The biological and ecological drivers of shell growth in bivalves

Purroy Albet, Ariadna

UNIVERSITY OF SPLIT, UNIVERSITY DEPARTMENT OF MARINE STUDIES
UNIVERSITY OF DUBROVNIK
INSTITUTE OF OCEANOGRAPHY AND FISHERIES, SPLIT

Postgraduate study of Applied Marine Sciences

Ariadna Purroy Albet

THE BIOLOGICAL AND ECOLOGICAL DRIVERS OF SHELL GROWTH IN BIVALVES

Doctoral thesis

Split, March 2017

This doctoral thesis was performed at the Institute of Oceanography and Fisheries, in the Laboratory of Fisheries Science and Management of Pelagic and Demersal Resources under the guidance of Prof. Melita Peharda Uljević Ph.D., in the framework of the inter-university postgraduate studies of Applied Marine Sciences at the University of Split and University of Dubrovnik. This research has been carried out in the framework of the ARAMACC Project "Annually Resolved Archives of Marine Climate Change" (FP7-PEOPLE-2013-ITN) under an ESR Marie Curie Fellowship.

"It is a curious situation that the sea, from which life first arose, should now be threatened by the activities of one form of that life. But the sea, though changed in a sinister way, will continue to exist; the threat is rather to life itself."

Rachel Carson

TABLE OF CONTENTS

BASIC DOCUMENTATION CARD

University of Split and University of Dubrovnik **Ph.D. thesis**

Ph.D. in Applied Marine Sciences

THE BIOLOGICAL AND ECOLOGICAL DRIVERS OF SHELL GROWTH IN BIVALVES

Ariadna Purroy Albet

Thesis was performed at the Institute of Oceanography and Fisheries, Split

Abstract

Bivalve mollusks incorporate life-history traits in their shells during growth making them valuable archives of environmental, biological and evolutionary information. This thesis provides insights into the biological and environmental drivers of shell growth in *Callista chione*, *Glycymeris bimaculata* and *Glycymeris pilosa*. The study was performed in the middle-eastern Adriatic Sea (Pag Bay, Cetina river mouth and Pašman Channel) from May 2014 until October 2015. A characterization of the feeding ecology of these species within their habitat analyzed several biochemical parameters including stable isotope and fatty acid composition. The reproductive behavior was studied applying two complementary approaches, histology and gonadosomatic index. Lastly, stable isotope analyses of carbonate samples were linked to high-resolution temperature records to describe shell microgrowth patterns. Spring and summer were identified as the periods with the best food quality in the particulate matter. Food resource partitioning was observed between *C. chione* and *G. bimaculata* at each site and the nitrogen isotopic composition of bivalve tissues was influenced by the presence of diazotroph biomass which differentiated among sites. Inter-site variations in the spawning timing and duration of *C. chione* were likely associated with temperature whereas in *Glycymeris* sp. spawning was not directly connected. Such small-scale biological responses are essential to address climate oscillation influences. Shell accretion took place between May and December pointing (i) temperature as an important determinant of shell growth (ii) food availability setting the limits for the growth season and (iii) the onset of gametogenesis close to the growth line formation, evidencing higher energy requirements for reproduction. These results contribute to knowledge on bivalve ecology in the Adriatic Sea and outlined the importance of coupling sclerochronology to ecological studies for a better understanding of species life-history traits.

(202 pages, 52 figures, 18 tables, 414 references, original in English)

Thesis deposited in National and University Library in Zagreb, Split University Library, and Library of Institute of Oceanography and Fisheries in Split

Keywords: bivalves, feeding ecology, fatty acids, stable isotopes, histology, gonadosomatic index, shell growth, sclerochemistry, sclerochronology, Adriatic Sea

Supervisor: Prof Melita Peharda Uljević Ph.D. / Senior Research Scientist

Reviewers: 1. Prof Nedo Vrgoč Ph.D. / Full professor
2. Ivana Bočina Ph.D. / Associate professor
3. Ivan Župan Ph.D. / Assistant professor

Thesis accepted: March 3rd 2017

TEMELJNA DOKUMENTACIJSKA KARTICA

Sveučilište u Splitu i Sveučilište u Dubrovniku **Doktorska disertacija**

BIOLOŠKI I EKOLOŠKI ČIMBENICI KOJI UTJEČU NA RAST LJUŠTURA ŠKOLJKAŠA

Ariadna Purroy Albet

Rad je izrađen u Institutu za oceanografiju i ribarstvo u Splitu

Sažetak

Školjkaši u svoje ljušture ugrađuju osobine životnog ciklusa, što ih čini vrijednim arhivima okolišnih, bioloških i evolucijskih podataka. Ovaj rad pruža uvid u biološke i ekološke čimbenike koji utječu na rast vrsta *Callista chione*, *Glycymeris bimaculata* i *Glycymeris pilosa*. Istraživanje je provedeno u istočnom dijelu srednjeg Jadrana (Paška uvala, ušće rijeke Cetine i Pašmanski kanal) u periodu od svibnja 2014. do listopada 2015. Karakterizacijom ekologije prehrane ovih vrsta u okviru njihovog okolnog staništa analizirano je nekoliko biokemijskih parametara, uključujući stabilne izotope i sastav masnih kiselina. Reproduktivno ponašanje se proučavalo primjenom dva komplementarna pristupa, histologije i gonadosomatskog indeksa. Analize stabilnih izotopa karbonatnih uzoraka su povezane sa zapisima temperature visoke rezolucije kako bi se opisali uzorci mikro-rasta. Proljeće i ljeto su identificirani kao razdoblja s najboljom kvalitetom hrane u mikroćesticama. Raspodjela izvora hrane je zamijećena između vrsta *C. chione* i *G. bimaculata* na svakoj lokaciji, a izotopni sastav dušika u tkivu školjkaša je bio pod utjecajem diazotrofne biomase koja se razlikovala među lokacijama. Varijacije među lokacijama, u vremenu i trajanju mriještenja vrste *C. chione,* su vjerojatno povezane s temperaturom, dok je kod vrste *Glycymeris* sp. mriještenje nije bilo izravno povezao. Takvi manji biološki odgovori su bitni za razumjevanje utjecaja klimatskih promjena. Rast ljušture se odvijao između svibnja i prosinca naglašavajući (i) temperaturu kao bitnu odrednicu rasta ljušture (ii) dostupnost hrane koja određuje granice sezone rasta i (iii) nastup gametogeneze u doba formiranja linije rasta, pokazujući veću potrebu za energijom tijekom razmnožavanja. Rezultati ovog istraživanja pridonose poznavanju ekologije školjkaša u Jadranskom moru, a istaknuli su važnost povezanosti sklerokronologije s ekološkim studijama za bolje razumijevanje osobina životnog ciklusa školjkaša.

(202 stranica, 52 slika, 18 tablica, 414 literaturnih navoda, jezik izvornika: engleski)

Rad je pohranjen u Nacionalnoj i sveučilišnoj knjižnici u Zagrebu, Sveučilišnoj knjižnici u Splitu i knjižnici Instituta za oceanografiju i ribarstvo u Splitu.

Ključne riječi: školjkaši, ekologija ishrane, masne kiseline, stabilni izotopi, histologija, gonadosomatski indeks, rast ljušture, sklerokemija, sklerokronologija, Jadransko more

Mentor: Prof. dr. sc. Melita Peharda Uljević Ph.D. / Znanstvena savjetnica

Ocjenjivači: 1. Prof. dr. sc. Nedo Vrgoč / Redovni profesor
2. Dr. sc. Ivana Bočina Ph.D. / Izvanredni profesor
3. Dr. sc. Ivan Župan Ph.D. / Docent

Rad prihvaćen: 3. Ožujak 2017. godine

1. GENERAL INTRODUCTION

Marine bivalves are commonly found in littoral shores and they often live in large aggregations of individuals which play an important role as ecosystem engineers contributing in creating, modifying and maintaining the habitat (Dame, 1996; Jones et al., 1994). Due to their extensive geographic and bathymetric distribution bivalves are able to withstand a wide range of environmental conditions which regulate species' life history traits (Gosling, 2015) raising interest in their use as paleoclimate recorders. Bivalve mollusk shells incorporate this information during growth making them valuable archives of environmental, biological and evolutionary information (Richardson, 2001). Therefore, bivalve shells can reveal valuable data pertinent to the reconstruction of environmental variations and life history traits from polar to tropical regions, and from freshwater to saltwater ecosystems (Goodwin et al., 2001).

In recent years, studies on bivalve sclerochronology, aiming to investigate interannual variations in growth increment widths, as well as variations in geochemical composition have developed rapidly (Schöne & Gillikin, 2013). Mollusk shells have been recognized as useful archives of environmental data spanning from several years to millennia (Schöne et al., 2005; Butler et al., 2010; Reynolds et al., 2013). Bivalves preserve high resolution records of environmental conditions and life-history traits in their shell increments (Schöne et al., 2005) and e.g., studying oxygen isotope ratios ($\delta^{18}O$) in shell carbonates may reveal whether variations in their annual calcification rate are controlled by exogenous and endogenous factors (Gosling, 2015). Temperature is a crucial parameter when studying bivalve shell growth and fine-scale studies have been able to decipher even semi-diurnal growth patterns in some organisms (reviewed in Schöne & Surge, 2012). The importance of each of these factors (e.g. temperature, salinity, phytoplankton abundance, circadian cycles, age and the biological clock) in controlling the rate and timing of growth varies among species and along latitudinal gradients (Richardson, 2001). It is the combination of temperature, food availability and food quality the one typically controlling intra-annual shell growth (Ansell, 1968; Witbaard, 1996; Ambrose et al., 2012; Vihtakari et al., 2016; Kubota et al., 2017) although the combination of different growth factors is likely to be species-specific (Jones, 1980; Nishida et al., 2012).

Likewise, the timing and duration of physiological processes such as the reproductive cycle vary both spatially and temporally, even within species (Cardoso et al., 2007; Santos et al., 2011; Verdelhos et al., 2011; Magalhães et al., 2016). This is a result of complex interactions between exogenous and endogenous factors from which environmental variables, e.g., temperature and food supply, are the principal regulators triggering gametogenesis and spawning (Sastry, 1979; Sebens, 1987; Drent, 2004;

MacDonald & Thompson, 1986; Philippart et al., 2003; Sokolova et al., 2012; Carmichael et al., 2004; Honkoop & Beukema, 1997; De Montaudouin, 1996).

Whether the allocation of energy is balanced or directed more to either reproduction or growth might certainly be species-specific and can possibly depend on the latitudinal gradient at which these species live and are exposed to varying temperature or food availability (e.g. Cardoso et al., 2007). The nature of environmental and physiological controls driving shell growth remains to be determined for a majority of bivalves. Thus, studies on bivalve ecology and characterization of life-history traits is a basic step to interpret shell growth patterns prior to use of bivalves as target organisms for paleoclimatological and age determination studies.

The onset of bivalve sclerochronological studies in the Mediterranean requires the identification of target species that could be used as paleoenvironmental archives. This task needs a sound understanding of the species life-history traits to infer meaningful ecological interpretations when doing environmental reconstructions based on shell microgrowth patterns. The combination of fine-scale studies on environmental and biological factors leading shell growth has been rarely applied and is an extremely powerful tool to reveal present changes and test evolutionary hypothesis. High-resolution environmental data contribute to improve our understanding on physiological processes and other life-history traits, biogeographic distribution of species and to efficiently manage shellfish fisheries resources. On this basis, the present thesis analyzes the combined effects of seawater temperature, food availability and reproduction into shell growth, in bivalves from the Adriatic Sea.

1.1. Rationale and objectives

At the forefront of environmental policy making due to climate change effects (IPCC, 2014) there is a strong need to assess marine benthic environmental changes. Understanding the imprint of the environment on bivalve shells is fundamental to better understand the processes responsible for these changes as well as for anticipating potential perturbations on these organisms and the ecosystems they sustain. In recent years, an increasing number of bivalve sclerochronology studies attempt to reconstruct the North Atlantic climate in order to predict future scenarios. In this scenarios, the Mediterranean stands as an interesting region for bivalve sclerochronology. However, the knowledge on biological and ecological drivers of shell growth in this and other regions is still limited. Identifying growth history patterns from extant species at a local scale is extremely powerful to assess bivalves' adaptive capacity to favorable and unfavorable conditions, and provide useful information to reconstruct past conditions. This can be achieved setting shell growth patterns into a chronological

frame to estimate what controls intra-annual changes in calcification rates. The aim of this thesis is to assess the environmental and biological drivers of shell formation by analyzing: (1) environmental variables (2) reproduction (3) feeding ecology and (4) shell growth of target bivalve species. Three target species were selected based on their abundance, relatively long lifespans and ecological role in the Adriatic, Mediterranean and Atlantic Seas: *Callista chione* (Linnaeus, 1758), a commercially important species, and two glycymeridids, *Glycymeris bimaculata* (Poli, 1795) and *Glycymeris pilosa* (Linnaeus, 1767). Sampling was conducted at three locations in the eastern Adriatic coast including Pag Bay, Cetina River mouth and Pašman Channel aiming to account for inter- and intraspecies biological responses in different habitats. The objectives of the thesis are:

- Analyze the pelagic-benthic coupling in the shallow waters of the middle Adriatic coast through the characterization of suspended particulate matter (SPM) and sediment (Sed) at sampling locations
- Describe the reproductive cycle of the studied species applying two methodological approaches: histological analysis and gonadosomatic index
- Describe body mass index, reproductive investment, reproductive output and fecundity of *C. chione* and intraspecific comparison between two sites
- Assess the influence of environmental variables (e.g., temperature) and food supply on the reproductive processes
- Describe spatio-temporal variations in the feeding ecology of *Glycymeris* sp. and *C. chione* throughout the combined application of stable isotopes and fatty acid analysis, and other biomarkers (e.g., C:N ratio, Chl *a*, biogenic silica)
- Evaluate the isotopic and fatty acid feeding niches with the application of a two-source mixing model
- Describe microgrowth patterns of shell growth throughout sclerochemistry: micromilling from shell surface in *C. chione* and from cross-sections in *G. bimaculata*
- Interrelate previous environmental and biological responses to shell growth and concluding which are the driving factors of timing and rate of growth
- Identify whether these patterns are characteristic of a given species or of a given habitat

2. LITERATURE REVIEW

2.1. Species of study

2.1.1. *Callista chione*

The smooth clam *Callista chione* is a marine venerid bivalve inhabiting the soft bottoms of Atlantic and Mediterranean coastal areas (Poppe & Goto, 1993). It is a suspension-feeding organism that burrows in sediments in the shallow waters. In many Mediterranean countries this species is commercially harvested by dredging boats (Tirado et al., 2002; Ramón et al., 2005) and in the shallow coasts of Greece and Croatia, it is also collected by skin or scuba-diving (Ezgeta-Balić et al., 2011; Metaxatos, 2004). *Callista chione* is a moderately long-lived bivalve with a longevity of over four decades (Ezgeta-Balić et al., 2011) and a shell length up to 100 mm (Poppe et al., 1993). Due to social demands on the shellfish market (Ezgeta-Balić et al., 2011) and the ongoing scarcity of natural beds (Ramón et al., 2005; Baeta et al., 2014), a sustainable management and close monitoring on the stock assessment needs to be implemented to protect natural beds and secure the long term fishery of this species. Additionally, *C. chione* has been found in middle Miocene rocks in Hall et al., (1974) and recent Mediterranean archeological research documented it as a marine resource for Neanderthals (Cortés-Sánchez et al., 2011; Romagnoli et al., 2016).

2.1.2. *Glycymeris bimaculata*

Species *Glycymeris bimaculata* predominantly occurs in the Mediterranean (Poppe et al., 1993), although it has also been found in the east Atlantic Ocean off the Canary and Madeira Islands, Portugal and NW Morocco (Nolf & Swinnen, 2013; Poutiers, 1996). In the Mediterranean Sea, it is the largest species of the Glycymerididae family, usually attaining a length of around 80 mm and estimated to reach up to 123 mm (Poppe et al., 1993; Nicol, 1964). In the eastern Adriatic Sea, *G. bimaculata* is a common burrowing bivalve inhabiting sandy and gravelly shallow bottoms. The largest specimen found in the Adriatic measured 99 mm in length (Legac & Hrs-Brenko, 1999). An estimated maximum longevity of 65 years and a chronology spanning 16 years revealed its potential use as sclerochronological archive (Bušelić et al., 2015). It is mainly used as bait for fishing or ornamental purposes, thus, with no economic interest. Sporadically might be consumed by local people (Legac & Fabijanić, 1994).

2.1.3. *Glycymeris pilosa*

Glycymeris pilosa is distributed along the Mediterranean, and the east Atlantic Ocean off the Canary and Madeira Islands and the coasts of Morocco, Mauritania, Western Sahara and Portugal (Goud & Gulden, 2009; Nolf et al., 2013; Poutiers, 1996). The northernmost documented limit is the Ria de Arousa in NW

Spain (Goud et al., 2009). As its congeneric *G. bimaculata*, it can reach up to 96 mm length (Huber, 2010) and inhabits sandy, muddy or gravelly bottoms. In the Adriatic Sea, and most likely in other Mediterranean regions, records of *G. pilosa* have been traditionally mis-identified as *G. glycymeris* (Linnaeus, 1758) (Legac et al., 1999; Peharda, D Ezgeta-Balić, et al., 2010) as recently revealed (Purroy et al., 2016). The presence of *G. pilosa* has been confirmed in the coasts of Greece and Israel (Sivan et al., 2006; Lécuyer et al., 2012) and along the entire Croatian coast. The largest specimen found in the Adriatic measured 94.0 mm in length (Peharda unpublished data). A recent study established the maximum longevity of *G. pilosa* at 69 years and a robust chronology spanning 44 years, supporting its potential as sclerochronological archive in the Mediterranean (Peharda et al., 2016).

Overall, the three species inhabit Adriatic waters but all do not always coexist in the locations that were sampled for this thesis (Fig. 2.1).

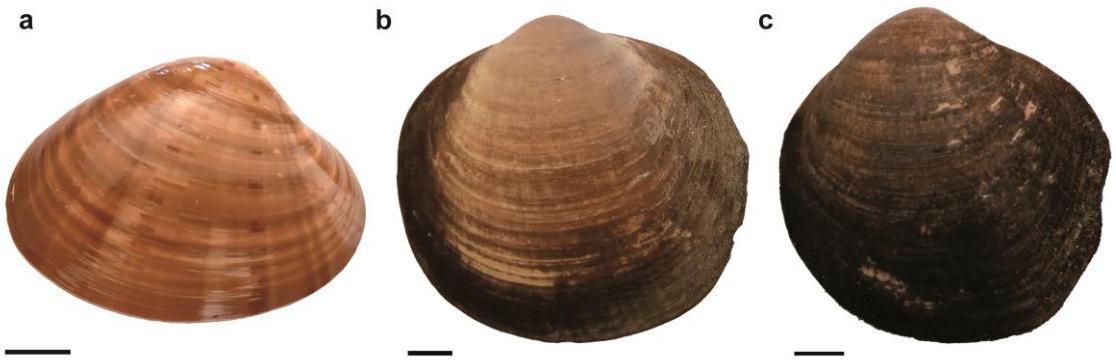

Figure 2.1. Target species: (**a**) *Callista chione*, (**b**) *Glycymeris bimaculata* and (**c**) *Glycymeris pilosa*. Scale bar 1 cm.

2.2. Feeding ecology

Bivalves are suspension-feeding organisms and participate on the transfer of particulate organic matter (POM) between the water column and the surface sediment layer (Schubert & Calvert, 2001). In the sediment-water interface, physical factors (e.g. currents, wind) and bioturbation enhance resuspension enabling a continuous supply of POM to suspension feeding organisms (Orvain et al., 2012; Dubois et al., 2014). Bivalves certainly feed upon phytoplankton but other sources such as detritus, bacteria, microphytobenthos and zooplankton constitute an important component of their diet (Peharda et al., 2012; Davenport et al., 2000; Grall et al., 2006; Kharlamenko et al., 2011; Ezgeta-Balić et al., 2012). In temperate areas, benthic consumers are able to shift their diets along the year adapting to the available material in suspended POM (Antonio et al., 2010), e.g. following the magnitude and seasonality of primary production. Filter feeding organisms can modify the chemical characteristics of particular

matter both in the pelagic and benthic pools (e.g. Page & Lastra, 2003; Prins et al., 1997; Charles et al., 1999; Ward & Shumway, 2004). Thus, investigating the origin and availability of food resources in POM in relation to their contribution to bivalve's diet allows to distinguish variations in the trophic activity, essential to better understand the role of selective feeding within the ecosystem (Riera & Richard, 1996; Carlier et al., 2007; Dubois et al., 2012). Assessing the role of bivalves in the benthic-pelagic coupling provides clues about the origin and preferential uptake of food within the pool of POM and potential limitations due to inter or intra-specific competition (Dame, 1996; Dubois et al., 2014) improving our understanding on the ecological and biogeochemical functioning in these systems. In aquatic ecosystems, stable isotopes (e.g. $\delta^{13}C$ and $\delta^{15}N$) and fatty acid concentrations have also been used to analyze the food web structure and infer trophic relationships within and between ecosystems (e.g. Kharlamenko et al., 2008; Kharlamenko et al., 2011; Antonio & Richoux, 2016b; Giraldo et al., 2016; Pérez et al., 2013).

2.2.1. Stable Isotope Analysis

Stable isotope (SI) analyses have been widely used to describe diet composition, trophic level and habitat characteristics in marine organisms (DeNiro & Epstein, 1978; Peterson & Fry, 1987; Lorrain et al., 2002; Lopez et al., 2016) due to a time integrated signal of the assimilated food sources in animal tissues (Peterson et al., 1987; Martínez del Rio et al., 2009; Ezgeta-Balić et al., 2014). The measurement of $\delta^{13}C$ allows the identification of the main primary producers (Post, 2002) and also discriminates sources from terrestrial and marine, and from benthic and pelagic systems (e.g. Savoye et al., 2003; Cloern et al., 2002). On the other hand, the $\delta^{15}N$ signature is useful to identify changes through the food chain, based on the principle that excretion and respiration of lighter isotopes by consumers increase their $\delta^{15}N$ content (Peterson et al., 1987; Carlier et al., 2015; Fry & Sherr, 1984) and even for identifying the so-called isoscapes, to trace geographic changes (Cherel & Hobson, 2007; MacKenzie et al., 2011). Additionally, SI may provide information on variations in productivity and nutrient levels (Riera, 2007), biological responses to anthropogenic influences such as pollution or recreational activities (Puccinelli et al., 2016; Alomar et al., 2015), and can also work as bioindicators (Post, 2002; Fry & Allen, 2003; Carriquiry et al., 2016). The recent development of models of trophic structure, known as mixing models, allow to place the trophic position of an organism in a food web in relation to the main food sources (Phillips et al., 2014 and references therein). The combination of several consumers allows to infer resource partitioning and to assess the degree of trophic variability at an inter- and intrapopulation level (Layman et al., 2012). In this way, SI are powerful to determine connections between the diet and the life-history traits of consumers or population dynamics.

2.2.1.1. Stable isotope analysis in food sources

In the particulate organic matter (POM) stable isotope signatures are used to decode biogeochemical coastal processes involving the production, origin and use of organic matter (OM), denitrification and deposition in sediments. In coastal and continental margin areas, SI are used to trace inputs of terrestrial or marine POM, and anthropogenic inputs such as sewage-derived organic matter, agricultural runoff, recreational boats or nutrients (Lee Van Dover et al., 1992; Carreira et al., 2002). Few studies have reported carbon and nitrogen isotope compositions of organic matter in the Adriatic Sea. The characterization of suspended particulate matter (SPM) in the Istra Peninsula (northern Adriatic), was conducted to assess the impact of OM derived from anthropogenic influence in coastal sites (Žvab Rožič et al., 2015). High $\delta^{15}N$ values and relatively depleted in $\delta^{13}C$ in SPM reflected insufficient local septic systems and the influence of riverine terrestrial material (4.2 to 13.8‰ $\delta^{15}N$ and -24.1 to -22‰ $\delta^{13}C$) whereas lighter ^{15}N values were associated with the effect of purification plants (-3.8 to 1.1‰ $\delta^{15}N$ and -22.5 to -21.3‰ $\delta^{13}C$). Additionally, nitrogen isotope analysis from water samples at sites with different amounts of anthropogenic contribution were also studied in the central eastern Adriatic which overall ranged from -1.3 to 13.8‰ (Žvab et al., 2010) and from 1.8 to 9.7‰ (Dolenec et al., 2011; Dolenec et al., 2007). The most ^{15}N-enriched values corresponded to those sites most influenced by human activities (Žvab et al., 2010; Dolenec et al., 2011).

Studies on the surface sediment layer were conducted in the north Adriatic (Ogrinc et al., 2005) and in Adriatic open waters (Faganeli et al., 1994). Average $\delta^{13}C$ values in surficial Adriatic sediments ranged from -28.6 to -23.5‰ pointing out a higher contribution of terrestrial origin in the western Adriatic (due to major influence of river Po) and in the southeastern Adriatic (also derived by riverine inputs), in contrast to eastern Adriatic coast which showed more marine derived values (-24.6 to -22.5‰) (Faganeli et al., 1994). In Ogrinc et al., (2005) values ranged from -25.5 to -21.5‰ ($\delta^{13}C$) and from 1.7 to 5.6‰ ($\delta^{15}N$), whereas the elemental organics composition revealed quite low values ranging from 0.5 to 1.3% (OC), 0.1 to 0.2% (N) and C:N atomic ratios from 4.2 to 38. The light isotopic values and C:N ~ 18 were distinguished under terrestrial influence whether more isotopically enriched values and C:N ~ 8 were linked to marine derived OM (Ogrinc et al., 2005).

2.2.1.2. Stable isotope analysis in consumers

Studies on $\delta^{15}N$ in tissues from benthic invertebrates in the central eastern Adriatic Sea reflected the local environmental conditions. Benthic organisms were generally enriched with respect to SPM varying from -1.3 to 11.9‰ (Žvab et al., 2010) and in *Mytilus galloprovincialis* Lamarck, 1819 values ranged from

3.3 to 8.2‰ (Dolenec et al., 2011). In Žvab et al., (2010), the enrichment of $\delta^{15}N$ values was suggested to be a result of untreated municipal, industrial and agricultural pollution in the areas. Dual nitrogen and carbon isotope analyses were studied in four bivalve species including *M. galloprovincialis*, *Ostrea edulis* Linnaeus, 1758, *Modiolus barbatus* (Linnaeus 1758) and *Arca noae* Linnaeus, 1758), from Mali Ston Bay (southern Adriatic), to observe seasonal variations in two different tissues, muscle and digestive gland (Ezgeta-Balić et al., 2014). Seasonal variations were more pronounced in the digestive gland, suggesting that this tissue better reflects recent food ingestion and trophic patterns. Mean $\delta^{15}N$ values ranged from 2.0 to 5.3‰ while mean $\delta^{13}C$ ranged from -24.0 to -21.8‰ and both values were more isotopically enriched in muscle tissue than in digestive gland (Ezgeta-Balić et al., 2014). These individuals were also analyzed for fatty acids (FA) to identify their main food sources (Ezgeta-Balić et al., 2012). In a like manner, *A. noae* from Pašman area (middle Adriatic Sea) was analyzed (Župan et al., 2014). Accordingly, muscle showed more isotopically enriched values averaging -19.1±0.8‰ ($\delta^{13}C$) and 5.5±0.7‰ ($\delta^{15}N$) than the digestive gland which had average values of -21.3±1.2‰ ($\delta^{13}C$) and 4.1±0.4‰ ($\delta^{15}N$). Results from these studies reveal the importance of choosing the right tissue accordingly to the main study goal.

Up to date, just one isotopic record in soft tissues has been found in the literature for *C. chione*, with mean values of -19.4±0.5‰ ($\delta^{13}C$) and 4.7±0.4‰ ($\delta^{15}N$), for a population from the NW Mediterranean (Carlier et al., 2007). The same holds true for the *Glycymeris* genus with only one study reported for *G. glycymeris* across a large depth gradient in the Bay of Brest (Nerot et al., 2012). These results showed more depleted values at the deepest station (~220 m) averaging values of -19±0.2‰ ($\delta^{13}C$) and 2.8±0.4‰ ($\delta^{15}N$) than at the shallowest one (6 m) where averaging values of -15.9±0.2‰ ($\delta^{13}C$) and 9.4±0.3‰ ($\delta^{15}N$) were noted (Nerot et al., 2012).

2.2.2. Fatty Acid Analysis

Fatty acids are involved in the organism's energy storage (Parrish et al., 2000) and are effective tracers of food sources, since they remain mostly invariable through trophic pathways, and are specific for different groups of organisms, e.g. primary producers, heterotrophs (e.g. Napolitano et al., 1997; Dalsgaard et al., 2003). However, the higher the trophic level, the more complex is the interpretation of FA as dietary indicators (Budge et al., 2002) due to the incorporation of multiple diet sources and diverse metabolic pathways (Dalsgaard et al., 2003). FA are good discriminators of food sources in suspended POM and sediment (Bergamino et al., 2014; Ricardo et al., 2015; El-Karim et al., 2016; Connelly et al., 2016) and they are also useful describing the seasonal and spatial variations in these pools as potential food sources for benthic organisms (Boon & Duineveld, 1996).

The composition of FAs in the digestive gland of bivalves play an important role as metabolic energy reserves; thus, their analysis have been employed to trace recent food ingestion (weeks–months) (Deudero et al., 2009; Ezgeta-Balić et al., 2012; Najdek et al., 2013). Few studies have considered the significance of incorporating spatial and temporal changes in environmental biochemical variations (e.g. SI, FA) to gain an insight in recent food assimilation in benthic organisms, particularly occupying different environments (Ventrella et al., 2008; Yurkowski et al., 2016; Gonçalves et al., 2012). Fine-scale studies describing spatio-temporal patterns in primary producers allow assessing the variability of the diet of secondary consumers within and among species which are essential for comprehensive ecological studies (Underwood et al., 2000; Antonio et al., 2012).

2.2.2.1. Fatty acids in food sources

Primary producers lay down the main FA profiles in marine food webs, consisting of phytoplankton (microalgae and photoautotrophic bacteria) and macroalgae. Microalgae support pelagic and offshore benthic food webs whereas macroalgae are present mostly in shallow coastal areas (Kayama et al., 1989). Photoautotrophic bacteria have a minor influence on the dynamics of marine ecosystems but heterotrophic bacteria contributing to microbial food web and terrestrial matter, are particularly important in coastal and estuarine ecosystems (Dalsgaard et al. 2003 and references therein). Numerous laboratory studies have examined the composition of fatty acids in marine microalgae (e.g. reviewed by Ackman et al., 1968; Kharlamenko et al., 2008; Kelly & Scheibling, 2012) concluding that individual FA cannot be used as taxonomic indicators but combinations of FA certainly reveal microalgae assemblages. The ratio of C16:1/C16:0 (>1) and the relative dominance of C20:5 (n-3) (EPA), C22:6 (n-3)/C20:5 (n-3) (DHA/EPA) (<1) and C14:0 are considered as diatom indicators (Ackman et al., 1968; Kharlamenko et al., 1995; Léveillé et al., 1997; Budge & Parrish, 1998) while the ratio of DHA/EPA (>1), DHA, 16:0 and C16:1/C16:0 (<1) are predominant in dinoflagellates (Dalsgaard et al., 2003; Budge et al., 1998). Herbivorous calanoid copepod markers are C20:1 and C22:1 (Falk-Petersen et al., 1987). A marker of zooplankton indicator of carnivory (Sargent & Falk-Petersen, 1988) and detrital matter (Fahl & Kattner, 1993) is C18:1(n-9). However, zooplankton is also characterized by 18:1(n-9), 18:2(n-6), 20:4(n-6) (ARA) and DHA (Kharlamenko et al., 2001). The level of (n-3) PUFA (EPA, DHA and ARA), considered as essential FA (EFA; Alkanani et al., 2007) are used as important food quality indicators (e.g. Antonio and Richoux 2016) which are transferred to microzooplankton (Ventrella et al., 2008). EFAs are necessary components of cell membranes and play an important role in many cellular activities in higher consumers (Ahlgren et al., 2009). Plants are the only organism able to biosynthesize de novo these PUFA and derivatives, 18:2(n-6) and 18:3(n-3) and i.e. EPA, DHA, ARA, which are essential for heterotrophic

organisms (Smith & Fitzpatrick, 1996). Usually, the C18:2(n-6) PUFA is associated with terrestrial sources when coupled to 18:3(n-3) at concentrations > 2.5 (Budge et al., 1998; Parrish et al., 1996; Fischer et al., 2014), seagrass (Kharlamenko et al., 2011), protozoa (Zhukova & Kharlamenko, 1999) and even to agricultural products (Napolitano et al., 1997). Main FA bacteria-specific are 15:0, 15:0ai, 15:1, 17:0, 17:0a1, 17:1 and 19:0, thus, combinations of FA are used to detect occurrence of bacteria (Mayzaud et al., 1989; Najdek et al., 2002; Fahl et al., 1993). Bacteria also biosynthesize, in common with eukaryotes, 16:1(n-7) and 18:1(n-7) FA. Therefore, if PUFA is present in large amounts, the origin would likely derive from eukaryotic production rather than bacterial (Dalsgaard et al., 2003). Marine heterotrophic bacteria abound in sediments, particularly after main phytoplankton blooms, as colonizers of settling particulate matter (Najdek et al., 2002); therefore, they are critical in recycling DOM and POM to higher trophic levels. For this reason, the FA composition in these systems is valuable to resolve the source of sediment particles, which is mainly dominated by SFA and MUFA. Further, elevated concentrations of 18:2(n-6) have been attributed to agricultural products scattered in the coast (Napolitano et al., 1997) or to some protozoa (Zhukova et al., 1999) and C16:0, C16:1 and C18:0 to domestic sewage (Boëchat et al., 2014). A summary of FA trophic markers (FATM) and their sources is listed in Table 2.1.

Table 2.1. Summary of FATM and their sources.

FATM	Sources	References
20:5(n-3) - EPA 16:1(n-7) 16:1(n-7)/16:0 > 1 22:6(n-3)/20:5(n-3) < 1 - DHA/EPA < 1 C14:0	Diatoms	Budge & Parrish (1998); Dalsgaard et al. (2003); Leveille et al. (1997)
22:6(n-3) - DHA 22:6(n-3)/20:5(n-3) > 1 - DHA/EPA > 1 16:1(n-7)/16:0 < 1 C16:0 C18:4	Dinoflagellates	Budge & Parrish (1998); Parrish et al., (2000); Dalsgaard et al. (2003)
18:1(n-9)	Zooplankton	Sargent & Falk.Petersen (1988); Kharlamenko et al. (2001); Zhukova & Kharlamenko et al. (1999)
C20:1 C22:1	Herbivorous calanoid copepods	Falk-Petersen et al. (1987)
Σiso- and anteiso- C15 and C17 18:1(n-7) 18:1(n-9) C20:0	Detritus/Bacteria	Mayzaud et al. (1989); Najdek et al. (2002); Fahl & Kattner (1993); Galap et al. (1999)
18:2(n-6) + 18:3(n-3) > 2.5	Terrestrial plants	Budge & Parrish (1998)
20:4(n-6) - ARA	Heterotrophic flagellates Invertebrate larvae	Lorrain et al. (2002)

Studies on the composition of FA in POM in the northern Adriatic Sea, one of the most productive regions of the Mediterranean largely influenced by the River Po inputs, revealed that sediment was mainly composed by SFA (mainly C16:0) and MUFA, mainly C16:1 and C18:1 (Najdek, 1993). These two FA are indicative of marine origin OM and were reported in higher concentrations during spring and summer, whereas the lowest concentrations occurred during the phytoplankton bloom in the winter-early spring. Other studies have focused on the mucilaginous aggregates which episodically are recorded in the area (Najdek et al., 2002). Studies on FA composition in SPM or Sed in other areas of the Adriatic haven't been found.

2.2.2.2. Fatty acids in consumers

During recent decades, fatty acid markers have been used to interpret bivalve diets usually only on one species and only few studies addressed spatial and/or temporal variability. In studies under laboratory conditions, bivalves have proved their ability to elongate or desaturate FA, e.g. 16:1(n-7) to 18:1(n-9) to 20:1(n-9) among others (Albentosa et al., 1996), what is hard to follow under natural conditions. PUFA are used as energy reserves during periods of nutritional shortage (Freitas et al., 2002). The ARA/EPA ratio and NMID (non-methylene-interrupted dienoic fatty acid) have been found to be higher in bivalve's larvae and eggs (e.g. Ahn et al., 2000) thus, their presence can be considered as a contribution of bivalve's larvae as food source (Ezgeta-Balić et al., 2012). Also, ARA is a precursor of prostaglandins which have an influence on the reproduction in mollusks (Soudant et al., 1999), by stimulating the contraction and release of gametes during the timing of spawning (Palacios et al., 2005). This association has been reported in studies in visceral mass (Galap et al., 1999) which showed higher concentrations of FA in general during the main spawning period and in the muscle (Ezgeta-Balić et al., 2012) pointing out a higher concentration of ARA during spawning. A high degree of unsaturation (UND) is characteristic of healthy mollusks (Dupčić Radić et al., 2014).

Detritus, diatom, dinoflagellate, zooplankton and EFA markers were the most abundant in consumer studies in the southeastern Adriatic Sea. Filter-feeders such as *Mytilus galloprovincialis*, *Ostrea edulis* and *Modiolus barbatus* (Ezgeta-Balić et al., 2012), *Pinna nobilis* Linnaeus, 1758 (Najdek et al., 2013), *Arca noae* (Ezgeta-Balić et al., 2012; Dupčić Radić et al., 2014) and *G. nummaria* (Linnaeus, 1758) (Najdek et al., 2016) have revealed ingestion of a mixed diet. Studies of FA indicated that different tissues had different carbon turnover rates (Tieszen et al., 1983) as demonstrated between the digestive gland and adductor muscle tissues (Ezgeta-Balić et al., 2012). For example, ARA, EPA and DHA decreased from May to September and increased until March. C16:1/C16:0 ratios were higher in spring-summer and lower in autumn-winter, conversely to DHA/EPA ratios (Ezgeta-Balić et al., 2012). In general, low levels of

dinoflagellate markers were found in this study, in contrast to important contribution of EFA, most likely reflecting a carnivorous diet. Additionally, larviphagy greatly contributed to their diet, likely associated with sampling in aquaculture farms. A high concentration of SFA has been previously reported in *G. nummaria* (Najdek et al., 2016) and *G. glycymeris* (Galap et al., 1999).

An effective way in identifying major sources of organic matter contributing to the diet of benthic invertebrates and investigating food web dynamics is combining SI and FA biomarkers analysis (Dalsgaard et al., 2003; Fry, 2006; Kharlamenko et al., 2008; Budge et al., 2008). Notwithstanding, other biomarkers are often used as indicators of the quality of organic matter by characterizing the composition of POM in coastal ecosystems. Among these, studies on elemental C:N ratios and Chlorophyll *a* (Chl *a*) abound, but few carry biogenic silica content analysis, which is a major component of marine biogenic matter fundamental for diatom growth (Ragueneau et al., 2002; Leblanc et al., 2003; Alomar et al., 2015). Therefore, an extended characterization including the above mentioned biological and environmental parameters (e.g., temperature, salinity) greatly contribute to an accurate determination of the sources of organic matter in relation to environmental conditions.

2.3. Reproduction

In marine invertebrates from temperate waters, sexual reproduction is cyclic with distinctive seasonal patterns (Gosling, 2015). In bivalves, the timing and duration of the reproductive cycle and in particular, spawning, are believed to be determined by the interaction between endogenous (genetic and physiological) and exogenous (environmental) factors (reviewed in Sastry, 1979; Gosling, 2003). Temperature and food availability are the main exogenous factors commonly attributed to influence the reproductive timing (Sastry & Blake, 1971; Gosling, 2003; MacDonald et al., 1986). Reproductive strategies between bivalve populations may depend on the latitudinal gradient (Santos et al., 2011; Verdelhos et al., 2011; Cardoso et al., 2007; Steingrimsson, 1989) and local environmental conditions (Verdelhos et al., 2011; Sola, 1997; Magalhães et al., 2016; Sebens, 1987). For instance, the transplant of specimens with particular latitudinal reproductive patterns followed the same reproductive strategy as in the original population, suggesting that a genetic component is controlling certain physiological mechanisms (Paulet et al., 1988) and evidencing that the adjustment to new environmental conditions it is not immediate. On the other hand, earlier spawning events (Philippart et al., 2003; Drent, 2004; Gam et al., 2010) or a decrease in the reproductive investment (Pörtner & Farrell, 2008; Sokolova et al., 2012) and output (Philippart et al., 2003; MacDonald et al., 1986) have been observed as a result of increasing temperatures.

Traditionally, the most applied methods for assessing the reproductive cycle in bivalves have been done through histological sectioning and squash preparations of gonads (Gosling, 2015). These methods are advantageous for determining the percentages of gonadal maturation stages and identifying stages of development, although they are time-consuming and rather subjective (Gosling, 2015). The somehow subjectivity when determining gametogenic stages is due to the coexistence of gametes in several developmental stages, leading macroscopic observations to errors (Tirado et al., 2002). Other methods quantifying the proportion of gonadal weight with respect to body mass (gonadosomatic index, GSI) (Santos et al., 2011; Cardoso et al., 2009a) have been used as a measure of reproductive effort, representing the main gametogenic events. An optimum approach to assess gametogenesis is the use of both qualitative, such as histology, and quantitative methods, such as GSI or oocyte size frequencies (Tirado et al., 2002; Gosling, 2003; Galimany et al., 2015).

In the Adriatic Sea, histological techniques have been used to document the reproductive cycle of several commercial and non-commercial bivalves. Most of these species showed a pronounced seasonal reproductive cycle with spawning occurring between June and August in *Modiolus barbatus* (Mladineo et al., 2007), spring–summer in *Glycymeris nummaria* (Crnčević et al., 2013) and during summer in *Arca noae* (Peharda et al., 2006) and *Venus verrucosa* Linnaeus, 1758, which was prolonged up to November (Popović et al., 2013). Condition index (CI) has been recognized as a reliable indicator of reproductive state for some species such *A. noae* (Peharda et al., 2006) and *V. verrucosa* (Popović et al., 2013) showing the highest values during periods prior to spawning. Based on this index, spawning was suggested to occur also during summer in *Mytilus galloprovincialis* Lamarck, 1819 (Peharda et al., 2007) and *Ruditapes decussatus* (Linnaeus, 1758) (Jurić et al., 2012). The CI can additionally increase in localities next to aquaculture farms due to the input of organic material (Župan et al., 2014). Therefore, the correlation of CI with gonadal development should be carefully addressed since experimental data has proven that low CI values may not correspond to the release of gametes, and can be influenced by other factors such as temperature, food or salinity (Tirado et al., 2002). During periods when food availability is not abundant, the energy of the individual goes to reproductive effort in detriment of loss of reserve tissue as seen in *R. decussatus* whereas low values of CI may coincide with ripe stages (Martínez-Pita et al., 2011; Delgado & Pérez-Camacho, 2007).

2.3.1. Reproduction in *Callista chione*

The reproductive cycle of *Callista chione* has been previously described for Atlantic (Moura et al., 2008) and Mediterranean populations (Valli et al., 1983; Valli et al., 1994; Tirado et al., 2002; Metaxatos, 2004;

Galimany et al., 2015) driven by the commercial interest for this species. In the southern coast of Spain, *C. chione* was found to spawn all year round primarily from February to September with the observation of three spawning peaks (February–March, spring and summer) and with a main gamete release in May (Tirado et al., 2002). Likewise, in the Catalan littoral, the smooth clam was able to reproduce all year round with a main spawning peak in spring (Galimany et al., 2015). In the Gulf of Trieste, Valli et al. (1983; 1994) identified one main spawning period from February to September with a maximum spawning release between May and August. In Greece, the reproductive cycle was also reported all year round with a continuous spawning from spring to beginning of winter and two main peaks in May and December (Metaxatos, 2004). In an Atlantic population from southwest Portugal three spawning peaks (January–March, April–May and August–October) were shown, immediately followed by a total gonadal restitution, indicating the start of a new gametogenic cycle (Moura et al., 2008).

The lack of a resting period has been claimed to be a strategy in the circalittoral, at depths around 10–20 m, where environmental conditions and a constant presence of Chl *a* are more stable for a successful recruitment than in shallower waters (Valli et al., 1983; Valli et al., 1994). A prolonged spawning period is advantageous for the species to avoid the risk of reproducing just once by spreading the settlement of spat throughout the year (Moura et al., 2008; Tirado et al., 2002) and compensating the high larvae mortality (Valli et al., 1994). The amount of reserves is constantly mobilizing from somatic to gonad tissues, and even during the most intense period of gametogenesis, the mobilization of reserve energy may exceed the one assimilated (Valli et al., 1994). As a result of these studies, an equal sex-ratio was observed and a consensus in the strong link between temperature and gonad maturation was confirmed. Also, latitudinal or small-scale variations have seen to influence the responses in gametogenesis and spawning mainly due to temperature changes rather than to phytoplankton biomass oscillations. First studies of *C. chione* did not account for hermaphrodites (Moura et al., 2008) or declared them very rare (Valli et al., 1983). Galimany et al., (2015) recently reported hermaphroditism in *C. chione*, a state that according to Heller (1993) occurs in 9% of all bivalves. The size at age maturity, defined as the length at which 50% of the population is mature, has been estimated at 50.8 mm for the populations in southern Portugal (Moura et al., 2008) and 30.3 mm for the Catalan littoral (Galimany et al., 2015). It is interesting to note that mature individuals 30 mm length were observed in the former, and mature females with a length of 20.6 mm in the latter. In contrast, gonadal maturation at the age of two has been reported by looking at smear samples (Metaxatos, 2004). A positive correlation between CI and periods prior to spawning was seen by Moura et al., (2008). All these studies were conducted in just one population during one breeding season, and none have assessed the quantitative allocation of energy into reproduction considering, for instance, environmental factors. Since differences in the growth rates of two relatively nearby populations of *C. chione* have been previously described in the

eastern Adriatic coast (Ezgeta-Balić et al., 2011), this region appears as an ideal experimental scenario for studies on the effects of temperature on natural populations.

2.3.2. Reproduction in *Glycymeris* sp.

The reproductive cycles of *Glycymeris bimaculata* and *G. pilosa* have not been assessed to date but reproduction characteristics of other members of the *Glycymeris* genus have been studied. In *G. glycymeris* from southern Brittany (France), ripe individuals represented at least 70% of the population throughout the year (Lucas, 1965). In populations from the Calf of Man (UK), Morris (1978) mentioned that *G. glycymeris* specimens were able to spawn all year round. Based on this knowledge, Steingrimsson (1989) studied *G. glycymeris* populations from around the Isle of Man using stereological analyses, since conventional techniques would not provide an accurate estimation of gametogenesis in a species with continuous spawning. His results showed that spawning occurred at small scales and confirmed that individuals were in the mature stage all year, thus indicating that most energy in the organism is allocated to reproduction. Under stress conditions, individuals might overcome spawning at larger scales to reach a maximum reproductive output (Steingrimsson, 1989). Height at sexual maturity was estimated at 20 mm (Lucas, 1965; Steingrimsson, 1989), which represented 12–13 year old specimens in the Isle of Man populations but just 4 year old in St. Malo (France), probably associated with differences in shell growth rates as reported by Berthou et al., (1986).

Another studied *Glycymeris* species is the Indian clam, *Glycymeris gigantea* (Reeve, 1843), from the Gulf of California (Mexico). The gonadal development for this species was studied bimonthly using common histological techniques and oocyte size frequencies (Villalejo-Fuerte et al., 1995). In this study, gametogenesis was shown to be most active from February to May, with the highest spawning peak in October, despite some degree of spawning being observed throughout the year. CI seemed to follow gametogenic activity, although it was not recommended as an indicator of reproduction due to the potential influence of changes in water content or nutritious mass in the soft tissue (Villalejo-Fuerte et al., 1995). On the other hand, a relationship between water temperature and main gamete release co-occured with a decrease in temperature of nearly 10°C (Villalejo-Fuerte et al., 1995).

The most recently studied glycymeridid is the cockle *Glycymeris nummaria* from Mali Ston Bay (southeastern Adriatic Sea). In this population, no differences in sex ratio were observed and a synchronous gonadal ripening took place between May–June, with one main annual spawning event (July–August) (Crnčević et al., 2013). For this species, CI generally followed gonad development and the highest mean gonad index (MGI) values were reported with increasing temperatures (May–July) while

the spawning peak coincided with the highest temperatures. Monthly mean mature oocytes of *G. nummaria* ranged from 9.2±2.8 µm to 41.9±23.7 µm with a maximum mature oocyte size around 80 µm (Crnčević et al., 2013) which is smaller than the one reported for *G. gigantea* (up to 150 µm) (Villalejo-Fuerte et al., 1995). This could be likely influenced by differences in shell length since *G. gigantea* attain a length of up to 99 mm (Nicol, 1964) whereas *G. nummaria* can occasionally reach lengths of 70 mm (Poppe et al., 1993). However, Lucas (1965) found mature oocytes between 160–180 µm for oval oocytes, suggesting these variations to be caused by different methodological approaches when measuring oocyte sizes. Hermaphrodites were also reported in *G. glycymeris* and *G. gigantea* (Lucas, 1965; Villalejo-Fuerte et al., 1995).

2.4. Shell growth

Bivalve shells, much like tree rings, are able to provide ultra high-resolution (tidal, daily, fortnightly, annual) records which allow a better understanding of species life history traits (Richardson, 2001). Bivalves can live in a wide biogeographic distribution ranging from poles to equator, from marine to freshwater ecosystems and from deep to shallow waters (Gosling, 2003). Consequently, the reconstruction of the physical and chemical environment during growth can be withdrawn from the shell imprint, for all these environments. Sclerochronology, firstly applied to study corals (Buddemeier et al., 1974), is successfully used in bivalves (Jones, 1980; Oschmann, 2009; Butler & Schöne, 2017) seeking to comprehend changes though an organism's life and reconstructing past environmental conditions. Jones et al., (2007) defined sclerochronology as "the study of physical and chemical variation in the accretionary hard tissues of organisms, and the temporal context in which they formed (…) seeks to deduce organismal life history traits as well as to reconstruct records of environmental and climatic change through space and time".

The application of growth pattern analysis is wide, including biology, ecology, archaeology and paleoclimate research (Schöne et al., 2012). Although most bivalves live for less than 10 years some are extremely long-lived. The astonishing finding of an *Arctica islandica* (Linnaeus, 1767) specimen dated 507 years as the longest lived non colonial animal (Butler et al., 2013) pointed out the important role of bivalves as potential paleoclimate archives. Uninterrupted climate reconstructions are the result of combining individual chronologies (cross-dating) of long-lived specimens (including fossils), known as master chronologies, allowing to extend the climate records beyond the lifetime of one organism (Marchitto et al., 2000; Schöne et al., 2003), covering centuries (Witbaard, 1996; Marchitto et al., 2000;

Butler et al., 2010; Schöne, 2003) to millennia (Reynolds et al., 2013; Wanamaker et al., 2012; Reynolds et al., 2017).

Sclerochronological techniques can be applied at several precision levels to trace the physico-chemical properties of the environment e.g., temperature, salinity (Koike, 1980; Marsden & Pilkington, 1995), water quality (Mutvei et al., 1996; Ravera et al., 2007), food availability (Sato, 1997) or biological responses such as the reproductive cycle (Sato, 1995; Jones, 1980). These records can be extracted through the combination of variable growth rates and geochemical properties of the shell. The identification of growth lines, formed by a different rate of shell deposition material due to chemical and crystallographic properties (e.g. Jones, 1980), is a first step prior to measuring growth rates. Growth line formation is usually associated with a period of slow growth with high amounts of organic material relative to calcium carbonate (Schöne et al., 2012). The growth increments, considered as the area in between the lines, are studied in the outer and middle shell layer of cross-sectioned valves as a measure of time (Richardson, 2001). Some bivalves form daily growth patterns, especially evidenced in the youngest portions of the shell, e.g. *Pecten maximus* (Linnaeus, 1758) (Chauvaud et al., 1998; Chauvaud et al., 2005) or *Tridacna spp* (Watanabe & Oba, 1999; Sano et al., 2012) associated with circadian periodicity. In intertidal bivalves, shell growth usually stops under aerial exposition, thus, in semidiurnal tide habitats, two growth lines can be formed per day (Schöne et al., 2007; Ramón & Richardson, 1990).

Traditionally, growth lines on the shell surface, which are used to age mollusks (e.g. Richardson, 2001 and references therein), represent the periods of growth slowdown or cessation, most likely associated with colder (e.g. Jones, 1980; Richardson, 2001) or warmer (e.g. Hall et al., 1974) months of the year. Several mark-recapture experiments have confirmed the formation of annually growth lines (Mannino et al., 2008; Peterson et al., 1983; Gosling, 2003; Sejr et al., 2002) and in some species the season of growth line formation has been seen to vary with latitude (Chauvaud et al., 2012; Cardoso et al., 2013; Lord & Whitlatch, 2014). Annual growth lines are characterized by dark lines which occasionally, especially in short-lived bivalves, can be easily discerned by the naked eye. To ensure reliable measurements and better distinguish annual growth lines from disturbance lines (caused e.g. by storms, food scarcity, fishing pressure) (Broom & Mason, 1978; Peharda, Ezgeta-Balić, Radman, et al., 2012; Witbaard, 1996; Leontarakis & Richardson, 2005), generally less prominent sections require to be cross-sectioned to analyze microgrowth bands (Richardson, 2001).

Shell growth rates vary through ontogeny and in response to several factors (e.g. Schöne et al., 2003). The environment (temperature, salinity, food availability and photoperiod), physiology (reproduction) and endogenous rhythms (tides) influence shell growth rates (Schöne et al., 2012). Most likely, an interaction of all these influences defines shell growth, and the precise effect of a single factor on

bivalve's growth is hard to quantify. Temperature has been recognized as the main driver of annual growth line formation (Jones et al., 1983; Bucci et al., 2009) which is dependent on species-specific temperature thresholds. Food availability and quality have also been reported to influence shell growth (Witbaard et al., 2001; Turekian et al., 1982). Furthermore, the reproductive cycle has also been associated with the growth line formation; as for instance in *Mercenaria* sp. (Castagna & Kraeuter, 1977), *Arctica islandica* (Jones, 1980) or *Phacosoma japonicum* (Reeve, 1850) (Sato, 1995). Accordingly, the timings of shell growth/cessation are sensitive to spatial variations (i.e. habitats) which may strongly increase or reduce shell biomineralization in a same species. Thus, studies on a single species in one habitat need to be interpreted with caution since they cannot be extrapolated.

To reveal microgrowth patterns shells are sectioned from the umbo to the shell margin along the axis of maximum growth, embedded in resin, and a series of grinding, polishing and etching is done prior to prepare acetate peel replicas of the shell (Richardson et al., 1979). Fluorescence spectroscopy is used as an alternative, with comparable results from acetate peel methods (Wanamaker et al., 2009). Sclerochemistry is used to combine shell growth patterns with geochemical analysis to use bivalve shells as paleoclimate recorders as high resolution environmental records. Stable isotopes (e.g. $\delta^{18}O$, $\delta^{13}C$) and trace element chemistry (Jacob et al., 2008) are used to unravel the environmental conditions in which shells were formed. The oxygen isotope is a proxy for temperature and a 1‰ change is considered to correspond to a temperature change of ~ 4.3°C (Grossman & Ku, 1986; Böhm et al., 2000). High $\delta^{18}O$ values correspond to low temperatures, whereas low $\delta^{18}O$ values to warmer periods. Some studies proved reliable increments of hourly to monthly resolved temperature, and bi-weekly to monthly $\delta^{18}O_{water}$ and salinity (Hallmann et al., 2008). Species-specific relationships between shell growth and temperature need to be fully understood to use them as temperature proxies. The carbon isotope ratio ($\delta^{13}C$) in carbonate shell materials is influenced by metabolic factors and by thermodynamic conditions (Fry et al., 1984; Kalish, 1991). Since metabolism is influenced by temperature and food supply, the effect of temperature on $\delta^{18}O$ is clearer than for $\delta^{13}C$. The analysis of stable isotopes has extensively been used to validate the seasonality in growth line deposition in other marine bivalves such as *Pinna nobilis* (Richardson et al., 2004), *Arctica islandica* (Schöne et al., 2004), *Panopea abrupta* (Conrad, 1849) (Goman et al., 2008), *Scrobicularia plana* (da Costa, 1778) (Santos et al., 2012), *Ensis directus* (Conrad, 1843) (Cardoso et al., 2013) or *Glycymeris bimaculata* (Bušelić et al., 2015) among others.

In the Adriatic Sea, the growth of some bivalves has been analyzed using the von Bertalanffy growth curve model (VBG). Overall, these studies have mainly focused on determining maximum longevities, growth rate estimates and timing of growth band formation but few included environmental or

biological variables in their analyses. Most of the studied bivalves are short-lived and the formation of annual growth rings varied among species. A longevity of over 16 years with a summer-autumn growth band (Peharda et al., 2002) has been estimated in *Arca noae*, which can extraordinarily grow up to the age of 25 years in non-exploited populations (Puljas et al., 2015). Growth bands were also formed during summer in the short-lived *Venus verrucosa* which reached 14 years of age (Peharda et al., 2013), *Acanthocardia tuberculata* (Linnaeus, 1758) which reached up to 11 years (Peharda et al., 2012) and *Modiolus barbatus* (Peharda et al., 2007) which reached 14 years of age. In *V. verrucosa*, growth band formation coincided with the timing of spawning and periods with minimum Chl *a* concentration. Alike, periods of fastest growth in *Mytilus galloprovincialis* were related to periods with higher concentration of Chl *a* (Peharda et al., 2007). The age of the oldest analyzed Mediterranean scallop *Pecten jacobaeus* (Linnaeus, 1758) was estimated at 13 years (Peharda et al., 2003). The short-lived *Ruditapes decussatus* formed annual growth bands in February during a period of slow growth and reached an age of up to 6 years (Jurić et al., 2012). Differences in growth rates between locations have evidenced a faster growth rate in Cetina than in Pag for *A. tuberculata* and *C. chione* (Peharda et al., 2012; Ezgeta-Balić et al., 2011). The combination of VBG and stable isotope analysis (δ^{18}O and δ^{13}C) was performed in the European date mussel *Lithophaga lithophaga* (Linnaeus, 1758), with an estimated longevity of 54 years, showing its potential as a geochemical sclerochronological archive (Peharda et al., 2015).

2.4.1. Shell growth in *Callista chione*

Age determination studies in *C. chione* by both external and internal rings have provided similar results during the early years of life (up to the age of 10 years). After this period, the growth rate decreased and the identification of rings close to the shell margin was unclear, especially when shells were damaged or presented other disturbance marks (Leontarakis et al., 2005). Therefore, acetate peel replicas have proven to be a good technique for age determination of this species (Leontarakis et al., 2005; Moura et al., 2009). *Callista chione* presents a predominantly aragonitic composition, although specimens collected in the Gulf of Trieste have shown a 10% of calcite (Keller et al., 2002). Daily or nearly daily growth increments have been observed in young shells (Hall et al., 1974). Specimens can attain a length of 90 mm and live for > 40 years in the Adriatic Sea (Ezgeta-Balić et al., 2011) and in the English Channel (Forster, 1981), although most common documented maximum ages are 16–17 years (Leontarakis et al., 2005; Moura et al., 2009; Metaxatos, 2004; Hall et al., 1974).

Environmental variables such as the influence of waves have proven to distress shell growth rate, showing lower rates and shorter longevity when measured at a wave-exposed site in comparison with a less wave-exposed one (Leontarakis et al., 2005). Up to date, just one study looked at the isotopic

composition (oxygen and carbon isotopes) from shell carbonates in *C. chione* (Keller et al., 2002) to age shells, estimating a 75 mm length individual to be 12 years old. These analyses also confirmed a fast deposition occurring during the first 5 years of life followed by a progressively marked decrease with increasing age (Keller et al., 2002; Ezgeta-Balić et al., 2011; Richardson, 2001; Moura et al., 2009). The deposition of growth lines during the summer months, coinciding with maximum peaks of temperature, has been agreed by several authors: from July up to October (Hall et al., 1974), during summer months (Keller et al., 2002) and from August until September (Ezgeta-Balić et al., 2011). The former related the shortest growth with the spawning time of the species (set in April), when temperature and food are optimum, speculating that growth deposition could be related to the beginning of oogenesis and spermatogenesis. In contrast, Moura et al., (2009) observed the deposition of growth lines between September and January coinciding with the slowest growth whereas the fastest growth took place during spring and summer. The latter study related the lower growth due to a mobilization of reserves for recovery of gonad stages, since gametogenesis in southwest Portugal occurred in November (Moura et al., 2008). In the eastern Adriatic Sea, several populations of *C. chione* were measured for age structure and growth rates, showing the fastest shell growth in the population from Cetina, which reached 70 mm at age of 7 years (Ezgeta-Balić et al., 2011). On the other hand, Kaštela and Pag Bays had lower growth rates, and these were similar to those reported in the southwest of Portugal (Moura et al., 2009).

2.4.2. Shell growth in *Glycymeris* sp.

Species of the *Glycymeris* genus have been recently used as high-resolution marine archives, reconstructing environmental conditions from modern *Glycymeris glycymeris*, *G. bimaculata* and *G. pilosa* (references below). Along with *Arctica islandica*, *G. glycymeris* is one of the most extended studied species for sclerochronology and so far its shells have been largely studied in the North Atlantic (Brocas et al., 2013; Reynolds et al., 2013; Royer et al., 2013; Ramsay et al., 2000). Due to the wide distribution of this genus, they arise as ideal candidates to provide uninterrupted records from decades up to several centuries, as seen for *G. glycymeris* (Schöne et al., 2013) from several settings. Growth increment widths have allowed the construction of dated chronologies from multidecadal to multicentennial time scales (Reynolds et al., 2013; Brocas et al., 2013). Annual growth lines in *G. glycymeris* from the North Atlantic are formed during winter, probably associated with minimum temperatures below the animal's threshold for growth (Royer et al., 2013; Berthou et al., 1986). In the Mediterranean Sea, the first robust master chronology was developed for *G. bimaculata* in Pag Bay (Bušelić et al., 2015). Annual growth lines were deposited at the beginning of spring and inter-annual

differences between growth increments were linked to variations in seawater temperature and salinity. The maximal longevity of analyzed shells in this study was over 60 years, indicating that growth rates are probably faster than its congeneric species *G. glycymeris* which can reach up to 200 years with a smaller size (Reynolds et al., 2013). Recently, *G. pilosa* was assessed as a potential environmental indicator in the Mediterranean, by studying a population from Pašman Channel (Peharda et al., 2016). The oldest analyzed shells were 69 years old and a master chronology spanned from 1969 to 2013. The relationship with environmental variables was somehow complex due to the highly variable conditions, common for shallow waters, but precipitation was positively correlated with growth, apparently indirectly associated with the supply of food to the bivalves (Peharda et al., 2016). The smallest of the glycymeridids in the Adriatic, *G. nummaria* was studied in Mali Ston Bay and a narrow growth line formation was observed after February (Peharda et al*.,* 2012). In this population, a short longevity of up to 20 years was estimated showing little potential for long term chronology construction. Although the longevity of *G. bimaculata* and *G. pilosa* is not comparable to that of *A. islandica* or *G. glycymeris*, they are good targets for sclerochronology and have a great potential to be used as key archives of high-resolution paleoceanographic variability in the Mediterranean and also in Atlantic areas. Since previous studies found differences in longevity of populations of *G. glycymeris* related to latitudinal gradients (Steingrimsson, 1989; Kaiser et al., 2000; Royer et al., 2013), further studies in other regions are highly recommended to corroborate this trend. Even ancient *Glycymeris* from Oligocene fossil records (*G. planicostalis*) have been analyzed, estimating shell growth to occur during winter and summer and an annual growth line deposition during late summer/early fall (Walliser et al., 2015). Overall, the timing and rate of shell growth can vary not only among congeneric species but also within a species (Jones & Quitmyer, 1996; Bušelić et al., 2015).

3. MATERIAL AND METHODS

3.1. Study area

The Adriatic Sea is considered a semi-enclosed sea within the Mediterranean basin, and it is considerably influenced by freshwater influxes derived from riverine and karstic flows characteristic for the eastern coast (Bonacci, 2015). Three sites located in the eastern part of the middle Adriatic Sea (Fig. 3.1, Table 3.1) were selected based on their different environmental settings and differences in bivalve growth recorded in earlier studies (Ezgeta-Balić et al., 2011). Pag Bay is located on the island of Pag with relatively well defined marine conditions, Cetina site (in Duće) is close to the mouth of the Cetina River and most likely influenced by fluvial inputs since its location on the direction of the river plume, and Pašman Channel is a marine exposed area with high current amplitudes (up to 10 cm/s) located in a traditionally important bivalve harvesting area. All locations are shallow coastal sites and samples were collected within a range of 1 to 5 m water depth. Previous studies on the distribution of benthic species (Peharda et al., 2010) identified these sites with sufficient population sizes for conducting a temporal collection based on monthly sampling, ensuring the collection of specimens throughout the study period.

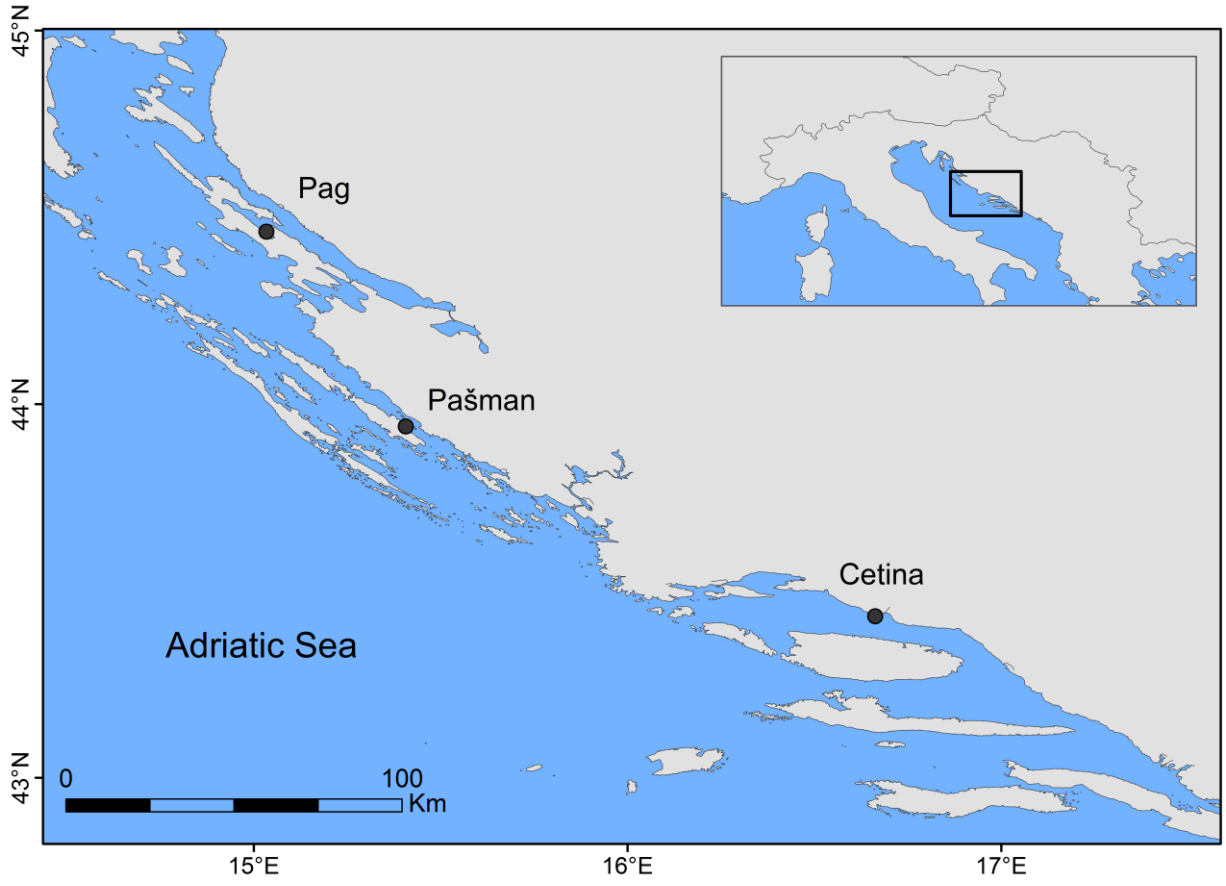

Figure 3.1. Location of study sites

Table 3.1. Geographic coordinates and description of study sites

	Pag	Cetina	Pašman
Location	44˚27'42'' N 15˚01'36''E	43˚26'13'' N 16˚41'14'' E	43˚56'49'' N 15˚23'18" E
Depth	3–6 m	2–4 m	1–3 m
Sediment type	gravelly sand	gravelly sand	gravelly sand

3.2. Environmental variables

3.2.1. Temperature, salinity and precipitation

Seawater temperature was measured hourly by data loggers (Tinytag, Gemini®) deployed at each location during the entire sampling period. Monthly salinity data was recorded *in situ* with an YSB probe. Monthly precipitation data for Pag, Cetina (Split) and Pašman (Biograd) meteorological stations were obtained from the Meteorological and Hydrological Service of the Republic of Croatia.

3.2.2. Characterization of water column and sediment

Seawater samples were collected ~0.5 m above the seafloor by SCUBA and skin diving using a Niskin bottle (between 10–20 L), transported in dark containers to keep the SPM from light and vacuum filtered in the laboratory. Prior to filtration water containers were gently agitated to homogenize seawater and filters were rinsed with distilled water. Pre-weighed nitrocellulose filters (Whatman™, 47 mm diameter, 0.45 µm mesh size) were used to measure bulk suspended particulate matter and biogenic silica content (BSi) while pre-combusted (450°C, 6 h) and pre-weighted glass fiber filters (Whatman™ GF/F, 25 mm diameter, 0.7 µm mesh size) were used to measure elemental composition and ratios of %C and %N, and their isotopic composition ($\delta^{13}C$ and $\delta^{15}N$; see 3.3.1), fatty acids and lipid concentrations (see 3.3.2). The concentration of SPM was determined on the dry mass of the total suspended particles retained per unit of volume after drying (60°C, 24 h) (expressed as mg/L). SPM filters were also used for BSi content analysis following a sequential alkaline digestion (2 to 5 h) with $NaCO_3$ to distinguish between biogenic and lithogenic silica sources (Mortlock & Froelich, 1989; DeMaster, 1991). Around 1 L of seawater per replicate was filtered for Chlorophyll *a* analyses through glass fiber filters which were folded, wrapped in aluminum foil, frozen and stored at -20°C. Chl *a* was extracted in 90% acetone (Strickland & Parsons, 1972) and measured in a Turner Systems (Sunnyvale, CA) Trilogy fluorometer. Triplicate samples were conducted for all chemical analysis. Additionally, satellite-derived Chl *a* data was extracted from the MODIS-Aqua Sensor provided by the EU Copernicus Marine Service (CMEMS).

Surface sediment samples (ca. upper 2 cm) (Sed) were collected monthly by SCUBA diving using a plastic core and preserved at -20°C. Homogenized and ground samples were used for %C, %N, BSi, SI (see 3.3.1) and FA (see 3.3.2) analyses, Chl *a* samples were extracted in 90% acetone (4°C, 12 h) (Lorenzen & Jeffrey, 1978), BSi content was measured following the procedure for SPM, and total carbon (TC) was measured in a LECO Truspec CN-2000 analyzer. Inorganic carbon (IC) (expressed in dry weight %) was calculated by the difference between TC and OC content. Grain size was determined in a HORIBA LA950V2 laser scattering particle size distribution analyzer after removal of organic matter in a 20% hydrogen peroxide solution (Table 3.2).

Table 3.2. Parameters measured in the different pools

	SPM	Sed	DG
Chl *a*	✓	✓	
BSi & total Si	✓	✓	
Granulometry		✓	
%OC, %N, $\delta^{13}C$, $\delta^{15}N$	✓	✓	✓
%IC		✓	
FA	✓	✓	✓
Lipids	✓	✓	✓

3.3. Feeding ecology

Bivalve shells were collected by SCUBA and skin diving. Ideally 20 living individuals per species were collected, measured for biometric analysis and processed within 3 hours by sectioning the muscle and dissecting the digestive gland (DG) from each individual. Digestive gland was chosen due to a fast isotopic turnover in this tissue reflecting recent signatures (days to weeks) (e.g. Ezgeta-Balić et al., 2012). Tissues from three specimens were pooled per each of three replicate samples. Each sample was stored at -20°C for subsequent analyses.

3.3.1. Isotopic analysis

Particulate organic carbon and nitrogen elemental and isotopic compositions were measured in SPM filters -dried at 50°C for 24 h-, 50 mg of Sed and 1 mg of DG. Sed and DG samples were freeze-dried and individually homogenized using an agate mortar and pestle. To remove carbonates, SPM filters and DG samples had a 6 h exposure to HCl fumes (Lorrain et al., 2003) while Sed samples were exposed to HCl fumes for 24 h (due to the high content of carbonates) prior to isotopic analyses. Further, to avoid effects of acidification in Sed (e.g. Walthert et al., 2010), non-acidified subsamples were used for the

analysis of $\delta^{15}N$. To eliminate residual HCl and water, all samples were ventilated overnight at room temperature and dried in a hotplate (50°C, 6 h). Filters were folded and placed into tin cups (12.5 mm x 5 mm) whereas Sed and DG samples were placed into tin cups wrapped by silver cups to avoid losses due to tin corrosion (8 mm x 5 mm). Stable isotope ratios of carbon ($^{13}C/^{12}C$) and nitrogen ($^{15}N/^{14}N$), and elemental %C and %N analyses were conducted on a Carlo Erba Elemental Analyzer EA1108 coupled to an isotope-ratio mass spectrometer ThermoFinnigan MAT253 in the Unidade de Técnicas Instrumentais de Investigación, University of A Coruña (Spain). Results are expressed in standard unit notation (VPDB for the carbon and atmospheric air for the nitrogen): δX = ([R sample / R standard] – 1) x 1000, where X represents ^{13}C or ^{15}N, and R is the ratio of $^{13}C/^{12}C$ or $^{15}N/^{14}N$, respectively. An acetanilide standard was used for the quantification of the amounts of %N and %C. Isotopic data are given in the conventional delta notation in units of parts per thousands (‰). Lipid content in tissues may affect $\delta^{13}C$ values, where high lipid concentrations result in depleted ^{13}C biasing the isotopic signal (DeNiro et al., 1978; Focken & Becker, 1998). However, previous studies in bivalves did not find this relationship (Lorrain et al., 2002; Ezgeta-Balić et al., 2014) therefore, lipid extraction was not conducted in the present study. A two-source isotopic mixing model was used in MixSIAR package, a graphical user interface (GUI) built on R software (Parnell et al., 2010), that uses an algorithm based on Bayesian statistics to determine the probability distributions for proportional food source contribution to the mix diet of consumers (Semmens et al., 2013). This model accounts for uncertainty in isotopic values when estimating the contribution of sources in the diet due to the incorporation of diet-tissue discrimination factors. Discrimination factors of 0.5±0.13‰ for $\delta^{13}C$ and 2.3±0.18‰ for $\delta^{15}N$ considered for benthic consumers (McCutchan et al., 2003; Alomar et al., 2015) were incorporated into the model. Despite the increasing number of studies for prey-predator fractionation values, there are no species-specific values for our target species; therefore, conventional fractionation values for benthic consumers can be applied as supported by Yokoyama et al., (2005). The Stable Isotope Bayesian Ellipses method in R (SIBER package) was used to investigate isotopic niches by examining the dispersion of $\delta^{13}C$ and $\delta^{15}N$ values.

3.3.2. Fatty acid analysis

SPM, Sed and DG samples were collected during one year period and freeze-dried prior to biochemical analyses. For total lipid analysis all samples were weighted (DG samples were blended) and later, a dichloromethane-methanol (DCM:MeOH) mixture (2:1) sonicated in a water bath at 30°C was added. After separation DCM phases were pooled and evaporated to dryness and weighed. Total lipids of digestive glands were re-dissolved in DCM and neutral lipids were separated according to Pernet et al., (2012). All extracts (total lipids of SPM and Sed and neutral lipids of DG) were saponified (1.2 M NaOH), acidified (6M HCl) and methylated (14% BF3 in methanol) then extracted in DCM. Fatty acid methyl

esters (FAMEs) were analyzed by Agilent gas–liquid chromatography (GLC) 6890 N GC System equipped with a 5973 Network Mass Selective Detector, capillary column (25 m x 0.3 mm x 0.25 µm; cross-linked 5% phenylmethylsiloxane) and ultra-high purity helium as the carrier gas. The GLC setting was programmed column temperature rise from 145°C by 4°C min^{-1} up to 270°C at a constant column pressure of 2.17 kPa. Retention times, peak areas and mass spectra were recorded with Chemstation software. Bacterial FAME standard mix, FAMEs mix C18-C20, polyunsaturated fatty acids standards (PUFA1 and PUFA3), cod liver oil and various individual pure standards of FAME were used.

FAs were reported as percentages of the total fatty acids (% TFA, mean ± SD) and grouped as saturated (SFA), monounsaturated (MUFA), PUFA, and detrital fatty acids (DETRITAL; 15:0+15iso+15anteiso+17:0+17iso+17anteiso+18:1(n-7); Najdek et al., 2002; Mayzaud et al., 1989). Unsaturation degree (UND) was calculated according to Pirini et al., (2007). The ratio of C16:1/C16:0 (> 1) and the relative dominance of C20:5 (n-3) (EPA) and C14:0 are considered as diatom indicators (Ackman et al., 1968; Kharlamenko et al., 1995; Léveillé et al., 1997) while the ratio of C22:6 (n-3)/C20:5 (n-3) (DHA/EPA) (>1.0), DHA, 16:0 and C16:1/C16:0 (< 1) are predominant in dinoflagellates (Dalsgaard et al., 2003; Budge et al., 1998). DHA, EPA and ARA (20:4 (n-6)) are considered Essential FA (EFA; Alkanani et al., 2007) and are transferred to microzooplankton (Ventrella et al., 2008). Herbivorous calanoid copepod markers are C20:1 and C22:1 (Falk-Petersen et al., 1987). A marker of carnivory indicator of zooplankton (Sargent et al., 1988) and detrital matter (Fahl et al., 1993) is C18:1(n-9).

3.4. Reproduction

Up to 40 standard-sized sexually mature individuals of target species per location were collected monthly by SCUBA and skin diving between June 2014 and October 2015 and transported alive to the laboratory.

3.4.1. Qualitative: Histological analysis of gonad tissue

Shell length (anterior-posterior axis), height (umbo-margin axis) and width (dorsal-ventral axis) were measured for each individual to the nearest 0.1 mm using Vernier calipers. Within three hours of collection, bivalves were sectioned, a piece of gonad tissue dissected, fixed in 4% formaldehyde and stored for later laboratory analysis. The tissue processing was conducted in the laboratory by dehydration in increasing concentrations of ethanol (70%, 80%, 96% and 100%) and clearing with a xylene substitute (Bioclear, Biognost). Following, the tissue samples were embedded in paraffin (Histowax, Leica), sectioned on a microtome at 5 µm and stained in hematoxylin and eosin. These histological sections were examined at 100x and 400x magnification using a Zeiss Axio Lab.A1 microscope, sexually identified and assigned to a descriptive gonad developmental stage. Stages were

adopted and modified from Valli et al., (1984) and Galimany et al., (2015), and described as early active (3), late development (4), ripe (5), spawning (2) and spent/inactive stage (1). Gonadal maturation stages were determined based on the size of gonadal acini, presence of interstitial tissue and density and prevailing stage of germ cells, and ranged from 1 to 5 for both sexes. When clams presented intermediate phases between two described stages, the one dominating the greatest part of the gonads was assigned. A detailed description of each stage is given in Table 3.3.

Table 3.3. Description of main developmental stages described for *Callista chione* (adopted from Valli et al., 1984).

Developmental stage	Females	Males
Early active	First recognizable stage of recovery after spawning. Oogonia and primary oocytes attached to the follicle walls. Follicles becoming larger and denser, connective tissue between them.	Spermatogonia and primary spermatocytes developing, partially lining the acini walls.
Late development	Secondary oocytes developing larger and thicker, still attached to the follicle wall. Starting formation of pedunculated oocytes. Follicles larger and closer together.	Spermatocytes and spermatids partially lining the acini walls. Starting to be radially arranged.
Ripe	Acini filled with pedunculated oocytes. Follicles are crowded with mature (free) oocytes. Follicle walls are very thin and connective tissue is reduced.	Spermatocytes and spermatids predominate. Follicles are packed with mature spermatozoa to periphery and organized into a rosette-like formation.
Spawning	Gonads retain differentiation. First signs of partial or total emission of gametes by evidence of empty zones. Areas with unspawned follicles and ripe oocytes. Increase presence of phagocytes. Scarce interfollicular connective and muscle tissues.	Majority of the follicles show signs of partial or total emission of gametes. Some spermatozoa arranged in spiral.
Spent/Inactive	Mature oocytes considerably shrunken in volume. High abundance of haemocytes attacking unspawned gametes for gonadial regression (lysis and resorption). Reorganization of follicles with broken acini walls; occasionally, the absence of gametes unables sex determination.	Some residual spermatozoa remain. Follicles collapsed with broken acini walls. High abundance of haemocytes for gonadial regression; occasionally, the absence of gametes unables sex determination.

A mean gonad index (MGI) was calculated separately for males and females by multiplying the number of individuals from each developmental stage by the numerical ranking assigned to that stage and dividing it by the total number of individuals in each sampling month (Gosling, 2003).

Histological analysis in *Callista chione* was performed on samples collected between July 2014 and July 2015. The collection of 20 individuals was not possible in each month and fewer individuals were collected in Pag in January 2015 (n=10), and in Cetina in November 2014 (n=15), December 2014 (n=10) and March 2015 (n=15). A total of 4 individuals from Pag and 3 individuals from Cetina were excluded from the stage determination due to artifacts with histological proceeding.

Glycymeris bimaculata samples were collected between July 2014 and August 2015. The collection of 20 individuals per month was performed at both Pag and Cetina. A total of 11 individuals were excluded from the stage determination in both Pag and Cetina due to artifacts with histological processing and infection.

Glycymeris pilosa samples were collected between September 2014 and August 2015 only at Pašman sampling site. This species was very rare at Pag and Cetina sampling sites, and Pašman was selected as a location with sufficient number of samples for this analysis. The collection of 20 individuals was not possible in each month and fewer individuals were collected in October 2014 (n=19), November 2014 (n=13) and December 2014 (n=19). A total of 21 individuals were excluded from the stage determination due to artifacts with histological processing and infection.

3.4.2. Quantitative: Gonadosomatic Index

Twenty monthly collected specimens were used to determine the gonad investment and to corroborate the main changes in the gametogenic cycle by following the seasonal changes in gonadal tissue between July 2014 and October 2015. After collection, samples were rapidly sorted out, stored at 5°C and processed within 24 h of collection. Analysis of GSI index of *Callista chione* was performed for samples collected from Pag and Cetina sampling sites. The collection of 20 individuals per month was not possible in Cetina in November 2014 (n=10) and May 2015 (n=19), and in Pag in January (n=15), September (n=7) and October (none) of 2015. A total of 591 individuals were processed for this analysis and 5 (0.85%) were discarded due to accidental handling. In *Glycymeris bimaculata* GSI index was performed in a total of 320 individuals only in Pag, due to smaller population of this species at Cetina sampling site.

Prior to dissection, morphometric measurements on each individual were taken for shell length, height and width to the nearest 0.1 mm with Vernier calipers and weighted, when dry, to the nearest 0.01 g. Bivalves were opened and gonads were carefully separated from the somatic tissue, and following, both

parts were placed in previously weighed porcelain dishes. Inorganic material, i.e. sand, was easily removable since it was accumulated in "sack-like" assemblages, thus, determination of just the dry mass was adequate. Samples were dried in an oven at 60°C for 48 h and weighed to get the estimated Somatic Mass Index (SMI) and Gonadal Mass Index (GMI). These indices were calculated as the dry weight of each part (soma and gonads) divided by the cubic shell dimensions expressed as mg/cm^3. To determine the relative investment in reproduction, the gonadosomatic index (GSI) was calculated as the gonadal dry mass (g) divided by the total body dry mass (g). Additionally, a Body Mass Index (BMI), determined as the sum of SMI and GMI, was used as a measure of body condition index. Complementary, the reproductive output was analyzed as the percentage of gametes released into the environment and fecundity as the differential in gonadal mass before and after spawning, an indication of the potential capability of an organism to produce reproductive units.

3.5. Growth

3.5.1. Micromilling on the shell surface of *Callista chione*

Shells of live collected young *Calllista chione* individuals from Pag and Cetina were analyzed for their shell microgrowth patterns using the surface micromilling method. Adult individuals of *C. chione* were not of use since they deposit shell material forming concentric lines, which added to the targeted short and narrow growth increments, would result in time-averaging and low sampling resolution. Three shells from each site were used for this analysis and based on shell lengths and shell microgrowth patterns investigated on the right valve they were all sexually mature. Analyzed shells from Pag were collected in June 2015, October 2015, and June 2016, respectively, while all analyzed shells from Cetina were collected in October 2015 and their age was identified by counting growth bands from shell cross-sections (Fig. 3.2). Shells from Pag had a length of 45.2 mm (AC1), 47.8 mm (AC2) and 36.4 mm (AC3) and shell lengths from Cetina were 53.9 mm (CC1), 52.7 mm (CC2) and 50.6 mm (CC3).

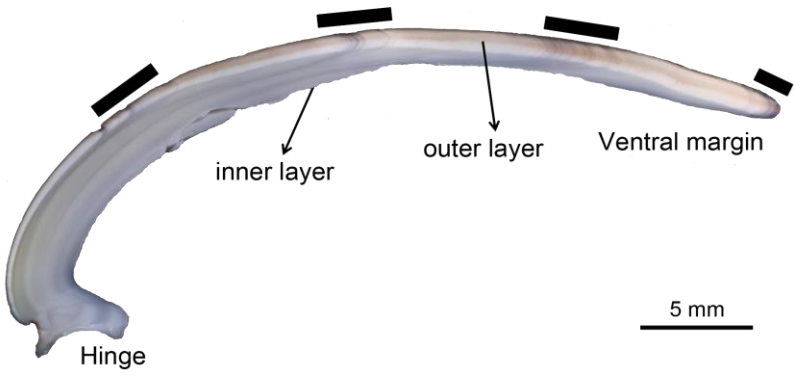

Figure 3.2. Cross-section of *Callista chione* CC2 specimen (length: 52.7 mm). Black rectangles indicate annually formed growth bands.

Shell powder (50 – 120 µg per sample) for isotope analysis was obtained by micromilling discrete and shallow sample swaths from the outer shell surface along the axis of maximum growth (Fig. 3.3), covering the last two years of life. Sampling was performed with a Dremel® Fortiflex drill equipped with a 0.3 mm cylindrical, diamond-coated bit (Komet/Gebr. Brasseler GmbH and Co. KG, model no. 835104010) which was coupled to a stereomicroscope equipped with reflective light (Olympus Europe Highlight 3100). Prior to sampling, the periostracum was physically removed. The distance between individual sample swaths was measured with the software ImageJ 1.48v. Each sample was then placed in temporal context (to the nearest month) as described in section 2.4.

Carbonate powder samples were reacted with 100% phosphoric acid in He-flushed borosilicate exetainers at 72°C. The liberated CO_2 gas was measured with a ThermoFisher MAT 253 gas source isotope ratio mass spectrometer in continuous flow mode coupled to a GasBench II. Analyses were conducted at the Institute of Geosciences of the University of Mainz. Stable oxygen and carbon isotope data are reported in δ-notation and given as parts per mil (‰) relative to the VPDB standard. To calibrate the samples, an in-house Carrara marble was used ($\delta^{18}O$ = -1.91 ‰; $\delta^{13}C$ = 2.01 ‰) that was calibrated against NBS-19. Internal precision (1σ) and accuracy (1σ) were better than 0.07 ‰ for both isotopes.

The majority of bivalves form shells in oxygen isotopic equilibrium with ambient water (Weidman & Jones, 1994; Marchitto et al., 2000). It is reasonable to assume that the same applies to the sampled aragonitic (tested with Feigl solution) shells. If so, the $\delta^{18}O_{shell}$ data can be used to compute ambient temperature during growth using the paleothermometry equation of Grossman and Ku (1986) (1) with a scale correction of -0.27 ‰ (Dettman et al. 1999). Accordingly, to enhance temperature reconstructions from $\delta^{18}O_{shell}$ values, $\delta^{18}O_{water}$ in seawater was measured. Salinity at the sample localities ranged from freshwater (derived from estuarine and underwater springs) to fully marine seawater. $\delta^{18}O_{water}$ measurements were also completed at the Institute of Geosciences of the University of Mainz using the equilibration method with CO_2. Exetainers were flushed with a mixture of 0.3 vol% CO_2 in helium and loaded with 0.5 ml of water sample. A total of 30 samples were collected between August 2014 and July 2015, at different sites within a ranging salinity gradient from freshwater to open seawater areas. Samples were equilibrated at 25°C for 24 hours. For calibration we used GISP2, SMOW2 and SLAP2 standards. Average internal precision was better than 0.1 ‰. $\delta^{18}O_{water}$ values were calculated against the Vienna Standard Mean Ocean Water (VSMOW). A salinity-isotope relationship (mixing line) was characterized from all these measurements allowing to estimate seawater properties during the sampling period to assign better $\delta^{18}O_{water}$ values. To determine the variability of temperatures on

seasonal to interannual time scales we applied the mixing line equation (2) developed for the studied Adriatic Sea region.

$T\delta^{18}O$ (°C) = 20.60 − 4.34 * ($\delta^{18}O_{shell}$ − ($\delta^{18}O_{water}$ −0.27)) (1)

$\delta^{18}O_{water}$ = 0.23 * salinity − 7.54 (2)

Monthly $\delta^{18}O_{water}$ values were then estimated using *in situ* measured monthly salinity values, and used to calculate monthly modeled $\delta^{18}O_{shell}$ values. The highest $\delta^{18}O_{shell}$ value was assumed to record the coldest period from the shell's growth whereas the lowest value was related to the warmest period, thus, data was arranged by using these extreme values as anchor points and aligned to the $\delta^{18}O_{shell}$ curve by adjusting the time axis. The temporal alignment allowed placing each $\delta^{18}O_{shell}$ value, that is, shell portion, in a calendar time. A $\delta^{18}O_{shell}$ derived-temperature curve was computed using equation 1 and data was re-arranged along the time axis to obtain the best fit with high resolution instrumental seawater temperatures.

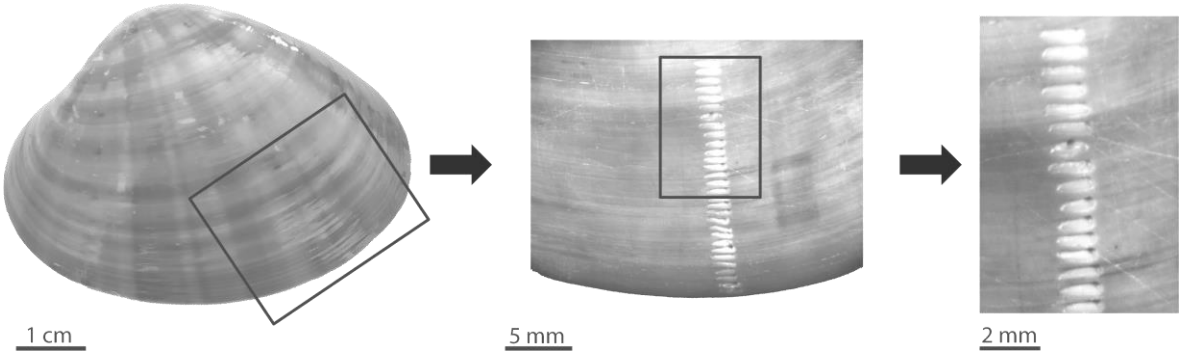

Figure 3.3. Illustration of the micromilled shell portion of the bivalve *Callista chione* (specimen CC2). Middle and rightmost figure show sample swaths.

3.5.2. Micromilling in the cross-sectioned valve of *Glycymeris bimaculata*

Shells from live collected individuals of *G. bimaculata* from Pag and Cetina were analyzed for their shell microgrowth patterns. Two adult shells from Pag (AB1 and AB3) and three adult shells from Cetina (CB1, CB2 and CB3) were used for this analysis. Shells from Pag had a length of 76.2 mm (AB1) and 84.4 mm (AB3) and shell lengths from Cetina were 66.4 mm (CB1), 75.0 mm (CB2) and 72.9 mm (CB3). All analyzed individuals were collected in October 2015.

One valve of each specimen was mounted on a Plexiglass cube with Epofix. A metal epoxy resin (WIKO Flüssigmetall) was used to embed the shells along the axis of maximum growth to avoid shell fracturing during cutting. Two 3 mm thin sections per specimen were cut perpendicular to the growth lines using a low-speed precision saw (Buehler Isomet 1000) equipped with a 0.4 mm thick diamond coated wafering

blade. Each thin section was mounted on glass slides with metal epoxy resin, ground on a series of wet silicon carbide papers (320, 800, 1200 grit), polished using 1 µm Al_2O_3 powder and ultrasonically rinsed in deionized water for few minutes. Micromilling was performed on one mounted thin section per specimen from the margin up to the last two years of growth. A Dremell® Fortiflex drill equipped with a 1 mm cylindrical, diamond-coated bit (Komet/Gebr. Brasseler GmbH and Co. KG, model no. H52104003) coupled to a stereomicroscope was used at the Geosciences Institute in Mainz University. Prior to analysis, the outer resin layer following the shell rim was carefully removed. Between 37–60 samples weighing between 50 and 120 µm each were continuously collected per individual after approximately covering the last 1.5 years of growth (Fig. 3.4). Analysis followed the same procedure as described in section 3.5.1.

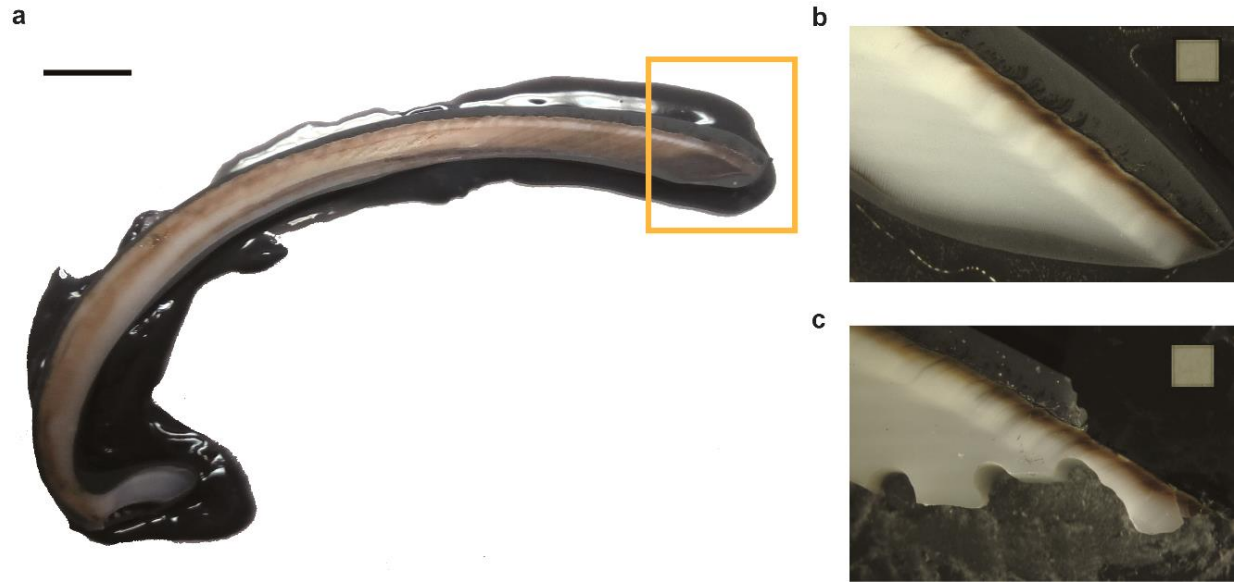

Figure 3.4. Resulting 3 mm thin section of *Glycymeris bimaculata* (**a**). Orange rectangle represents the ventral margin at which samples were collected. Detail of the shell margin before (**b**) and after (**c**) micromilling. Scales at 1 cm (a) and 1 mm (b,c).

The high-resolution $\delta^{18}O_{shell}$ values from cross-sections of *Glycymeris bimaculata* were fit following a polynomial function equation prior to the temporal alignment. The best fit minimizes differences between measured and modeled values. Following the same approach than in *C. chione*, high resolution instrumental seawater temperature were cross-dated to the $\delta^{18}O_{shell}$ derived-temperature curve, and these were re-arranged along the time axis to obtain the best fit.

The other thin section left from each specimen was used for their age determination. Following the previous mentioned steps (grinding and polishing) thin sections were immersed for ca. 20–40 min under constant stirring in Mutvei's solution (Schöne et al., 2005). The main component of this staining solution

is Alcian blue, which stains mucopolysaccharides and glucosamids. This treatment facilitates the ageing of specimens since it stains the carbonate material from the shell enhancing growth lines. Following staining, cross-sections were digitized with a Canon EOS 550D digital camera attached to a Wild Heerbrugg M8 stereomicroscope equipped with a double spotlight head illumination (Schott VisiLED MC 1000).

Since the period of growth line formation was hard to achieve based on adult specimens of *G. bimaculata*, two juvenile shells were sampled by surface drilling, aiming to place the approximate period of growth line formation. Shells were collected in Pag in April 2015 and had a length of 28.5 mm (AB68) and 28.6 mm (AB69). A 0.3 mm drill bit was used to collect samples through consecutive holes from margin inwards.

In addition, to get an estimate of metabolic carbon (C_M) incorporation inshell material, water samples were also measured during 4 months to get $\delta^{13}C_{DIC}$. Water samples were collected in the same glass vials and 200 µL of a $CuSO_4$ solution (stock solution 25.6 g $CuSO_4*5H_2O$ 100 mL^{-1}) were injected to inhibit biological activity following Taipale & Sonninen, (2009). Glass vials could not be Helium fluxed due to logistical constraints and caps were sealed with Parafilm. The mixing line equation from McConnaughey et al., (1997) and rewritten by Gillikin et al., (2009) was used:

$$C_M = \delta^{13}C_{shell} - \varepsilon_{shell\text{-}HCO3^-} - \delta^{13}C_{DIC})/(\delta^{13}C_M - \delta^{13}C_{DIC}) \quad (3)$$

Where $\varepsilon_{shell\text{-}HCO3^-}$ is the fractionation factor between aragonite and bicarbonate (2.7‰ according to Romanek et al., 1992) and $\delta^{13}C_M$ is that of metabolic carbon.

3.6. Statistical analysis

3.6.1. Environmental variables

Pearson correlation coefficients were used for testing relationships in temperature among each of the study sites.

3.6.2. Feeding ecology

3.6.2.1. Environmental variables

Two-way ANOVAs were used to test the effect of site (2 levels) and month (17 levels) in SPM, Chl *a*, BSi and lipids. A t-test was done for BSi in the sediment. Statistical assumptions for normality (Shapiro test) and homoscedasticity (Levene's test) were confirmed prior to all analyses.

3.6.2.2. Stable isotopes

Two-way ANOVAs were used to assess the effect of site and month on isotopic and C:N molar ratios in food sources and consumers. The isotopic niche overlap was tested with SIBER and SIAR packages in R (Jackson et al., 2011; Parnell et al., 2010). A Standard Ellipse Area (SEA), which is to bivariate data as SD is to univariate data, was applied to measure the isotopic niche width using Bayesian inference. SEAs are an alternative to Convex Hull methods since the ellipses are unbiased with respect to sample size and their estimation allows robust comparisons between data sets (Jackson et al., 2011). SEA values were corrected for small sample size (SEA_C) containing 95% of the data, and Bayesian estimates (SEA_B) were estimated as a measure to trophic width between species-sites. Analyses were performed in R v3.1.3 (R Core Team 2015).

3.6.2.3. Fatty acids

Analyses of similarities (ANOSIM) were performed in all detected FA profiles in SPM and Sed to determine resemblance among sampling periods and sites, and among consumer groups across sampling periods: PC-CC, PG-CG, PG-PC and CG-CC. This coding refers to *Callista chione* from Pag (PC) and Cetina (CC) and to *Glycymeris bimaculata* from Pag (PG) and Cetina (CG). All replicated data were used and log(x+1) transformed to improve normality prior to analysis. Results based on a global R statistic and p-value were reported. Non-metric multidimensional scaling (nMDS) and a Bray-Curtis similarity matrix were used to visualize the temporal compositional differences of all detected monthly mean FA profiles in each pool with respect to site. Similarity percentage analysis (SIMPER) and principal component analysis (PCA) were applied to identify the main contributors of dissimilarities in the FA profiles between sites in each pool. SIBER was also used to analyze feeding niche overlap using the *x* and *y* coordinates of the nMDS analysis of FA profiles of consumer groups following Antonio and Richoux (2014). SIBER analyses were performed using R v3.2.3 (Jackson et al., 2011; R Core Team, 2015) and multivariate analysis (ANOSIM, nMDS, SIMPER and PCA) using PAST 3.0 (Hammer et al., 2001).

3.6.3. Reproduction

For sex-ratio analysis, a chi-square test was applied considering an expected ratio of 1:1. The Levene's test was used to check for homogeneity of variances prior to any ANOVA or ANCOVA tests and normality of residuals was assessed by the Shapiro test. A Mann-Whitney test was applied to BMI and GSI data to test for differences between sites. A two-way ANOVA was performed to test for differences in between sex and shell length along the sampled period and also to test the seasonality between GSI and BMI between populations. These values were squared root transformed to obtain normality and used to test for these indices. To test for sex differences in MGI, the synchronicity between GSI and BMI, and the

influence of temperature on BMI and GSI, linear regression analysis using Pearson's correlation were done for each site. Differences in gonadal mass and GSI during months prior to spawning between sites were tested using a one-way ANCOVA controlling for shell length. All statistical analyses were carried out using Rv3.2.3 (R Core Team, 2015).

3.6.4. Growth

To quantitatively calculate shell accretion, shell growth rates were calculated in % based on one annual cycle. With increasing ontogenetic age, growth rate (and variance) decreases. To compare seasonal growth rates of years formed during different ontogenetic stage, such age-related growth trends need to be removed. This is accomplished by estimating the growth trend with an appropriate function (for example, a linear function) and removing the age trend from the growth increment time-series by dividing the observed increment width at each time interval by the predicted shell growth. The average of the resulting growth index chronology will equal 1. Oxygen data from surface micromilling of *Callista chione*, was combined with measured distances between each growth record from shell margin (described in 3.5.1).

Pearson correlations were calculated to observe relationships between $\delta^{13}C_{shell}$ and $\delta^{18}O_{shell}$ values. Furthermore, a set of environmental and biological variables, including temperature (T), salinity (S), body mass index (BMI), gonadosomatic index (GSI), precipitation (Prec), $\delta^{13}C_{SPM}$ ($\delta^{13}C$) and $C{:}N_{SPM}$ molar ratio (C:N) were compared (Pearson correlation) to monthly shell growth indices (GR). Statistics were calculated using R (R Core Team, 2015) and transformations were applied when needed.

4. RESULTS

4.1. Environmental variability

The mean monthly temperature values showed a clear seasonal trend at all sites with ranges from 8.9 to 25.1°C in Pag, 12.7 to 26.4°C in Cetina and 10.7 to 24.9°C in Pašman. All were highly correlated between each other ($r > 0.97$, $P < 0.001$). Minimum recorded temperatures were of 7.4, 10.9 and 6.1°C and maximum ones of 28.6, 28.6 and 28.3°C in Pag, Cetina and Pašman, respectively.

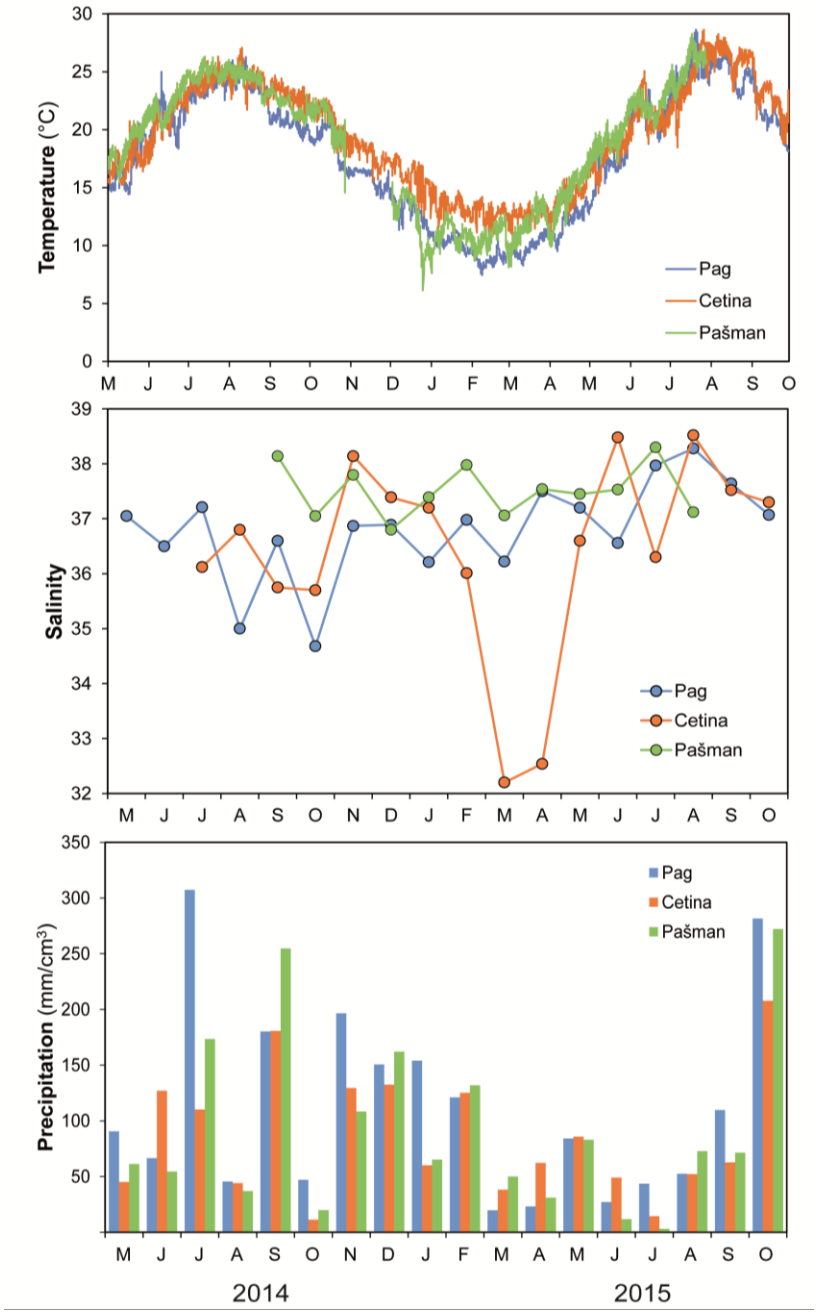

Figure 4.1. Seawater temperature from hourly measurements, monthly salinity values and monthly average precipitation values at three sampling sites.

Monthly salinity ranges oscillated from 34.7 to 38.3 in Pag, 32.2 to 38.5 in Cetina and 36.8 to 38.3 in Pašman. Precipitation was measured in mm/cm^3 and showed the highest monthly average in Pag with 111.1±86.0, followed by Pašman 92.4±78.3 and Cetina 85.4±55.5. The month with maximum precipitation in Pag was June 2014 whereas September 2014 recorded the most rain both in Cetina and Pašman. Overall, besides the unusual rain in July and September 2014 and October 2015, the period with higher precipitation was between November and February (Figure 4.1).

4.2. Feeding ecology

4.2.1. Trophic ecology of *Callista chione* and *Glycymeris bimaculata* from two populations: Pag and Cetina

4.2.1.1. Food sources: Environmental variables as food quality indicators

SPM concentrations had means of 1.02±0.33 mg/L in Pag and 0.92±0.35 mg/L in Cetina (Table S1) and didn't significantly differ ($P > 0.05$) between sites (Table S2). In Pag, monthly values ranged from 0.43 to 3.98 mg/L and highest values were observed in both summers with a small peak in March 2015, whereas in Cetina ranges were from 0.53 to 1.99 mg/L with two main peaks observed in February and June 2015. Temporal variation of Chl a_{SPM} were similar between sites ($P > 0.05$) ranging from 0.2 to 0.6 µg/L in Pag and 0.2 to 0.7 µg/L in Cetina (Tables S1, S2). In Pag, the maximum Chl a_{SPM} peaks were observed in October 2014 and in January, March and October 2015 whereas the lowest concentration of Chl a_{SPM} was observed in both summers. In Cetina, the highest concentration of Chl a_{SPM} was observed during winter and spring and major peaks were in October 2014 and in April and May 2015. Between June-September 2014 and June-August 2015, the low values of both Chl a_{SPM} and % of Chl *a* in SPM, suggested that this period was the poorest for Chl a_{SPM} availability in the water column (Fig. 4.2.1a, Table S1). A similar annual trend was supported from satellite Chl a_{SPM} extracted from the MODIS-Aqua sensor with overall low Chl a_{SPM} values in summer and fall and high values during spring and winter in the Eastern Adriatic Sea (Figure S1). Significant differences were observed in Chl a_{Sed} between sites ($p < 0.001$) with ranges from 0.4 to 5.0 µg/g in Pag and 1.1 to 11.8 µg/g in Cetina; the latter showed particular high values between November 2014 and March 2015. The annual patterns of Chl a_{SPM} and Chl a_{Sed} were significantly correlated in Cetina ($r = 0.49$, $P < 0.05$) but not in Pag ($r = 0.15$, $P > 0.05$), suggesting a more efficient pelagic-benthic coupling in Cetina.

The concentration of BSi_{SPM} showed a high temporal variability ranging from 0.03 to 0.2 mg/L in Pag and from 0.02 to 0.2 mg/L in Cetina and non-significant differences between sites (Tables S1, S2). Summer 2014 presented the highest values in BSi_{SPM} and no significant correlation was found between BSi_{SPM} and Chl a_{SPM} at any site (all at $r < 0.28$, $P > 0.05$) (Fig. 4.2.1).

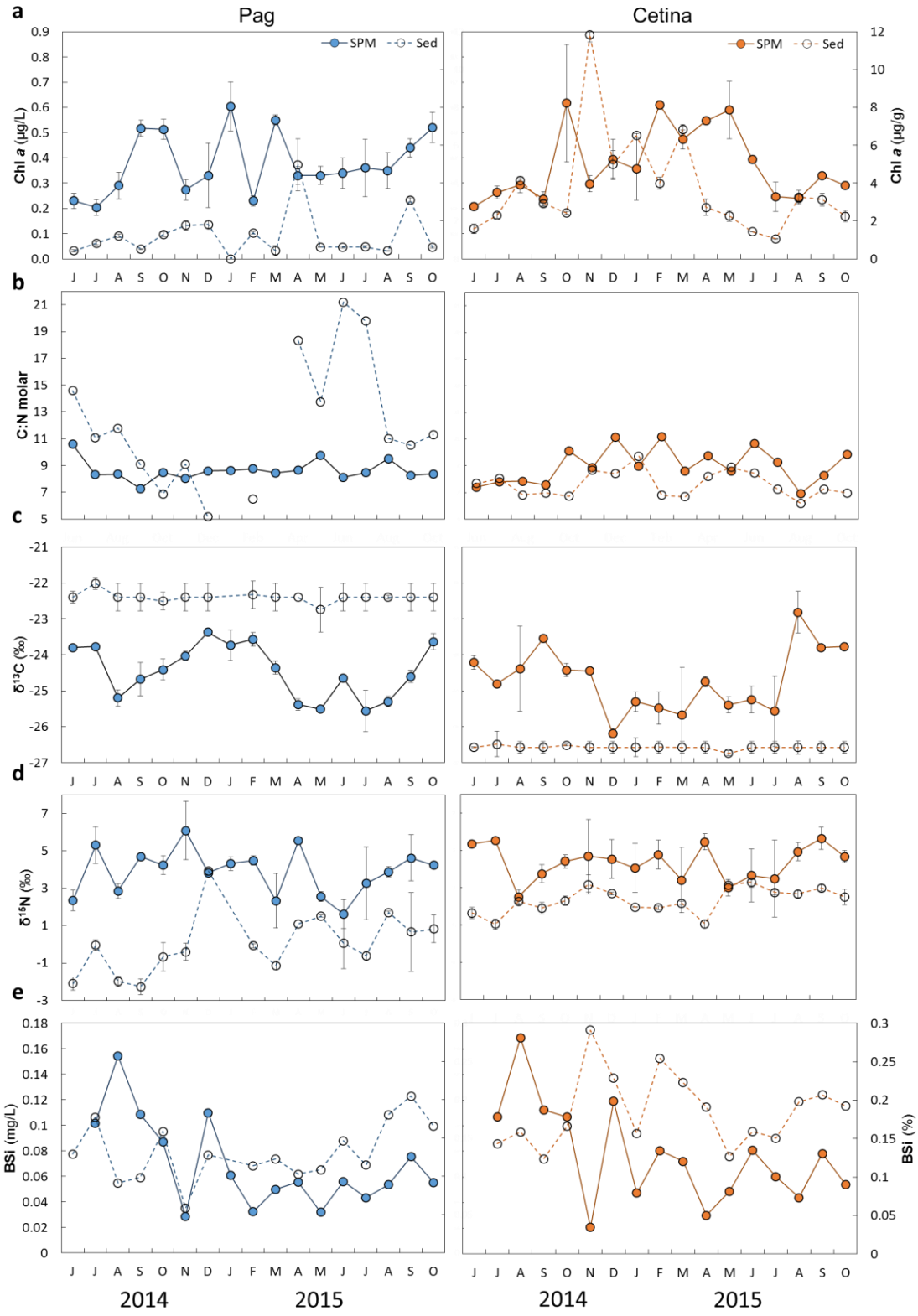

Figure 4.2.1. Temporal variations in (**a**) Chlorophyll *a* concentration (Chl *a*) (note different units in both vertical axis), (**b**) C:N molar ratio, (**c**) $\delta^{13}C$, (**d**) $\delta^{15}N$ and (**e**) biogenic silica (BSi) (note different units in both vertical axis) in suspended particulate organic matter (SPM) and sediment (Sed) at two sites Pag and Cetina. Error bars represent standard deviations.

The concentrations of BSi_{Sed} ranged from 0.06 to 0.2% in Pag and 0.1 to 0.3% in Cetina and showed significant differences between sites (t-test, $P < 0.05$). BSi_{SPM} and BSi_{Sed} were coupled during most of the study period (Fig. 4.2.1e). Sediment grain size was relatively constant with a high content of sand and gravel, and low content of silt and clay (fine sediment; < 63 µm), which accounted for < 2%. Sand (2 mm–63 µm) represented a higher portion in Cetina (87%) than in Pag (74%) whereas gravel (> 2 mm) was more abundant in Pag (26% vs 11%).

Stable isotopes. In water column samples the isotopic temporal variation ranged from -25.56 to -23.37‰ for $\delta^{13}C_{SPM}$ and 1.63 to 6.09‰ for $\delta^{15}N_{SPM}$ in Pag and from -26.19 and -22.82‰ for $\delta^{13}C_{SPM}$ and 0.03 to 5.64‰ for $\delta^{15}N_{SPM}$ in Cetina. Two-way ANOVAs indicated significant differences between month and the interaction with site in $\delta^{13}C_{SPM}$ (at $P < 0.001$) but not between sites ($P > 0.05$), whereas for $\delta^{15}N_{SPM}$ there were significant differences between sites, month and their interaction (all at $P < 0.001$; Table 4.2.1). More enriched isotopic values were observed during summer and fall at both sites. In the sediment, the isotopic temporal variation ranged from -22.74 to -22.0‰ for $\delta^{13}C_{Sed}$ and -2.26 to 3.92‰ for $\delta^{15}N_{Sed}$ in Pag, and from -26.74 to 26.48‰ for $\delta^{13}C_{Sed}$ and 1.05 to 3.30‰ for $\delta^{15}N_{Sed}$ in Cetina. There were significant differences in $\delta^{13}C_{Sed}$ between sites (at $P < 0.001$), whereas significant differences were neither found across months nor in their interaction with site ($P > 0.05$; Table 4.2.1). More depleted values in $\delta^{13}C_{Sed}$ than $\delta^{13}C_{SPM}$ were observed in Cetina whereas the contrary was observed in Pag. Significant differences in $\delta^{15}N_{Sed}$ (all at $P < 0.001$) evidenced the more depleted and variable values in Pag and more enriched and constant in Cetina (Fig. 4.2.1d). On the other hand, $\delta^{15}N_{SPM}$ showed more enriched values than in $\delta^{15}N_{Sed}$ at both sites.

The $C:N_{SPM}$ molar ratios did not significantly differ between sites ($P = 0.055$), with ranges from 7.3 to 10.6 in Pag and from 6.9 to 11.2 in Cetina; but temporal differences within site were significant (at $P < 0.001$), and Pag showed a lower annual mean (Table 4.2.1). There was no evident annual trend at any site (Fig. 4.2.1b). A significant correlation was shown between $C:N_{SPM}$ and SPM at both sites ($r = 0.50$, $P < 0.05$), which reflected the incorporation of degraded material into the water column. Also, a significant correlation between $C:N_{SPM}$ and Chl a_{SPM} in Cetina was found ($r = 0.60$, $P < 0.05$), which is illustrated with the coincidence of peaks in October 2014 and February and April-June 2015 (Fig. 4.2.1). BSi_{SPM} and $C:N_{SPM}$ were not significantly correlated at any site (all at $r < 0.47$, $P > 0.05$). In all cases, POC_{SPM}/Chl a_{SPM} values were > 200 (Table S1).

$C:N_{Sed}$ molar ratios in Pag varied from 5.2 to 21.2 whereas in Cetina it was from 6.2 to 9.7. In Pag, high values were recorded from spring to mid-summer. The range of $C:N_{Sed}$ values in Cetina was similar to that observed in $C:N_{SPM}$ (Fig. 4.2.1b, Table 4.2.1). Inorganic carbon varied from 10.7 to 12.1% in Pag and

from 7.6 to 11.6% in Cetina (Table S1). The values in Pag were closer to the weight % of C in the $CaCO_3$ molecule. Overall, more than 93% of TC was inorganic in both sites. Total N values ranged from 0–0.05% at both sites (Table S1).

Fatty acids. FA values > 0.01 (1% of total FA) are represented in Table S4 for SPM and Sed and in Table S5 for DG. All pools showed the higher proportions on saturated fatty acids (SFA) with higher TFA% during fall and in DG also during winter. The lowest SFA values were observed during the summer, when PUFA was more abundant.

Considering all FA_{SPM} (n = 33) and FA_{Sed} (n = 24), a two-way ANOSIM and nMDS showed significant differences between sites and month ($r > 0.99$, $P < 0.001$ and $r > 0.84$, $P < 0.001$, respectively) and nMDS revealed the large temporal spread of the data between sites, which was more evident in SPM than in Sed (Fig. 4.2.2a,b).

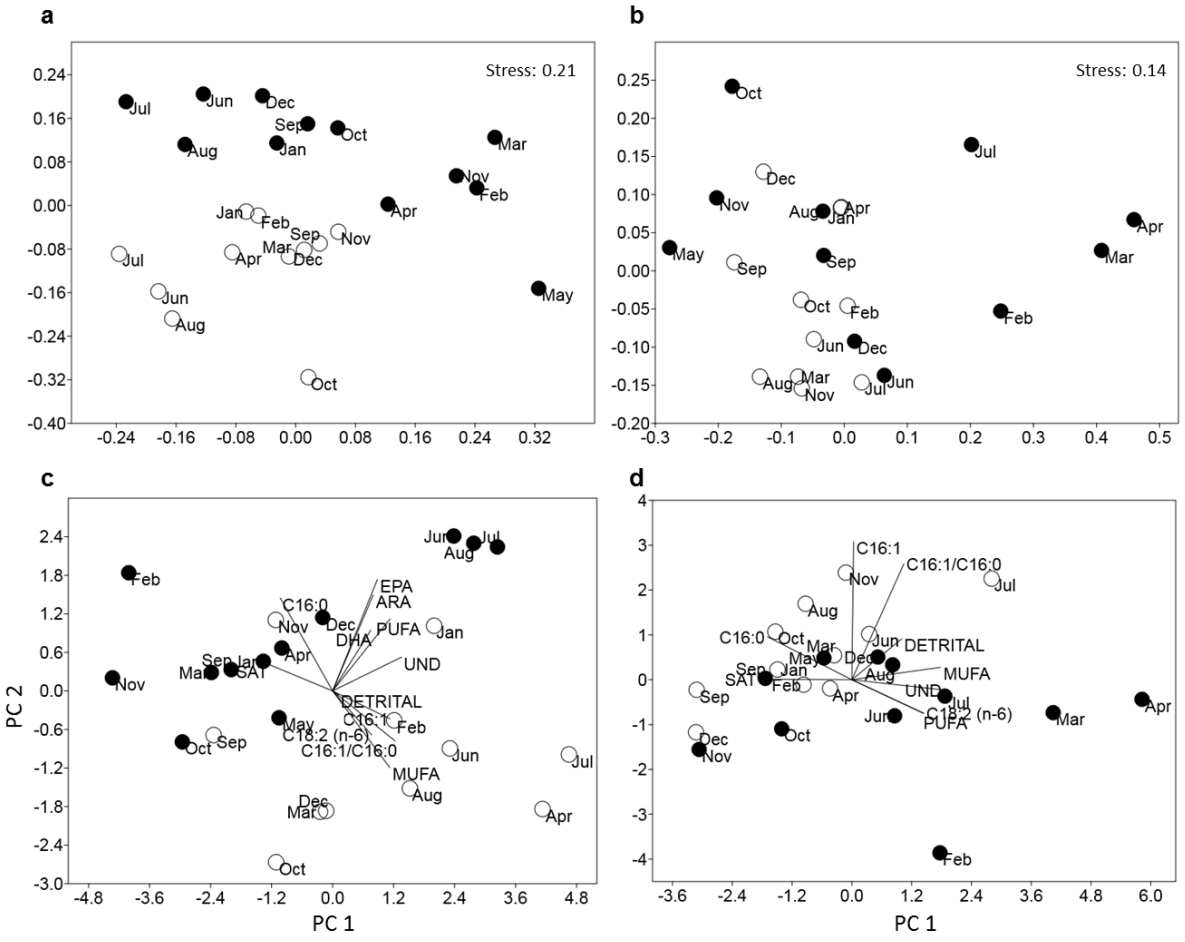

Figure 4.2.2. Above, non-metric multidimensional scaling (nMDS) of suspended particulate organic matter (SPM) (**a**) and sediment (Sed) (**b**) considering all FA profile means. Below, principal component analysis (PCA) output using most influential FA profiles in SPM (**c**) and Sed (**d**). Both sites are represented, Pag (filled) and Cetina (blank).

SIMPER revealed C16:1, C18:2 (n-6) and PUFA as the main contributors of dissimilarities in FA profiles between sites in SPM and Sed, with a cumulative contribution of nearly 50% in both pools (Table S6). PCAs revealed the temporal variations of the most contributing FA profiles in SPM and Sed, where PC1 explained 53% and 57% and PC2 18% and 20% of variance, respectively (Fig. 4.2.2). In FA_{SPM}, C16:1 showed much higher and constant values in Cetina; in Pag, comparable values were observed only in summer. Similarly, C18:2 (n-6) was higher in Cetina with comparable values in Pag only during fall. PUFA was the highest fraction during summer, particularly in Pag, and a subsequent peak during winter at both sites. Within PUFA, EPA and DHA were the largest contributors, with a higher abundance in Pag, particularly during summer. The contribution of MUFA and detrital was higher in Cetina (Fig. 4.2.2c; Table S4). Overall, the high values of PUFA and other indicators of fresh material (EFAs) in the summer and later in winter suggested that these are the periods of the highest food quality in the water column. Among FA_{Sed}, PUFA and MUFA were also higher in Pag, especially in summer and spring. The highest abundance in the sediment during summer coincided with the highest abundance in SPM, which was not the case during winter. Also, the FA_{Sed} contributing the most within PUFA was C18:2 (n-6), a marker of terrigenous input with higher abundance in Pag mostly during spring and summer. Within MUFA, C16:1 showed a higher predominance in Cetina. Detrital FAs were more abundant in Cetina, and overall, the lowest values were observed during fall (Fig. 4.2.2d; Table S4).

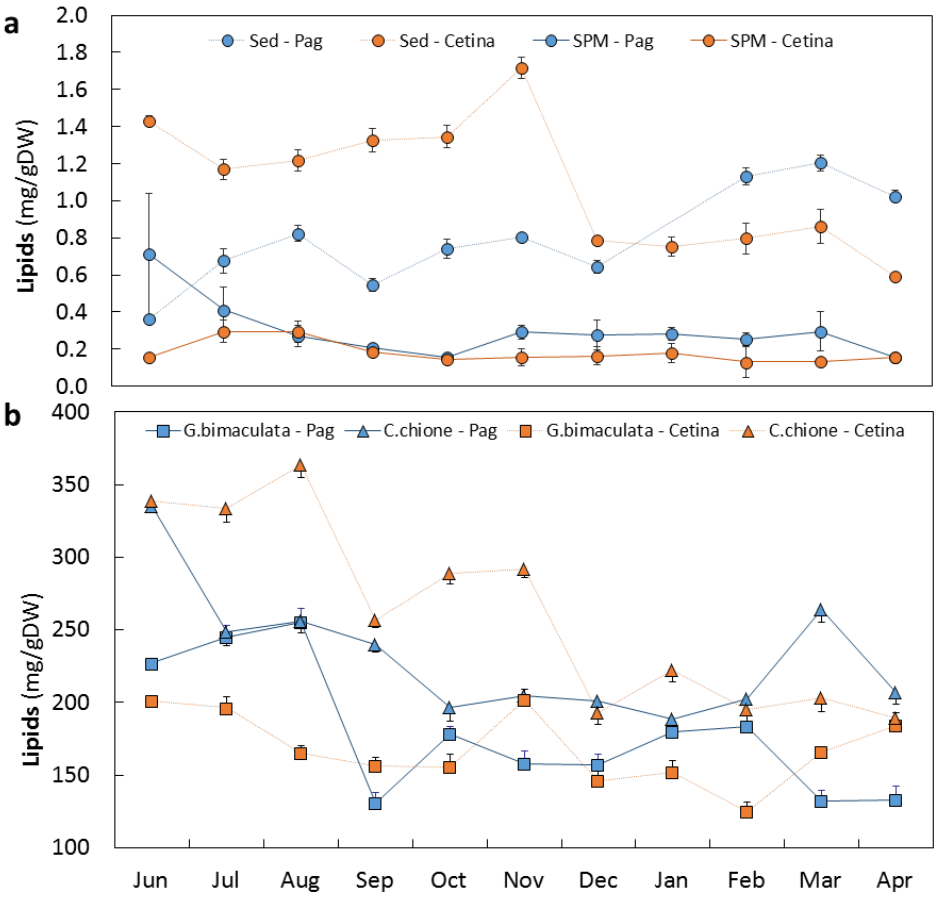

Figure 4.2.3. Temporal variation of lipid concentration in (**a**) sediment (Sed; dashed line) and suspended particulate organic matter (SPM; continuous line) and (**b**) *Glycymeris bimaculata* (*G. bimaculata*) and *Callista chione* (*C. chione*) at Pag (fill) and Cetina (blank).

The concentration of $lipids_{SPM}$ differed significantly between sites; however, it followed a similar temporal pattern ($P < 0.001$; Table S2) ranging from 0.16 to 0.71 mg/L in Pag and from 0.13 to 0.3 mg/L in Cetina (Fig. 4.2.3). At both sites, the lowest concentration of lipids took place between August and October (Fig. 4.2.3a). In $lipids_{Sed}$, values ranged from 0.36 to 1.20 mg/g in Pag and 0.59 to 1.72 mg/g in Cetina; the concentration was significantly higher in Cetina and there was an opposite temporal pattern between sites ($P < 0.001$; Table S2). $Lipids_{SPM}$ were one order of magnitude lower than $lipids_{Sed}$.

4.2.1.2. Consumers: *Glycymeris bimaculata* and *Callista chione*

Stable isotopes. The carbon isotopic signature in the digestive gland showed a temporal variation that ranged from -25.6 to -23.0‰ in Pag and -25.8 to -23.1‰ in Cetina in *C. chione*, and slightly more enriched $\delta^{13}C_{DG}$ in *G. bimaculata*, from -24.5 to -22.1‰ in Pag and -25.2 to -22.4‰ in Cetina (Fig. 4.2.4a). In *C. chione* the $\delta^{15}N_{DG}$ varied from 0.02 to 0.4‰ in Pag and 1.6 to 3.2‰ in Cetina and in *G. bimaculata* from 0.2 to 1.8‰ in Pag and 1.9 to 3.2‰ in Cetina (Fig. 4.2.4b). Two-way ANOVAs revealed significant differences in $\delta^{13}C_{DG}$ between sites, month and their interaction in both species (at $P < 0.001$) and also in $\delta^{15}N_{DG}$ except for temporal changes between sites for *C. chione* ($P > 0.05$) (Table 4.2.1). These results indicated that $\delta^{13}C_{DG}$ variation was species-dependent with slightly more ^{13}C-depleted values in *C. chione*. Contrarily, variation in $\delta^{15}N_{DG}$ was site-dependent, with more ^{15}N-enriched values in Cetina. A slight temporal offset between $\delta^{13}C_{SPM}$ and $\delta^{13}C_{DG}$ was observed, where the variation in $\delta^{13}C_{DG}$ followed that of $\delta^{13}C_{SPM}$ weeks later (Figs. 4.2.1c, 4.2.4a). Overall, enriched isotopic values were observed between June 2014 to January 2015 and July to October 2015 whereas a decrease towards more depleted values occurred from February to June 2015. The $C{:}N_{DG}$ molar ratio showed significant differences between site, month and their interaction for *C. chione* ($P < 0.001$) but they were less evident for *G. bimaculata* ($P > 0.001$) (Fig. 4.2.4c; Table 4.2.1).

	Consumer									Food source								
	Callista chione					*Glycymeris bimaculata*					SPM				Sed			
	df	SS	MS	*F*	p	df	SS	MS	*F*	p	df	SS	MS	*F*	p	df	SS	MS	*F*	p
δ^{13}C (‰)																				
site	1	6.48	6.48	40.97	< 0.001*	1	1.30	1.30	12.55	< 0.001*	1	0.65	0.65	3.70	0.058	1	179.88	179.88	2248.55	< 0.001*
month	16	37.57	2.35	14.86	< 0.001*	16	40.06	2.50	24.23	< 0.001*	17	54.53	3.21	18.33	< 0.001*	16	0.51	0.03	0.40	0.945
site*month	16	27.20	1.70	10.76	< 0.001*	16	6.02	0.38	3.64	< 0.001*	17	28.18	1.66	9.47	< 0.001*	15	0.17	0.01	0.14	0.999
Residuals	68	10.75	0.16			68	7.03	0.10			71	12.43	0.18			8	0.64	0.08		
δ^{15}N (‰)																				
site	1	49.01	49.01	1136.02	< 0.001*	1	54.12	54.12	2567.67	< 0.001*	1	9.42	9.42	10.70	< 0.001*	1	78.35	78.35	231.41	< 0.001*
month	16	17.67	1.11	25.61	< 0.001*	16	19.55	1.22	57.98	< 0.001*	17	101.56	5.97	6.79	< 0.001*	16	67.37	4.21	12.44	< 0.001*
site*month	16	1.08	0.07	1.56	0.105	16	1.38	0.09	4.09	< 0.001*	17	43.26	2.54	2.89	< 0.001*	15	39.62	2.64	7.80	< 0.001*
Residuals	68	2.93	0.04			68	1.43	0.02			71	62.51	0.88			34	11.51	0.34		
C:N molar																				
site	1	28.21	28.21	31.15	< 0.001*	1	2.81	2.81	9.22	0.003	1	2.28	2.28	3.80	0.055					
month	16	88.69	5.54	6.12	< 0.001*	16	33.90	2.12	6.94	< 0.001*	17	46.28	2.72	4.53	< 0.001*					
site*month	16	52.69	3.29	3.64	< 0.001*	16	8.39	0.52	1.72	0.064	17	68.10	4.01	6.67	< 0.001*					
Residuals	68	61.57	0.91			68	20.75	0.31			70	42.06	0.60							

Table 4.2.1. Two-way ANOVA results of the δ^{13}C (‰), δ^{15}N (‰) and C:N molar ratio in consumer's digestive gland (*Callista chione* and *Glycymeris bimaculata*) and food sources (suspended particulate matter [SPM] and sediment [Sed]).

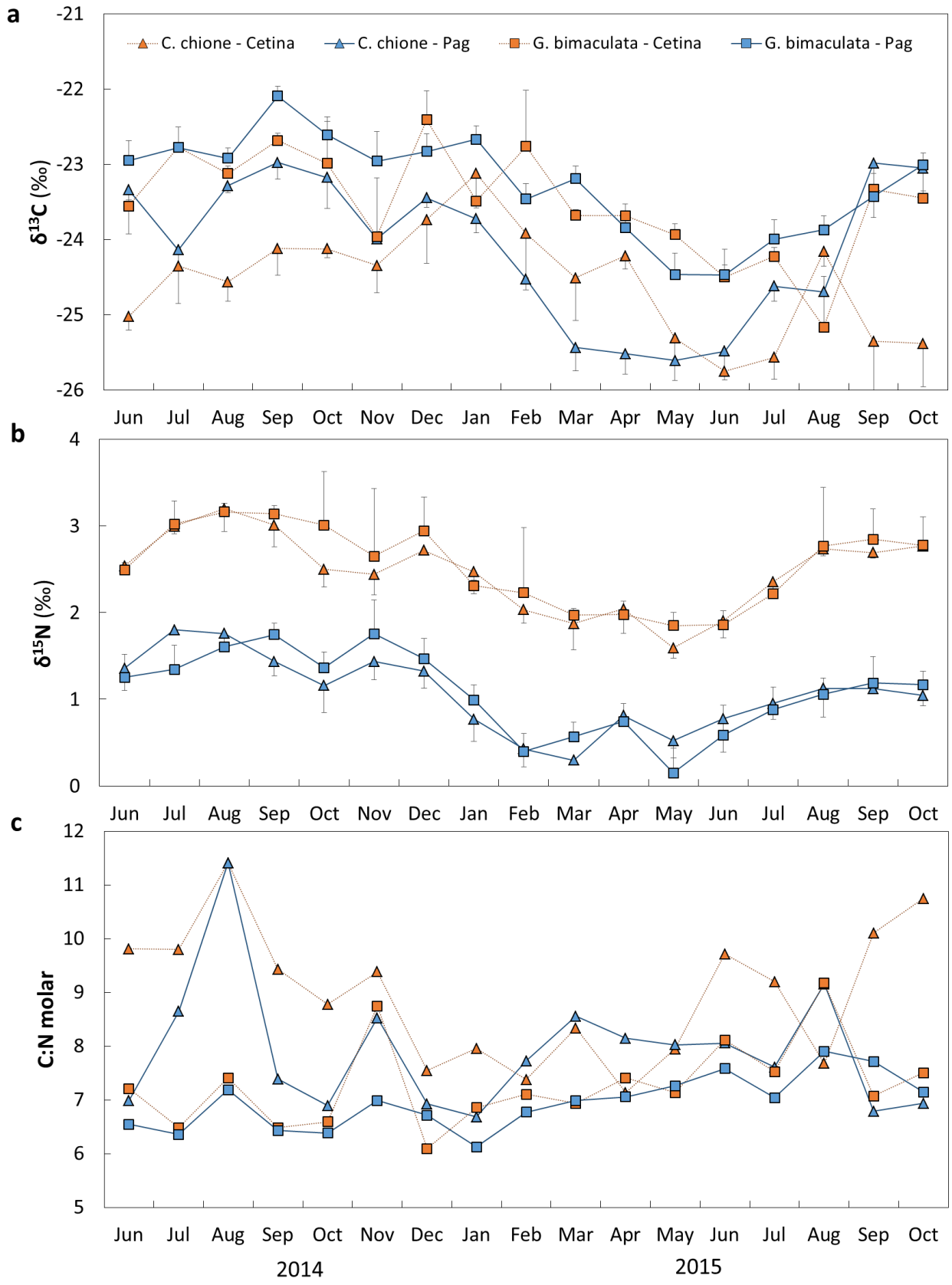

Figure 4.2.4. Temporal variation in (**a**) $\delta^{13}C$ (‰), (**b**) $\delta^{15}N$ (‰) and (**c**) C:N molar ratio in the consumer's digestive gland from both sites. *Callista chione* (*C. chione*) and *Glycymeris bimaculata* (*G. bimaculata*) from Pag and Cetina.

The proportion of each food source on the consumer diets estimated by MixSIAR models revealed that the sampled bivalves used both SPM and Sed, supported by a Gelman-Rubin diagnostic for each model <1.05 (values <1.2 for all model parameters are indicative that convergence between multiple Markov chains has been reached, therefore, fairly confident). However, the relative importance of each food source differed between sites. Sed as food source was more important for Pag populations and during summer there was a slight contribution of SPM, whereas in Cetina it was SPM that contributed the most to their diet. The highest contribution of Sed in Gly_{Cetina} was in August, whereas in $Call_{Cetina}$ it was precisely in the same period when it showed an evident decrease (Fig. 4.2.5). The temporal isotopic spreads of all pools within each population is illustrated as part of each model output corroborating previously described patterns (Fig. 4.2.6). The output from SIBER analysis revealed a large overlap from both convex hull and SEA, between species isotopic niche at each site, indicating an overall proximity in their feeding isotopic niche (Fig. 4.2.7a).

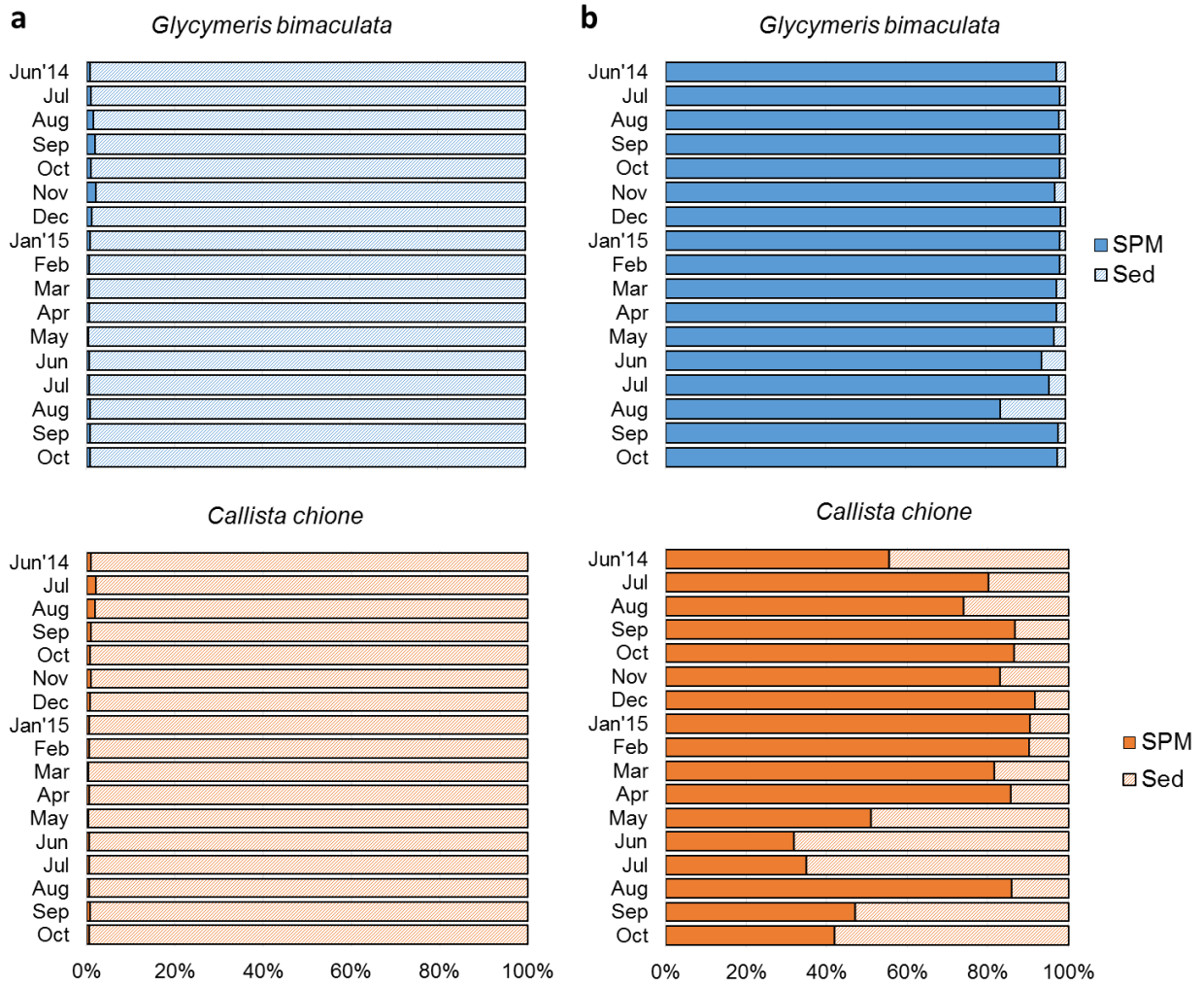

Figure 4.2.5. Contribution of food sources: suspended particulate organic matter (SPM) and sediment (Sed) to the diet of *Glycymeris bimaculata* and *Callista chione* at two sites: (**a**) Pag and (**b**) Cetina. Output from a two-source MixSIAR model for each population.

According to the above mentioned results, an isotopic feeding niche overlap occurred just in November and March, revealing different composition of food sources throughout the year. Individuals of Gly_{Pag} showed the smallest isotopic feeding niche with a completely SEA overlap and a substantial convex hull overlap. $Call_{Pag}$ had a wider niche, where the most enriched values overlapped with those from Gly_{Pag}. Based on SEA_B results, $Call_{Pag}$ and Gly_{Cetina} have a greater plasticity than the other species at these locations (Fig. 4.2.7c).

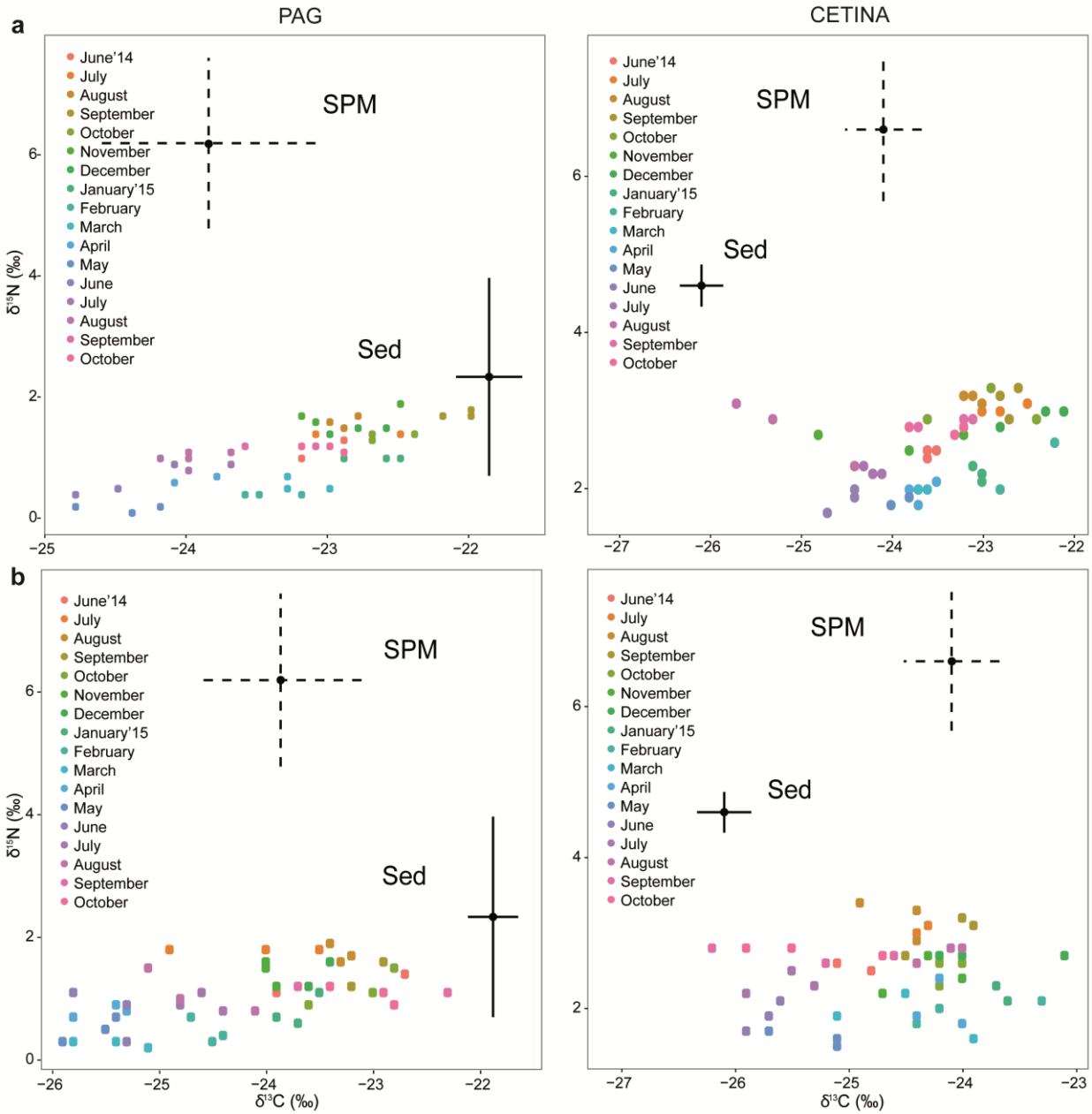

Figure 4.2.6. MixSIAR output on the contribution of each food source (suspended particulate matter [SPM] and sediment [Sed]) in each population of (**a**) *Glycymeris bimaculata* and (**b**) *Callista chione* along a temporal gradient (17 months).

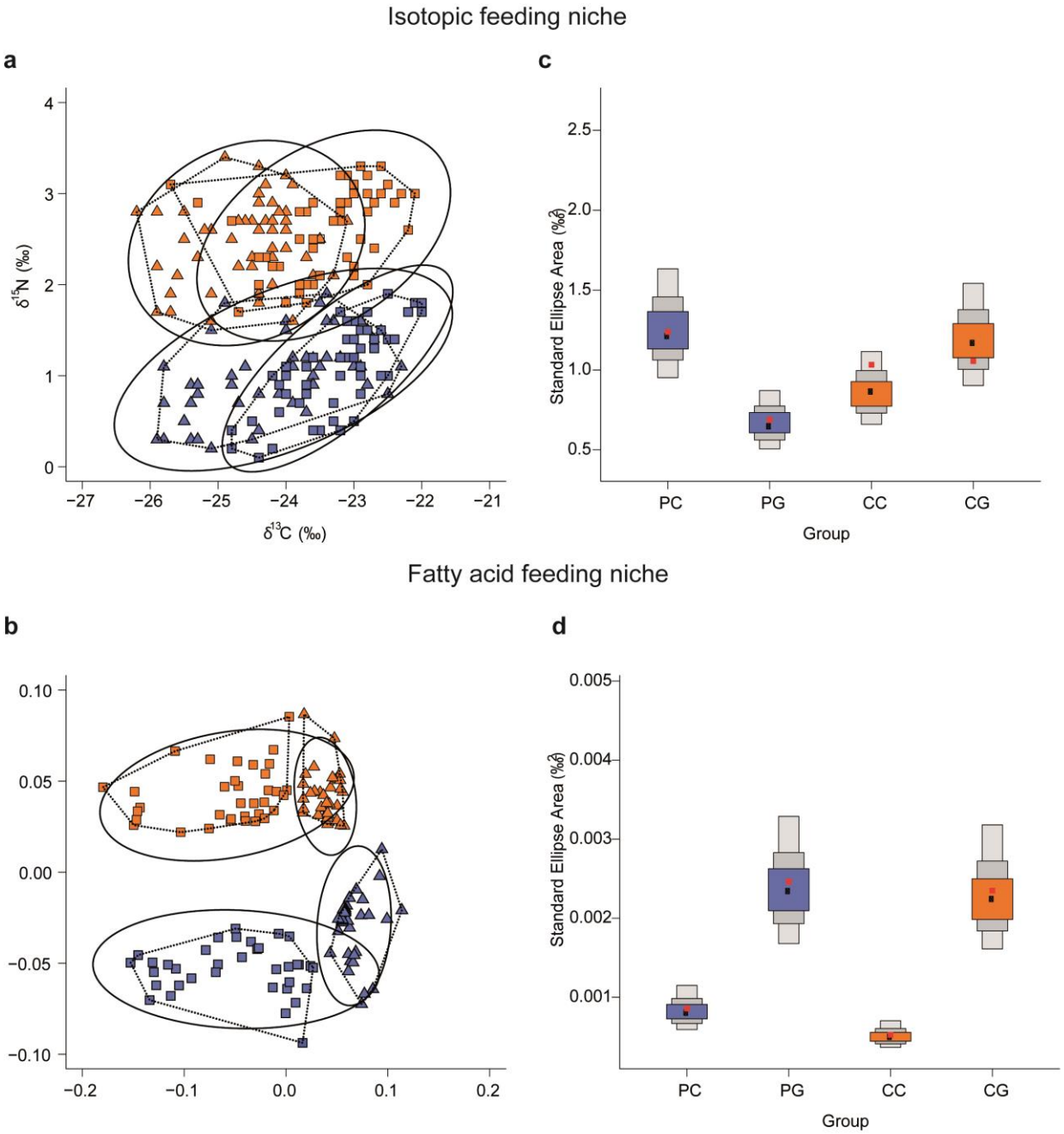

Figure 4.2.7. Isotopic (SI) and fatty acid (FA) feeding niche of two benthic suspension feeders at two sampling sites during 17 months. SIBER output using (**a**) pooled stable isotope bi-plot and (**b**) nMDS x-y ordinates of pooled FA profiles. *Glycymeris bimaculata* (squares) and *Callista chione* (triangles) in Pag (blue) and Cetina (orange). The continuous line represents the small sample size corrected standard ellipse areas (SEA_C) and the convex hulls areas are the dotted lines of calculated feeding niche widths for each species. Mean standard ellipse area (SEA) estimates for each group (PC= *Callista chione* from Pag; CC= *C. chione* from Cetina; PG= *Glycymeris bimaculata* from Pag (CG) and *G. bimaculata* form Cetina (CB) for SI (**c**) and FA (**d**). Boxed areas indicate the SEA_B with Bayesian 50, 75 and 95% credible interval with the mode indicated by black squares. The maximum likelihood estimate for the corresponding SEAc is indicated by red squares.

Fatty acids. Results for FA_{DG} derive from the same pooled individuals as for SI. Most predominant FA group were SFA (> 58 TFA%), followed by MUFA (> 23 TFA%) and PUFA (> 5 TFA%). ANOSIM revealed significant differences on all FA profiles (n = 38) among each group formed by species-site (r = 0.83, P < 0.001) and these were more evident between species than sites in the pairwise comparison (r = 1, P < 0.001, between species; r < 0.53, P < 0.001between sites). SIMPER analyses and PCA revealed the FA profiles that most contributed to temporal differences for each consumer group, with PC 1 explaining more than 77% and PC 2 between 5-11% (Table S7; Fig. 4.2.8). PUFA, C20:5 and C22:6 contributed to nearly 50% of the differences between each group.

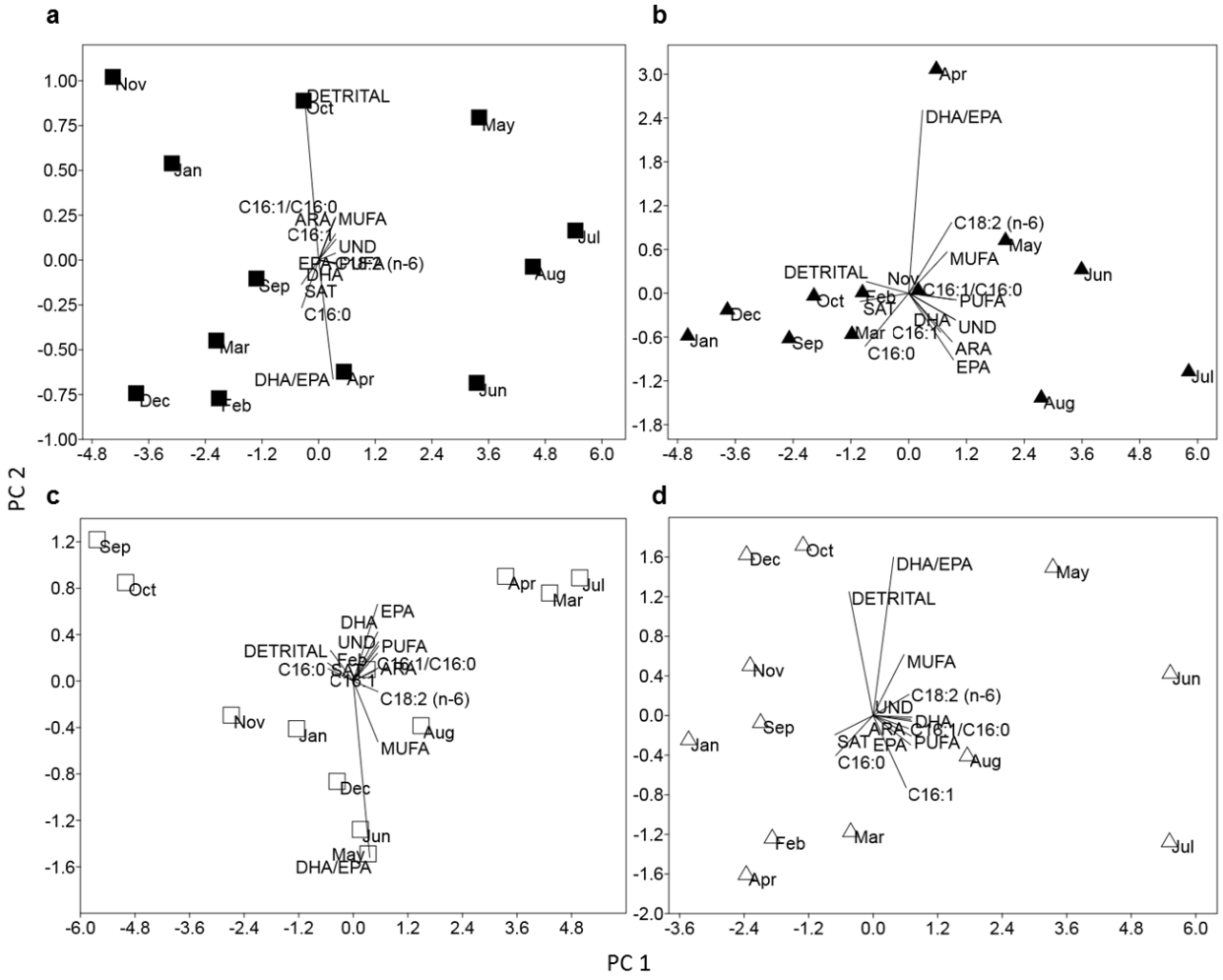

Figure 4.2.8. Principal component analysis (PCA) output using most influential fatty acid profiles in Pag for (**a**) *Glycymeris bimaculata* (**b**) *Callista chione* and Cetina for (**c**) *G. bimaculata* (**d**) *C. chione*.

In Pag, first PCA axis clearly separated spring and summer months from fall and winter. MUFA, PUFA, C18:2, EPA, DHA, UND and C16:1 were the highest during summer, particularly in $Call_{Pag}$. Detrital FA were more abundant during fall and winter, although present during all year (Fig. 4.2.8a,b; Table S5). In Cetina, a similar temporal trend was observed, and both species showed higher values of MUFA, PUFA,

C18:2, EPA, DHA and UND during summer and spring. Individuals of Gly_{Cetina} had similar concentrations in spring and summer, whereas in $Call_{Cetina}$ these concentrations were more evident (higher) in the summer. Detrital FA were slightly lower in spring-summer (Fig. 4.2.8c,d; Table S5).

MUFA values decreased after fall in Gly_{Pag} and after summer in Gly_{Cetina}, and they started to increase during winter-spring in the latter. Overall, summer was the season when the abundance of detrital was the lowest in contrast to fall and winter, whereas C18:2 (n-6) abounded the most during spring and summer. The herbivorous calanoid copepod markers (C20:1 and C22:1) were more abundant in spring and summer; oleic acid (C18:1) characteristic of zooplankton was more abundant in *C. chione*, and a diatom marker (C14:0) was more abundant in *G. bimaculata*. SIBER analysis of FA revealed a substantial overlap between SEA but not in the convex hulls from each consumer group (Fig. 4.2.7b). The FA feeding niche plot also showed that consumers were grouped by site and the highest niche plasticity corresponded to *G. bimaculata* at both sites (Fig. 4.2.7d).

The concentration of $lipids_{DG}$ ranged from 188.34 to 335.39 mg/g in $Call_{Pag}$, 189.59 to 363.90 mg/g in $Call_{Cetina}$, 130.53 to 255.36 mg/g in Gly_{Pag} and from 125.07 to 201.78 mg/g in Gly_{Cetina}. Overall, there was a decreasing trend from summer to spring (Fig. 4.2.3b).

4.2.2. Trophic ecology of *Glycymeris pilosa* from two populations: Pag and Pašman

4.2.2.1. Food sources: Environmental variables as food quality indicators

Mean SPM concentration was lower in Pašman (0.81±0.31 mg/L) than in Pag (1.02±0.33 mg/L) (Table 4.2.2) and significant differences between sites were found throughout the year (all at $P < 0.001$) (Table 4.2.3). In Pašman, monthly values ranged from 0.44 to 1.45 mg/L and the highest value was associated with a high resuspension event observed in the area in November 2014. SPM values were the lowest in spring while increasing values were recorded in summer as also observed in Pag sampling site. Chl a_{SPM} values were significantly similar between sites ($P > 0.05$) ranging from 0.2 to 0.7 µg/L in Pašman and 0.2 to 0.6 µg/L in Pag (Tables 4.2.2, 4.2.3). The maximum Chl a_{SPM} peaks were observed in November 2014 and August 2015 whereas the lowest concentration of Chl a_{SPM} was observed in March 2015, opposite to Pag. Significant differences were observed through time and with the interaction with site (all at $P < 0.001$). All Chl a_{SPM} concentration values coincided with the % of Chl a_{SPM} in SPM except those shown in November 2014 which showed contrasting values, as a result of the high resuspension event previously mentioned in the area (Fig. 4.2.9a, Table 4.2.2).

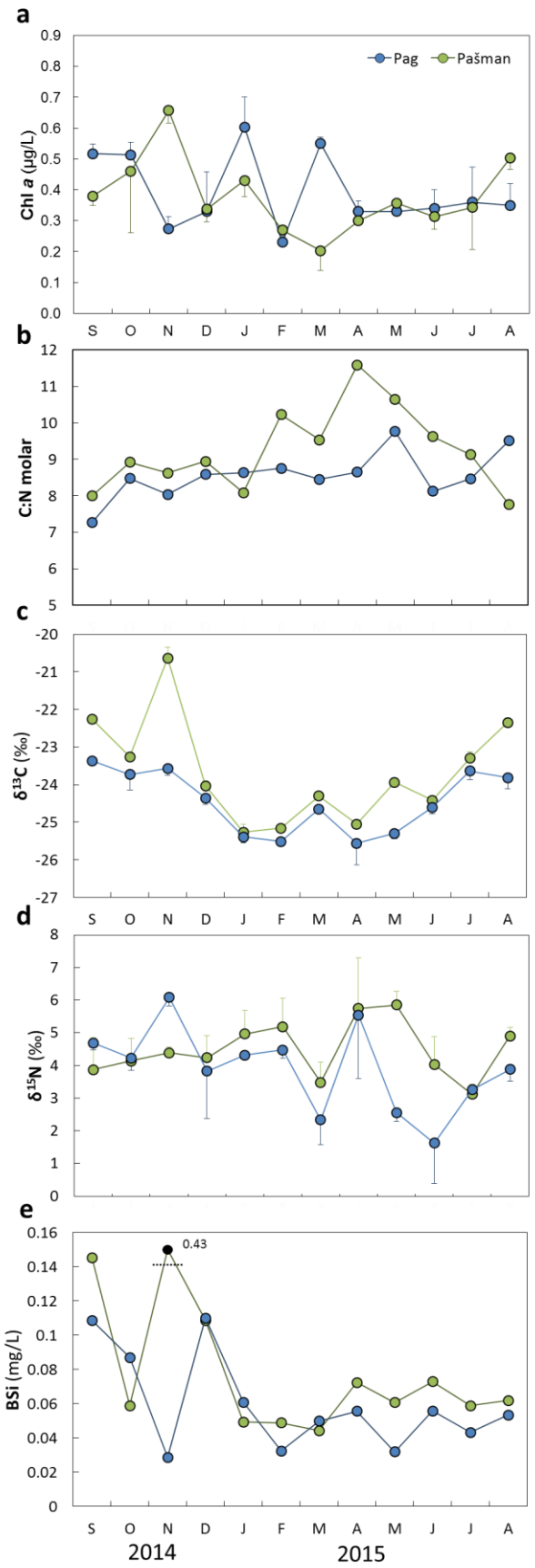

Figure 4.2.9. Temporal variations in (**a**) Chlorophyll *a* concentration (Chl *a*), (**b**) C:N molar ratio, (**c**) $\delta^{13}C$, (**d**) $\delta^{15}N$ and (**e**) biogenic silica (BSi) in suspended particulate organic matter at two sites Pag and Pašman. Error bars represent standard deviations.

The concentration of BSi_{SPM} also showed a high temporal variability in Pašman ranging from 0.04 to 0.44 mg/L (that of November 2014) (Fig. 4.2.9e). It is interesting to note, that the second highest value was only 0.15 mg/L, which is closer to values observed in Pag (0.02 to 0.2 mg/L). Statistical analysis confirmed that there were no significant differences between sites, time and their interaction (all at $P < 0.001$) (Tables 4.2.2, 4.3.3). September 2014 and later summer 2015 presented the highest values in BSi_{SPM} and a significant positive correlation was found between BSi_{SPM} and Chl a_{SPM} (at $r < 0.72$, $P < 0.05$). Sediment grain size was constituted of 83% sand, 13% gravel and a 4% of silt and clay (fine sediment).

The concentration of lipids in SPM showed overall higher values in Pag, ranging from 0.16 to 0.29 mg/g, than in Pašman, which varied from 0.12 to 0.38 mg/g. Again, the relatively higher values in November are likely associated with resuspension. If this month is excluded, average values in Pašman were 0.14±0.02, which were clearly lower than those in Pag, 0.23±0.02 (Fig. 4.2.10).

Table 4.2.2. Descriptive table of environmental and biochemical parameters in suspended particulate matter (SPM) in Pašman (mean ± SD). Abbreviations: Temperature (T; °C), Salinity, Suspended particulate matter concentrations (SPM; mg/L), Chlorophyll *a* (Chl *a*; µg/L), Chl *a* fraction within SPM (Chl *a*/SPM; %), Biogenic silica (BSi; mg/L), BSi fraction within SPM (BSi/SPM; %), Particulate organic carbon and Chl *a* ratio (POC/Chl *a*).

				SPM					
Season	**Month**	**T (°C)**	**Salinity**	**SPM (mg/L)**	**Chl *a* (µg/L)**	**Chl *a*/SPM (%)**	**BSi (mg/L)**	**Bsi/SPM (%)**	**POC/Chl *a***
	Sep	22.46	38.14	1.4±0.2	0.4±0.0	0.028	0.15±0.0	10.72	395.55
Fall	Oct	21.11	37.05	0.8±0.3	0.5±0.2	0.057	0.06±0.0	7.28	456.34
	Nov	19.00	37.80	8.3±1.6	0.7±0.0	0.008	0.44±0.1	5.26	475.98
	Dec	13.23	36.80	0.7±0.2	0.3±0.0	0.050	0.11±0.0	15.42	504.07
Winter	Jan	10.69	37.39	0.7±0.2	0.4±0.1	0.059	0.05±0.0	6.75	295.21
	Feb	10.73	37.98	0.4±0.1	0.3±0.0	0.062	0.05±0.0	11.17	459.97
	Mar	11.58	37.06	0.6±0.3	0.2±0.1	0.019	0.04±0.0	7.76	549.13
Spring	Apr	13.76	37.54	0.5±0.2	0.3±0.0	0.070	0.07±0.0	13.31	525.39
	May	18.43	37.45	0.6±0.2	0.4±0.0	0.063	0.06±0.0	10.46	744.62
	Jun	21.77	37.53	0.7±0.1	0.3±0.0	0.027	0.07±0.0	9.95	662.05
Summer	Jul	24.88	38.30	1.0±0.1	0.3±0.1	0.036	0.06±0.0	6.00	538.08
	Aug	26.40	37.12	0.8±0.1	0.5±0.0	0.070	0.06±0.0	7.59	349.51

Table 4.2.3. Two-way ANOVA results of environmental parameters in Pašman. Suspended particulate matter (SPM) in mg/L, Chlorophyll *a* (Chl *a*) in µg/L and Biogenic silica (BSi) in mg/L. Probabilities are expressed as: ** P < 0.001.

Two-way ANOVA					
	df	**SS**	**MS**	***F***	**P**
SPM (mg/L)					
site	1	7.00	7.00	44.51	< 0.001**
month	11	81.13	7.38	46.88	< 0.001**
site*month	11	78.13	7.10	45.15	< 0.001**
Residuals	48	7.55	0.16		
Chl *a* (µg/L)					
site	1	0.00	0.00	0.82	0.371
month	11	0.43	0.04	6.82	< 0.001**
site*month	11	0.53	0.05	8.32	< 0.001**
Residuals	47	0.27	0.01		
BSi (mg/L)					
site	1	0.03	0.03	65.06	< 0.001**
month	11	0.20	0.02	36.77	< 0.001**
site*month	11	0.22	0.02	42.05	< 0.001**
Residuals	48	0.02	0.00		

The **isotopic** temporal variation in SPM ranged from -25.26 to -20.63‰ for $\delta^{13}C_{SPM}$ and 3.12 to 5.86‰ for $\delta^{15}N_{SPM}$ in Pašman. These values were more enriched in both isotopes than in Pag, although when discarding $\delta^{13}C$ from November 2014, the most enriched value was -22.26‰. Two-way ANOVAs indicated significant differences between site, month and their interaction in $\delta^{13}C_{SPM}$ (all at $P < 0.001$) and $\delta^{15}N_{SPM}$ (all at $P < 0.05$) (Table 4.2.4). The isotopic cycle was quite synchronous between sites, and more ^{13}C-enriched values were observed during summer and fall at both sites. A pattern was less clear for $\delta^{15}N_{SPM}$ which showed decreasing values during summer 2015. Lopez et al. (1995) in Ryan et al. (1990)

Although $C:N_{SPM}$ molar ratios followed a similar pattern during fall and winter, they significantly differed between sites ($P < 0.001$), with ranges from 7.7 to 11.6 in Pašman, higher than those observed in Pag (from 7.3 to 10.6) (Table 4.2.4). A pattern was shown in Pašman with increasing values in late winter/spring followed by a steady decrease towards the summer (Fig. 4.2.9b), unlike in Pag. Also, non-significant correlations were found neither between $C:N_{SPM}$ and Chl a_{SPM} ($r = 0.55$, $P > 0.05$) nor $C:N_{SPM}$ and BSi_{SPM} ($r = 0.24$, $P > 0.05$), as had also been shown in Pag. As in Pag, POC_{SPM}/Chl a_{SPM} values in Pašman were > 200, indicating a predominance of heterotrophic/mixotrophic organisms, or detrital carbon (Table 4.2.2).

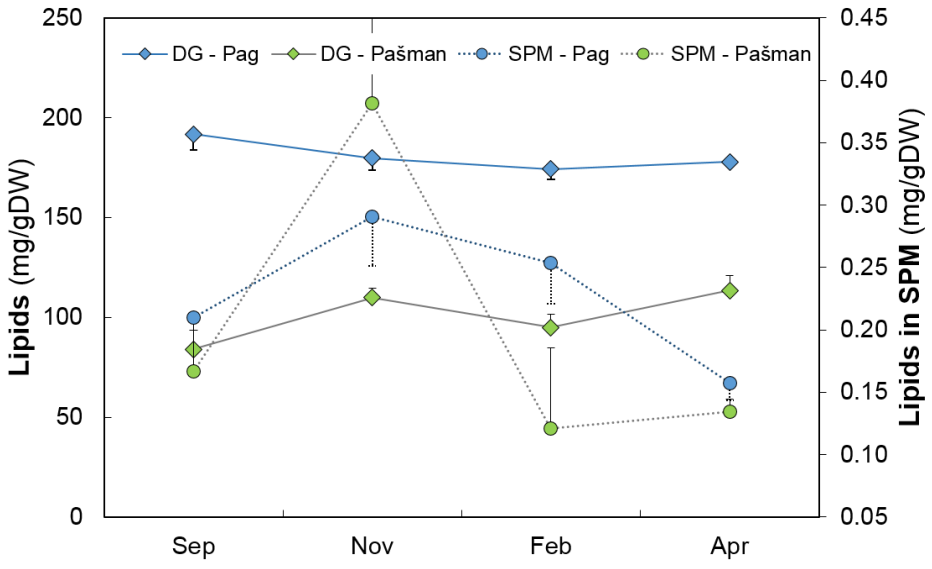

Figure 4.2.10. Seasonal variation of lipid concentration in the digestive gland of *Glycymeris pilosa* (DG; continuous line) and in suspended particulate matter (SPM; dashed line) at Pašman (green) and Pag (blue).

4.2.2.2. Consumer: *Glycymeris pilosa*

The carbon isotopic signature in DG showed a temporal variation that ranged from -22.5 to -19.7‰ in Pašman and -25.2 to -22.8‰ in Pag (Fig. 4.2.11a). The $\delta^{15}N_{DG}$ varied from 3.5 to 4.7‰ in Pašman and 0.3 to 1.4‰ in Pag for the same period (Fig. 4.2.11b). Two-way ANOVAs revealed significant differences in $\delta^{13}C_{DG}$ and $\delta^{15}N_{DG}$ between sites and month (all at $P < 0.001$) and also their interaction (at $P < 0.05$) at both sites (Table 4.2.4). These results are consistent with the lack of overlap between populations. Overall, ^{13}C-depleted values were observed during the end of winter and spring whereas an increase towards more enriched values varied between populations. In Pašman, values were more enriched in fall and summer, while in Pag the highest values were shown in fall and early winter. The $C:N_{DG}$ molar ratio showed significant differences between site and month (all at $P < 0.001$) but not in their interaction ($P > 0.05$) indicating that temporal isotopic values behaved in a similar pattern between populations (Fig 4.2.11c, Table 4.2.4).

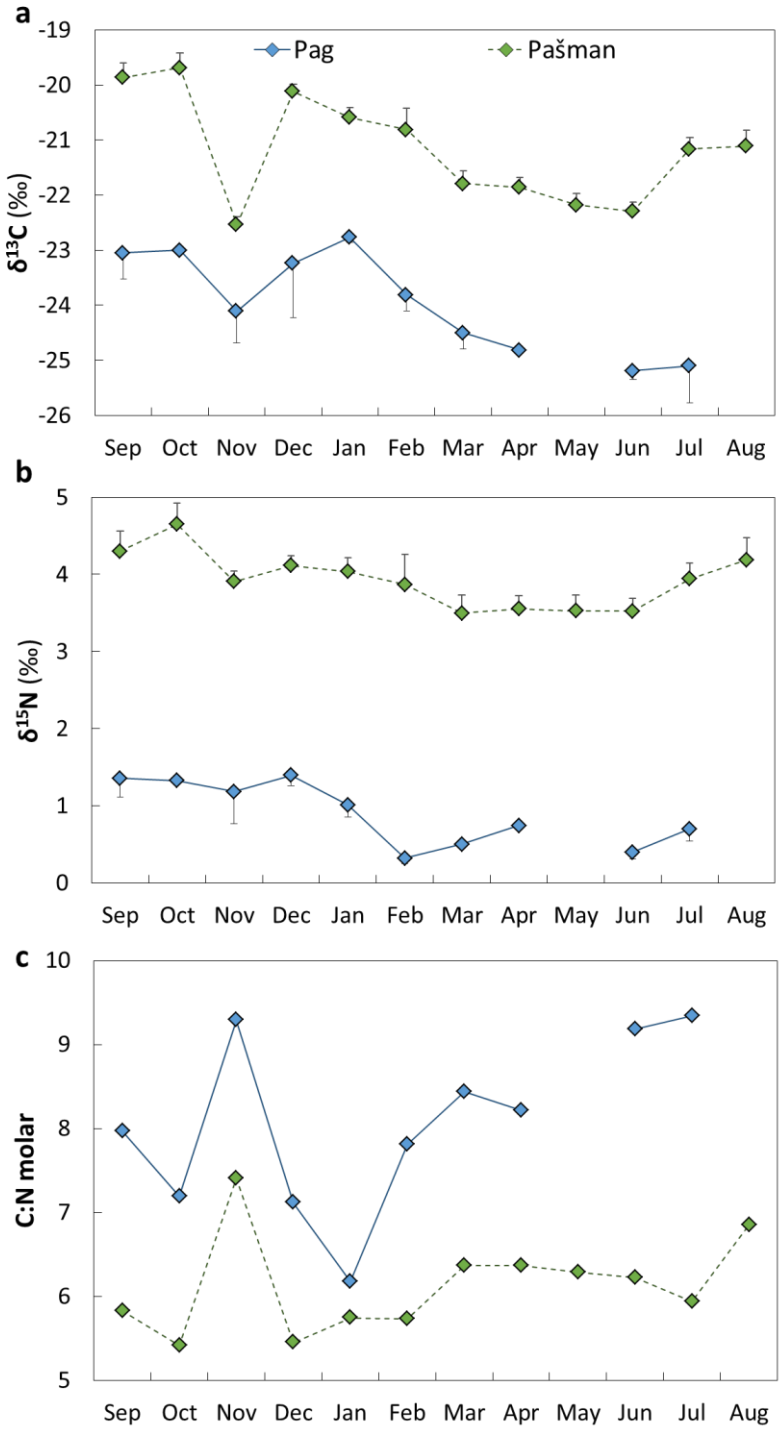

Figure 4.2.11. Temporal variation in (**a**) $\delta^{13}C$ (‰), (**b**) $\delta^{15}N$ (‰) and (**c**) C:N molar ratio in the digestive gland of *Glycymeris pilosa* from Pag and Pašman.

The concentration of lipids in DG was also analyzed seasonally in Pašman, and it was compared to the same months in Pag. Average values in Pašman were 100.6±7.1 mg/g and those in Pag were considerably higher, 180.9±5.3 mg/g (Fig. 4.2.10).

Table 4.2.4. Two-way ANOVA results of the $\delta^{13}C$ (‰), $\delta^{15}N$ (‰) and C:N molar ratio in the digestive gland of *Glycymeris pilosa* and suspended particulate matter (SPM) between Pašman and Pag.

	Glycymeris pilosa					**SPM**				
	df	**SS**	**MS**	***F***	**P**	**df**	**SS**	**MS**	***F***	**P**
$\delta^{13}C$ (‰)										
site	1	111.32	111.32	577.82	< 0.001*	1	10.97	10.97	109.06	< 0.001*
month	11	43.03	3.91	20.31	< 0.001*	11	75.03	6.82	67.83	< 0.001*
site*month	9	4.92	0.55	2.84	0.01	11	11.26	1.02	10.18	< 0.001*
Residuals	39	7.51	0.19			48	4.83	0.10		
$\delta^{15}N$ (‰)										
site	1	132.25	132.25	3408.11	< 0.001*	1	6.60	6.60	10.38	0.002
month	11	7.76	0.71	18.18	< 0.001*	11	51.08	4.64	7.30	< 0.001*
site*month	9	0.99	0.11	2.83	0.012	11	29.08	2.64	4.16	< 0.001*
Residuals	39	1.51	0.04			48	30.52	0.64		
C:N molar										
site	1	57.43	57.43	128.85	< 0.001*	1	8.74	8.74	16.85	< 0.001*
month	11	24.96	2.27	5.09	< 0.001*	11	35.40	3.22	6.21	< 0.001*
site*month	9	5.01	0.56	1.25	0.30	11	21.19	1.93	3.72	< 0.001*
Residuals	39	17.38	0.45			48	24.88	0.52		

As observed from the isotopic biplot there is a clear separation between populations based on digestive gland values whereas ranges between SPM did not differ that much (Fig. 4.2.12).

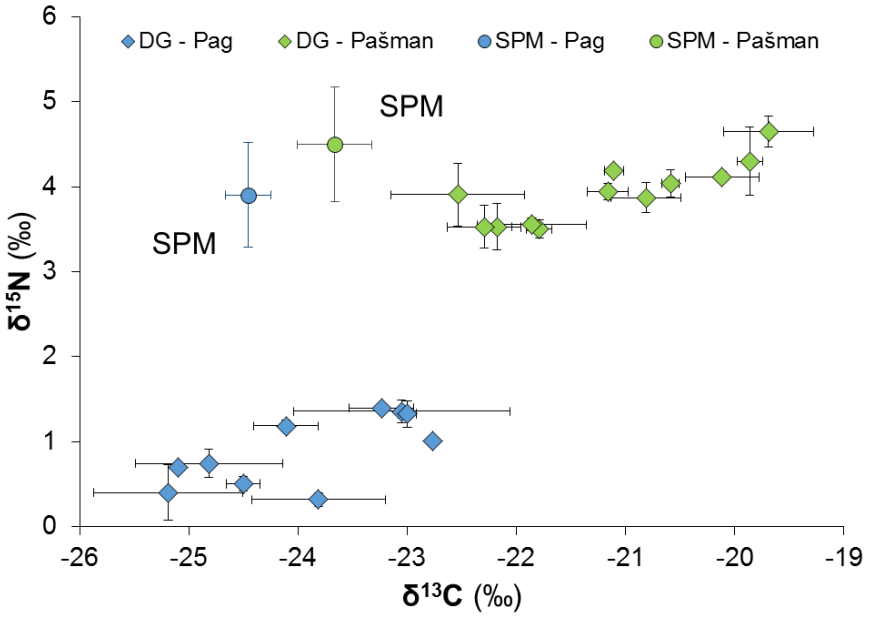

Figure 4.2.12. Stable isotope biplot ($\delta^{13}C$, $\delta^{15}N$) (‰; mean ± SD) showing the isotopic values in the digestive gland (DG) of *Glycymeris pilosa* and suspended particulate matter (SPM) from Pašman and Pag populations.

4.3. Reproduction

4.3.1. Reproductive cycle of *Callista chione* at two study sites

4.3.1.1. Histological analysis

Specimens from Pag and Cetina used for histological analysis had a mean shell length of 67.8±4.7 mm (n=245) and 64.7±5.7 mm (n=220), respectively. There were no significant differences in shell length between males and females with respect to sampling site (two-way ANOVA F = 2.278, P = 0.133 in Pag and F = 0.251, P = 0.617 in Cetina). A total of 133 males (54.3%), 105 females (42.9%) and 7 hermaphrodites (2.8%) were identified in Pag population, while 116 males (52.7%), 97 females (44.1%), 3 hermaphrodites (1.4%) and 4 sexually undifferentiated individuals (1.8%) were determined in samples from Cetina. The sex ratio did not differ significantly from 1:1 (chi-square = 3.294, P = 0.069 in Pag and chi-square = 1.695, P = 0.193 in Cetina).

The resulting histological sections showing the main characteristics of female and male gonad developmental stages are shown in Fig. 4.3.1. Hermaphroditic samples are shown in Fig.4.3.2.

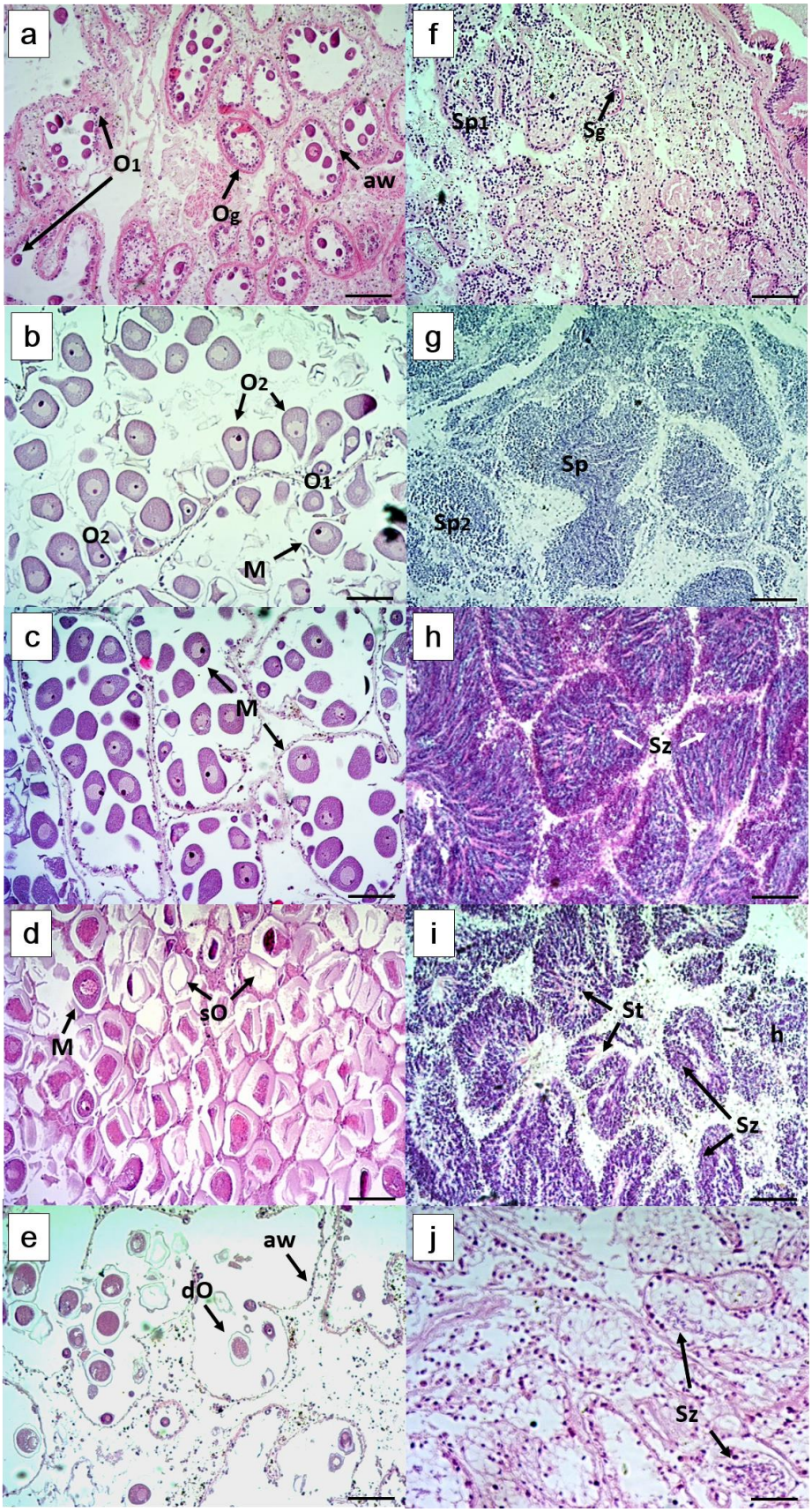

Figure 4.3.1.

Photomicrographs of the histological sections of female (left) and male (right) gonads of *Callista chione* characterizing each stage of gonadal maturity: (**a**,**f**) early active (**b**,**g**) late development (**c**,**h**) ripe (**d**,**i**) spawning and (**e**,**j**) spent/inactive. Scale bar 100 µm.

Og: oogonia

O1: primary oocytes O2: secondary oocytes

M: mature oocytes sO: spawned oocytes dO: degenerative oocyte under resorption

aw: acinus wall;

Sg: spermatogonia, Sp1: primary spermatocyte

Sp2: secondary spermatocyte

Sz: sperm cells

St: sperm tails

h: haematocytes.

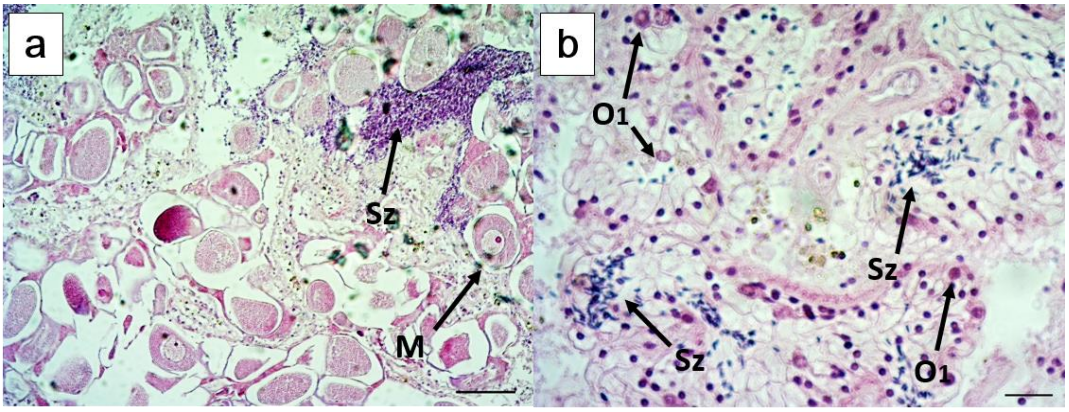

Figure 4.3.2. Two hermaphrodite individuals of *Callista chione* shown at different magnifications and stages. (**a**) A spawned individual with both free oocyte and spermatocytes, scale bar 100 µm. (**b**) A spent to early stage with new acini walls and development of oogonia and primary oocytes as well as free sperm cells under reabsorption, scale bar 20 µm. O1: primary oocytes, M: mature oocytes, Sz: sperm cells.

The monthly relative frequencies of the various gonad developmental stages were used to estimate the timing of the reproductive cycle at each site, using qualitative histological analysis (Fig. 4.3.3). The main period of gamete release at Pag started at ~12°C and extended over approximately 4 months from April until July 2015, accompanied with an increase in temperatures (Fig. 4.3.3a,c). The maximum spawning peak occurred in July 2015, coinciding with nearly the highest temperatures in the area (> 24°C). In October 2014 around 15% of females were in ripe stage which may have occasioned the small spawning peak observed during December 2014 and January 2015, and consequently, the presence of four different gonadal stages was identified in December 2014.

The spawning allocation in the population at Cetina started in January 2015 (particularly in females) at ~14°C, and it included the time with the lowest mean temperature (12.7°C) that could reach down to 10.9°C, what is 4°C higher than the minimum temperature recorded in Pag. The main spawning event was identified between May and June 2015, coupled with the increasing temperatures (Fig. 4.3.3b,d). Interestingly, females were in slightly advanced gonad developmental stages and presented a higher percentage of spawning (Fig. 4.3.3b). Likewise, a spent/inactive stage was barely identified for females and those with gonads at the end of the spawning period, were represented in more than 80% of the samples by an early active stage. Regardless of sex, the population remained in ripe stage for a long period during winter and early spring.

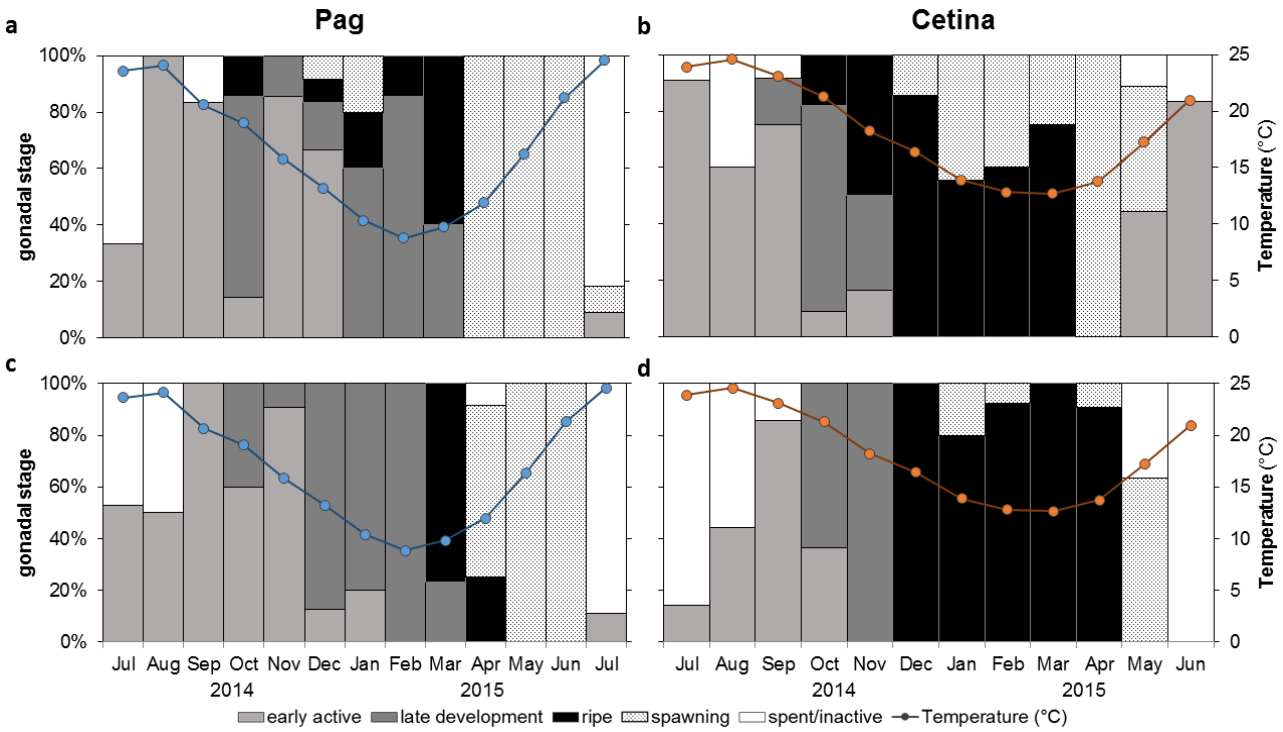

Figure 4.3.3. Monthly relative frequencies of gonad development stages of *Callista chione* and mean monthly temperature at Pag and Cetina sampling sites (**a**,**b**) females and (**c**,**d**) males.

Overall, *Callista chione* was determined to be sexually active during almost the whole year at both study sites and individuals coped with a wide range of temperature at both sites: 21.2°C and 17.6°C, respectively. A main spawning peak was identified representing the end of gametogenesis, and it took place earlier at Cetina (May/June 2015) than at Pag (July 2015). Unlike Cetina population, individuals from Pag were in early active and late development stages for a longer period, and there was just a small transition to ripe stage prior to the spawning timing. The spent/inactive stages lasted for a little longer at Pag and in males from Cetina, than in females from Cetina. Also, specimens analyzed from Pag had a more synchronous cycle. The end of gametogenesis and start of new formation was identified for two consecutive years coinciding with the high temperature peaks, July 2014 and June/July 2015. It is important to highlight the maximum mean temperatures recorded during two consecutive years which were higher in 2015 than 2014, with an increase of 1°C (Pag) and nearly 2°C (Cetina) (in August 2014, 24.1°C and 24.6°C, respectively).

The Mean Gonad Index (MGI) indicated that despite the slight advancement of gonadal stage in females during certain periods, both female and male cycles showed a highly significant synchronicity at both sites ($r = 0.86$, $P < 0.001$ at Pag and $r = 0.88$, $P < 0.001$ at Cetina) (Fig. 4.3.4). The highest MGI values, that is, when gonads were the ripest, were identified between January and March 2015 (excluding the small

peak observed in October 2014) at Pag, and during December 2014 and April 2015 at Cetina, when temperatures were at their lowest. Contrary, the release of gametes was coupled with an increase of temperatures where the lowest MGI values coincided with the highest mean temperatures at both sites during two consecutive years.

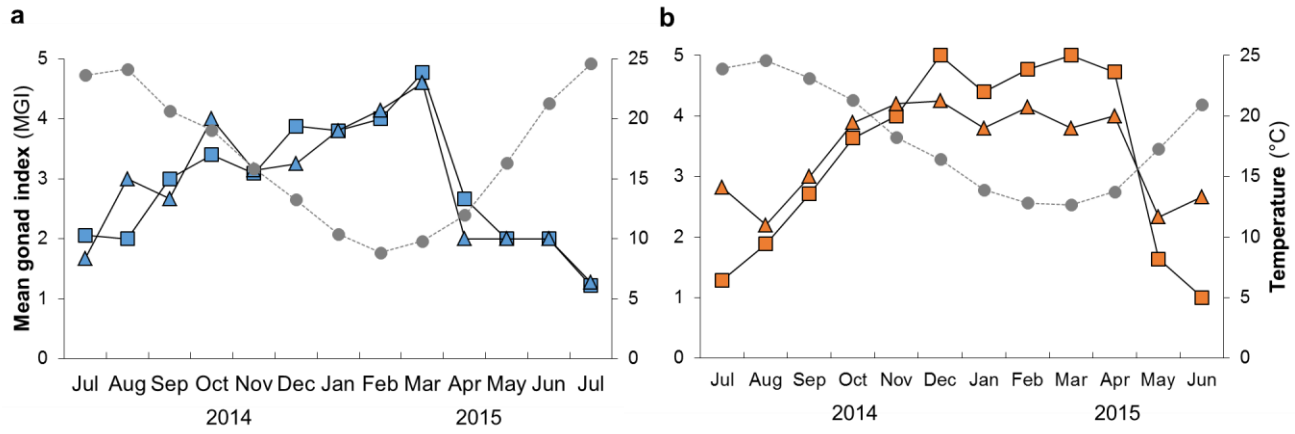

Figure 4.3.4. Mean monthly gonad index values of *Callista chione* and mean monthly temperature (circles); males (squares) and females (triangles) from (**a**) Pag and (**b**) Cetina.

It is important to note that during this study the presence of parasites and signs of tissue infection where evidenced in histological preparations at both sites, although in a much lesser extent than in *G. bimaculata*, as reported later on.

4.3.1.2. Gonadosomatic Index

Individuals used for determining the gonadosomatic index (GSI) had a mean shell length of 64.0±3.8 mm in Pag and 61.6±2.9 mm in Cetina. Based on shell length ranges all individuals were sexually mature and the moment of spawning was considered with the decrease in GSI.

Complementary, body mass index (BMI) was determined to better understand temporal patterns in GSI and the reproductive investment for each population. BMI values of specimens collected in Pag (31.86±4.64) were significantly greater than those from Cetina (28.73±4.22) (Mann-Whitney, $P < 0.001$). The largest mean BMI values were 37.94 and 36.42 in Pag (corresponding to April and May 2015) and 33.56 and 30.95 in Cetina (corresponding to July 2014 and June 2015). Overall, the BMI showed higher amplitude following the temperature changes in Pag whilw smaller ranges were observed in Cetina (Fig. 4.3.5a).

Similarly, GSI values from Pag (0.050±0.046) were significantly greater than those from Cetina (0.037±0.031) (Mann-Whitney, $P < 0.001$) (Fig. 4.3.5b). The combination of both indices showed a positive correlation ($r = 0.77$, $P < 0.001$) in Pag, indicating a synchrony along the temporal pattern. This

pattern was not observed in Cetina (r = 0.13, P > 0.05), where the highest BMI values corresponded to low GSI values. There were statistically significant differences in BMI and GSI values between sites, month and their interaction, thus, confirming the different spatial and temporal timing of somatic and gonadal growth (Table 4.3.2).

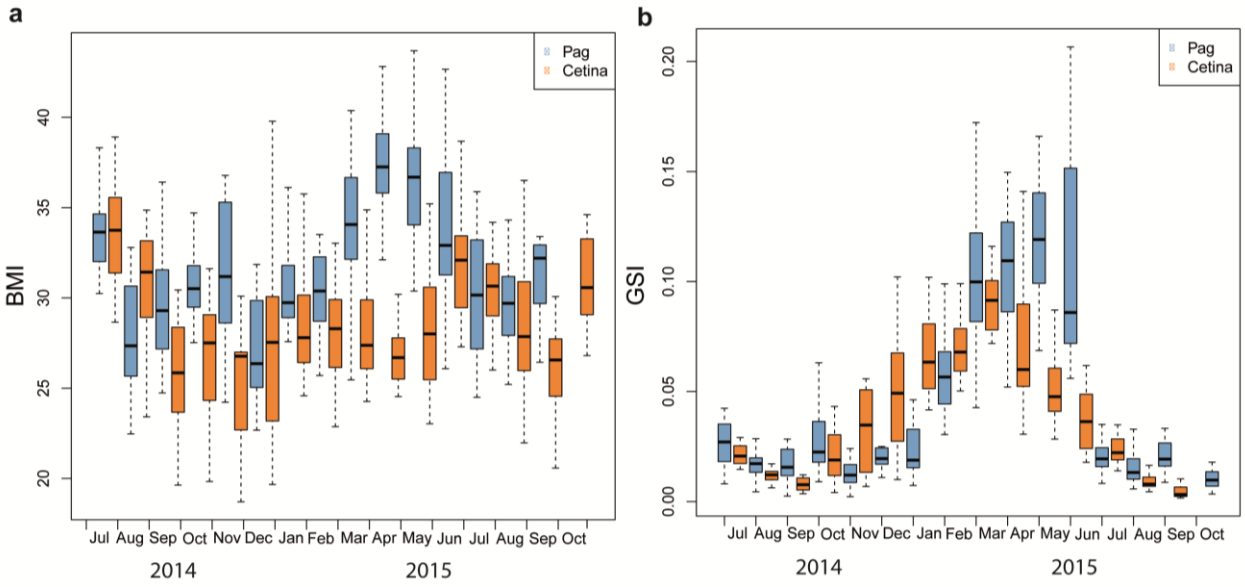

Figure 4.3.5. Seasonal variation in body mass index (BMI) (**a**) and gonadosomatic index (GSI) (**b**) of *Callista chione* for Pag and Cetina populations. Horizontal bars indicate median value respectively, boxes span the interquartile range –where 50% of the values fall– and discontinuous whiskers represent the data range excluding the outliers.

Table 4.3.2. Analysis of variance for comparison of body mass index and gonadosomatic index between two populations of *Callista chione*. Month was a considered continuous variable during the total length of the sampled period; ***P < 0.001

Effect	df	SS	Mean Sq	F-ratio	P-value
Body mass index					
Location	1	1.3354	1.3354	123.387	< 0.001
Month	15	2.5205	0.16803	15.526	< 0.001
Location * Month	14	1.6214	0.11582	10.701	< 0.001
Error	547	5.9201	0.01082		
Gonadosomatic index					
Location	1	14.65	14.6499	86.799	< 0.001
Month	15	381.22	25.4146	150.58	< 0.001
Location * Month	14	63.12	4.5083	26.711	< 0.001
Error	546	92.15	0.1688		

In Pag, GSI started to increase in the late winter/early spring and reached a maximum peak in June 2015, showing quite steady values for the entire spring. The gonadal investment in Pag population reached its maximum along the increasing temperatures and persisted for a few months (between March and June). A small peak was observed during October 2014 but a marked drop was identified as the main spawning discharge in July 2015, at temperatures around 24°C, and a resting stage was nearly immediately reached after that (August 2015) coinciding with the highest annual temperatures. A positive correlation was found between temperature and mean GSI, however it was not statistically significant ($r = 0.45$, $P > 0.05$) (Fig. 4.3.6a).

In Cetina, increasing GSI values were observed during the winter months reaching maximum values in early spring (March 2015), when the lowest mean monthly temperatures were recorded (12.7°C). Spawning took place as a series of consecutive events, indicating liberation of gametes in different pulses, during late spring and summer, reaching a nearly complete resting stage in September, observed for two consecutive years. The start of a new gametogenic cycle took place in the late summer/early autumn, with the maximum temperatures. The GSI in Cetina was strongly negative correlated to temperature ($r = -0.95$, $P < 0.001$) (Fig. 4.3.6b).

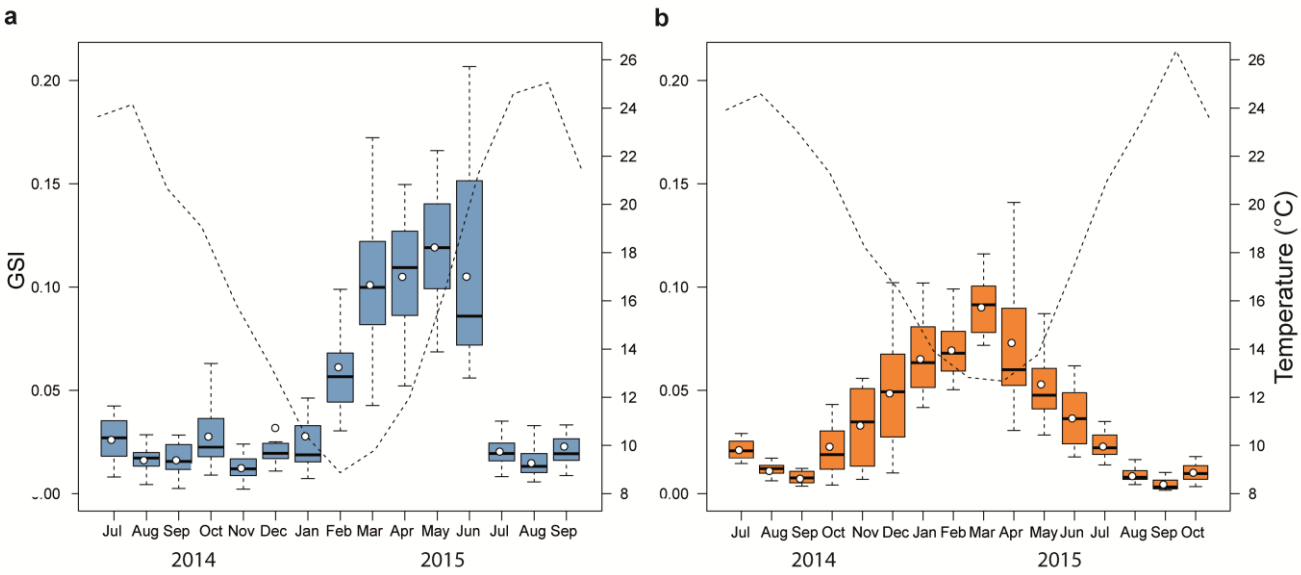

Figure 4.3.6. Relationship between the seasonal variation in gonadosomatic index (GSI) of *Callista chione* and mean monthly temperature (dashed line) for populations of Pag (**a**) and Cetina (**b**). White circles and horizontal bars indicate mean and median value respectively; boxes span the interquartile range, where 50% of the values fall, and discontinuous whiskers represent the data range excluding the outliers.

Whereas temperature did not influence the spawning events the same way at both sites, the start of gametogenesis coincided with the decrease of temperatures in both populations, evidenced during two consecutive years and the reproductive cycle was characterized by a unimodal distribution.

4.3.1.3. Reproductive investment, output and fecundity

Seasonal changes in gonadal mass were present in both populations. During the ripest stages, prior to spawning, the highest gonadal production was observed in Pag with a mean weight of 348±13 mg whereas in Cetina it was 165±6.70 mg. Observed differences were statistically significant between sites (ANOVA, $F = 168.5$, $P < 0.001$) and shell length did not significantly influence this variation in the response variable (ANCOVA, $F = 0.587$, $P > 0.05$), indicating a higher reproductive investment in Pag. The maximum recorded gonadal mass in this period was 699 mg (Pag) and 411 mg (Cetina).

A linear relationship between gonadal mass and total body mass from individuals with highly developed gonads (in mature stages) was also significant ($r = 0.57$, $P < 0.001$) (Fig. 4.3.7). Gonads represented a 16% of total body mass in Pag population, and around 7% in Cetina during months preceding the gamete release. At full maturity, gonadal occupation in Pag was 20.7% and reached a mean value of 2.1% after spawning, implying a drop of up to 18% and representing a loss of gonadal mass of about 260 mg. In Cetina, GSI increased up to 12.2% in March 2015 and reached a mean value of 0.9% after spawning, a drop of up to 11% and an accumulated loss of about 160 mg (considering the continuous spawning events) (see Fig. 4.3.6). Therefore, differences in the reproductive output were evidenced between sites and showed similar results for two consecutive years, being higher in Pag.

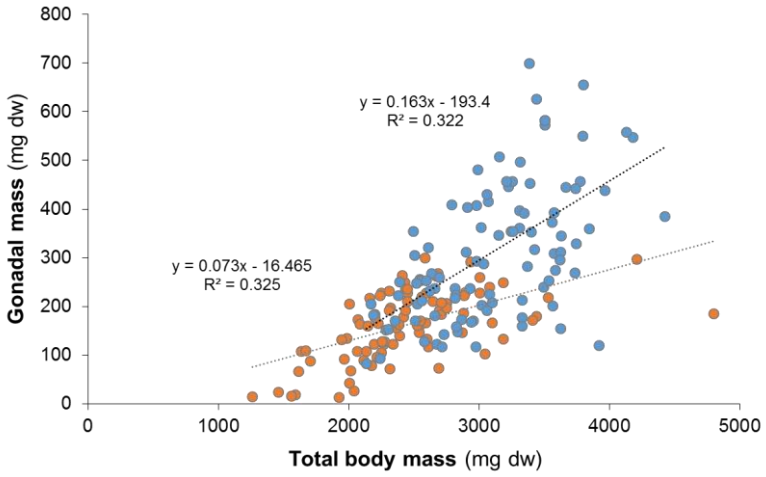

Figure 4.3.7. Relationship between gonadal mass (mg dw) and total body mass (mg dw) before spawning in Pag (blue) and Cetina (orange)

Overall, based on mean population values, specimens from Pag released 82% of the gonads whereas those from Cetina released nearly the totality of its gonadal mass (96%). In terms of fecundity per brood, and assuming an equal weight for males and females, a higher proportion of gonadal mass into reproduction was invested in Cetina, despite the highest investment and output from Pag population (Fig. 4.3.6).

4.3.1.4. Comparative analysis of methods

Considering the seasonal pattern of the reproductive cycle, the estimation by means of qualitative histological analysis and gonadosomatic index, led to similar results (Fig. 4.3.8). Both methodologies determined the same main spawning periods where the highest values of GSI corresponded to months with ripe and spawned gonad stages. On the other side, low GSI values were coupled with the spent/inactive and early developmental stages. Overall, the maximum values were between March and June 2015 in Pag, and between January and May 2015 in Cetina, coinciding with the ripe/spawning stages. The identification of the transition between the last spawning event and spent/inactive period is evidenced by the drop in GSI values.

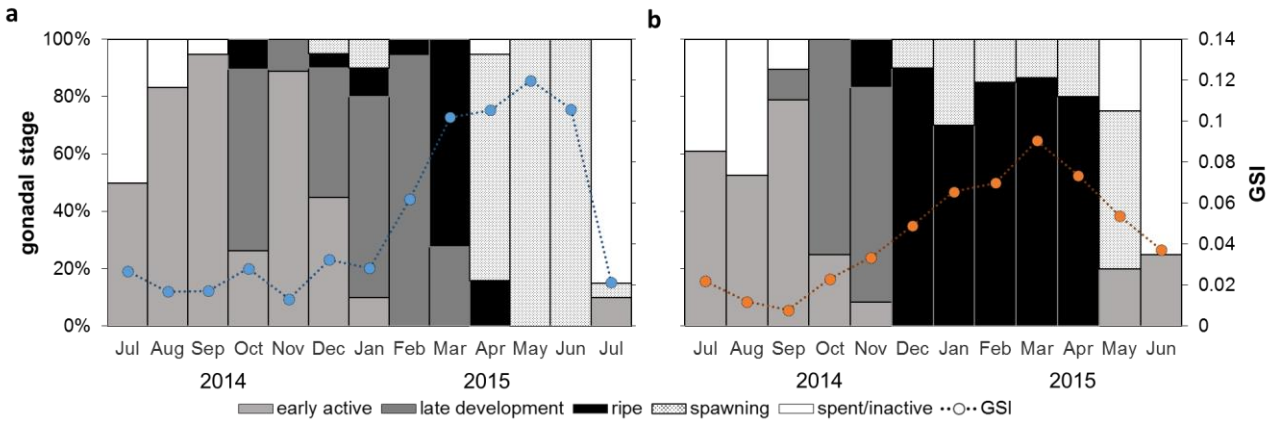

Figure 4.3.8. Combination of two methodologies for determining reproductive cycle in *Callista chione* from population in Pag (**a**) and Cetina (**b**). Histogram shows monthly relative frequencies of developmental stages for the entire population based on histological analysis and dashed line shows the temporal pattern of gonadosomatic index (GSI); white circles correspond to monthly mean GSI values.

4.3.2. Reproductive cycle of *Glycymeris bimaculata* at two study sites

4.3.2.1. Histological analysis

Specimens from Pag and Cetina used for histological analysis had a mean shell length of 76.9±6.2 mm (n=320) and 65.8±4.8 mm (n=280), respectively. Macroscopic sexual determination is feasible except during periods of gonadal inactivity. Female gonads are pink/purple colored whereas males are characterized by a whitish/yellowish coloration. There were no significant differences in shell length between males and females across time with respect to sampling site (two-way ANOVA, F = 1.296, P = 0.204 in Pag and F = 1.137, P = 0.328 in Cetina). A total of 178 males (55.6%), 141 females (44.1%) and 1 hermaphrodite (0.3%) were identified in Pag population, while 149 males (53.2%), 129 females (46.1%), 1 hermaphrodite (0.4%) and 1 sexually undifferentiated individual (0.4%) were determined in samples from Cetina. The sex ratio was 1.0:1.3 in Pag (chi-square = 4.292, P = 0.038) whereas in Cetina did not significantly differ from 1:1 (chi-square = 1.439, P = 0.230).

The resulting histological sections showing the main characteristics of female and male gonad developmental stages (given in Table 3.4.1) are shown in Fig. 4.3.9. A detail of male components during spermatogenesis is shown in Fig. 4.3.10a and a hermaphroditic sample in Fig. 4.3.10b.

As observed in *C. chione*, histological preparations of *G. bimaculata* individuals revealed a high degree of infection by parasites which in some cases added difficulties during the gonadal stage interpretation (Fig. 4.3.11). Gonadal neoplasia was particularly present in the majority of individuals throughout the year, and it was more evidenced during early active stages as illustrated in the stage representation shown in Fig. 4.3.9f, which is stained in pink.

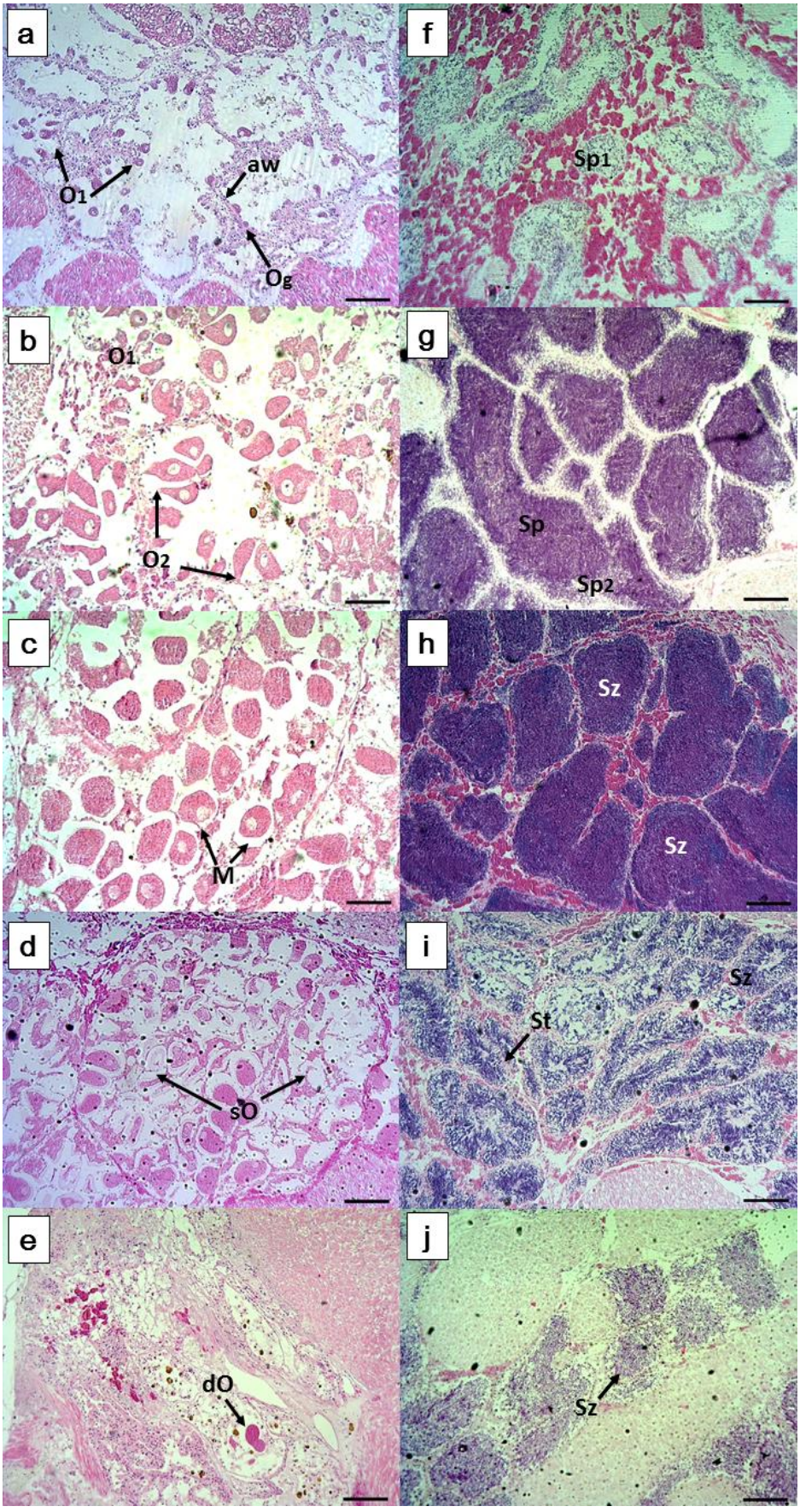

Figure 4.3.9.
Photomicrographs of the histological sections of female (left) and male (right) gonads of *Glycymeris bimaculata* characterizing each stage of gonadal maturity: (**a**,**f**) early active (**b**,**g**) late development (**c**,**h**) ripe (**d**,**i**) spawning and (**e**,**j**) spent/inactive. Scale bar 200 µm.
Og: oogonia
O1: primary oocytes O2: secondary oocytes
M: mature oocytes sO: spawned oocytes dO: degenerative oocyte under resorption
aw: acinus wall;
Sg: spermatogonia, Sp1: primary spermatocyte
Sp2: secondary spermatocyte
Sz: sperm cells
St: sperm tails.

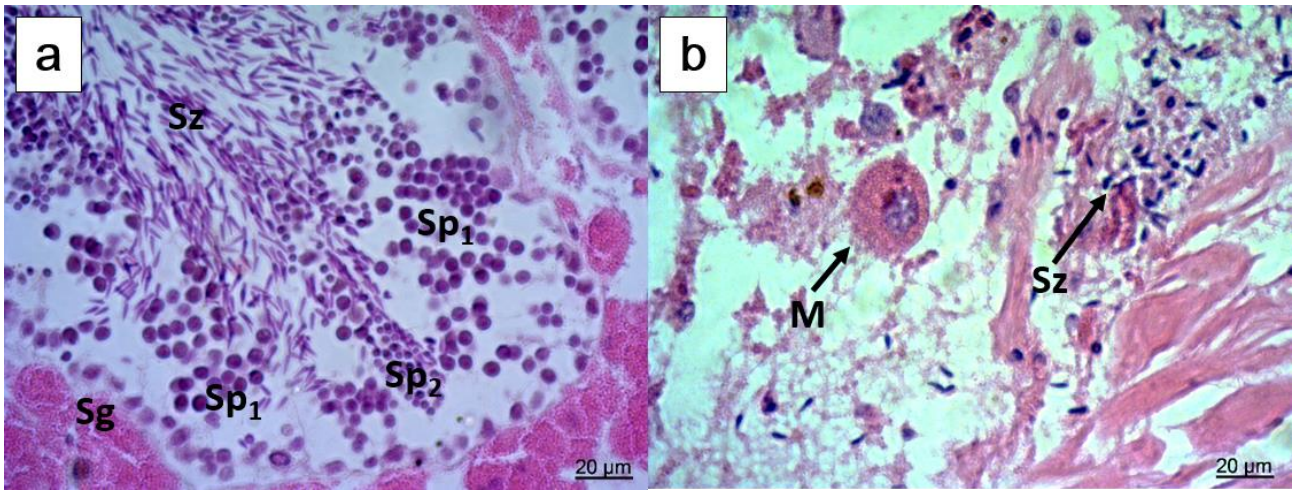

Figure 4.3.10. (**a**) Detail of male spermatogenesis components. Sg: spermatogonia, Sp1: primary spermatocyte, Sp2: secondary spermatocyte and Sz: sperm cells. (**b**) Hermaphrodite individual of *Glycymeris bimaculata* in a spent stage. M: mature oocytes, Sz: sperm cells.

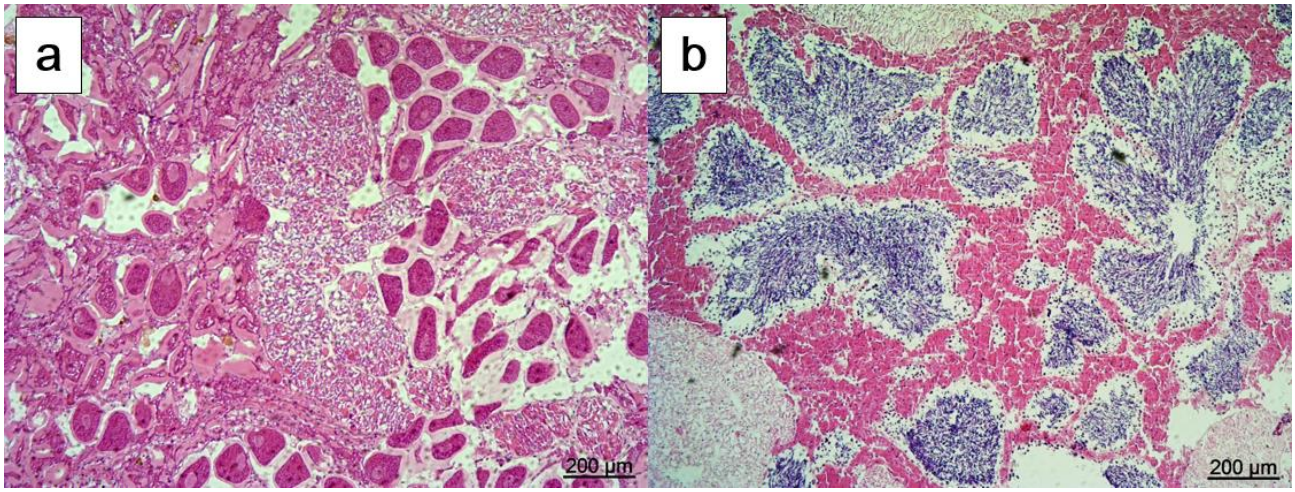

Figure 4.3.11. Specimens showing signs of gonadal infection in (**a**) female and (**b**) male in *Glycymeris bimaculata*.

The monthly relative frequencies of gonad developmental stages, as a result of qualitative histological analysis, estimated the reproductive cycle at each site (Fig. 4.3.12). The main period of gamete release at Pag coincided with the highest temperatures in both years; in 2014 a short spawning duration was observed in females in August and in males during September whereas in 2015 spawning started in July/August and it was prolonged until September/October (Fig. 4.3.12a,c). Therefore the spawning peaks were observed in September 2014 and October 2015 with the decline of temperatures. A new gametogenic cycle started right after spawning and the early active stage, shared with a certain percentage of individuals in spent stage, was dominant for a few months, particularly in males. Females had a long period with a high percentage of individuals in late development stage between February and June, whereas the ripe stage was briefly reached represented by a small percentage of individuals in

May, June and July 2015 and rapidly followed by the spawning stage. In males, late development represented a lower percentage of individuals prior to the ripe stage, suggesting a quick transition from early active to ripe stages which extended from November until June.

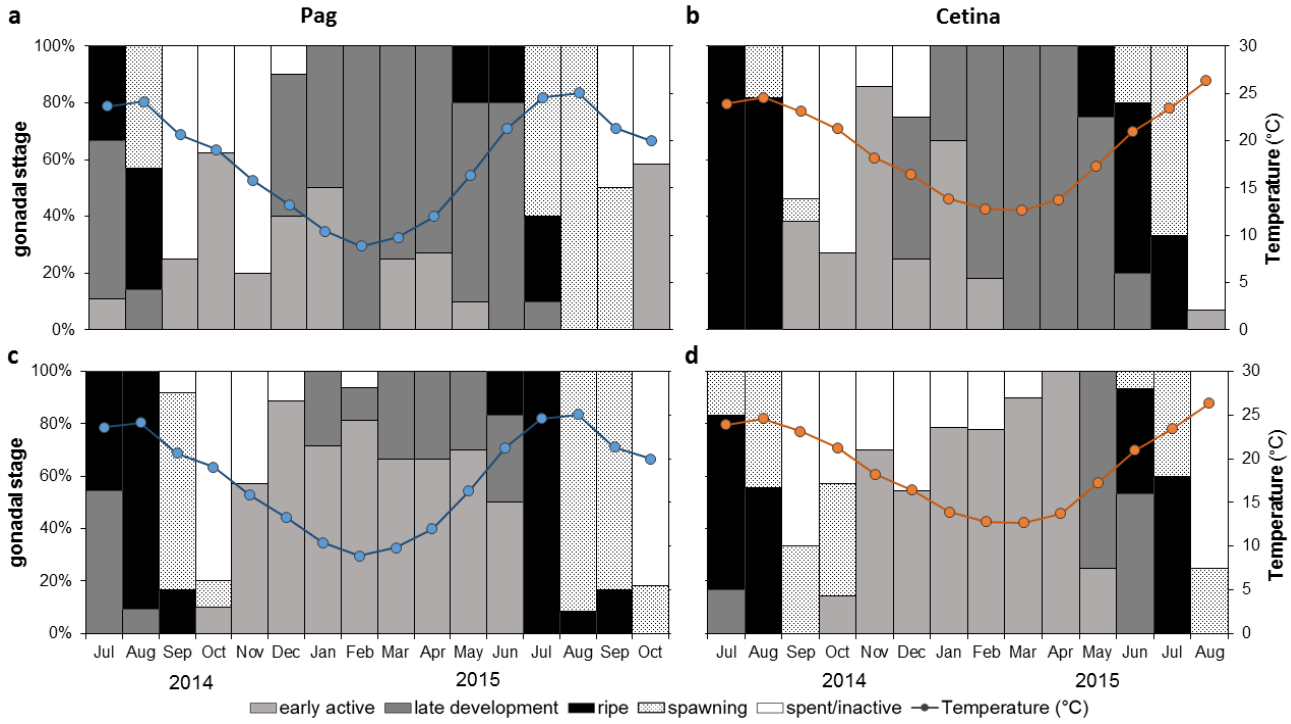

Figure 4.3.12. Monthly relative frequencies of gonad development stages of *Glycymeris bimaculata* and mean monthly temperature at Pag and Cetina sampling sites (**a**,**b**) females, (**c**,**d**) males.

The spawning allocation in the population from Cetina took place between August and September 2014 and in 2015 it started earlier, around June and up to July/August. In both females and males, the spawning stage represented again a short period, and in 2014 the main spawning peak was in September with the decreasing temperatures whereas in 2015 it occurred a month earlier, in August, when temperatures were at its highest (Fig. 4.3.12b,d). A resting stage was not completely observed, and a small percentage of individuals were in spent stage; this was especially evident in males, where this stage was present up to March 2015. Similarly like in Pag population, a late development stage quickly overtook the early active stage in females whereas early active was predominant in males for a long period (nearly 6 months), followed by a short transition between late development and ripe individuals between May and June 2015.

Overall, *Glycymeris bimaculata* was determined to be sexually active during the whole year at both study sites, with a short period of individuals in spent stage and high synchronous cycles in both populations. Females were in slightly advanced gonad developmental stages at both sites and showed a shorter period of individuals in early active stage than males. Mature individuals in the ripe stage were

found, at most, during 2 months rapidly followed by spawning. The spawning peak in Pag population was nearly similar between years (September/October). Interestingly, the population from Cetina, had an earlier spawning peak in 2015 (August) than in 2014 (September), being 2015 a year characterized with the highest temperatures recorded since many years.

The MGI indicated that despite the slight advancement of gonadal stage in females during certain periods, both female and male cycles showed a synchronicity at both sites, more highly significant in Cetina ($r = 0.65$, $P < 0.05$ at Pag and $r = 0.86$, $P < 0.001$ at Cetina) (Fig. 4.3.13). The highest MGI values were identified in August 2014 and July 2015 at Pag coupled to the highest temperatures and during July/August 2014 and May-July 2015 at Cetina, the later when temperatures were still increasing. Contrary, the release of gametes up to the lowest MGI values was coupled to decreasing temperatures, and values of 3-4 corresponding to early active and late development stages coincided with the lowest temperatures recorded at both sites (Fig. 4.3.13).

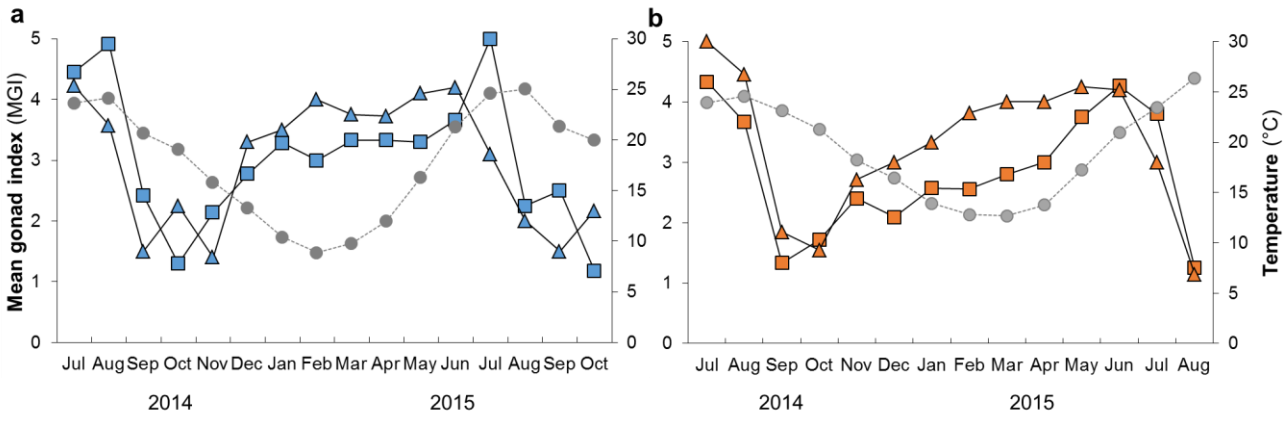

Figure 4.3.13. Mean monthly gonad index values of *Glycymeris bimaculata* and mean monthly temperature (circles); males (squares) and females (triangles) from (**a**) Pag and (**b**) Cetina.

4.3.2.2. Gonadosomatic index at Pag

Individuals used for determining the GSI had a mean shell length of 75.7±4.2 mm. No significant differences were shown in shell length along the sampled period (ANOVA, F = 0.261, P > 0.05). Based on shell length ranges all individuals were sexually mature and the decrease in GSI was considered as the moment of spawning. There were no significant differences between sex and GSI (ANOVA, F = 2.334, P > 0.05) as illustrated in Fig. 4.3.14; therefore, data from both sexes were analyzed together to increase sample size for analysis. GSI values averaged 0.106±0.073. The highest mean monthly GSI values were 0.192, 0.204 and 0.208 (in August 2014, August and September 2015, respectively) and the lowest ones were recorded in October of both years, 0.012 (in 2014) and 0.018 (in 2015) (Fig. 4.3.15b). Complementary, temporal patterns in BMI were also illustrated in this study to assess their relationship with GSI. Over the study period, BMI values averaged 22.4±3.1. The largest mean monthly BMI value was 26.1 shown in summer (August 2015) and the lowest mean was 18.4 shown in winter (December 2014) (Fig. 4.3.15a). These two indices had a positive correlation (r = 0.63, P < 0.001), indicating a synchrony along the temporal pattern.

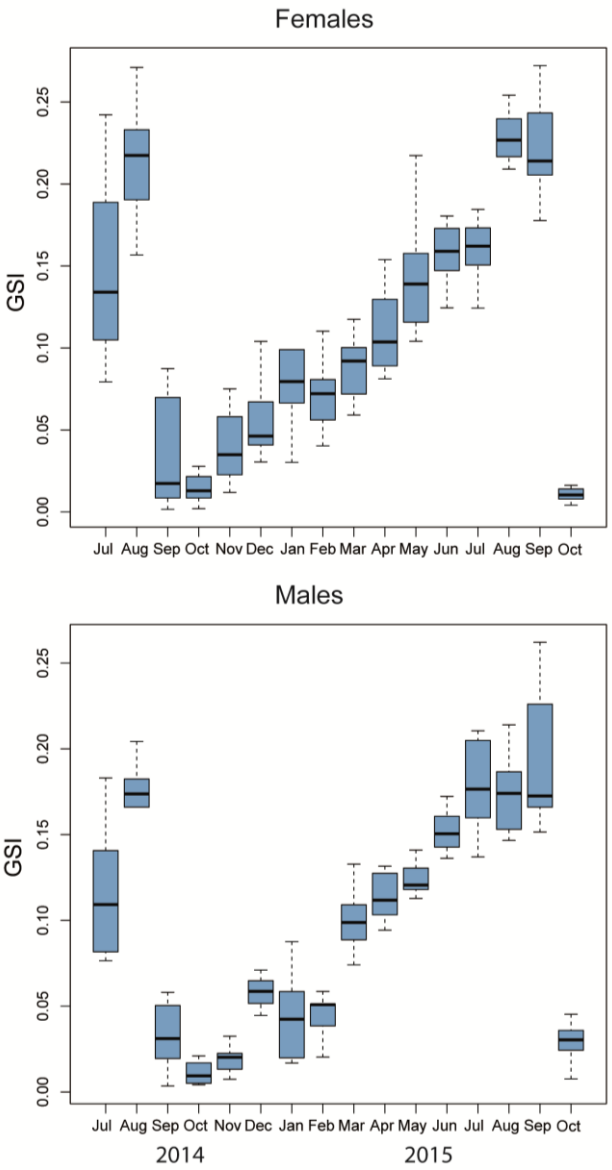

Figure 4.3.14. Seasonal variation in gonadosomatic index (GSI) of *Glycymeris bimaculata* between females and males. Horizontal bars indicate mean and median value respectively; boxes span the interquartile range, where 50% of the values fall, and discontinuous whiskers represent the data range excluding the outliers (above Figure).

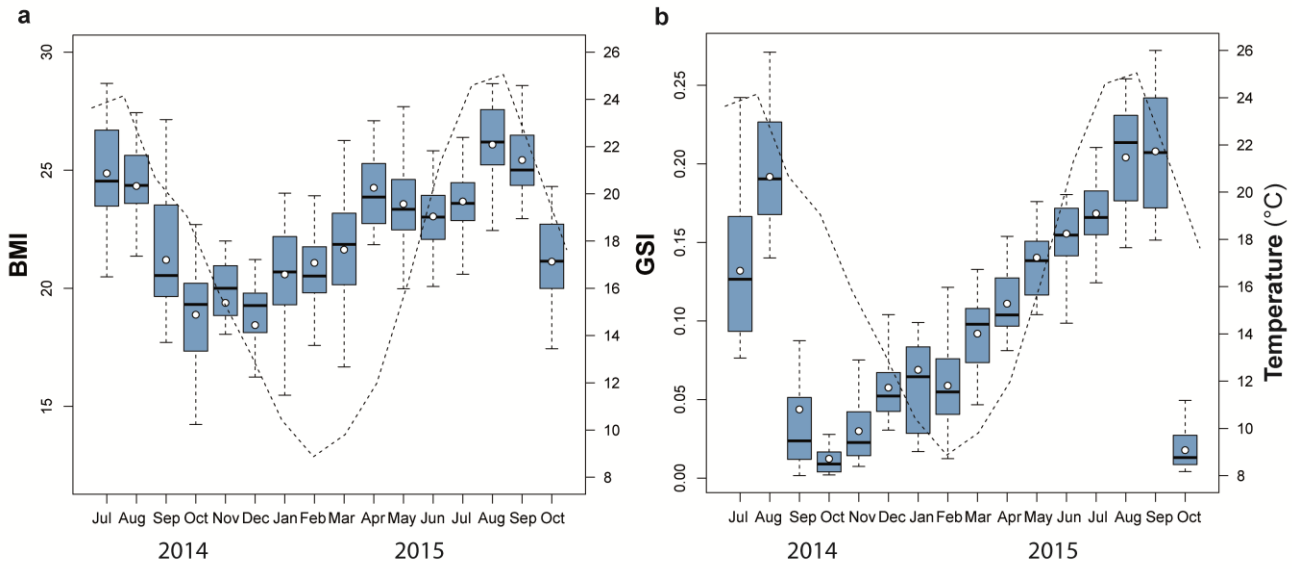

Figure 4.3.15. Relationship between the seasonal variation in body mass index (BMI) (**a**) and gonadosomatic index (GSI) (**b**) of *Glycymeris bimaculata* and mean monthly temperature (dashed line) at Pag. White circles and horizontal bars indicate mean and median value respectively; boxes span the interquartile range - where 50% of the values fall - and discontinuous whiskers represent the data range excluding the outliers.

GSI started to increase in the late fall/early winter and it was during spring when the values highly increased reaching a maximum peak in August–September 2015. This summer peak was also suggested from the previous year in August. The gonadal investment reached its highest values along with the temperature maxima in both years and GSI considerably dropped with decreasing temperatures. The main spawning discharge in 2014 was identified in September, at temperatures between 20 – 24°C, and a resting stage was nearly immediately reached after that (October). In the following year, the spawning timing was even more distinct and took place in October. Interestingly, October also showed a narrower spread of data, indicating that most of the sampled specimens reached the lowest content of gonadal mass while in previous months the variation between specimens was higher. A positive correlation was significantly found between temperature and mean GSI ($r = 0.56$, $P < 0.05$). The onset of gametogenesis was observed late in 2014 with a moderate GSI increase at decreasing temperatures; GSI values started to increase considerably with the temperature rising. The reproductive cycle was characterized by a unimodal distribution as evidenced by two consecutive years (Fig. 4.3.15b).

4.3.2.3. Reproductive investment, output and fecundity

Seasonal changes in gonadal mass were present in this population. During the ripest stages, prior to spawning, the highest mean gonadal mass was of 4.7±1.3 g in August 2014 and of 5.3±1.0 g in both

August and September from 2015. The maximum gonadal occupation in this period was 6.8 g (August 2014) and 7.4 g (September 2015).

A linear relationship between gonadal mass and total body mass from individuals with highly developed gonads (in mature stages) also showed to be significant ($r = 0.66$, $P < 0.001$) (Fig. 4.3.16). Gonads represented about 36% of total body mass during months preceding the gamete release. At full maturity, gonadal occupation in 2014 was up to 27.1% and reached a mean value of 1.2% after spawning, implying a drop of up to 26% and representing an average loss of gonadal mass of about 0.93 g. In 2015, gonadal occupation increased up to 20.8% in September and reached a mean value of 1.8% after spawning, a drop of up to 19% and an average gonadal mass loss of about 1.21 g. Therefore, differences in the reproductive output were shown for two consecutive years, and these were higher in 2014. Overall, based on mean population values, specimens from 2014 released 93.8% of the gonads and those from 2015 released 92.5%. In terms of fecundity per brood, a high percentage of gonadal mass was invested into reproduction (Fig. 4.3.16).

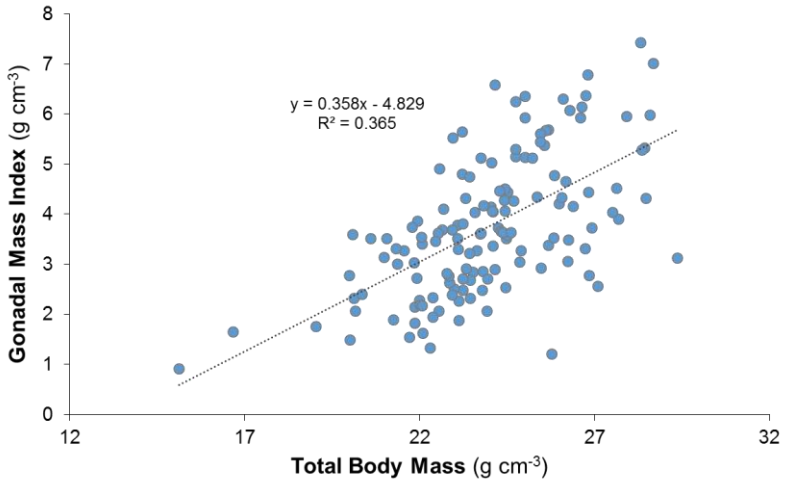

Figure 4.3.16. Relationship between gonadal mass (m dw) and total body mass (g dw) before spawning *Glycymeris bimaculata*.

4.3.2.4. Comparative analysis of methods

As in the case of *C. chione*, the combination of qualitative histological analysis and gonadosomatic index to assess the seasonal pattern of the reproductive cycle, led to similar results (Fig. 4.3.17). Both methodologies also determined the same main spawning periods where the highest values of GSI corresponded with ripe and spawned months. On the other side, low GSI values were coupled with months with the highest percentage of individuals in the spent/inactive stage, followed by increasing GSI values as the gametogenic cycle was advancing. Overall, the maximum values were in August 2014

and August and September in 2015. Similarly, a sharp decrease is evidenced between the last spawning event and the spent/inactive period.

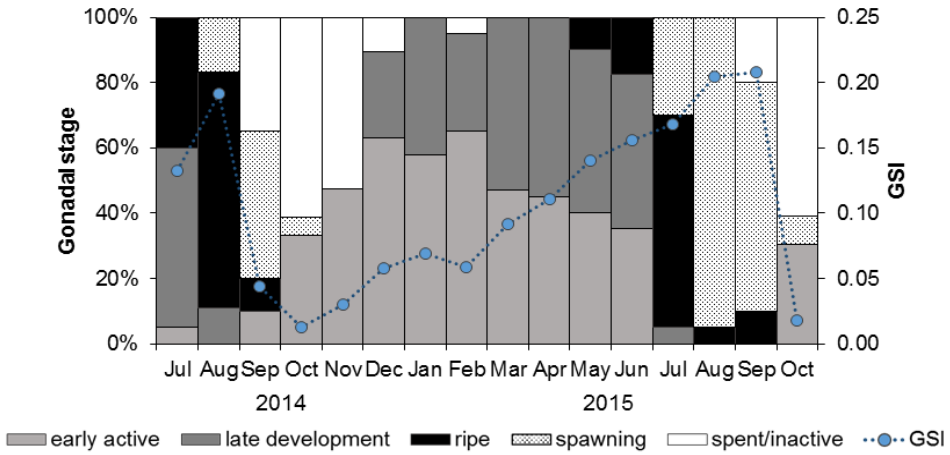

Figure 4.3.17. Combination of two methodologies for determining the reproductive cycle in *Glycymeris bimaculata*. Histogram shows monthly relative frequencies of developmental stages for the entire population based on histological analysis and dashed line shows the temporal pattern of gonadosomatic index (GSI); blue circles correspond to monthly mean GSI values.

4.3.3. Reproductive cycle of *Glycymeris pilosa* from Pašman

4.3.3.1. Histological analysis

Specimens of *Glycymeris pilosa* used for histological analysis had a mean shell length of 71.0±5.7 mm (n=231). Macroscopic sexual determination is feasible except during periods of gonadal inactivity. Female gonads are pink/purple colored whereas males are characterized by a whitish/yellowish coloration. There were no significant differences in shell length between males and females with respect to sampling month (ANOVA, $F = 1.319$, $P > 0.05$). A total of 129 males (51.1%), 121 females (48.5%) and 1 sexually undifferentiated specimen (0.4%) were identified. The sex ratio did not differ significantly from 1:1 (chi-square = 0.256, $P = 0.613$). The resulting histological sections showing the main characteristics of female and male gonad developmental stages (given in Table 3.4.1) are shown in Fig. 4.3.18.

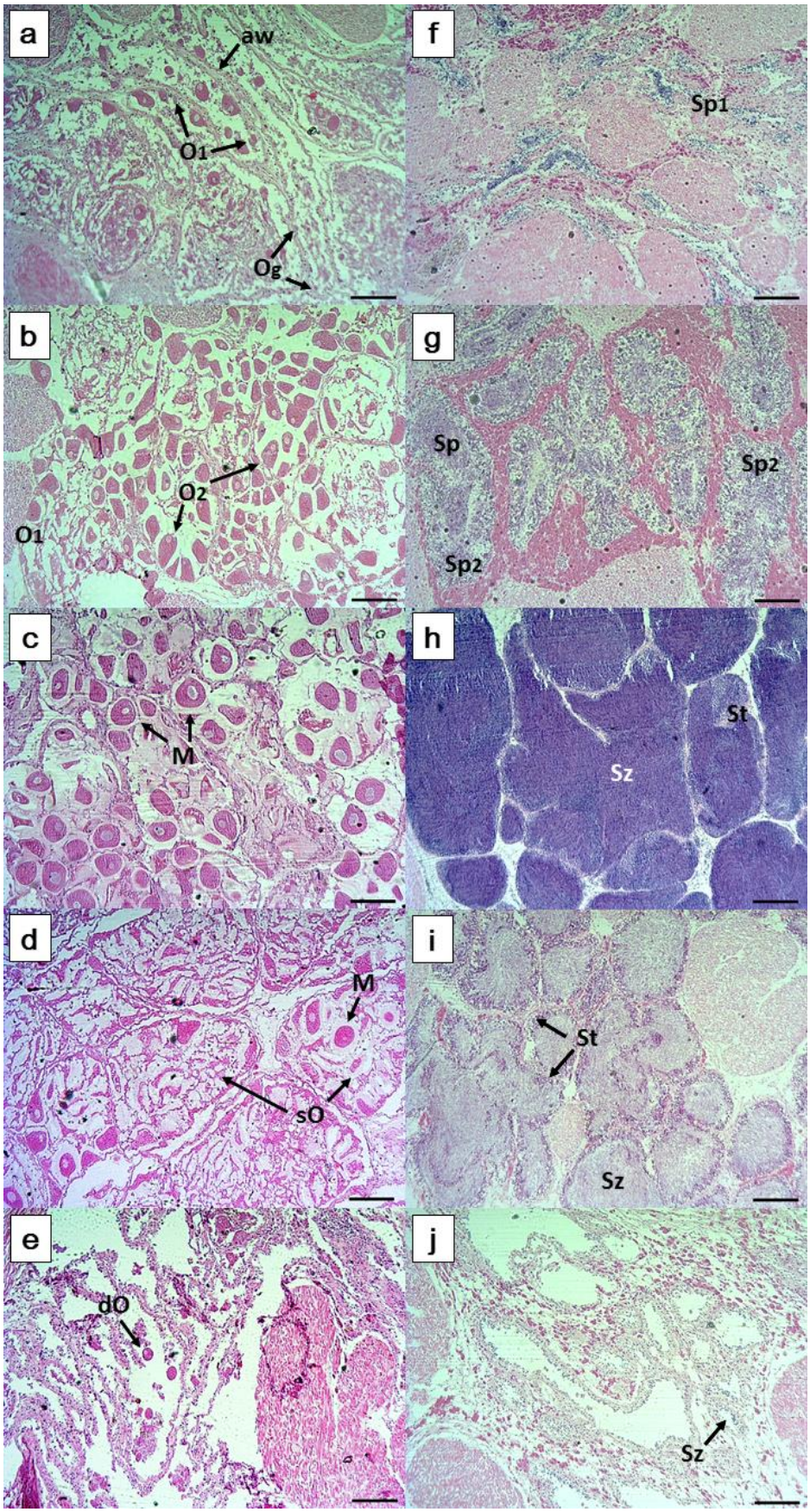

Figure 4.3.18.

Photomicrographs of the histological sections of female (left) and male (right) gonads of *Glycymeris pilosa* characterizing each stage of gonadal maturity: (**a**,**f**) early active (**b**,**g**) late development (**c**,**h**) ripe (**d**,**i**) spawning and (**e**,**j**) spent/inactive. Scale bar 200 µm.

Og: oogonia

O1: primary oocytes O2: secondary oocytes

M: mature oocytes sO: spawned oocytes dO: degenerative oocyte under resorption

aw: acinus wall;

Sg: spermatogonia, Sp1: primary spermatocyte

Sp2: secondary spermatocyte

Sz: sperm cells

St: sperm tails.

In this study, the reproductive cycle over 12 months was estimated by looking at the monthly relative frequencies of gonad developmental stages on basis of histological analysis (Fig. 4.3.19). Due to sampling design, the end of the 2014 reproductive cycle and nearly all 2015 cycle were covered. Samples collected in 2014 showed a little percentage of ripe individuals in September whereas the release of gonads, as indicated by the spawning stage, was nearly prolonged for three months in females. A low percentage of individuals in spent stage was shown between October and December. After this short stage, the onset of the new gametogenic cycle took place in December when temperatures were reaching the lowest values. Between January and May individuals were found both in early and late development stages, and as temperatures were increasing, the late development stage had a higher coverage. Males had a more extensive period in early development stage that lasted for nearly 4 months. In June, first individuals with mature gonads were present in the sampled population. Ripe individuals were also present in July, with a greater percentage of males in this stage that seems to be rather short. Spawning started between July and August 2015, at temperatures between 24–26°C and lasted longer predominant in females. As observed from this 12 month study, females were slightly advanced in reaching maturation stage. Due to the lack of a clear spent stage, our results indicated a long preparation of gonads (early and late development stages) and a short period of maturation which rapidly lead to gonad release, followed by a longer spawning period.

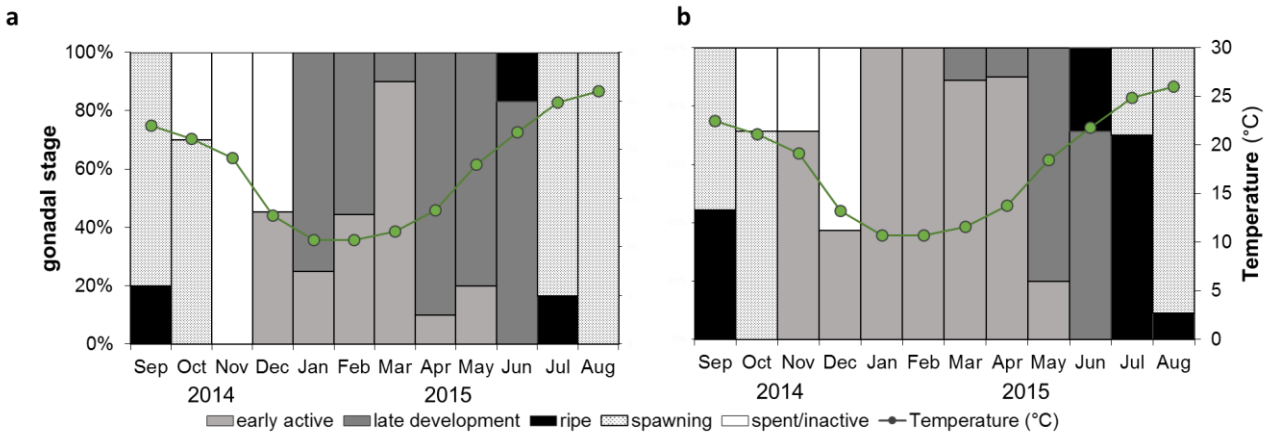

Figure 4.3.19. Monthly relative frequencies of gonad developmental stages of *Glycymeris pilosa* and mean monthly temperature at Pašman (**a**) females, (**b**) males.

The MGI indicated a slight advancement of female gonadal stages although both female and male cycles showed a highly significant synchronicity ($r = 0.70$, $P < 0.05$) (Fig. 4.3.20). The lowest MGI values in 2014 preceded the lowest temperatures whereas the highest MGI values (barely exceeding 4) were identified in May and June 2015 in both sexes, evidencing the short length of the ripe stage. The onset of gamete release took place with an increase of temperatures which reached the highest values in August 2015

(Fig. 4.3.19). Gonadal neoplasia in histological preparations was observed in many analyzed individuals of this species.

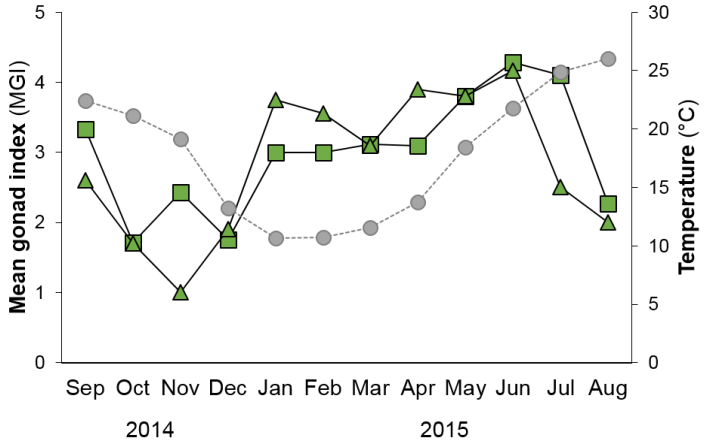

Figure 4.3.20. Mean monthly gonad index values of *Glycymeris pilosa* and mean monthly temperature (circles); males (squares), females (triangles).

4.4. Growth

The mixing line equation developed for the study area had an R^2 = 0.95 (Fig 4.4.1) enabling a high confidende estimation of $\delta^{18}O_{water}$ from monthly salinity measurements. The average $\delta^{18}O_{water}$ value from all 30 measured samples was -0.94±3.24‰. Reconstructed $\delta^{18}O_{water}$ values from Pag ranged from 0.45 to 1.28‰ whereas those from Cetina ranged from -0.12 to 1.34‰.

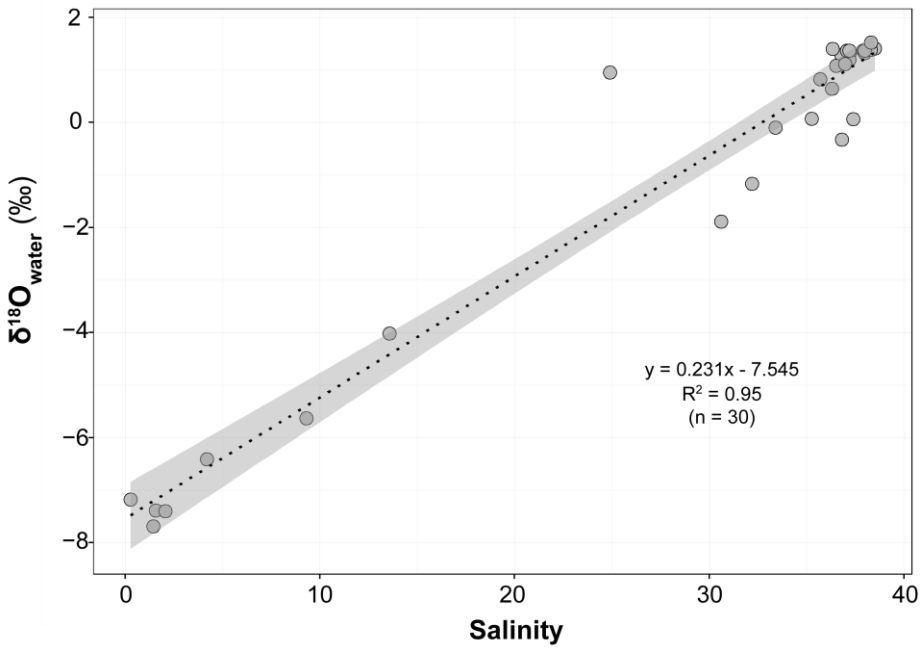

Figure 4.4.1. Mixing line equation obtained from salinity and $\delta^{18}O_{water}$ (‰) measurements. Grey-shaded area represents the 95% confidence interval.

4.4.1. Micromilling on the shell surface of *Callista chione*

The shell stable isotope curves of all studied *Callista chione* shells showed distinct sinusoidal oscillations (Fig. 4.4.2). Seasonal $\delta^{18}O_{shell}$ amplitudes of shells from Pag were fairly similar from -0.82 to 2.24‰ in AC1, from -0.78 to 2.25‰ in AC2 and from -0.77 to 2.46‰ in AC3. Those from Cetina showed a slightly larger variance, from -0.73 to 1.79‰ in CC1, from -0.91 to 1.71‰ in CC2 and from -0.84 to 1.51‰ in CC3. Distinct major growth lines were visible on external shell surfaces and in cross-sections of *C. chione* permitting to determine the ontogenetic ages. Specimens from Pag lived for 3 to 6 years while those from Cetina were 4 years-old. Since specimens had different shell lengths and ages, amplitudes of annual $\delta^{18}O_{shell}$ variation and distances within each annual cycle varied among individuals. In Fig. 4.4.2b, a significant shortening over the sampled transect became apparent in the spacing between maximum to minimum $\delta^{18}O$ values reflecting a decrease in the shell growth rate through ontogeny, widely recognized in organisms which grow their shell by periodic accretion. The variation between seasonally depleted and enriched extremes is nearly defined by linear series, anticipating the seasonal variation in seawater temperature. Since depleted values represent the highest temperatures while enriched values are representative of the coldest periods, a wider amplitude was observed in individuals from Pag similar to larger mean annual seawater temperature variation observed at this site. The amplitudes of $\delta^{13}C_{shell}$ values from Pag shells were quite similar and ranged from -1.20 to 0.03‰ in AC1, from -1.51 to -0.16‰ in AC2 and from -0.42 to -0.06‰ in AC3. Those from Cetina ranged from -1.36 to 0.02‰ in CC1, from -1.02 to -0.07‰ in CC2 and from -1.08 to -0.21‰ in CC3. Correlations between both oxygen and carbon isotopes were performed to assess whether they exhibited any analogous seasonal evolution between their profiles. Significant negative correlations existed between $\delta^{18}O_{shell}$ and $\delta^{13}C_{shell}$ except for shell CC3 (Table 4.4.1).

Table 4.4.1. Summary of stable isotope values determined in shells of *Callista chione* from Pag (AC1-AC3) and Cetina (CC1-CC3). All values are reported in ‰ (VPDB standard). Pearson correlation between $\delta^{18}O_{shell}$ and $\delta^{13}C_{shell}$ for each specimen at * $P < 0.05$ and ** $P < 0.001$.

ID	$\delta^{18}O_{shell}$				$\delta^{13}C_{shell}$				Pearson correlation	
	Average	Max	Min	Amplitude	Average	Max	Min	Amplitude	R	P
AC1	0.58	2.24	-0.82	3.06	-0.58	0.03	-1.20	1.24	-0.723	< 0.001**
AC2	0.53	2.25	-0.78	3.03	-0.78	-0.16	-1.51	1.35	-0.412	0.046*
AC3	1.02	2.46	-0.77	3.22	-0.42	-0.06	-0.80	0.74	-0.438	0.025*
CC1	0.39	1.79	-0.73	2.51	-0.57	0.02	-1.36	1.38	-0.528	0.001*
CC2	0.11	1.71	-0.91	2.63	-0.52	-0.07	-1.02	0.95	-0.639	< 0.001**
CC3	0.49	1.51	-0.84	2.36	-0.64	-0.21	-1.08	0.87	-0.189	0.318

The identification of the timing of shell growth band formation targeted a series of growth lines which were deposited between summer and early fall; these observations are likely the result of increasing shell growth rates during the summer followed by a waning of shell growth after the temperature maxima leading to a main growth deposition during this period (Fig. 3.5.1).

Modeled $\delta^{18}O_{shell}$ values at each site compared well with each other (Fig. 4.4.3). Aligning the time-axis of $\delta^{18}O_{shell}$ derived-temperature curve to high resolution instrumental seawater temperatures using Equation 1 allowed the best fit placing data in a calendar time. The temperature amplitudes of annual $\delta^{18}O_{shell}$ variation (Table 4.4.1) were revealed and the growth season was estimated to mainly occur between May and December. According to Equation 1, each 4.34°C change in temperature results in a one permil shift in shell carbonate, therefore, reconstructed temperatures of $\delta^{18}O_{shell}$ values from individuals in Pag covered a range of 13.2–14°C while those from Cetina ranged from 10.2–11.4°C, representing a lower amplitude than measured seawater temperature (16.2°C in Pag; 13.7°C in Cetina).

Reconstructed temperatures in Pag ranged from 13.9 to 28.2°C in AC1, 13.8 to 27.5°C in AC2 and 13.6 to 26.9°C in AC3, whereas in Cetina ranges oscillated between 16.4 to 28.4°C in CC1, 16.7 to 27.7°C in CC2 and 16.8 to 28.2°C in CC3. These values are within the range of maximum recorded temperatures which was 28.6°C at both sites. Minimum temperatures were 7.4°C at Pag and 10.9°C at Cetina (Fig. 4.4.4).

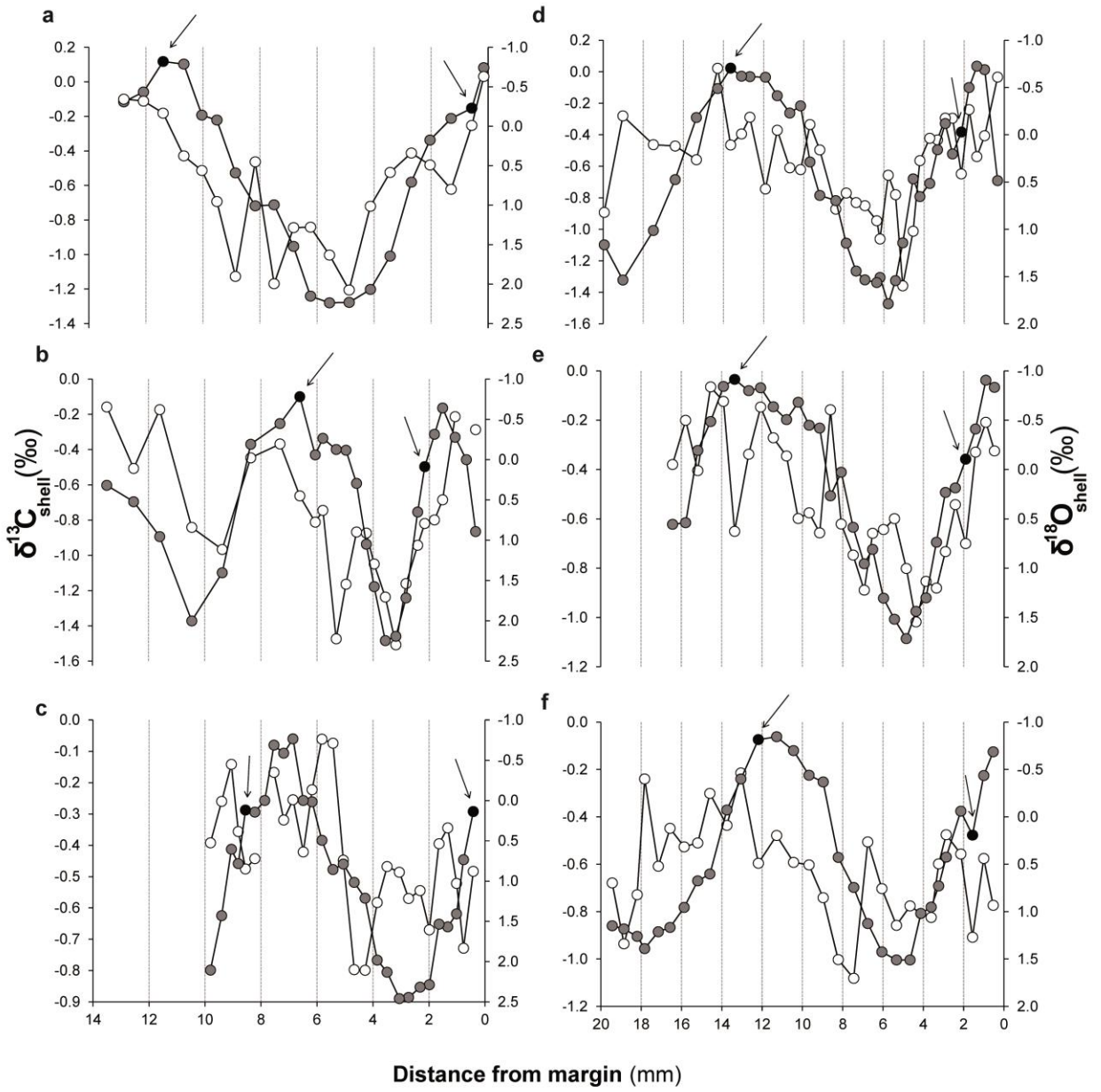

Figure 4.4.2. Isotopic composition of $\delta^{18}O$ (grey circles) and $\delta^{13}C$ (white circles) from sampled shells at each location. The oxygen data is presented on a reversed scale to simplify the interpretation in terms of temperature. Replicates from Pag (**a**) AC1, (**b**) AC2 and (**c**) AC3 and from Cetina (**d**) CC1, (**e**) CC2 and (**f**) CC3. Black circles represent the edges of the annual period used to calculate growth rates.

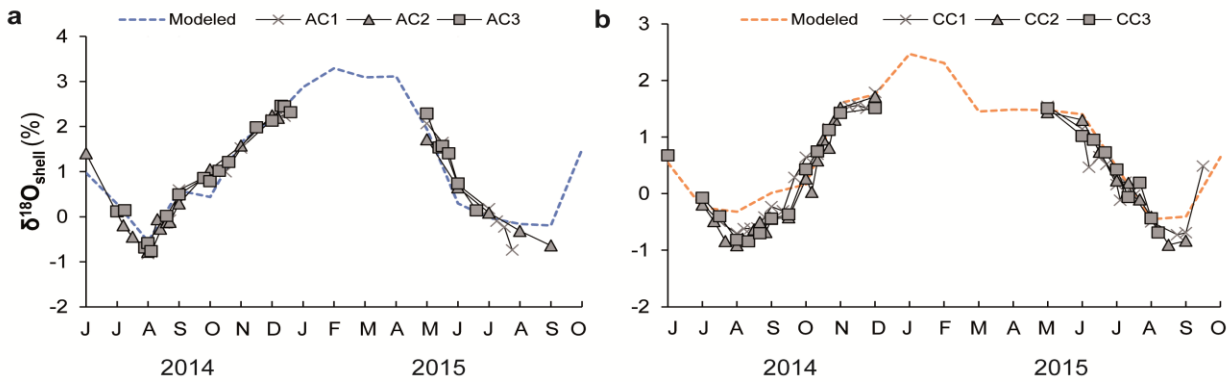

Figure 4.4.3. Alignment of each $\delta^{18}O_{shell}$ values using the modeled $\delta^{18}O_{shell}$ according to sampling sites (**a**) Pag and (**b**) Cetina.

Based on the $\delta^{18}O_{shell}$ alignment, estimation of growth rates was accomplished by considering one annual cycle, from August to July, except for AC3 which were calculated between July and June (Fig. 4.4.5).

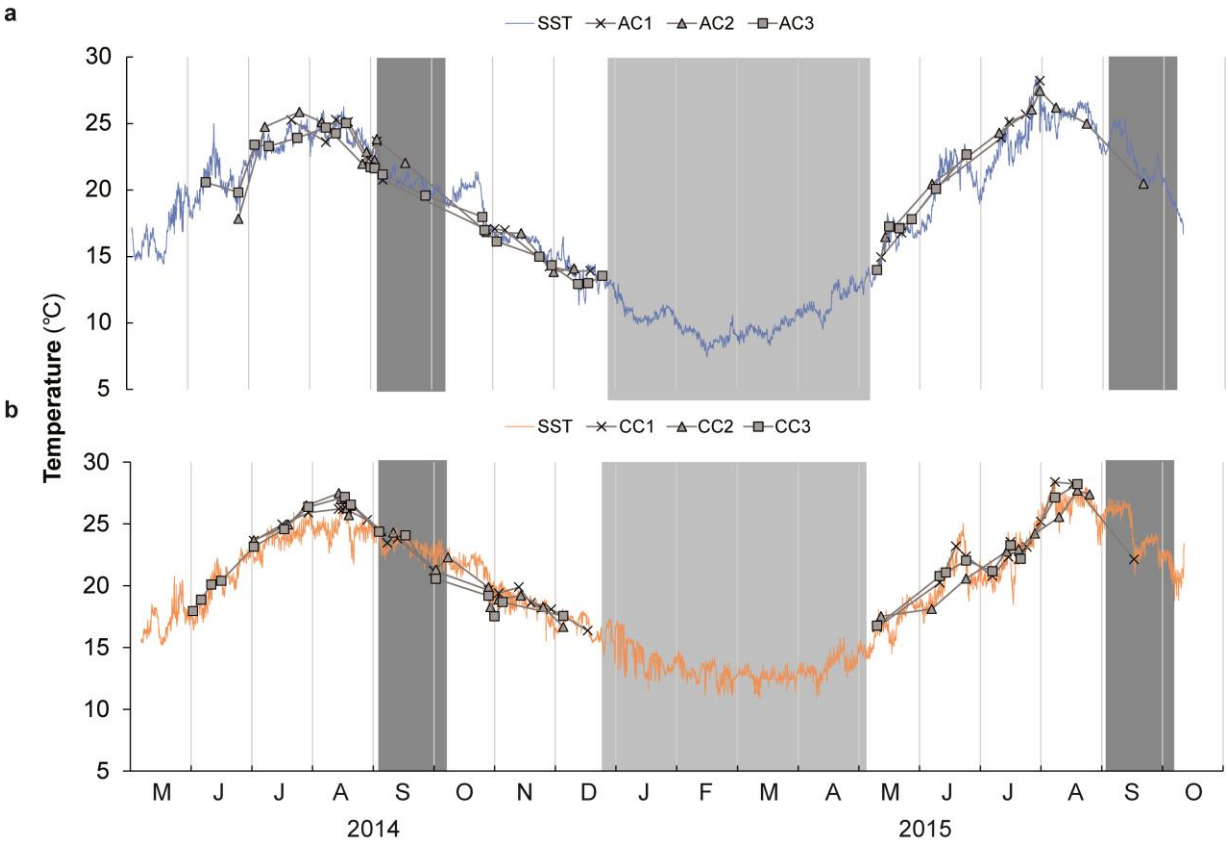

Figure 4.4.4. Temporal alignment of reconstructed $\delta^{18}O_{shell}$ temperatures from instrumental SST in (**a**) Pag and (**b**) Cetina. Dark shaded area represents the approximate period of growth line formation. Light shaded area represents a period of slow/negligible growth.

Data for monthly mean growth rates is presented in percentages showing the seasonal patterns of annual shell growth within a one year period. The highest growth rates occurred during the summer months, while a decreasing tendency was shown towards the winter and this started to increase in the following spring. Some differences between sites were observed. In Pag, decreasing growth rates were not as sharp as in Cetina, particularly during fall; similarly, the increasing growth rates during spring were uninterrupted in Cetina, while in Pag showed some decrease at the beginning of summer. Shell growth rates between January and April were extremely low or rather negligible at both sites, as supported from microstructure results (data not shown).

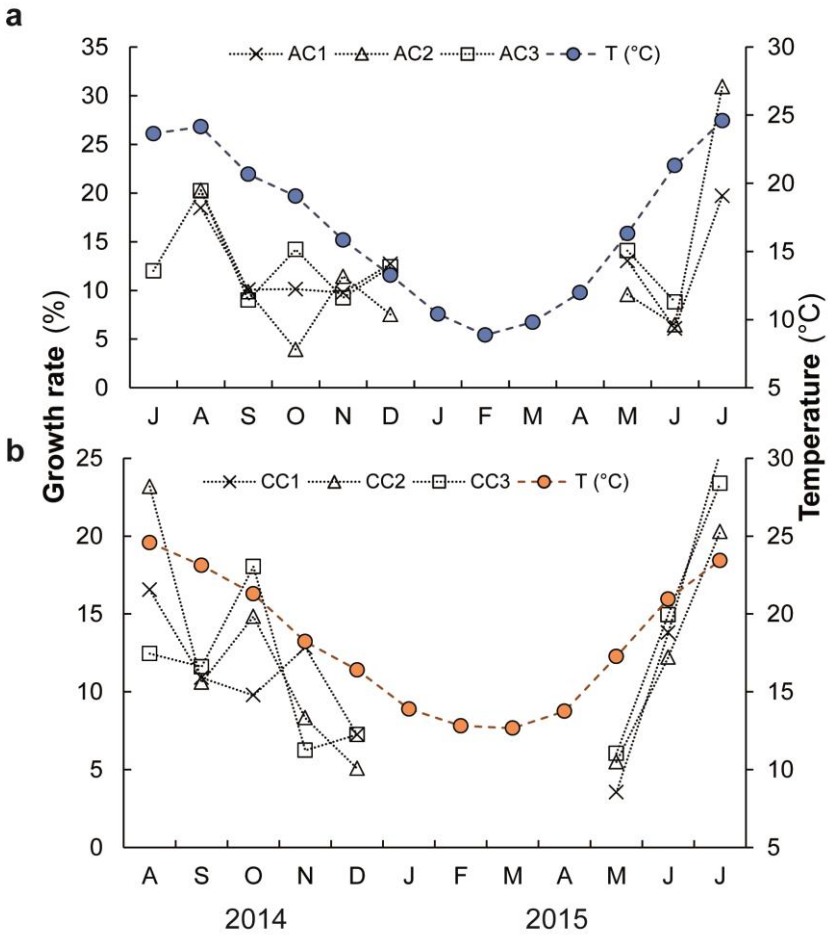

Figure 4.4.5. Seasonal changes in the monthly shell growth rates (%) for each replicate of *Callista chione* at (**a**) Pag and (**b**) Cetina and corresponding temperature values (colored circles) at each site.

4.4.1.1. Correlating growth with environmental and biological variables

The test the potential influence of environmental (temperature, salinity and precipitation) and biological variables ($\delta^{13}C$ and C:N ratios from suspended particulate matter and GSI) on *C. chione* shell growth, we compared these set of data to estimated shell growth rates.

Shell growth rates and **temperature** were positively correlated both in Pag ($r = 0.84$, $P < 0.01$) and Cetina ($r = 0.94$, $P < 0.01$) (Figs. 4.4.6 and 4.4.7). A stronger correlation in Cetina is evidenced by the decreasing shell growth rates between August and December and the increasing values between May and July, along with seawater temperature records. In comparison with the preceding and following months, the growth rates in October 2014 were remarkably high. This month was characterized by unusual high temperatures following a colder and rainier September than previous years. Salinity and precipitation did not significantly correlate with shell growth rates (all at $P > 0.05$) (Figs. 4.4.6 and 4.4.7).

By comparing shell growth rates with **GSI** values, fast shell growth rates occurred in specimens from Pag during December, coinciding with the beginning of gametogenesis. This would suggest a low energy investment on gonadal mass, as shown by low GSI values (Fig. 4.4.8), although no significant correlation was observed between both shell growth rates and GSI ($r = -0.50$, $P > 0.05$) (Fig. 4.4.6). In contrast, at Cetina specimens a higher investment in gonadal development was shown in both November and December which could likely explain the lower shell growth rates observed these periods, as strengthened by the high negative correlation between both variables ($r = -0.83$, $P < 0.01$). Despite the synchronous timing of negligible shell growth, some differences between sites were also observed in relation to the gonadal production. In Pag, June was the month with the highest GSI values prior to the spawning timing and showed lower growth rates than the previous month. After spawning, both sites showed increasing percentages in shell growth rates which were tightly coupled to temperature and food supply. The temporal variation in BMI was not correlated to shell growth rates.

The carbon isotope and C:N molar ratios measured from the suspended particulate matter were used as **food quality** indices. $\delta^{13}C_{SPM}$ showed a positive correlation with shell growth rates at Pag ($r = 0.64$, $P < 0.001$) but none from Cetina (all at $P > 0.05$), whereas the C:N ratio was not significantly correlated to shell growth rates at any site (all at $P > 0.05$).

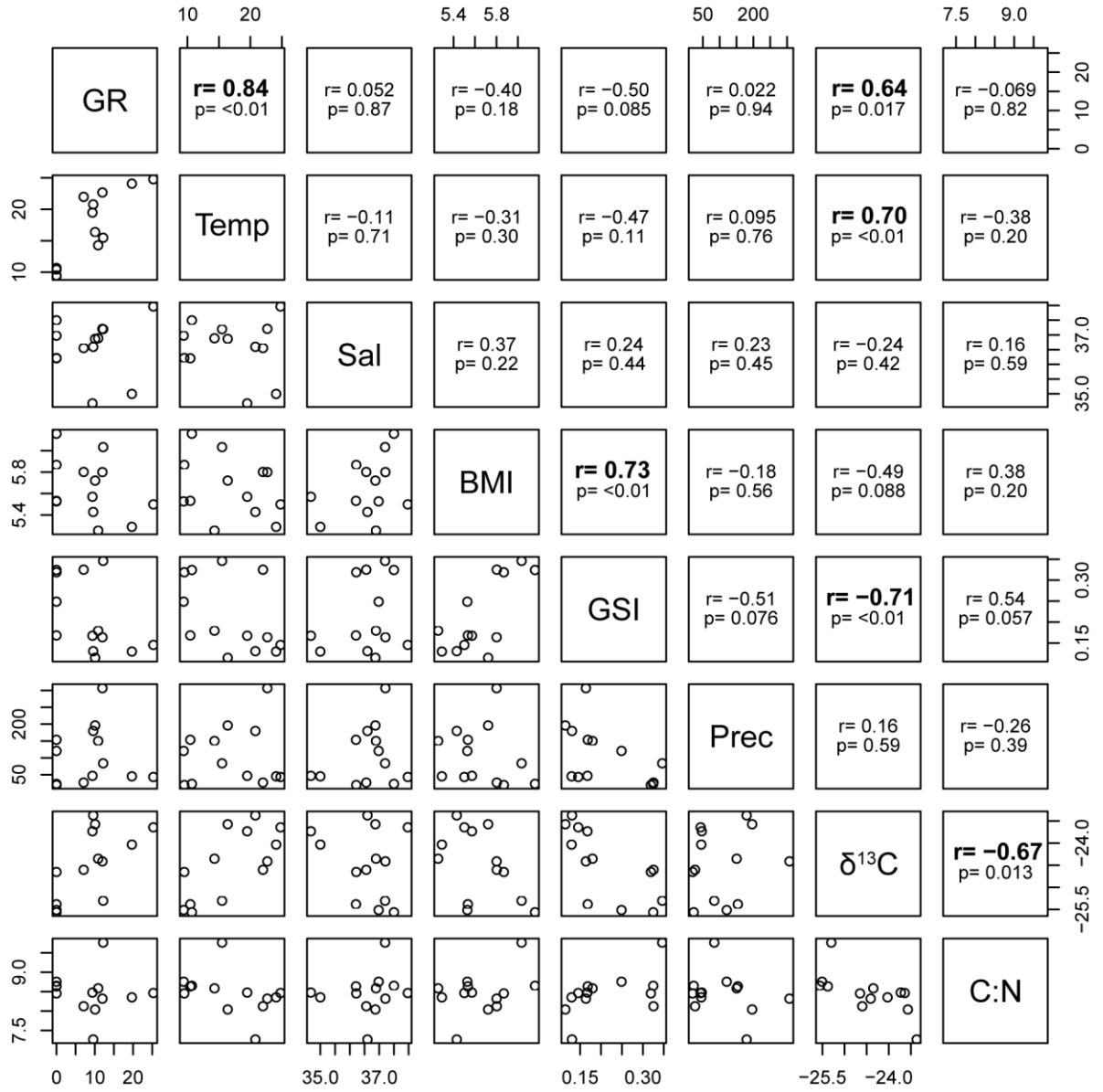

Figure 4.4.6. Scatter-plot matrix displaying the correlation output in Pag between monthly mean values of growth rates (GR), temperature (T), salinity (S), body mass index (BMI), gonadosomatic index (GSI), precipitation (Prec), $\delta^{13}C_{SPM}$ ($\delta^{13}C$) and $C{:}N_{SPM}$ molar ratio (C:N).

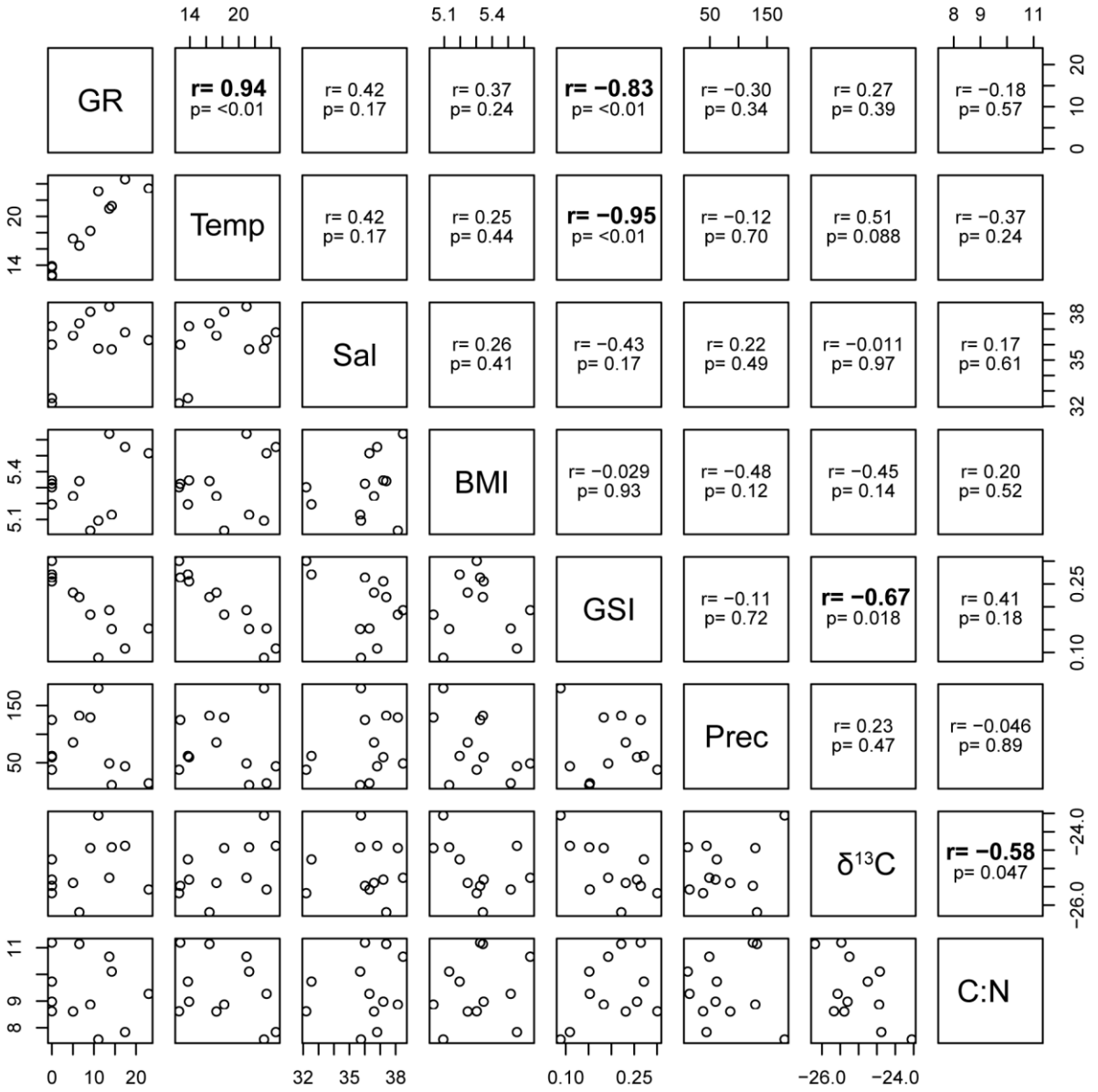

Figure 4.4.7. Scatter-plot matrix displaying the correlation output in Cetina between monthly mean values of growth rates (GR), temperature (T), salinity (S), body mass index (BMI), gonadosomatic index (GSI), precipitation (Prec), $\delta^{13}C_{SPM}$ ($\delta^{13}C$) and $C{:}N_{SPM}$ molar ratio (C:N).

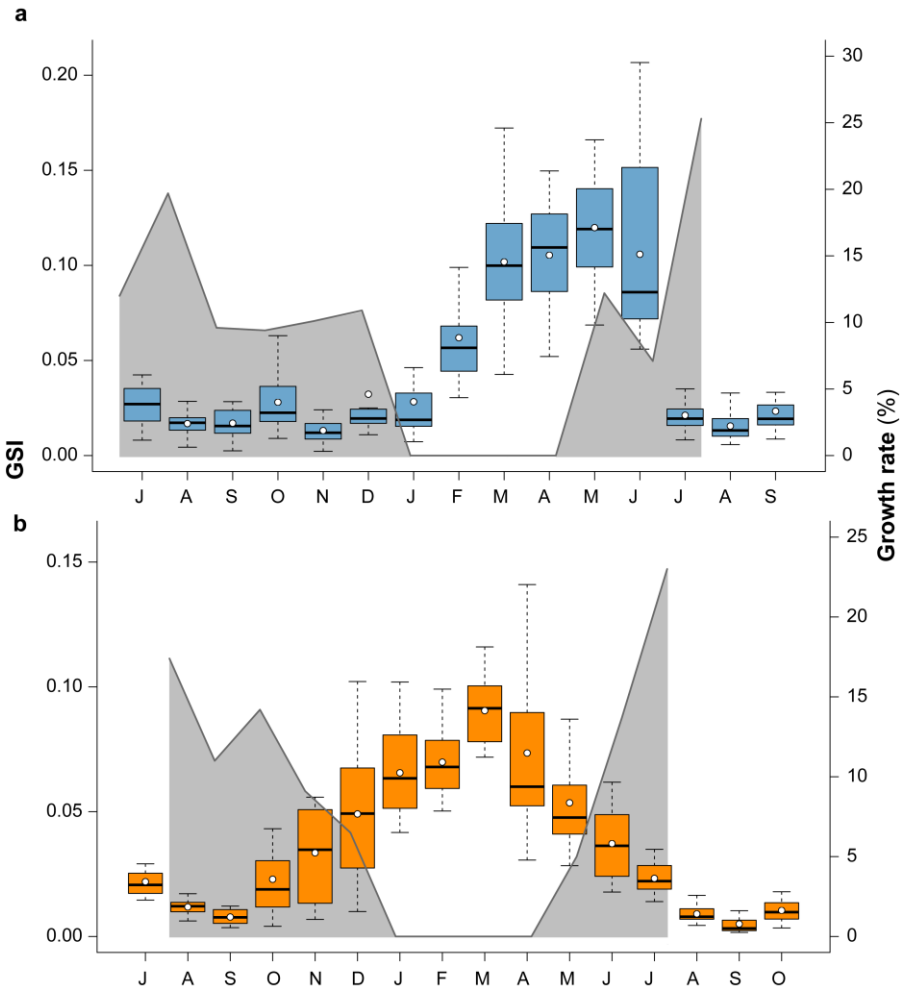

Figure 4.4.8. Combined gonadosomatic index (GSI) and mean growth rates of *C. chione* within a year period in (**a**) Pag and (**b**) Cetina

4.4.2. Micromilling in the cross-sectioned valve of *Glycymeris bimaculata*

Geochemical analysis in adult specimens of *Glycymeris bimaculata* through continuous-sampling also revealed sinusoidal shell $\delta^{18}O_{shell}$ curves (Fig. 4.4.9). Complete annual intervals were covered for AB1, AB3 and CB2, whereas CB1 and CB3 covered half curves between maximum and minimum $\delta^{18}O_{shell}$ values. Seasonal $\delta^{18}O_{shell}$ amplitudes from Pag shells were from -0.49 to 1.84‰ in AB1 and from -0.47 to 1.67‰ in AB3. Those in analyzed shells from Cetina ranged from -0.83 to 2.24‰ in CB1, from -0.33 to 1.54‰ in CB2 and from -0.57 to 2.44‰ in CB3.

The seasonal $\delta^{13}C_{shell}$ amplitudes from Pag ranged from 0.03 to 1.25‰ in AB1 and from -0.52 to 0.38‰ in AB3. In analyzed samples from Cetina these amplitudes ranged from 0.35 to 1.77‰ in CB1, from 0.33 to 0.95‰ in CB2 and from 0.49 to 1.72‰ in CB3. Correlations between $\delta^{18}O_{shell}$ and $\delta^{13}C_{shell}$ varied between specimens, showing a significant positive correlation in AB3 and negative correlations in the other

sampled shells, although only in CB1 and CB3 these were significant (Table 4.4.2). These last results from Cetina specimens could be biased since they include just half of the annual signal.

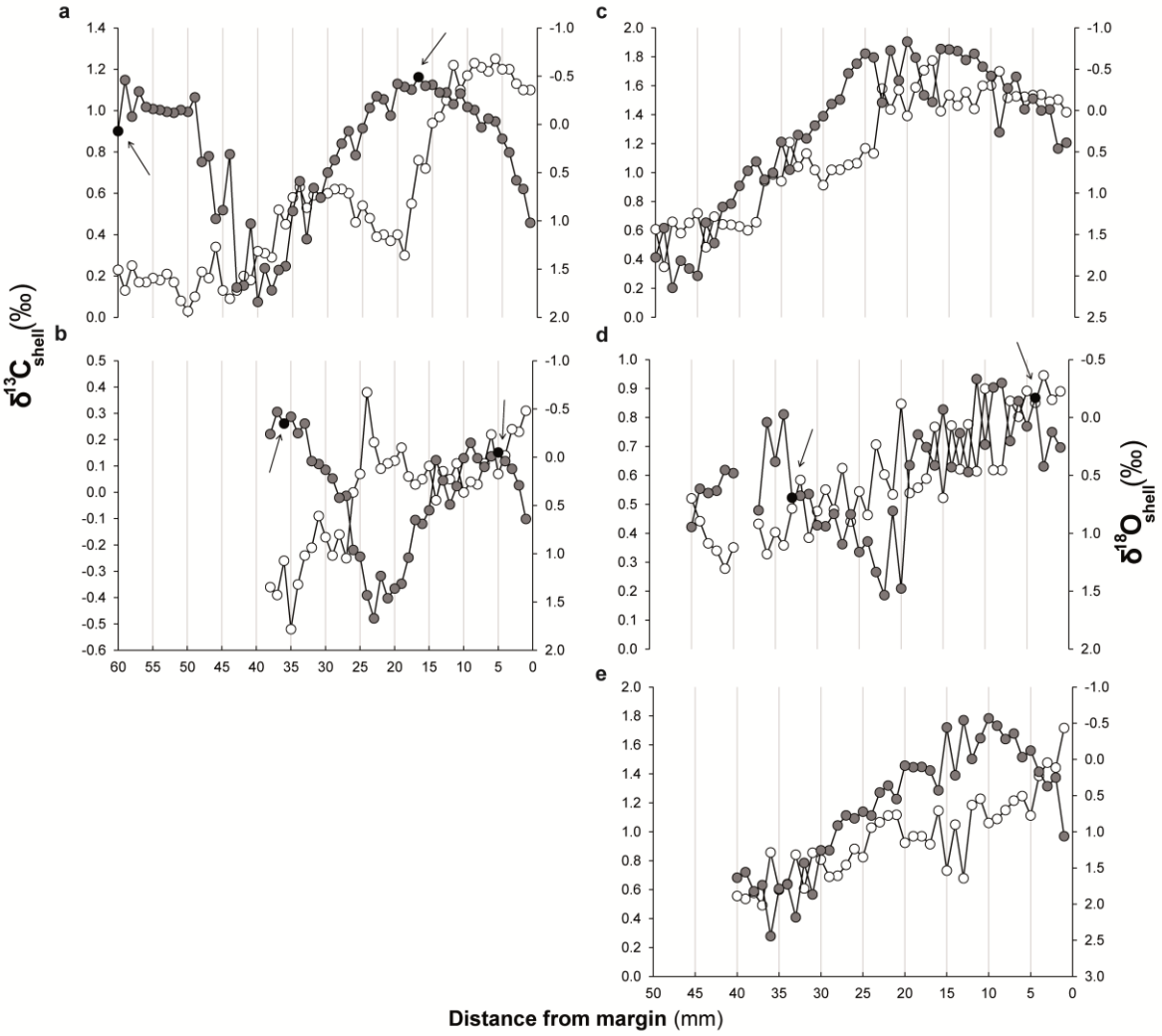

Figure 4.4.9. Isotopic composition of $\delta^{18}O$ (grey circles) and $\delta^{13}C$ (white circles) from sampled shells at each location. The oxygen data is presented on a reversed scale to simplify the interpretation in terms of temperature. Two replicates from Pag (**a**) AB1 and (**b**) AB3 and three from Cetina (**c**) CB1, (**d**) CB2 and (**e**) CB3. Black circles and arrows represent the edges of the annual period used to calculate growth rates.

Macroscopic observations of growth lines and growth increments on the cross-sectioned valves was sometimes indiscernible and they were easier to distinguish in the hinge region (Fig 4.4.10). Estimated age of individuals from Pag was ca. 16 (AB1) and 25 (AB3) years whereas those from Cetina were aged 10 (CB1), 13 (CB2) and 13 (CB3) years.

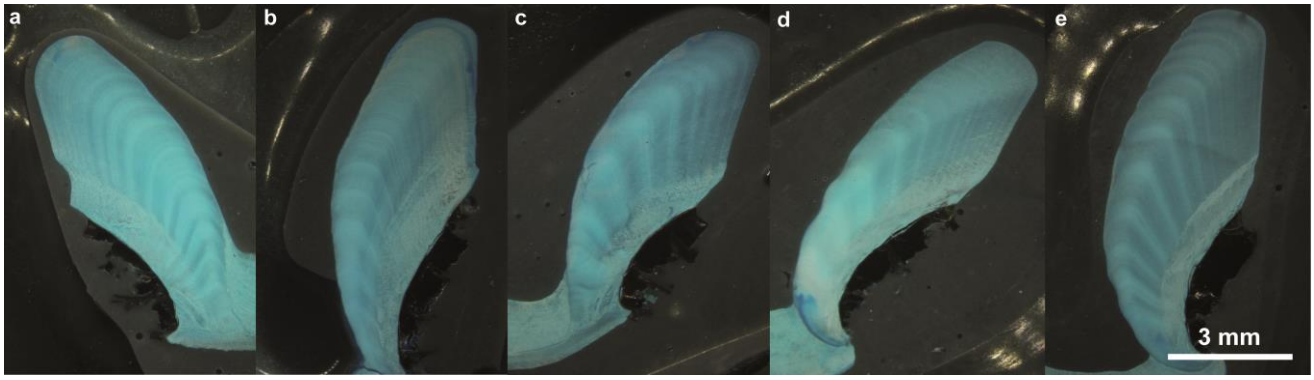

Figure 4.4.10. Mutvei staining to age *Glycymeris bimaculata* shells from hinge cross-sections. Specimen IDs: (**a**) AB1, (**b**) AB3, (**c**) CB1, (**d**) CB2 and (**e**) CB3.

The curve-fitting algorithm on $\delta^{18}O_{shell}$ values had R^2 of 0.85 and 0.91 from Pag specimens (AB1 and AB3, respectively) and 0.93, 0.73 and 0.93 from Cetina specimens (CB1, CB2 and CB3, respectively). These values were used to firstly align them with modeled $\delta^{18}O_{shell}$ values derived from $\delta^{18}O_{water}$ reconstructions per each month (Fig. 4.4.11).

Reconstructed temperatures in Pag ranged from 13.4 to 27.1°C in AB1 and 15.2 to 26.0°C in AB3, whereas in Cetina ranges oscillated between 14.0 to 28.9°C in CB1, 17.4 to 26.5°C in CB2 and 13.5 to 27.7°C in CB3. These values are within the range of maximum recorded temperatures which were 28.6°C at both sites. Minimum temperatures were 7.4°C at Pag and 10.9°C at Cetina indicating a growth shutdown during the coldest period of the year (Fig. 4.4.12).

Table 4.4.2. Summary of stable isotope values determined in adult shells of *Glycymeris bimaculata* from Pag (AB1 and AB3) and Cetina (CB1-CB3). Juvenile shell values of *G. bimaculata* are also included (AB68 and AB69). All values are reported in ‰ (VPDB standard). Pearson correlation between $\delta^{18}O_{shell}$ and $\delta^{13}C_{shell}$ for each specimen at * P < 0.05 and ** P < 0.001.

ID	$\delta^{18}O_{shell}$				$\delta^{13}C_{shell}$				Pearson correlation	
	Average	Max	Min	Amplitude	Average	Max	Min	Amplitude	R	P
AB1	0.28	1.84	-0.49	2.33	0.55	1.25	0.03	1.22	-0.164	0.207
AB3	0.39	1.67	-0.47	2.14	-0.01	0.38	-0.52	0.90	0.604	<0.001**
CB1	0.25	2.14	-0.83	2.98	1.16	1.77	0.35	1.43	-0.775	<0.001**
CB2	0.48	1.54	-0.33	1.87	0.63	0.95	0.33	0.62	-0.172	0.308
CB3	0.65	2.44	-0.57	3.01	0.96	1.72	0.49	1.22	-0.519	<0.001**
AB68	0.71	2.07	-0.61	2.68	0.78	1.04	0.57	0.47	-0.359	<0.189
AB69	0.72	2.62	-0.73	3.35	0.71	1.23	0.17	1.06	0.256	0.172

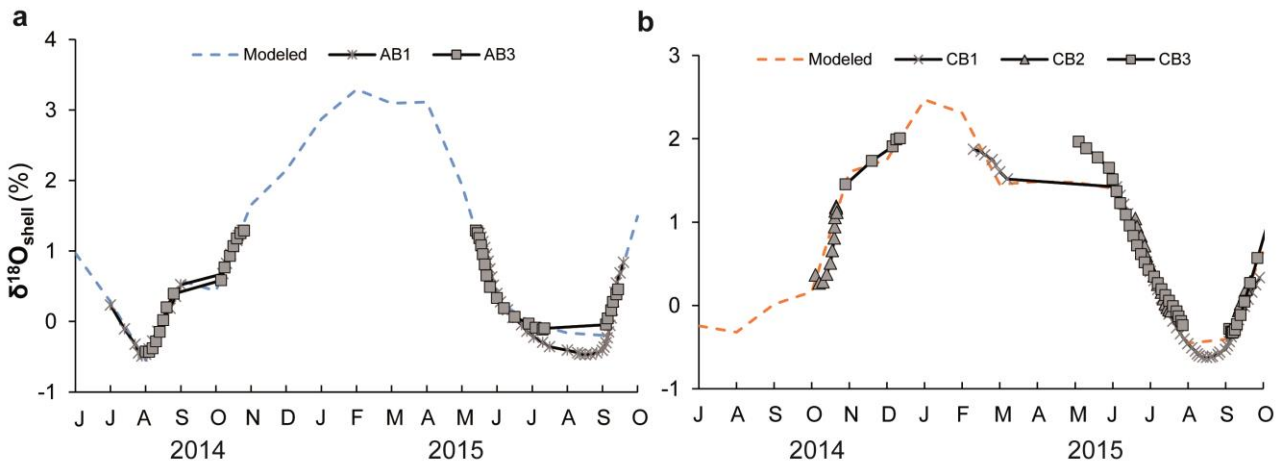

Figure 4.4.11. Alignment of each $\delta^{18}O_{shell}$ values using the modeled $\delta^{18}O_{shell}$ in (**a**) Pag and (**b**) Cetina.

The estimation of growth rates was only possible for the two specimens from Pag which covered a complete annual period with sufficient high resolution. Periods with the highest growth in AB1 were June with 13.6%, August with 22.7% and July with 29.5%. In shell AB3, the highest growth rate periods were May with 16.1%, July with 22.6% and June with 25.8%. Months with the lowest shell growth were November with 4.5 and 6.5% and December with 4.5 and 0% for AB1 and AB2, respectively. The CB2 specimen from Cetina suggested June and July to be the months with the highest shell growth rates, although a more detailed study of this and other replicates is needed. Therefore, statistical analysis with environmental and biological indices were not performed due to lack of enough specimens to corroborate these results. Notwithstanding, based on the availability of environmental and biological data, some relationships can be drawn which are discussed further on.

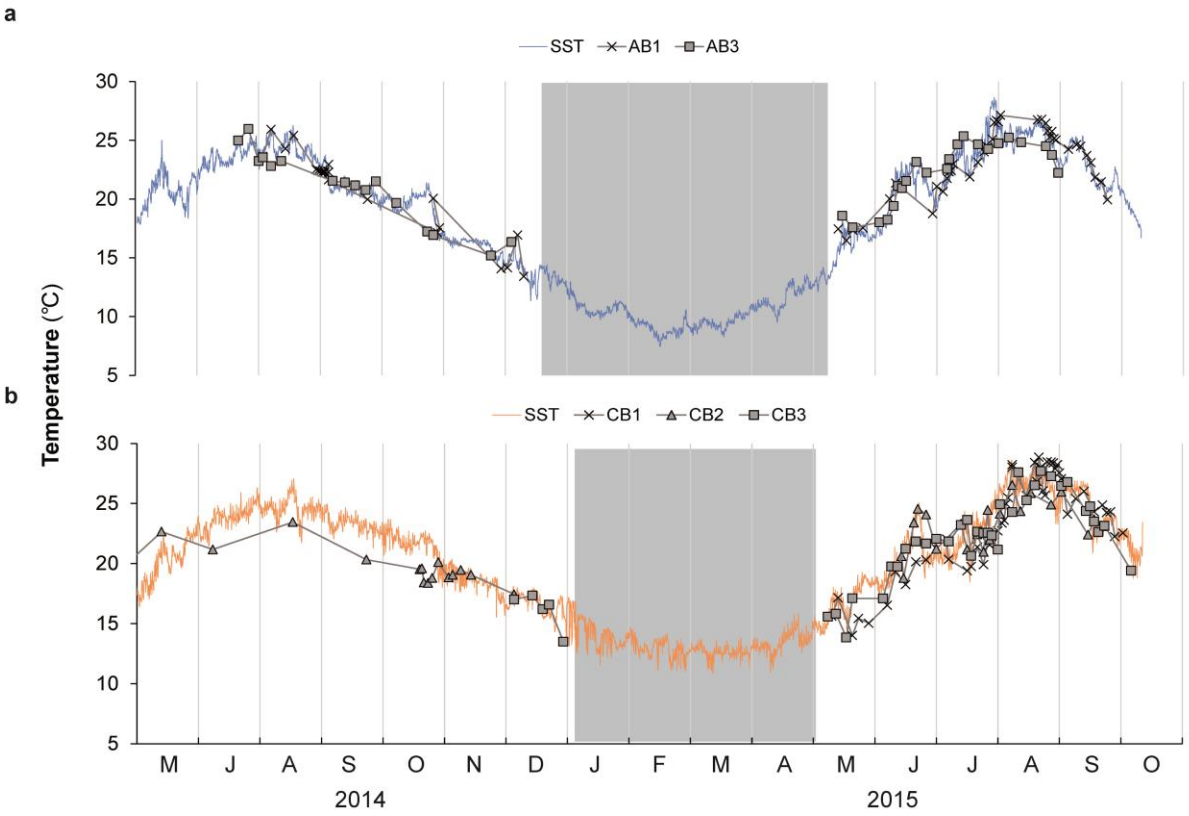

Figure 4.4.12. Temporal alignment of reconstructed $\delta^{18}O_{shell}$ temperatures from instrumental SST in (**a**) Pag and (**b**) Cetina. Shaded area represents a period of slow/negligible growth.

Oxygen and carbon isotope values obtained from drilled samples in two *G. bimaculata* juveniles are displayed in Table 4.4.2. There were no significant correlations between intra-annual isotopic values (all at $P > 0.05$). Based on these results and in macroscopic observations of the growth line formation, this took place around the $\delta^{18}O_{shell}$ minima in both sampled three year old specimens. The timing of growth line formation was representing the highest temperatures in 2 (AB68) and 3 (AB69) consecutive years (Fig. 4.4.13).

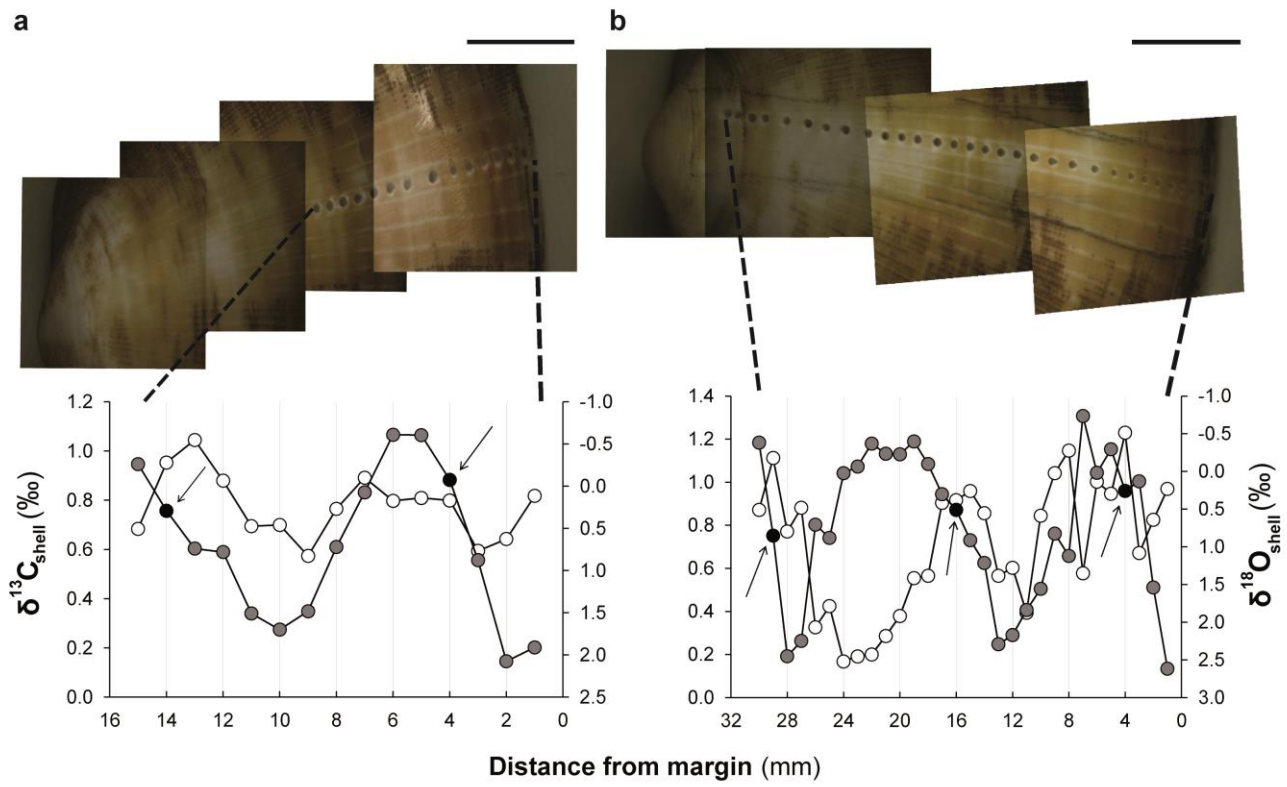

Figure 4.4.13. Isotopic composition of $\delta^{18}O$ (grey circles) and $\delta^{13}C$ (white circles) in two *Glycymeris bimaculata* juvenile shells (**a**) AB68 and (**b**) AB69 from Pag site. Scale bar 50 mm. The oxygen data is presented on a reversed scale to simplify the interpretation in terms of temperature.

An estimation of metabolic carbon in *G. bimaculata* shells was performed. Although the full annual variability of $\delta^{13}C_{DIC}$ could not be captured throughout the year, the average of 4 samples (0.02‰) collected between July and October 2015 was used and calculated in Equation 3 (see 3.5.2). The $\delta^{13}C_{shell}$ represents the mean composition of three replicated shells (CB1-CB3; 0.92), $\varepsilon_{shell\text{-}HCO3^-}$ of 2.7‰ and $\delta^{13}C$ from digestive gland tissue of sampled specimens (-23.45‰) was used to represent $\delta^{13}C_M$. This organ was used since it has the highest carbon incorporation compared to gonad > adductor muscle (Paulet et al., 2006). Therefore, it is the best organ to use so $\delta^{13}C$ variations, which are linked to organ activity and growth, are removed.

5. DISCUSSION

5.1. Feeding

5.1.1. Characterization of food sources

In coastal zones, marine particulate organic matter is composed of a mixture of living and detrital material derived from plankton, bacteria, fecal pellets or zooplankton remains such as exoskeletons (Savoye et al., 2012; Berto et al., 2013). To our knowledge, this is the first study investigating the biochemical composition of particulate matter at an interannual scale (17 months) in the central eastern Adriatic. Additionally, the biochemical composition of suspended particulate matter was measured at an intra-annual scale (12 months) in Pašman. Results from parameters measured in the water column showed negligible spatial differences in SPM, Chl *a*, BSi, lipids and C:N molar ratios and isotopic composition ($\delta^{13}C$, $\delta^{15}N$) signatures but revealed large temporal variations. These variations were consistent with the environmental conditions in the area (i.e. light, temperature) which are known to influence, among others, isotopic fractionation (Fry, 2006). The observed temperature and salinity values at all study sites are typical for coastal eastern Mediterranean waters (Vilibić et al., 2015).

5.1.1.1. Identifying the origin of organic matter through stable isotope analysis

As indicated by the $\delta^{13}C$ pattern, a mixed terrestrial-riverine and marine OM origin characterized SPM, typical of these types of environments (Fig. 4.2.1c) (e.g. Savoye et al., 2003; Berto et al., 2013). Isotopically lighter carbon was observed during winter and spring (down to -26‰) likely due to high precipitation events associated with river discharge. In contrast, more enriched $\delta^{13}C$ values during summer and fall (up to -22.8‰) were closer to those of coastal marine environments (~-22‰ in marine phytoplankton) (Fry et al., 1984; Harmelin-Vivien et al., 2008) suggesting a progressive mixing of terrestrial and marine materials after phytoplankton blooms.

Few previous studies have reported the isotopic composition of sediment in the Adriatic Sea, and these were conducted in its northern part (Ogrinc et al., 2005) or in the open sea (Faganeli et al., 1994). Unlike SPM, large spatial rather than temporal variations were shown in the carbon isotope values, which averaged -22±0.4‰ at Pag and -26±0.2‰ at Cetina. These ranges are within those reported in Ogrinc et al., (2005), Faganeli et al., (2009) and Žvab-Rožić et al., (2015) which studied locations that receive both marine and terrigenous origin inputs as also shown in other estuarine influenced coastal systems (e.g. Ramaswamy et al., 2008). The differences between SPM and Sed pools at each site may reveal

differences in organic matter sources throughout the year, suggesting a shift of available material at the water-sediment interface. In Pag, a more enriched $\delta^{13}C$ in the upper sediment layer could be attributed to resuspension of fresh material induced by Bora wind events or to microphytobenthic production, which could significantly contribute in other areas in the Adriatic Sea (Šestanović et al., 2009). The Bora is a katabatic wind, most common in winter, blowing from the northeast with gusts up to 200 km/h, inducing big waves and resuspension in the Adriatic Sea. These events are particularly strong and recurrent in this area (Surić et al., 2015), enhancing recycling of nutrients (Berto et al., 2013), hence production. Also, the degradation of ^{13}C-enriched mixture of organic matter such as macroalgae detritus could be associated with this isotopic carbon enrichment (Dias et al., 2016). In contrast, the proximity to the river mouth suggests that the influence of terrestrial matter in Cetina could be responsible for the ^{13}C-depleted signal as it occurred in other estuarine areas (Hedges et al., 1997).

Interpreting the nitrogen isotope signal is not straightforward due to the potential contribution of more than one nitrogen source, namely N_2, NO_3^-, NH_4^+ or DON (e.g. Berto et al., 2013; Currin et al., 1995; Peterson, 1999). The range of the $\delta^{15}N$ signature of phytoplankton and bacterioplankton is of the order of -2 to 5‰ (Rees et al., 2006). The oligotrophic nature of the Eastern Mediterranean basin is ^{15}N-depleted in OM (Pantoja et al., 2002; Sachs & Repeta, 1999) as it is in other oligotrophic areas, e.g. Sargasso Sea (Montoya et al., 2002). The $\delta^{15}N_{SPM}$ ranges in Pag (1.6 to 6.1‰), Cetina (2.5 to 5.5‰) and Pašman (3.1 to 5.9‰) were within those previously reported for the Adriatic (Žvab et al., 2010; Žvab Rožič et al., 2015; Faganeli et al., 2009) and other Mediterranean areas (Vizzini & Mazzola, 2006; Carlier et al., 2007; Carlier et al., 2008). The mixture of freshwater and marine water was expected to occur in all study sites. In Cetina, there is the influence of the river, whereas in Pag and Pašman the influence comes from the underground freshwater discharges typical of the karstic nature of the area (Hamer et al., 2010; Surić et al., 2015). This is supported by the significant temporal variation in ~4‰ units observed along the sampled period where peaks (Figs. 4.2.1d, 4.3.2.1) coincided with months with high precipitation events (Fig. 4.1) which potentially enhanced this enrichment. These episodic peaks might be related to a higher river discharge (Cetina area) and to pulses of underwater springs (characteristic from Pag and Pašman areas) (Surić et al., 2015) which seem to increase the nitrogen isotopic composition. The influence of karstic springs on SPM has also been reported in a Mediterranean lagoon with $\delta^{15}N$ values of 4.9‰ (Carlier et al., 2015), and in environments associated with pristine soils and terrestrial plant organic matter (Peterson et al., 1987). Further, bacteria, zooplankton and fecal pellets have greater $^{15}N/^{14}N$ ratios than phytoplankton (Minagawa & Wada, 1984; Vander Zanden & Rasmussen, 2001); therefore a higher content of degraded phytoplankton material (Harmelin-Vivien et al., 2008) could increase the signal in months with higher $\delta^{15}N_{SPM}$ values.

In the sediment layer, more depleted and variable $\delta^{15}N$ values were observed at Pag (ranging from 3.9 to -2.3‰) in contrast to more constant but also relatively low values in Cetina. This is probably supported by a rather constant discharge from the Cetina river throughout the year (Bonacci & Roje-Bonacci, 2003), averaging 2.3±0.2‰, similar to those in Mediterranean estuarine areas (Carlier et al., 2007). Relatively low $\delta^{15}N$ values in organic matter deficient sediments, as indicated by light $\delta^{13}C$ in Cetina, have been attributed to the diagenetic alteration of nitrogen isotopic ratios in the presence of oxygen (Sachs et al., 1999). However, the present results cannot test this hypothesis. In oligotrophic water bodies, diazotroph biomass is responsible for atmospheric nitrogen fixation (Rees et al., 2006; Pantoja et al., 2002; Wada et al., 2012), particularly by blue-green algae (Currin et al., 1995; Minagawa & Wada, 1986). Studies of cultured cyanobacteria revealed that nitrogen isotope ratios ranging from -1.5 to -3.0‰ during N_2 fixation were associated with high $\delta^{13}C$ in cyanobacteria cells (Wada et al., 2012). Such negative values were found in the sediment samples from Pag. Additionally, studies of cyanobacteria in sedimentary organic matter in the NW Mediterranean with $\delta^{15}N$ ranges from -2 to 2‰ support this explanation (Kerhervé et al., 2001). Also, in the Eastern Mediterranean $\delta^{15}N$ values ~-2‰ are suggested to be a result of remineralization of organic matter (Möbius, 2013). Low $\delta^{15}N_{Sed}$ could also be attributed to the excess of P from enhanced riverine inputs and changes in the composition of sediment (Krom et al., 2004). Within the overall assumptions, these results support the hypothesis that more depleted and variable $\delta^{15}N_{Sed}$ values in Pag were likely associated with benthic bacteria, probably related to diazotroph biomass, suggesting that nitrogen fixation is a main contributor to the $\delta^{15}N$ signal in PON. Other reports of anthropogenic influence reported $\delta^{15}N$ values > 10‰ in the particulate matter (Cifuentes et al., 1988; Carlier et al., 2008; Puccinelli et al., 2016; Žvab Rožič et al., 2015; Liénart et al., 2016) which are far outside the ranges observed in this study for both pools.

5.1.1.2. Biogenic parameters as indicators of particulate matter quality

Another indicator commonly used to identify degraded marine organic matter and distinguish marine from terrestrial OM is the C:N Redfield ratio, which associates the value of ~6 with live phytoplankton (Redfield, 1958). The presence of fresher material in Pag was suggested by the constant $C:N_{SPM}$ values close to those of marine derived phytoplankton (4 – 8) (e.g. Schubert & Calvert, 2001) throughout the year. At Cetina, $C:N_{SPM}$ ranges from 7 to 11 represented a mixture of phytoplankton with marine degraded and/or terrestrial OM as seen in other estuarine systems (Hedges et al., 1997; Dias et al., 2016; Savoye et al., 2003). The presence of several C:N ratio peaks (e.g. October 2014, December, February and June 2015; Fig. 4.2.1b) was most probably related to resuspension events, supported by the coincidence with high suspended particulate matter values, which may reflect the incorporation of

degraded material into the water column. At Pašman, $C:N_{SPM}$ ranges were closer to those from Cetina (7.8–11.6) but the temporal pattern resembled that in Pag, except for a peak shown in spring. The low relationship between $C:N_{SPM}$ and biogenic silica at all sites strengthens the view that fresh siliceous phytoplankton is not a main constituent of the OM in the water column and that other inputs of organic carbon, e.g. terrestrial, or degraded marine material may be more abundant. Bacterial cells have lower C:N than phytoplankton due to preferential mineralization of N (Newton et al., 1994); therefore, in periods of food scarcity, C:N ratios may decrease due to bacterial presence.

The sediment at Pag showed a large temporal variation in the C:N ratio with lower values during fall and winter suggesting higher abundance of bacteria during those months, on the same direction as the N isotopic signature (Fig. 4.2.1b,d). The spring peak observed at this site strongly suggests that an important terrestrial input took place during this season which is further supported with FA results (discussed in the next section). In Cetina, $C:N_{Sed}$ ratios were more constant averaging 7.7 and a high percentage of biogenic silica was observed, suggesting a relatively high concentration of fresh OM with diatom abundance. Contrastingly, the FA marker for diatom was quite low (as discussed in the next section). Therefore, the presence of empty frustules better explain the high BSi values and gives further support to the presence of bacteria in the OM pool. This is supported by the fact that the low %C and %N in the sediment are in the range of those reported in the Adriatic, 0.5-1.3 %C and 0.1-0.17 %N (Ogrinc et al., 2005) and 0.02-0.15 %N (Matijević et al., 2009), corroborating the poor nutritional quality of the sediment in this oligotrophic basin.

In addition, the POC/Chl *a* ratio was explored, finding that all values were > 200 indicating the strong presence of heterotrophic/mixotrophic organisms (Galois et al., 1996; Bentaleb et al., 1998) as reported in estuarine areas in the Adriatic Sea (Šolić et al., 2015). Overall, the temporal variations observed at local scales are common in temperate coastal ecosystems, especially within the influence of river mouth areas (Cresson et al., 2012; Berto et al., 2013).

5.1.1.3. Identifying the composition of organic matter through fatty acid analysis

Along with SI estimates, FA patterns showed seasonal changes within the pool of SPM elucidating different sources of organic matter at both analyzed sites, Pag and Cetina. The most important components of SPM and Sed lipids were 14:0, 18:0, 18-1(n-9), 20:1, 20:0 and detrital FA (Fig. 4.2.2). Within SFA, C20:0 was higher during winter and this FA has been linked to bacteria associated with detrital matter (Galap et al., 1999), which were more abundant in Pag, coincident with SI results. The

high proportion of MUFA, 16:1, 18-2(n-6) and detrital FA in Cetina suggested that terrestrial sources predominate in the OM in SPM also supporting the observations of SI results. Usually, the FA marker C18:2(n-6) is associated with terrestrial sources (Budge et al., 1998; Parrish et al., 1996; Fischer et al., 2014), seagrass (Kharlamenko et al., 2011), protozoa (Zhukova et al., 1999) and even agricultural products (Napolitano et al., 1997). This FA marker has also been associated with brown algae when coupled to higher concentrations of 18:3(n-3) (Li et al., 2002). In the present study this coupling was not observed; thus, brown algae are unlikely to be responsible for this marker increase, hypothesizing that seagrass, which is present at both sites but particularly in Cetina (pers. obs), might be responsible for the observed values. The FA 18:1(n-9) was particularly abundant during spring and summer, and besides its association with zooplankton (Sargent et al., 1988) it has also been related to cyanobacteria (Antonio et al., 2016b), again supporting the results of SI analyses. The best OM quality indicated by high PUFA concentrations took place during summer and was higher in Pag, in agreement with relatively low C:N and high BSi_{SPM} values. Accordingly, phytoplankton represented by diatom (EPA) and dinoflagellate (DHA) markers were most abundant during this period and least abundant in the fall (Fig. 4.2.2).

Herbivorous calanoid copepods markers were more abundant in Cetina during fall and winter, apparently following the phytoplankton peaks. The Chl *a* pattern from monthly values in this study, Chl *a* derived from satellite observations (Fig. S1), and data from previous studies in the eastern Adriatic, showed that the highest phytoplankton biomass develops during fall-winter and spring and is followed by summer stagnation (Ninčević-Gladan et al., 2015; Ninčević Gladan et al., 2009). In contrast, phytoplankton FA markers, $\delta^{13}C$, C:N ratios and BSi_{SPM} values suggested that SPM is of better quality during spring and summer. Often, $\delta^{13}C$ is positively correlated to Chl *a* concentrations (e.g. Miller & Page, 2012) indicating the limitations of having only monthly Chl *a* measurements in shallow coastal areas. These findings stress the importance of including a large suite of parameters to better assess the environmental characteristics, which change rapidly, particularly in shallow waters. The temporal mismatch between Chl *a* and the rest of the variables is most likely influenced by the high amount of resuspended material other than phytoplankton (e.g. bacteria and empty diatom frustules) that may obscure the phytoplankton Chl *a* signal. Increases of Chl a_{SPM} during winter as observed in Cetina might be associated with river nutrient inputs (Antolić et al., 2010).

These changes obviously affect the trophic behavior in bivalves which rely on potential food sources from the sediment as an alternative to the water column. Therefore, characterizing the chemical composition of sediment to identify potential food sources is an essential part of the assessment of their trophic ecology. For example, it is known that bivalves may largely feed on benthic microalgae (Kang et al., 1999; Page et al., 2003; Dubois et al., 2014; Navarro et al., 2016). Our results showed C18:0 and C16:0 as the most abundant FA in the sediment as seen in other estuarine (Boëchat et al., 2014; El-Karim

et al., 2016) and marine sediments (Volkman et al., 2007); however, they have been considered ambiguous biological markers of microalgae (El-Karim et al., 2016).

The highest contribution of terrigenous, carnivorous and herbivorous calanoid copepod markers to Sed was observed at Pag, contrasting with the results from SPM, and suggesting that Sed provides a major fraction of these sources to higher level consumers. Interestingly, the highest abundance of PUFA (in very low concentrations ~2.7%, annual mean) and MUFA took place during spring and summer, especially in Pag. This temporal pattern coincided with that observed in the water column indicating an abundance of fresh material sources in both pools, and an effective pelagic-benthic coupling, whereas the winter increase in SPM was not reflected in Sed. One possible explanation could be the efficient uptake of fresh material from the water column by consumers in a period of relatively less available food. Another explanation could be the transport to other areas (i.e. via currents) supported by the strong influence of Bora wind events during the winter time. Resuspension favors the availability of food sources to suspension-feeders and results in frequent exchanges between SPM and Sed pools (Carlier et al., 2007; Dubois et al., 2014). As a result, both pools consisted of a mixture of detritus, bacteria, phytoplankton and zooplankton.

The combination of SI and FA profiles described an alternation between a freshwater dominated system in winter and a marine-water dominated system in summer, as seen in the Kowie estuary in South Africa (Antonio et al., 2014). Indeed, the particulate matter in Pag would seem to be of better quality, indicated by the abundance of EFA within PUFA in both pools and by the lighter values of $\delta^{13}C$ and reduced SFA observed in the sediment. However, the nitrogen isotopic signature better distinguished the sources contributing to the organic matter pool at each site indicating that it is a better tracer of environmental changes than the carbon isotope (Fig. 4.2.4a). Cyanobacteria seemed to play a major role in Pag where more ^{15}N-depleted values clearly separated it from Cetina; however, detrital FA showed that bacteria were abundant in both pools at both sites, indicating their importance as a food source (Šestanović et al., 2009; Galois et al., 1996). The combined assessment of the pelagic and benthic pools is necessary for the comprehensive analysis of the functioning of marine ecosystems and considerably improves our understanding when consumers are incorporated in the analyses (Danovaro et al., 2001; Frangoulis et al., 2011; Braeckman et al., 2015).

5.1.2. Spatial and temporal variation in bivalve diet: *C. chione* and *G. bimaculata* study

Few studies have included spatial and temporal fluctuations of biochemical parameters of particulate matter in combination with organism tissues to trace the contribution of different food sources to bivalve's diet (e.g. Doi et al., 2005; Bergamino et al., 2014). This study revealed, for the first time, the isotopic composition of the digestive gland of the clam *Callista chione* and the cockle *Glycymeris bimaculata*, which showed a pronounced temporal variation in their diet at two sampling sites. The carbon isotopic variation appeared to be species-specific, with slightly more enriched values in *G. bimaculata* while large differences in the nitrogen isotope were site-specific, with more enriched values shown in Cetina (Fig. 4.2.4a,b). The temporal variation in $\delta^{13}C_{DG}$ was coupled to that in $\delta^{13}C_{SPM}$, indicating that bivalves adjusted their dietary shifts depending on the availability of food in SPM (Figs. 4.2.1, 4.2.4); this coupling suggested that SPM is an important food source, in agreement with other studies (DeNiro et al., 1978; Riera et al., 1996; Kang et al., 1999; Kasai et al., 2004; Antonio et al., 2014).

Results presented here showed a slight ^{13}C-enrichment in DG with respect to SPM. Bivalves enrich their $\delta^{13}C$ concentration in their tissues because they preferentially release the lighter ^{12}C during respiration (Kharlamenko et al., 2001; Page et al., 2003; Kang et al., 1999). A mixed diet is often composed of plant material and sediment detritus in invertebrates (Bacon et al., 1998; Guest et al., 2004; Navarro et al., 2016). In this study, *G. bimaculata* presented slightly heavier $\delta^{13}C$ values than *C. chione* indicating that they feed more upon autochthonous particles (i.e. phytoplankton derived organic matter) and suggesting a stronger dependence on primary producers as seen in other studies (Kharlamenko et al., 2008; Kang et al., 2003; Nadon & Himmelman, 2006; France, 1995). A shift towards more depleted values was observed for both species between February and June 2015, associated with terrestrial material with more depleted values in *C. chione* (-27‰) than in *G. bimaculata* (-25‰). Lighter $\delta^{13}C$ values in organisms have often been associated with high lipid content (e.g. Thompson et al., 2000) since these are ^{13}C-depleted (DeNiro et al., 1978; Focken et al., 1998). This association was not observed in *C. chione* where higher lipid concentrations and high C:N molar ratios, especially during summer and fall, were not coupled to low $\delta^{13}C$ values (Figs. 4.2.3, 4.2.4).

Similar findings have been reported in other filter feeders (Ezgeta-Balić et al., 2014; Lorrain et al., 2002) indicating that lipids might did not bias the present results. The more depleted $\delta^{13}C$ values observed in *C. chione* do not seem to be specific for this species since the one stable isotope study in the literature for *C. chione* reported in the NW Mediterranean showed a more enriched isotopic signature than in

these results ($\delta^{13}C$: -19.4±0.5‰, $\delta^{15}N$: 4.7±0.4‰, n=5 in Carlier et al*.,* 2007). In the present study, both species showed similar $\delta^{13}C$ signals regardless of site, suggesting that there are regional differences across the Mediterranean Sea.

A shift in $\delta^{15}N$ of about 1‰ was identified between the Pag and Cetina populations (Fig. 4.2.4a). This $\delta^{15}N$ variation was not associated with a different trophic level but with the different environments (i.e. food sources) which allowed a clear identification of bivalve population location. The ranges of $\delta^{15}N$ in specimens from Cetina were consistent with those from other filter-feeders in the Adriatic Sea (Ezgeta-Balić et al., 2014) whereas the lower $\delta^{15}N$ signature from the Pag populations has not been reported for bivalves in the Adriatic Sea, suggesting particular environmental conditions in Pag. Seasonal changes in $\delta^{15}N$ were coupled with those from the carbon isotope which showed more depleted values during winter and spring. In the Pag populations, these values were closer to those of Sed, suggesting an important contribution of Sed to their diet (further discussed in the next section). These results emphasize the need to conduct temporal studies in order to detect the rapid imprint that environmental changes have on animal tissues. The observed spatio-temporal intraspecific variation support the use of the digestive gland as a good indicator of fast turnover tissue (Deudero et al., 2009; Ezgeta-Balić et al., 2014).

FA profiles complemented the information on the spatio-temporal variation of the diet composition provided by isotopic signatures. For all populations, temporal differences in FA profiles were more evident than spatial ones as seen in *Mytilus edulis* from the western Mediterranean (Ventrella et al., 2008). For all consumers, combined SFA and MUFA dominated the composition of the DG with percentages of around 90%, followed by PUFA and detrital material. Detrital material was found in similar concentrations in all bivalves with lower values during the summer. SFA concentrations in *G. bimaculata* were higher than those in *C. chione* (up to 84% TFA) especially during fall and winter, and these were higher at Pag. These SFA values were similar to those reported in *Glycymeris nummaria* (up to 82% TFA) (Najdek et al., 2016). These results suggest that SFA greatly contribute to the diet of *Glycymeris* sp*.* in the eastern Adriatic, unlike *C. chione* and other bivalves in the southern Adriatic (Ezgeta-Balić et al., 2012; Najdek et al., 2013). Within the SFA pool, the bacteria marker associated with detrital matter (C20:0) was slightly higher in *G. bimaculata*, especially at Cetina. PUFA were higher in *C. chione* especially during summer, particularly in Pag, even in periods with low PUFA abundance (Table S5). This difference suggests that *C. chione* has a preferential uptake of high quality food compared with *G. bimaculata*. Diatoms and dinoflagellates contributed most to the bivalves' diet during spring and summer, particularly in *C. chione*. PUFA, especially EFA, are essential for growth but also a high degree

of unsaturation (UND) is characteristic of healthy mollusks (Dupčić Radić et al., 2014). Therefore, it can be inferred that *C. chione* has a better condition than *G. bimaculata*. Herbivorous calanoid copepod markers identified this group as a main component in the bivalves' diet especially during spring and summer. Since oleic acid, a marker of zooplankton, was more abundant in *C. chione*, zooplankton seems to be a preferential food source for this bivalve. There were no large changes in the proportions of PUFAs, EFAs and bacterial FAs between sites suggesting that the general quality of food sources was similar but slight differences were shown between species.

Overall detritus, diatom, dinoflagellate, zooplankton and EFA markers were the most abundant components in analyzed bivalves what is in agreement with other studies in the south-eastern Adriatic Sea. In these studies, other filter-feeders such as *Mytilus galloprovincialis*, *Ostrea edulis* and *Modiolus barbatus* (Ezgeta-Balić et al., 2012), *Pinna nobilis* (Najdek et al., 2013), *Arca noae* (Ezgeta-Balić et al., 2012; Dupčić Radić et al., 2014) and *G. nummaria* (Najdek et al., 2016) revealed the ingestion of a mixed diet. The higher concentration of lipids in bivalves coincided with those months with the best indicators of food quality in SPM. Analogously, lipid concentrations in *C. chione* showed a sharp decline between August and September 2014, potentially linked with early gametogenic stages and the building up of gonadal storage (Fig. 4.2.3). In *G. bimaculata* populations, results are less pronounced but seem to support the same hypothesis; these observations are in line with other studies (Chu & Greaves, 1991) since it is known that large oocytes are enriched in lipids (Gabbott, 1975).
Callista chione fed more upon fresher material than *G. bimaculata* which relied largely on bacteria-derived detritus, as observed in other species of the same genus, *Glycymeris glycymeris* (Galap et al., 1999) and *Glycymeris nummaria* (Najdek et al., 2016). The importance of bacteria in the bivalve diet has also been reported in other shallow coastal areas (Kang et al., 2003; Antonio et al., 2012) corroborating the importance of heterotrophic bacteria contributing to the carbon cycle through the microbial loop in oligotrophic waters such as the Adriatic Sea (Šantić et al., 2013).

5.1.3. Contribution of food sources to bivalve diet and feeding niche: *C. chione* and *G. bimaculata* study

To quantify food web relationships, estimates of the enrichment/depletion in $\delta^{13}C$ and $\delta^{15}N$ values between consumer and prey, known as trophic fractionation (Vander Zanden et al., 2001) or trophic enrichment factor (TEF) are required. In marine systems it is often assumed that a consumer is isotopically enriched relative to its food source (Post, 2002; Minagawa et al., 1984) although in benthic communities, the trophic fractionation between primary producers and consumers is highly variable and

unpredictable (Nadon et al., 2006). Here, results showed a slight ^{13}C-enrichment but ^{15}N-depletion in the signal between consumers and SPM and no clear relationship between consumers and Sed. A two source mixing model was used to elucidate the contribution of each source to the diet of the bivalves through time (Fig. 4.2.5). Often, SPM signatures are assumed to be relatively constant in space and time, leading to erroneous outputs and ecological misinterpretations (Miller et al., 2012). To avoid biased results, this temporal and spatial variation was integrated in the mixed model. Although TEFs vary among tissues and through time (Paulet et al., 2006), common enrichment factors for benthic invertebrates have been uniformly used (McCutchan et al., 2003) due to the lack of species-specific studies in our target individuals; therefore, these enrichment factors were used for the whole sampling period as the best approach. Based on these results, the contribution of Sed dominated in the populations from Pag with a slight contribution of SPM during summer when a major concentration of fresh material was available in the water column. In contrast, SPM was the main contributor to the diet composition at Cetina especially for *G. bimaculata* (> 97%). Interestingly, the highest contribution of Sed to this species took place in August 2015, whereas for *C. chione*, the opposite pattern was observed precisely in this period (Fig. 4.2.5). This contrasting figure suggested that in August 2015 there was a potential peak of available fresh material upon which *C. chione* largely fed and which did not greatly influence the nutritional resources of *G. bimaculata*.

Dual isotope and fatty acids analyses characterized each site as different feeding niches, and this difference was more evident with fatty acids results (Fig. 4.2.7b). Both species showed a similar temporal isotopic variation with more enriched values during summer and fall and more depleted values during winter and spring. The turnover time integrated in the digestive gland (days to weeks) is short enough to reflect the characteristics of the environment, in our case, the higher phytoplankton concentration during spring and summer, as discussed earlier. The isotopic feeding niche showed an overlap only in November and March at Cetina, revealing different composition of food sources during the rest of the year, whereas at Pag, the overlap was evident during fall and winter. A larger contribution of Sed was clear in the Pag populations, supported by the ^{15}N-depleted values in DG. This is not unusual since isotopic ratios of animals are closely related to their food (DeNiro et al., 1978; Minagawa et al., 1984; Post, 2002; Antonio & Richoux, 2016a). At Pag, the highest niche plasticity was observed for *C. chione* suggesting its ability to consume more isotopically diverse food sources than *G. bimaculata*. Niche plasticity allows the reduction of intraspecific competition when food is scarce (Gutt, 2006) by consumption of different fractions of POM (Riera, 2007). The narrower isotopic range in *G. bimaculata* would suggest that both species compete for food in a period of food scarcity; however, the fatty acid feeding niche revealed that despite the overlap, *G. bimaculata* is more opportunistic.

This behavior matches with the trophic activity of *C. chione* which appears to be more selective within the available organic pool. Morphological differences could also play a role in the selection of food particles. The presence of a siphon in *C. chione* could restrict its ability to pick particles from the environment. In contrast, little is known about the feeding habitats of *G. bimaculata* which has no inhalant siphon and potentially has the ability to feed also upon particles in the interstitial water. Food quantity and quality may affect different bivalve species in different ways since they (i) might assimilate food at different rates (Bacon et al., 1998), (ii) have a different biochemical composition in their soft tissues as a consequence of changes in food supply (Baker & Hornbach, 2000) or (iii) relocate differently the assimilated food towards different functions (Lewis & Cerrato, 1997). The similar isotopic and C:N ratio patterns observed between populations at each site may indicate that resuspension events make benthic diatoms available for consumers (e.g. Miller et al., 1996) ensuring the availability of organic material in SPM throughout the year. Therefore, both species have the capacity to ingest particles from both SPM and Sed pools. This type of intraspecific variation was also observed in *Crassosstrea gigas* in France (Riera et al., 1996). SPM is a dynamic pool of autochthonous and allochthonous material thus, to facilitate the identification of the origin of SPM, multiproxy approaches have been used, such as in the Yura estuary (Antonio et al., 2012).

In the present study, the combination of a dual isotope model with a set of biochemical parameters (FA, Chl *a*, C:N ratio, and BSi) gave insights into the origin of food sources. It can be concluded that each species obtained their carbon from different sources and that the nitrogen isotopic composition in the Sed strongly separated populations based on $\delta^{15}N_{DG}$ (Fig. 4.2.7a). The larger dispersion of FA in *G. bimaculata* could be linked to a wider range of bacteria FA markers than in *C. chione*. Although the detrital contribution is quite high in both species, bacteria just constituted a small proportion of the diet in *C. chione* in other areas (Charles et al., 1999). Bivalves are proficient at sorting material for its consumption (reviewed in Ward & Shumway, 2004). *Glycymeris bimaculata* might act as an opportunistic feeder in this respect, incorporating resuspended particles with more detrital-derived material such as seen in *P. magellanicus* (Shumway et al., 1987). Bacteria seems to contribute significantly to bivalve nitrogen requirements in periods of food scarcity (Langdon & Newell, 1990), which is likely the case in the present study especially for Pag populations. Therefore, both species have the ability to switch from suspension to deposit feeding depending on the environmental conditions, as seen for *Abra alba* (Sampaio et al., 2010).

5.1.4. Spatial and temporal variation in bivalve diet: *G. pilosa* study

Spatio-temporal fluctuations in the isotopic composition of the digestive gland of *Glycymeris pilosa* were also evaluated. Analysis of stable isotopes revealed a pronounced temporal variation in the diet of *G. pilosa*. The isotopic variation appeared to be site-specific, with more enriched values of both carbon and nitrogen isotopes in Pašman population (Fig. 4.2.9). This site-specificity was also apparent when comparing *G. pilosa* values from Pag to those of previously studied species in the same location. The temporal variation in $\delta^{13}C_{DG}$ was coupled to that in $\delta^{13}C_{SPM}$, indicating that *G. pilosa* also adjusted their dietary shifts depending on the availability of food in SPM (Figs 4.2.9, 4.2.11). For both *C. chione* and *G. bimaculata*, these results showed a slight ^{13}C-enrichment in DG with respect to SPM (up to 2‰).

On the other hand, *G. pilosa* from Pašman presented significantly heavier $\delta^{13}C$ values, up to 3‰, than in Pag specimens. These results indicated that despite the similar $\delta^{13}C_{SPM}$ between sites, the population in Pašman fed more upon autochthonous particles. This is corroborated by $C:N_{DG}$ ratio ranges in this population (5.4–7.4). One hypothesis could be associated with reduced inter-specific competition in the area, but since other bivalve species are present in the Pašman Channel, i.e. *Venus verrucosa*, *Arca noae*, *Pinna nobilis* or *C. chione* (Peharda et al., 2009); pers. obs) this is probably not the reason. The $\delta^{15}N_{DG}$ ranges in the Pašman population were also the highest observed in all studied populations, suggesting that they did not largely rely on heterotrophic benthic bacteria. Although sediment samples were not analyzed at this site, $\delta^{15}N_{DG}$ resembled $\delta^{15}N_{SPM}$ likely indicating that suspended particulate matter was the main nitrogen source (Fig. 4.2.12). Since lower $\delta^{15}N$ values in bivalve tissues have also been associated with lower metabolic rates when compared at different depth gradients (Nerot et al., 2012), one could suspect that the *G. pilosa* population from Pašman has a higher metabolic activity than the population in Pag. However, both are very shallow sites with similar characteristics, with specimens collected from Pag at 3–5 m and from Pašman at 1–2 m, so this hypothesis would poorly explain these differences. It is important to note the considerably higher concentration of lipids in the Pag population rather than in Pašman, indicating a lower concentration of carbon in the diet and suggesting reduced energy reserves in the later. In spite of this, both populations had higher concentrations than those observed in other bivalves from the southeastern Adriatic (Ezgeta-Balić et al., 2012).

5.2. Reproduction

5.2.1. Reproductive cycle & temperature

Environmental factors have a strong influence on reproduction in bivalves (e.g. Sastry & Blake, 1971; Gosling, 2003; Gaspar, 2004; Drent, 2004; Drummond et al., 2006; Gam et al., 2010) and this has been corroborated in the present work. Temperature and food availability are considered as the main factors triggering reproduction, most likely influencing distinct periods of the cycle (Gosling, 2003 and references therein). For many species, the initiation of gametogenesis is temperature dependent (Sastry et al., 1971; Bayne, 2009) whereas gonadal development requires a nutritional input to produce mature cells (Sastry, 1966; Iglesias & Navarro, 1991). However, this complex interplay between both factors is considered to be species-dependent (Gosling, 2003). In the present study, temperature played a significant role where the warmest period was mainly associated with spawning events. Based on previous information (see Section 5.1) the highest quality of food supply took place during spring and summer and monthly Chl *a* biomass values were quite similar among sites ranging from 0.2 to 0.7 μg/L. To assess which were the triggering factors for reproduction, two populations of *Callista chione* and *Glycymeris bimaculata* were evaluated and compared for intra and inter-specific differences. Additionally, a population of *Glycymeris pilosa* from Pašman was also evaluated. Our results on the reproductive cycle of *C. chione, G. bimaculata and G. pilosa* in the middle Adriatic confirmed the dioecious nature of the species and the ability to reproduce nearly all year around. However, observed differences in the timing and duration of the reproductive cycle revealed that temperature is not the sole factor triggering spawning among all studied populations.

In *C. chione*, these observations were previously reported in other Atlantic (Moura et al., 2008) and Mediterranean populations (Valli et al., 1983; Valli et al., 1994; Metaxatos, 2004; Galimany et al., 2015; Tirado et al., 2002). An equal sex ratio was described from histological analyses since macroscopic determination based on the coloration and consistency of gonads (Moura et al., 2008), did not allow for identifying sex. Previous studies of this venerid bivalve did not report hermaphrodites (Moura et al., 2008) or declared them very rare (Valli et al., 1983). However, in the present research hermaphroditism was occasionally observed, as recently documented in Galimany et al., (2015).

Based on our population comparison results, seawater temperatures in Pag and Cetina sites oscillated between 7.4 and 28.6°C. Similar maximum mean monthly values were observed between sites (25–26°C) while minimum values were lower at Pag, differing by ~4°C, indicating large spatio-temporal variations. Differences in temperature primarily influences the timing and duration of spawning (Valli et al., 1994; Galimany et al., 2015) which apparently, appeared to be linked with the inter-site variations in

the reproductive cycle observed in this study. Gametogenesis was initiated when temperatures were the highest, during two consecutive periods in both populations, and reached maximum gonadal mass indices in spring. The spawning period started earlier at Cetina (in January 2015), a period with milder temperatures (at ~14°C) which would have favored an earlier maturation of gonads, with a main spawning peak in spring prolonged up to June/July. For this species, it is presumed that an extended spawning period is advantageous over one single event per year (Moura et al., 2008; Tirado et al., 2002) and it compensates its high larvae mortality (Valli et al., 1994). At Pag, the spawning period started later on, in April 2015 (at ~12°C), and the main peak took place during summer, with a short time period of gamete release (mainly during July) indicative of a major gonad storage during gametogenesis. Both spring and summer have been documented as the main spawning period in other populations in the Mediterranean (Valli et al., 1983; Valli et al., 1994; Metaxatos, 2004; Galimany et al., 2015; Tirado et al., 2002) and overall in bivalves (Zwarts, 1991).

A synchrony between female and male cycles was observed, typical of organisms with external fertilization to ensure their reproductive success by increasing probabilities of fertilization (Levitan, 1993). The highest stages of maturation were represented by high mean gonad index (MGI) values and were inversely correlated to temperature, showing increasing values during gametogenesis and a clear drop with increasing temperatures, as previously described for *C. chione* by Galimany et al., (2015) and also observed for other bivalves (Cruz et al., 2000; Gosling, 2003). Commonly, spawning takes place before highest temperatures are reached, a strategy to ensure the viability of eggs (lower during the warmest period) and to reduce metabolic demands (Honkoop & van der Meer, 1998). The small spawning peak identified for females from Pag in October 2014 could be explained by the unusual conditions in the area during that year. After a cold and rainy summer, relatively higher temperatures were recorded in October 2014, suggesting the high sensitivity of the species to changes in temperature and adaptation capacity. Studies on populations with milder seawater temperatures have reported several intra-annual peaks (Tirado et al., 2002; Metaxatos, 2004; Moura et al., 2008) supporting this assumption.

Up to date, this is the first study evaluating the reproductive cycle in *G. bimaculata* and *G. pilosa*. In the *G. bimaculata* population in Pag, males were more abundant than females (1.0:1.3) whereas in Cetina and in the *G. pilosa* populations, the sex ratio equaled one. Unlike in *C. chione*, gametogenesis started later in time, around October in *G. bimaculata* and November in *G. pilosa*, and were therefore decoupled from the temperature maxima. On the other hand, the spawning period and timing of the *G. bimaculata* populations in comparison with those of *C. chione* showed some similarities. Even though

the spawning period was shorter in *G. bimaculata* than in *C. chione*, the main spawning peak also took place earlier in Cetina (September 2014 and August 2015) than in Pag (September/October 2014 and September/October 2015) during two consecutive periods. However, temperatures didn't seem to have an influence since they averaged ~26°C in Cetina and ~20–22°C in Pag. In the *G. pilosa* 12-month-study, the timing of spawning took place towards the fall, between October/November 2014 at ~21°C and a short maturation period was observed in the oncoming cycle. *Glycymeris* sp. were characterized by a long period in late development stage in females, and in early development stage in males. Likewise, both species reached maximum gonadal mass indices during summer and the relationship between MGI and temperature was less clear. Based on these results it is hypothesized that in *Glycymeris* sp. from the Adriatic Sea, although the periodicity in temperature may initiate gametogenesis, the spawning period and timing was delayed (when compared to that observed in *C. chione*) likely linked to the need for more time to build sufficient energy storage under the presence of food supply. As studied in other bivalves, the coupling between temperature and food supply to trigger spawning is required (MacDonald et al., 1986; Santos et al., 2011).

The reproductive cycle has been studied in other members of the *Glycymeris* genus. In *G. glycymeris*, populations from southern Brittany (France) and the Isle of Man (UK) presented different patterns to the ones observed here. In France, ripe individuals represented at least 70% of the population throughout the year (Lucas, 1965), and Morris (1978) mentioned that UK specimens were able to spawn all year around. Based on this knowledge, Steingrimsson (1989) studied *G. glycymeris* populations from around the Isle of Man using stereological techniques, and confirmed that individuals were in mature stage all year, thus indicating that most energy in the organism is allocated into reproduction. Under stress circumstances, individuals might overcome spawning at larger scales to reach a maximum reproductive output (Steingrimsson, 1989). Thus, the observed differences are likely associated with different environmental settings, showing once again large differences between North Atlantic and Mediterranean species.

On the other hand, the reproductive cycle in the Indian clam, *Glycymeris gigantea* (Reeve, 1843) from the Gulf of California (Mexico) resembled these results more closely. The gonadal development for this species was studied bimonthly using common histological techniques and gametogenesis was most active from February to May, with a main spawning peak in October (Villalejo-Fuerte et al., 1995). However, this study showed a relationship between gamete release and a decrease in temperature of nearly 10°C (Villalejo-Fuerte et al., 1995). In the southeastern Adriatic Sea, the dog cockle *G. nummaria* also showed no differences in sex ratio and a synchronous gonadal ripening took place between

May–June, with one main annual spawning event (July–August) (Crnčević et al., 2013). In this population, the highest MGI values were reported with increasing temperatures (May–July) while the spawning peak coincided with the highest temperatures (Crnčević et al., 2013). Hermaphrodites represented a small proportion of all sample sizes (< 0.5%) and their presence was also reported in both *G. glycymeris* and *G. gigantea* (Lucas, 1965; Villalejo-Fuerte et al., 1995).

It is important to note that gonadal neoplasia was observed in histological preparations of all species. It was in *G. bimaculata* and *G. pilosa* that this parasitic infectation was very marked, especially during early active stages. As tumors grow, they invade and destroy normal follicles, as described in other bivalve molluscs (Peters et al., 1994). In addition, infection by protozoa parasites were also shown in the gills and mantle tissues surrounded by many haematocytes, which could be associated with the presence of *Perkinsus* sp., Nematopsis or Porospora as previously reported in *C. chione* specimens from the North Adriatic (Canestri-Trotti et al., 2000).

The combination of histological analysis and gonadosomatic index (GSI) was applied for the first time in *C. chione* and *G. bimaculata* revealing that both methods successfully describe the main changes in the gametogenic cycle and can be applied for assessing the reproductive effort of these species. Microscopic examination has been traditionally used to interpret the reproductive cycle within several main gametogenic stages for different marine bivalve species including scallops, mussels and clams (e.g.Taylor, 1983; Gray et al., 1997; Delgado & Pérez-Camacho, 2007; Peharda et al., 2006; Popović et al., 2013). Despite its advantage in determining and identifying the main stages of development during the gametogenic cycle, as observed from our samples, it is a labor intensive method (Gosling, 2003). On the other hand, GSI is used to determine the storage and release of gonad material providing a quantitative estimate of gonad proportion in a short time interval (Gosling, 2003), although it would not be an appropriate tool to determine the main stages of gametogenesis. Whereas in *C. chione* GSI comprised data from both sexes, in the population of *G. bimaculata* GSI was initially analyzed for both males and females. Since no significant differences were shown between GSI and sex, the data were pooled together. As a result, GSI proved to be a reliable method for representing the main changes in the reproductive cycle as seen in other bivalves (Royer et al., 2008; Uddin et al., 2012; Cardoso et al., 2009a; Santos et al., 2011), even when sexual differentiation is not contemplated. In addition, this index enables determination of the variation in the reproductive output and fecundity.

5.2.2. Body mass index

Body mass index (BMI) values were measured to recognize physiological responses to variations in environmental factors (Sebens, 1987; Honkoop et al., 1997). Increasing BMI during the coldest period were described in poikilotherms as a response to a reduced metabolic activity (Clarke, 1987; Brey, 1995) whereas losses in BMI were enhanced by low food availability in some bivalves (e.g. Honkoop & Beukema, 1997; Cardoso et al., 2007; Cardoso et al., 2009b; Santos et al., 2011). In the *C. chione* population from Pag, temporal variations in BMI showed increases during the winter time and early spring, with subsequent losses during the summer and fall, as previously observed in this species using the condition index (CI) (Moura et al., 2008). In this population, the coupled growth in BMI and GSI was evidenced and had a considerably higher amplitude, indicating a proportional investment into soma and gonads and higher losses in body mass after spawning. In *C. chione* from the Cetina population, the highest gonadal mass period was coupled with a slightly low BMI, followed by an increase towards the summer when spawning was taking place, suggesting a faster recovery and a higher investment into somatic growth rather than reproduction, as previously described for populations of *Cerastoderma edule* from northern Spain (Iglesias et al., 1991). In other bivalves, the decrease in body condition during summer months was associated with the release of gametes during spawning events and with increasing temperatures which would demand a higher metabolic cost (Cardoso et al., 2007; Rueda & Smaal, 2004).

In *G. bimaculata* BMI and GSI were well correlated, with increasing BMI values along with gametogenesis. The only previous information in *Glycymeris sp.* contemplating body mass weight is CI in *G. gigantea*. In this species, CI seemed to follow gametogenic activity, although particularly in this case, it could be potentially influenced by changes in water content or nutritious mass in the soft tissue (Villalejo-Fuerte et al., 1995).

Therefore, BMI or CI should be used with caution as indicators of gonadal development in bivalves (e.g. Gaspar & Monteiro, 1998; Gribben et al., 2004; Drummond et al., 2006) since factors such as temperature, food or salinity might be masked and have an influence on the cycle (Tirado et al., 2002). In addition, body size could also play a role in the reliability of CI as an indicator of gametogenesis. Based on our results and those from congeneric species, in *Glycymeris* sp. BMI coupled best to GSI; this is likely associated with a larger size and highest body condition, compared with *C. chione*. Further, a better somatic condition after spawning implies that once reproductive demands are satisfied, there is more energy left over for growth, as suggested in Jokela & Mutikainen, (1995) for *Anodonta piscinalis*.

Accordingly, leaving aside the temperature influence, a higher investment into both soma and gonads in *C. chione* Pag population could potentially result in lower shell growth. This is supported by the lower shell growth rate documented for this population by Ezgeta-Balić et al., (2011) and discussed further on.

5.2.3. Reproductive investment, output and fecundity

The reproductive investment has been widely reported in bivalves to better interpret the allocation of energy into somatic and gonadal mass (Royer et al., 2008; Santos et al., 2011; Velasco, 2013). For example, seasonal variations in gonadal mass linked to environmental conditions were described at the population (Brey, 1995) and species (Jokela et al., 1995) level. Such conditions may influence the constant mobilization from somatic to gonadal tissues (Valli et al., 1994) resulting in different reproductive strategies as seen in the *C. chione* case study presented here. A positive relationship between gonadal mass and body mass index was shown in both populations, with a higher reproductive investment at Pag (16%) than at Cetina (7%). Further, as a result of spawning, a higher percentage of gonad release with respect to the preceding state at full maturity was also observed in the population from Pag, contributing to a higher reproductive output. In terms of fecundity, individuals from Cetina had higher values (96%), indicating that most of their gonadal mass was invested into reproduction.
The presence of gonads in resorption stage and spawning taking place during a period of high metabolic demand (summer) in the population at Pag, suggests the use of gonad storage as a reserve. Under unfavorable conditions, the resorption of gametes is common to survive periods of food scarcity, as seen in *Mytilus edulis* (Bayne et al., 1978) and *Mya arenaria* (Coe & Turner, 1938), which may fluctuate at each gametogenic period depending upon food availability (Sastry, 1966; Honkoop et al., 1998; Gosling, 2003). *Callista chione* individuals from Pag possibly use energy reserves stored from the previous gametogenic cycle by gonadal resorption to ensure the generation of a new cycle as described for *Mya arenaria* (Coe et al., 1938). Contrarily, in individuals from Cetina gonads were most likely produced from newly available food since there was hardly any gonad mass left after spawning was completed, as also seen in *Cerastoderma edule* populations (Cardoso et al., 2009a).

Only in *G. bimaculata* from Pag could these parameters be determined; therefore, a comparison between two reproductive seasons was attempted. Both higher investment and fecundity per brood were shown in 2014 (26% and 94%, respectively) compared with 2015 (19% and 92%). A hypothetical explanation for these intra-annual differences could be the higher temperatures measured in 2015 (as discussed further on).

As analyzed in Brey, (1995), the evolutionary adaptation of benthic invertebrate populations living in colder environments influence the mode of reproduction, by maintaining the energy invested into reproduction while gonad productivity may be reduced. In this context, a lower fecundity in the coldest environment is selected as safeguard for guaranteeing next year's survival and offspring. The same strategy was suggested in populations of *Scrobicularia plana* (Santos et al., 2011). Therefore, from an energetic allocation point of view, it seems that the intraspecific variation in the reproductive condition of *C. chione* as a response to different environmental conditions was proven to be advantageous for the species.

5.2.4. Future scenario/ implications

This work was partly carried out in the context of one of the highest global temperature recorded since 1880, with an average temperature across global land and ocean surface 0.90°C above 20th century average in 2015 (NERC, 2015). Our studied populations experienced an increase of up to 2°C between two consecutive years with no apparent differences observed in their reproductive behavior based on GSI. Shallow-water marine invertebrates are considerably tolerant to short-term variations in temperature (Clarke, 1987; Viladrich et al., 2016). Notwithstanding, habitats characterized by temperatures above or below an organism optimum can cause an increase in their physiological stress. Mass mortality events attributed to high temperatures have been recently witnessed in benthic invertebrates in the Mediterranean (Rivetti et al., 2014; Verdelhos et al., 2015). Changes in temporal trends of seawater temperature can have an effect on an individual's body size (Kaustuv et al., 2001) and can cause earlier spawning, a higher reproductive investment (Jablonski, 1996; Morgan et al., 2013), a lower reproductive output (Philippart et al., 2003) or alterations in growth rate in bivalves (Zucchetta et al., 2012). Further, variations in temperature patterns may lead to changes in population dynamics causing shifts in bivalve distribution (Root et al., 2003; Jones et al., 2010; Beukema et al., 2009; Gosling, 2015; Philippart et al., 2011). Considering the overall greater gonadal investment at Pag and the greater weight loss during spawning at Cetina, recovery after unfavorable changes seems uncertain for both populations. Additionally, potential forthcoming increases of temperature in Pag may alter the reproductive strategy and cause a shift in the timing of spawning. The reduction of energy available for reproduction due to higher metabolic costs (Brey, 1995; Philippart et al., 2003) and changes in the thermal optimum interval (Verdelhos et al., 2015) could cause an extension of gametogenesis, with the consequent lack of sufficient resting period for recovery. Thus, small-scale studies taking into account both local extrinsic and intrinsic factors (Burdon et al., 2014) in detecting biological responses such as

reproductive performance are essential to address climate oscillation impacts, particularly in species of management concern.

Due to a high commercial and economic value of *C. chione* (Ezgeta-Balić et al., 2011; Tirado et al., 2002; Metaxatos, 2004; Galimany et al., 2015) and the ongoing scarcity of natural beds in other Mediterranean regions (Ramón et al., 2005; Baeta et al., 2014) a close monitoring of the stock assessment is needed to ensure the species health. Furthermore, studies on growth energetics coupled with an increased knowledge on the ecological patterns and life strategies will contribute to the understanding of how a changing environment affects population dynamics.

5.3. Growth

5.3.1. Use of $\delta^{18}O$ and $\delta^{13}C$ as proxies

Shell microgrowth increments preserve information about the environmental and physiological conditions in which mollusks live (Jones et al., 1983), thus, proving to be a good proxy for ecological research. In the present study, the reconstructed temperatures estimated from $\delta^{18}O_{shell}$ values in combination to high resolution instrumental seawater temperature allowed a precise determination of the seasonal growth patterns in *Callista chione* shells from two different sites. Shells faithfully recorded the ambient temperature between April/May and December, and showed little or no growth during the winter months.

The carbon isotope signature of biogenic carbonates and its ambiguous relationship to shell growth make it a less clear proxy for palaeoenvironmental reconstructions (McConnaughey & Gillikin, 2008). Shell $\delta^{13}C$ is derived from dissolved inorganic carbon (DIC) in seawater and organic carbon sources from food (incorporated via the metabolic pathway). Distinguishing between the two sources can be difficult (Lartaud et al., 2010; McConnaughey et al., 1997). Likewise, $\delta^{13}C_{shell}$ is also influenced by metabolic carbon from respired CO_2 which initially was thought to be a rather negligible contribution (McConnaughey et al., 1997; Lorrain et al., 2004; Gillikin et al., 2006). According to later studies, metabolic carbon was shown to contribute > 10% in some species (Gillikin et al., 2009; Gillikin et al., 2007). For instance, *Mercenaria mercenaria* showed high ranges of metabolic carbon observed through ontogeny (5–37%) resulting in a decrease in $\delta^{13}C_{shell}$ (Gillikin et al., 2007) while in others, no discernable decrease in $\delta^{13}C_{shell}$ through ontogeny was shown (Buick & Ivany, 2004; Gillikin et al., 2005; Butler et al., 2011). The $\delta^{13}C_{shell}$ ranges in *C. chione* were quite consistent among replicates and between sites, averaging negative values and extreme ranges from -1.51 to 0.03‰. A similar $\delta^{13}C_{shell}$ range was found in a young specimen of *C. chione* measured in the Northern Adriatic (-0.99 to -0.06‰; Keller et al., 2002).

In this work, the authors suggested that the shell isotopic composition of both oxygen and carbon did not have marked variations through ontogeny. In *G. bimaculata*, just one specimen showed $\delta^{13}C_{shell}$ below 0‰ whereas maximum values reached 1.77‰; therefore, interspecific differences could be raised due to metabolic differences even if these did not vary through ontogeny. Accordingly, interspecific variation at the same locality could be increased due to metabolic differences even if these do not vary through ontogeny.

The onset of reproduction may have also affected the $\delta^{13}C_{shell}$ variation. For example, more negative $\delta^{13}C_{shell}$ values have been explained by higher metabolic rates after as a consequence of restoring the energy lost during spawning (Gillikin et al., 2006). According to other studies based on laboratory experiments with different diets more negative $\delta^{13}C_{shell}$ values were associated with higher metabolic activity as a result of increased food availability (Lartaud et al., 2010; Sejr et al., 2004). Based on the detailed biological and ecological dataset and their covariation with $\delta^{13}C_{shell}$, spring/summer presented the highest values with a decreasing pattern towards the winter. These findings suggest that the decrease in $\delta^{13}C_{shell}$ in *C. chione* is not a consequence of the aftermath of spawning. Instead, this covariation is most probably associated with low food availability given that spring and summer are the periods with the highest availability of food in the study area. The role of both gametogenesis and food supply in interpreting proxy records needs more attention, especially in relation to $\delta^{13}C$.

In summary, the incorporation of light carbon from metabolic CO_2 into the shells may result from environmental and physiological effects, and the relative proportion of these two factors may vary amoing species. Hence, its use as a $\delta^{13}C_{DIC}$ or salinity proxy still remains unclear. In addition, the relationship between oxygen and carbon isotopes still present challenging interpretations potentially associated with ontogenetic effects. Based on these results in *C. chione* specimens and in younger specimens of *G. bimaculata* (those from Pag), both isotopes were inversely co-varying.

5.3.2. Growth patterns: timing and rate of shell growth

5.3.2.1. Growth patterns in *Callista chione*

The current study presents a monthly resolved and temporally aligned growth record for young specimens of *C. chione* in the eastern Adriatic Sea, allowing an estimate of the timing and rate of shell growth. The annual cycle of $\delta^{18}O_{shell}$ values showed a unimodal distribution whereas the growth curve presented a bimodal pattern with maximum values up to 2.46‰ and 1.79‰ and minimum values down to -0.82‰ and -0.91‰ in Pag and Cetina populations, respectively. These amplitudes were higher in

specimens from Pag since maximum values differed between the populations by nearly 1‰, whereas the minimum values were quite similar between sites, indicating that populations in Pag grew during a colder temperature period. Maximum reconstructed temperatures from $\delta^{18}O_{shell}$ values coupled well with high resolution instrumental SST and these were ~ 1°C lower at Pag than at Cetina sampling sites (26.9 vs 28.1°C). Evaporation rates may increase during summer due to higher temperatures and a decrease in precipitation, causing more positive $\delta^{18}O_{water}$ values, and consequently, $\delta^{18}O_{shell}$ values tend to be underestimated (Radermacher et al., 2009; Goodwin, Flessa & Schöne, 2001). This could explain the slight differences between reconstructed and instrumental temperature maxima. Likewise, the temperature minima did not compare well with reconstructed temperatures (7.4 vs 13.6°C and 10.9 vs 16.6°C for Pag and Cetina, respectively). The overall reconstructed temperatures suggest an extremely slowdown of shell growth or growth cessation between winter and late spring (January – April). Periods of very limited growth could lead to biased $\delta^{18}O_{shell}$ temperature reconstructions due to time-averaging (Schöne, 2008). Generally, $\delta^{18}O_{shell}$ values are analyzed on the carbonate material obtained by drilling or milling in the shell, an amount oscillating between 50 – 120 µg. During periods of slow growth, this amount is likely to contain material formed during a longer period of time. Therefore, the resulting overall $\delta^{18}O$ signal derives from a large average between multiple $\delta^{18}O_{shell}$ values, which is likely to slightly bias the reconstructed temperatures (Goodwin et al., 2004). The $\delta^{18}O_{shell}$ ranges are within those of a young specimen (slightly over 3 years old) measured by Keller et al., (2002) which oscillated between -1.5 to 2‰ and whose reconstructed temperatures fell between 13.2 and 30.6°C. In that study, maximum reconstructed temperatures were too high for the area, possibly caused by assuming a $\delta^{18}O_{water}$ value of 1‰ for the whole year. Coastal areas are very likely influenced by freshwater influxes altering the annual variation of $\delta^{18}O_{water}$ which may result in biased temperature reconstructions.

Growth bands were observed macroscopically on the shell surfaces and in cross-sectioned valves and consisted of a series of more densely packed (intra-annual) growth lines. Annually resolved growth lines during this period have also been documented in other populations from the Adriatic Sea (Ezgeta-Balić et al., 2011; Hall et al., 1974). In contrast, in the SW of Portugal, growth lines were deposited between September and January (Moura et al., 2009). A closer examination revealed a series of closely spaced and distinct shell growth bands deposited at the end of summer/early fall most probably representing a waning of shell growth. These results are in line with those anticipated by Hall et al., (1974) for a North Adriatic population and are supported by the lower density of samples (more spaced data points) observed around the growth band regions (Fig. 4.4.4). Therefore, annual growth bands in *C. chione* shells from the Adriatic Sea are indicators of a slow growth preceding a sharp decrease in shell growth.

5.3.2.2. Growth patterns in *Glycymeris bimaculata*

Uninterrupted $\delta^{18}O_{shell}$ records were obtained by milling from *G. bimaculata* cross-sections. Micromilling, rather than the drilling of individual holes, is considered the best sampling technique ensuring a complete growth record from the sampled specimens and thus enabling a higher temporal resolution (Schöne, 2008). Additionally, micromilling favors the sampling of equal fractions in shell increments, minimizing spacing between samples and ideally completed at equidistant intervals. As in the *C. chione* results, a unimodal distribution was shown based on the annual cycle of $\delta^{18}O_{shell}$ values which overall, showed higher amplitudes in specimens from Cetina. In addition, contrary to that observed in *C. chione*, maximum $\delta^{18}O_{shell}$ values were obtained from the Cetina populations (maximum of 2.44‰ compared with 1.84‰ in Pag), which could be related either to time-averaging, species-specific thresholds or to an ontogenetic trend. Even though milling is a high sampling resolution technique, time-averaging could be responsible for the lower amplitude observed in shell CB2. Time-averaging effects occur when sample sizes differ, and it generally takes place in those increments where growth slows down and the sample interval remains the same, thus, the same sample size represents (averages) more time (Goodwin et al., 2004) reducing the amplitude of $\delta^{18}O_{shell}$ values.

The observed differences between sites do not seem to be species related since maximum and minimum $\delta^{18}O_{shell}$ values between both species fell within similar ranges regardless of site. Additionally, on a previous study of *G. bimaculata* from Pag, $\delta^{18}O_{shell}$ values oscillated from -0.5 to 2.3‰ (Bušelić et al., 2015), indicating that shells can also record similar amplitudes to those from Cetina. It is frequently assumed that bivalves have a similar growth season through ontogeny; however ontogeny is likely associated with these variations in our study sites since specimens sampled at Pag were much older (16 and 25 years) than those in Cetina (10–13 years). Furthermore, based on the oxygen isotope values from *G. bimaculata* juvenile shells from Pag, the ranges showed higher values (-0.61 to 2.62‰) than in adults, and these were similar to those from Cetina (-0.83 to 2.44‰). Moreover, the amplitude of $\delta^{18}O_{shell}$ values in *C. chione* has been shown to decrease through ontogeny (Keller et al., 2002). Previous studies of shell increments based on stable oxygen isotopes in other species also revealed wider isotopic amplitudes in juveniles and even a longer growth season, as seen in *Spisula solidissima* (Say, 1822) (Ivany et al., 2003), *Phacosoma japonicum* (Schöne et al., 2003) and *Mercenaria stimpsoni* (Gould, 1861) (Kubota et al., 2017). Maximum reconstructed temperatures from $\delta^{18}O_{shell}$ values also coupled well with high resolution instrumental SST, with very similar ranges between sites. These results indicated that shell growth is extremely slow or rather negligible between January and April.

The identification of shell growth bands in adult *G. bimaculata* specimens is not straightforward even microscopically. Previous studies of *G. bimaculata* validated the annual growth line formation in spring coinciding with the increase of seawater temperatures (Bušelić et al., 2015). By contrast, the timing of growth line formation in two congeneric species, *G. glycymeris* and *G. nummaria*, coincided with the seawater temperature minima. Whereas in *G. glycymeris* from the western English Channel the growth line was deposited between December and March (Berthou et al., 1986), marginal increment analysis of *G. nummaria* from the Adriatic Sea showed that the growth line was laid down by March (Peharda et *al.,* 2012). On the other hand, small *G. bimaculata* (3 years old) specimens from the present study had clearer visible lines with the naked eye and, which based on the measured stable oxygen isotopes, these corresponded to the end of summer/early fall. These results should be treated with caution until more replicates corroborate these observations. In a recent study of a fossil *Glycymeris* sp., *G. planicostalis*, Walliser et al., (2015) postulated higher shell growth rates during spring and summer rather than fall and winter, suggesting the need to sample slow-growing portions of the shell at a higher resolution. Looking at these results, it can be inferred that *Glycymeris* species from this genus are likely to present a season of shell growth cessation.

Optimum temperature ranges for shell growth are species-specific (Chauvaud et al., 2005; Ivany et al., 2003). Here, both studied species presented the highest growth rates during the summer months, especially during July and August, although some peaks differed according to site. Site-specific differences in growth rates are not surprising, as previously observed in other mollusks (Radermacher et al., 2009). For instance, in the bivalve *P. japonicum*, the length and rate of growth were mainly controlled by temperature, showing differences between two nearby sampling sites (Schöne et al., 2003).

5.3.3. Environmental and physiological controls of shell microincrement growth

Environmental stimuli such as temperature, photoperiod or food supply are known to influence growth patterns in marine benthic invertebrates. Whether temperature or food availability is the main driver of shell growth rate is a fundamental question raised by many authors (e.g. Goodwin et al., 2001; Ivany et al., 2003). There is a close agreement between $\delta^{18}O_{shell}$ derived temperature estimates and observed temperatures, suggesting *C. chione* and *G. bimaculata* shells act as good environmental recorders. As observed from these results, the interpretation of geochemical signals is sensitive to the season of growth and it can vary within species even at short-scale distances (ca. 200 Km). These observations together with high correlations between shell growth and temperature at both sites provide further evidence of the influence of temperature in shell growth control. In addition, decreasing temperatures

are likely influencing the deposition of shell growth line in *C. chione*. In other venerid bivalves from the NW Pacific, *Mercenaria stimpsoni* (Kubota et al., 2017) and *Phacosoma japonicum* (Tanabe 1988, Schöne 2003) and from NE Pacific coast *Chione cortezi* Carpenter, 1864 (Goodwin et al*.,* 2001; Goodwin et al., 2003) $\delta^{18}O_{shell}$ seasonality was suggested to be driven by the annual variation of seawater temperature, where shell growth ceased during the cold season. While maximum summer temperatures were recorded consistently at both Pag and Cetina sites, the lowest recorded temperatures varied between them, suggesting that temperature is not the only driver of the winter slowdown in growth.

Food. In ectothermic organisms, the growth rate tends to increase with temperature as a result of a higher metabolic rate as long as the food supply is abundant (Broom et al., 1978). Even when temperatures are high, a minimum amount of available food is required for organism maintenance and therefore, growth (Broom et al., 1978). Similarly, when temperature thresholds for growth are not reached, the amount of available food is insufficient for growth. Certainly, the quality of food determines the growth rate in organisms that mainly rely on fresh phytoplankton and other components of suspended particulate matter (Pernet et al., 2012). This represents the major source of food for filter-feeding bivalves, where phytoplankton provides the best source of energy (Witbaard et al., 2001). Often, the interpretation of food availability and quality based on phytoplankton concentration is hard to assess when it is not measured *in situ*, since available satellite data has a coarse resolution over coastal areas.

Based on the measurement of several environmental parameters previously analyzed in the present thesis, the periods with the best quality of food in these two settings are spring and summer. Both bivalves are filter-feeders and feed upon a mixed diet composed of phytoplankton, zooplankton, microphytobenthos and detritus including bacteria-derived detritus. The significant positive correlation between $\delta^{13}C_{SPM}$ in Pag and shell growth rates indicates that food supply is an important driver. Similarly, the growth rate decrease during fall could be influenced by a shortage in food supply. This correlation did not prove significant in Cetina; however, the lack of environmental record in shells (from reconstructed $\delta^{18}O_{shell}$ values) over this time period suggest a similar hypothesis.

Therefore, whereas temperature stands as an important determinant of shell growth, food availability could set the limits of the shell growth season, considering that during winter food is scarce and its quality is the poorest in the area. Other studies have attributed the onset of the growth season to phytoplankton blooms. Higher growth rates were observed in *M. galloprovincialis* during the period of highest primary productivity (March – May) when temperatures were relatively low in contrast to that observed at the highest temperatures (Peharda et al., 2007). In Arctic ecosystems, where mean annual

temperature ranges are quite narrow, shells of *Serripes groenlandicus* (Mohr, 1786) and *Clinocardium ciliatum* (Fabricius, 1780) deposit winter growth lines as a response to insufficient food supply (Ambrose et al., 2012; Vihtakari et al., 2016). Also, in *M. stimpsoni* from the NW Pacific food availability was suggested to be an indicator of the winter growth break (Kubota et al., 2017). In other mollusks such as the gastropod *Strombus gigas* Linnaeus, 1758, shell growth was largely controlled by food supply rather than by temperature; according to Radermacher et al., (2009), it is possible that rainfall acts to increase the amount of nutrients and thus primary productivity and shell growth, as revealed in their study area.

Reproduction.

Interruptions of shell growth can also be a response of endogenous rhythms, which in turn, fall in synchrony with the above mentioned environmental stimuli (Brockington & Clarke, 2001). For instance, an endogenous time-keeping mechanism is gametogenesis, which several studies have shown to play a role in decreasing shell growth rates and shell growth line formation. In most multicellular animals, there is an initial period of growth and development before reaching sexual maturity when the production of gametes starts. Endogenous shell growth rhythms may be a result of a varying resource allocation towards growth as a trade-off to other requirements for the physiological processes (Abele & Philipp, 2013). In the present study, gonadosomatic index was negatively correlated to shell growth rates in the *Callista chione* population from Cetina and a negative pattern was also observed in the Pag population. These results indicated that spawning events occurred prior to the highest shell growth rates whereas the onset of gametogenesis (October – December) coincided with a shell growth decline. Gametogenesis is a high-energy consumption period for egg and sperm production for which bivalves usually prepare by building up nutrient reserves before it takes place. The slow growth could be associated with a preferential allocation of energy to reproduction rather than growth. The population in Cetina typically experiences a fall/winter gonadal growth under periods of food scarcity, as seen in other species (e.g. Seed, 1976). Alternatively, the Pag population would develop gametogenesis in a shorter period, late winter/spring, when favorable conditions were at their maximum, possibly explaining the relatively higher growth rates observed in December and May. In another population of *C. chione* from the north Adriatic, spawning was presumed to occur between spring and summer, with the growth line deposition coinciding with the start of gametogenesis (estimated at the end of summer/early fall) (Hall et al., 1974). In another venerid bivalve, *P. japonicum*, slow growth was observed between June – July during the ripe gonadal phase, and growth was resumed after spawning thus, named as spawning break (Sato, 1995). Gonadal maturation was also associated with decreasing shell growth rates in one of the Arctic populations studied by Vihtakari et al., (2016).

Likewise, as firstly described in mytilid bivalves, a decline in growth efficiency was observed with increasing size, due to the increasing metabolic demands (Jørgensen, 1976). Thus, the relative allocation of energy towards growth and reproduction has an ontogenetic shift (von Bertalanffy growth equation assumption). In *Cerastoderma edule* (Linnaeus, 1758), sexually immature individuals barely slowed shell growth during the summer, contrasting to adult specimens which showed a distinctive growth line during this season (Milano et al., 2017). These summer growth lines were also observed in a separate study (Ramón, 2003) although it still remains unclear if these are associated with reproduction. In *P. undulata*, high growth rates in spring occurred presumably prior to the spawning timing, which took place over the summer together with lower shell growth rates (Yan et al., 2014). On the other hand, in *M. stimpsoni*, the hypothesis of spawning triggering the summer growth band was ruled out, since this was produced in both adult and immature juveniles and although the reason remained unknown, a possible explanation could be the higher temperatures reported in that study area (Kubota et al., 2017). Yet, bivalve may mimic reproduction during pre-maturity so that immature juveniles may show similar responses to adults (Thompson et al., 1980). In *A. islandica*, the growth break observed in adults during gametogenesis was suggested to be mimicked by juveniles (Schöne et al., 2005) although a later study showed that different populations form the annual growth line at the same time although reproductive events occur at different timings (Schöne, 2013). An Antarctic species, *Yoldia eightsi* (Courthouy, 1839) might have its shell growth constrained by gametogenesis (Román-González et al., 2017). In *M. edulis* from Tokio Bay, slower shell growth rates during winter were possibly controlled by a combination of environmental and physiological factors (Okaniwa et al., 2010). Our results showed a correspondence between the annual biocheck formation and the post-spawning and regeneration stage in *C. chione*. This periodicity was coincident with decreasing of both temperatures and food supply, and therefore is difficult to determine which of these factors was the main driver.

Shell growth rates in *G. bimaculata* specimens were highest during late spring and summer, which coincided with the spawning timing at both sites (July – September). Considering a growth line formation at the end of summer (as discussed previously from young shells), a relationship with the end of gametogenesis and the onset of a new cycle could be inferred. In *Scapharca broughtonii* (Schrenck, 1867), an Arcidae family species, summer growth breaks were observed during the highest temperature peak based on microstructure analysis, and these were in turn associated with spawning events (Nishida et al., 2012). Therefore, this hypothesis cannot be disregarded. As supported by the above mentioned literature, resource allocation differences during gametogenesis are species-specific. Whether this physiological process or environmental drivers are the main triggers for shell growth is a continuing topic for discussion.

To conclude, the species-specific physiological optimum is a combination of warm temperatures and quality and quantity of food supply in areas where predation is not a major threat; therefore, species from Cetina have a better condition in terms of higher shell growth rates associated with milder temperatures and higher quality of food. Shell growth and gonad development were active at several intervals, but coincided the most with periods of the highest food quality in the surrounding environment. Our results showed that both *C. chione* and *G. bimaculata,* despite showing varying ecological characteristics between sites, do share a period of growth slowdown, suggesting the coincidental food supply in the region as a limiting factor. The reduced shell growth during late fall and winter, when seawater temperatures and food availability were the lowest, coupled with the onset of gametogenesis suggested a reduced shell growth as a result of unfavorable environmental conditions and a higher requirement of reproductive effort. Unlike in mark-recapture or lab-cultured experiments, where animals may suffer the newly provided conditions (e.g. Iglesias & Navarro, 1991), growth studies presented in this thesis allow reporting changes in an environmental context which reflects natural conditions.

5.3.4. Potential for paleoclimate reconstructions

Sclerochemical analysis performed on *C. chione* and *G. bimaculata* shells provided feasible data for reconstructing maximum temperatures. Shells do not monitor the environment uninterruptedly (Goodwin et al., 2003; Ivany et al., 2003) and are faithful recorders of environmental conditions only during growth, as shown in this study. Therefore, the reconstruction of the seawater temperature minima from $\delta^{18}O_{shell}$ values in this region is not feasible due to the negligible shell growth during the coldest months. These results further support studies in ontogenetically younger portions of the shell, since these regions are more reliable indicators of past temperature reconstructions not only due to faster growth rates (enabling higher resolution) but also because they cover a wider spectrum of past temperatures. A clear example of this is shown in Kubota et al., (2016), where studies in *M. stimpsoni* postulated shell growth between spring and fall in juveniles, whereas adults deposited shell material almost exclusively during the summer. These observations highlight the importance of considering both juvenile and mature shell portions when studying shell growth patterns. Certainly, because of its longevity, *Glycymeris* sp. has a great potential for sclerochronology. Comparing growth dynamics in congeneric species at close-by locations may indicate the range of potential differences associated with their longevity. To reliably compare shell growth rates between our studied populations, sclerochemical analysis in shell replicates need to be extended (further milled) to cover the same annual periods.

The Glycymerididae is a cosmopolitan family from the Cenozoic, inhabiting temperate to warm-water environments (Thomas, 1975; Nicol, 1964). Glycymeridid bivalve records have been found in shallow-marine deposits from the northeast Pacific upper Cretaceous and Paleocene (Squires, 2010). Sclerochronological studies have been conducted on the Oligocene bivalve *G. planicostalis* (Walliser et al., 2015). Pliocene fossils have also been recorded from the North Sea Basin and *G. radiolyrata* was suspected to evolve from *G. bimaculata* (Moerdijk et al., 2000). Additionally, fossil *Glycymeris* sp. and *Callista* sp. shells have been found in Venus-Ancilla assemblages from the Miocene in northern Italy (Bernasconi & Robba, 1993), while Pleistocene marine deposits from the Mediterranean (Torres et al., 2013; Crippa, 2013; Crippa et al., 2016) and northern Patagonia (Bayer & Gordillo, 2013) contain fossil shells of several *Glycymeris* sp. Radiocarbon studies in shells of *G. nummaria* (before *G. insubrica*) have been aged 5500 years BP during the Holocene (Sivan et al., 2006). Gutierrez-Mas, (2011) suggested that *Glycymeris* sp. shell accumulations may shed light on recent sea-level changes as studied in Cadiz Bay. Altogether and the use of *Glycymeris* sp. and *Callista chione* shells by Neanderthals along the northern Mediterranean (Cortés-Sánchez et al., 2011; Romagnoli et al., 2016) make them interesting targets for palaeoecological studies.

5.3.5. Future research

A wide range of techniques and applications to sclerochronology are currently under development. Studies relating crystallographic properties with geochemical analysis in the shell in relation to the surrounding environment have recently postulated that higher metabolic rates, as a result of warmer temperatures and high-availability of food, likely synthesize larger amounts of organic material in the shell matrix (Nishida et al., 2012; Milano et al., 2017). Different microstructures contain different mixtures of organics, thus, their study may identify periods of major growth line formation or line disturbances (Stemmer & Nehrke, 2014; Cuif et al., 2013). On the other hand, trace elements have also been used as environmental proxies, providing insights into physiological, environmental and even anthropogenic effects on shell growth variation (Carroll et al., 2009; Elliot et al., 2009; Gillikin, 2005; H. Yan et al., 2014) and recently improved techniques have revealed high resolution periodicities of elemental ratios such as Mg/Ca, Sr/Ca, B/Ca or Ba/Ca from fossil and modern clams (Zhao et al., 2017; Schöne, 2013; Hori et al., 2015) although distinguishing between environmental and physiological factors is challenging. These new approaches should be carried out to gain a better understanding of proxy incorporation in natural settings and thus, revealing more details of bivalve life history traits given the extensive environmental and biological data collection from this thesis.

6. CONCLUSION

- A mixture of marine and terrestrial sources constitutes the particulate matter in the coastal central Adriatic Sea and also presents a temporal variation. A terrestrial influence is evident in winter and spring, while a progressive mixing with marine waters is observed in summer and fall, after the main phytoplankton blooms.

- Low %C and %N characterize the sediment, corroborating its poor nutritional quality in this oligotrophic sea.

- Stable isotopes and fatty acid analysis revealed spring and summer as the periods with best nutritional quality of the particulate matter.

- The $\delta^{13}C$ in the digestive gland was species-specific, with more enriched values in *Glycymeris bimaculata* than *Callista chione*, whereas $\delta^{15}N$ was site-specific, with more enriched values in Cetina.

- No feeding overlap between *G. bimaculata* and *C. chione* was observed suggesting resource partitioning. Populations in Pag showed a higher contribution of sediment to their diet, and the presence of benthic diazotroph biomass was likely responsible for the low $\delta^{15}N$ in their diet.

- Site-specificity was dominant when comparing the isotopic composition of two populations of *G. pilosa*, with more isotopically enriched values in Pašman.

- The present work accentuated the importance of assessing spatial and temporal changes of a large set of biochemical parameters in feeding ecology studies.

- Histology and Gonadosomatic index successfully described the main changes in the gametogenic cycle of two different species, *C. chione* and *G. bimaculata*.

- Inter-site variations in the spawning timing and duration of *C. chione* were most likely due to temperature, taking place earlier and for a more prolongued period in Cetina, the warmest site.

- Different reproductive strategies between *C. chione* populations were shown by a resorption of gonads in Pag population, as a result of the species adaptation capacity to unfavorable conditions (e.g. temperature).

- A later spawning period and timing in *Glycymeris* sp. relative to *C. chione* was most likely related to insufficient time to develop enough energy storage during periods of sufficient food supply.
- Body mass index is not always an indicator of body condition in bivalves.
- Seasonal variation in $\delta^{18}O_{shell}$ values measured from *C. chione* and *G. bimaculata* specimens from the Adriatic Coast revealed that shell accretion took place mainly between May and December.
- Annual growth bands were clearly deposited at the end of summer and early fall in *C. chione* as a result of slow growth. In *G. bimaculata* growth lines in young specimens were laid down at the temperature maxima but in adults it remains unclear.
- Temperature is an important determinant of shell growth whereas food availability set the limits of the shell growth season. The onset of gametogenesis coincided with periods of slow growth suggesting a preferential allocation of energy to reproduction rather than growth.
- These results document extensively several aspects of bivalve ecology in the Adriatic Sea and a comprehensive relationship with shell growth, establishing baseline information for further studies on the studied species and other bivalves.
- Sclerochronology coupled to physiological and ecological studies contribute to a better understanding of species life-history traits.

7. LITERATURE

Abele, D. & E. Philipp. 2013. Environmental Control and Control of the Environment: The Basis of Longevity in Bivalves. Gerontology, 59(3): 261–266.

Ackman, R., C. Tocher & J. MacLachlan. 1968. Marine phytoplankter fatty acids. J. Fish. Res. board Canada, 25: 1603–1620.

Ahlgren, G., T. Vrede & W. Goedkoop. 2009. Fatty acid ratios in freshwater fish, zooplankton and zoobenthos—are there specific optima? In M. Arts, M. Brett, & M. Kainz, eds. *Lipids in aquatic ecosystems*. London, New York: Springer Science, pp. 147–178.

Ahn, I.-Y., K. Woong Cho, K.-S. Choi, Y. Seo & J. Shin. 2000. Lipid content and composition of the Antarctic lamellibranch, *Laternula elliptica* (King & Broderip) (Anomalodesmata: Laternulidae), in King George Island during an austral summer. Polar Biol., 23(1): 24–33.

Albentosa, M., U. Labarta, M. Fernández-Reiriz & A. Pérez-Camacho. 1996. Fatty acid composition of *Ruditapes decussatus* spat fed on different microalgae diets. Comp. Biochem. Physiol. Part A, 113: 113–119.

Alkanani, T., C.C. Parrish, R.J. Thompson & C.H. McKenzie. 2007. Role of fatty acids in cultured mussels, *Mytilus edulis*, grown in Notre Dame Bay, Newfoundland. J. Exp. Mar. Bio. Ecol., 348(1-2): 33–45.

Alomar, C., M. Vázquez-Luis, K. Magraner, L. Lozano & S. Deudero. 2015. Evaluating stable isotopic signals in bivalve *Pinna nobilis* under different human pressures. J. Exp. Mar. Bio. Ecol., 467: 77–86.

Ambrose, W.G., P.E. Renaud, W.L. Locke, F.R. Cottier, J. Berge, M.L. Carroll, B. Levin & S. Ryan. 2012. Growth line deposition and variability in growth of two circumpolar bivalves (*Serripes groenlandicus*, and *Clinocardium ciliatum*). Polar Biol., 35(3): 345–354.

Ansell, A. 1968. The rate of growth of the hard clam *Mercenaria mercenaria* (L) throughout the geographical range. J. du Cons. Perm. Int. pour l'Exploration la Mer, 31: 364–409.

Antolić, B., D. Bogner, N. Bojanić, I. Cvitković, M. Despalatović & B. Grbec. 2010. *Kontrola kakvoče obalnog mora 2009? Projekt Pag-Konavle*, Split.

Antonio, E. & N. Richoux. 2014. Trophodynamics of three decapod crustaceans in a temperate estuary using stable isotope and fatty acid analyses. Mar. Ecol. Prog. Ser., 504: 193–205.

Antonio, E.S., A. Kasai, M. Ueno, Y. Ishihi, H. Yokoyama & Y. Yamashita. 2012. Spatial-temporal feeding

dynamics of benthic communities in an estuary-marine gradient. Estuar. Coast. Shelf Sci., 112: 86–97.

Antonio, E.S., A. Kasai, M. Ueno, Y. Kurikawa, K. Tsuchiya, H. Toyohara, Y. Ishihi, H. Yokoyama & Y. Yamashita. 2010. Consumption of terrestrial organic matter by estuarine molluscs determined by analysis of their stable isotopes and cellulase activity. Estuar. Coast. Shelf Sci., 86(3): 401–407.

Antonio, E.S. & N.B. Richoux. 2016a. Influence of diet on the metabolic turnover of stable isotope ratios and fatty acids in the omnivorous shrimp *Palaemon peringueyi*. Mar. Biol., 163(7): 154.

Antonio, E.S. & N.B. Richoux. 2016b. Tide-Induced Variations in the Fatty Acid Composition of Estuarine Particulate Organic Matter. Estuaries and Coasts, 39(4): 1072–1083.

Bacon, G.S., B.A. Macdonald & J.E. Ward. 1998. Physiological responses of infaunal (*Mya arenaria*) and epifaunal (*Placopecten magellanicus*) bivalves to variations in the concentration and quality of suspended particles I. Feeding activity and selection. J. Exp. Mar. Bio. Ecol., 219: 105–125.

Baeta, M., M. Ramón & E. Galimany. 2014. Decline of a *Callista chione* (Bivalvia: Veneridae) bed in the Maresme coast (northwestern Mediterranean Sea). Ocean Coast. Manag., 93: 15–25.

Baker, S.M. & D.J. Hornbach. 2000. Physiological Status and Biochemical Composition of a Natural Population of Unionid Mussels (*Amblema plicata*) Infested by Zebra Mussels (*Dreissena polymorpha*). Am. Midl. Nat., 143(2): 443–452.

Barker Jørgensen, C. 1976. Growth efficiencies and factors controlling size in some mytilid bivalves. Especially *Mytilus edulis* L.: review and interpretation. Ophelia, 15(2): 175–192.

Bayer, M. & S. Gordillo. 2013. A new Pleistocene species of *Glycymeris* from Northern Patagonia. Ameghiniana, 50(2): 265–268.

Bayne, B.L. 2009. Carbon and nitrogen relationships in the feeding and growth of the Pacific oyster, *Crassostrea gigas* (Thunberg). J. Exp. Mar. Bio. Ecol., 374(1): 19–30.

Bayne, B.L., D.L. Holland, M.N. Moore, D.M. Lowe & J. Widdows. 1978. Further studies on the effects of stress in the adult on the eggs of *Mytilus edulis*. J. Mar. Biol. Ass. U. K., 58(04): 825–841.

Bentaleb, I., M. Fontugne, G. Descolas-Gros, C. Girardin, A. Mariotti, C. Pierre, C. Brunet & A. Poison. 1998. Carbon isotopic fractionation by plankton in the Southern Indian Ocean: relationship between $\delta^{13}C$ of particulate organic carbon and dissolved carbon dioxide. J. Mar. Syst., 17: 39–58.

Bergamino, L., T. Dalu & N.B. Richoux. 2014. Evidence of spatial and temporal changes in sources of organic matter in estuarine sediments: Stable isotope and fatty acid analyses. Hydrobiologia, 732(1): 133–145.

Bernasconi, M. & E. Robba. 1993. Molluscan palaeoecology and sedimentological features: an integrated approach from the Miocene Meduna section, northern Italy. Palaeogeogr. Palaeoclimatol. Palaeoecol., 10: 267–290.

Berthou, P., M. Blanchard, P. Noel & C. Vergnaud-grazzini. 1986. The analysis of stable isotopes of the shell applied to the determination of the age of four bivalves of the "Normano-Breton" Gulf, Western Channel. ICES, K16: 1–13.

Berto, D., F. Rampazzo, S. Noventa, F. Cacciatore, M. Gabellini, F.B. Aubry, A. Girolimetto & R.B. Brusà. 2013. Stable carbon and nitrogen isotope ratios as tools to evaluate the nature of particulate organic matter in the Venice lagoon. Estuar. Coast. Shelf Sci., 135: 66–76.

Beukema, J.J., R. Dekker & J.M. Jansen. 2009. Some like it cold: populations of the tellinid bivalve *Macoma balthica* (L.) suffer in various ways from a warming climate. Mar. Ecol. Prog. Ser., 384: 135–145.

Boëchat, I.G., A. Krüger, R.C. Chaves, D. Graeber & B. Gücker. 2014. Science of the Total Environment Land-use impacts on fatty acid profiles of suspended particulate organic matter along a larger tropical river. Sci. Total Environ., 482-483: 62–70.

Böhm, F., M.M. Joachimski, W.C. Dullo, A. Eisenhauer, H. Lehnert, J. Reitner & G. Worheide. 2000. Oxygen isotope fractionation in marine aragonite of coralline sponges. Geochim. Cosmochim. Acta, 64: 1695–1703.

Bonacci, O. 2015. Karst hydrogeology / hydrology of dinaric chain and isles. Environ. Earth Sci., 74: 37–55.

Bonacci, O. & T. Roje-Bonacci. 2003. The influence of hydroelectrical development on the flow regime of the karstic river Cetina. Hydrol. Process., 17(1): 1–15.

Boon, A. & G. Duineveld. 1996. Phytopigments and fatty acids as molecular markers for the quality of near-bottom particulate organic matter in the North Sea. J. Sea Res., 35(4): 279–291.

Braeckman, U., P. Provoost, K. Sabbe, K. Soetaert, J.J. Middelburg, M. Vincx & J. Vanaverbeke. 2015. Temporal dynamics in a shallow coastal benthic food web: insights from fatty acid biomarkers and

their stable isotopes. Mar. Environ. Res., 108: 55–68.

Brey, T. 1995. Temperature and reproductive metabolism in macrobenthic populations. Mar. Ecol. Prog. Ser., 125: 87–93.

Brocas, W.M., D.J. Reynolds, P.G. Butler, C.A. Richardson, J.D. Scourse, I.D. Ridgway & K. Ramsay. 2013. The dog cockle, Glycymeris glycymeris (L.), a new annually-resolved sclerochronological archive for the Irish Sea. Palaeogeogr. Palaeoclimatol. Palaeoecol., 373: 133–140.

Brockington, S. & A. Clarke. 2001. The relative influence of temperature and food on the metabolism of a marine invertebrate. J. Exp. Mar. Bio. Ecol., 258(1): 87–99.

Broom, M.J. & J. Mason. 1978. Growth and spawning in the pectinid *Chlamys opercularis* in relation to temperature and phytoplankton concentration. Mar. Biol., 47(3): 277–285.

Bucci, J.P., W.J. Showers, B. Genna & J.F. Levine. 2009. Stable oxygen and carbon isotope profiles in an invasive bivalve (*Corbicula fluminea*) in North Carolina watersheds. Geochim. Cosmochim. Acta, 73(11): 3234–3247.

Buddemeier, R., J. Maragos & D. Knutson. 1974. Radiographic studies of reef coral exoskeletons: rates and patterns of coral growth. J. Exp. Mar. Bio. Ecol., 14: 179–200.

Budge, S., S. Iverson, W. Bowen & R. Ackman. 2002. Among- and within-species variability in fatty acid signatures of marine fish and invertebrates on the Scotian Shelf, Georges Bank, and southern Gulf of St. Lawrence. Can. J. Fish. Aquat. Sci., 59: 886–898.

Budge, S. & C. Parrish. 1998. Lipid biogeochemistry of plankton, settling matter and sediments in Trinity Bay, Newfoundland. II. Fatty acids. Org. Geochem., 29: 1547–1559.

Budge, S.M., M.J. Wooller, A.M. Springer, S.J. Iverson, C.P. McRoy & G.J. Divoky. 2008. Tracing carbon flow in an arctic marine food web using fatty acid-stable isotope analysis. Oecologia, 157(1): 117–129.

Buick, D.P. & L.C. Ivany. 2004. 100 years in the dark: Extreme longevity of Eocene bivalves from Antarctica. Geology, 32(10): 921.

Burdon, D., R. Callaway, M. Elliott, T. Smith & A. Wither. 2014. Mass mortalities in bivalve populations: A review of the edible cockle *Cerastoderma edule* (L.). Estuar. Coast. Shelf Sci., 150(PB): 271–280.

Bušelić, I., M. Peharda, D.J. Reynolds, P.G. Butler, A.R. González, D. Ezgeta-Balić, I. Vilibić, B. Grbec, P.

Hollyman & C.A. Richardson. 2015. Glycymeris bimaculata (Poli, 1795) — A new sclerochronological archive for the Mediterranean? J. Sea Res., 95: 139–148.

Butler, P.G., C.A. Richardson, J.D. Scourse, A.D. Wanamaker, T.M. Shammon & J.D. Bennell. 2010. Marine climate in the Irish Sea: analysis of a 489-year marine master chronology derived from growth increments in the shell of the clam Arctica islandica. Quat. Sci. Rev., 29(13-14): 1614–1632.

Butler, P.G. & B.R. Schöne. 2017. New research in the methods and applications of sclerochronology. Palaeogeogr. Palaeoclimatol. Palaeoecol., 465: 295–299.

Butler, P.G., A.D. Wanamaker, J.D. Scourse, C.A. Richardson & D.J. Reynolds. 2011. Long-term stability of δ13C with respect to biological age in the aragonite shell of mature specimens of the bivalve mollusk Arctica islandica. Palaeogeogr. Palaeoclimatol. Palaeoecol., 302(1-2): 21–30.

Butler, P.G., A.D. Wanamaker, J.D. Scourse, C.A. Richardson & D.J. Reynolds. 2013. Variability of marine climate on the North Icelandic Shelf in a 1357-year proxy archive based on growth increments in the bivalve Arctica islandica. Palaeogeogr. Palaeoclimatol. Palaeoecol., 373: 141–151.

Canestri-Trotti, G., E.M. Baccarani, F. Paesanti & E. Turolla. 2000. Monitoring of infections by protozoa of the genera Nematopsis, Perkinsus and Porospora in the smooth venus clam *Callista chione* from the North-Western Adriatic Sea (Italy). Dis. Aquat. Organ., 42: 157–161.

Cardoso, J.F.M.F., G. Nieuwland, R. Witbaard, H.W. van der Veer & J.P. Machado. 2013. Growth increment periodicity in the shell of the razor clam *Ensis directus* using stable isotopes as a method to validate age. Biogeosciences Discuss., 10(3): 4303–4330.

Cardoso, J.F.M.F., S. Santos, J.I. Witte, R. Witbaard, H.W. van der Veer & J.P. Machado. 2013. Validation of the seasonality in growth lines in the shell of *Macoma balthica* using stable isotopes and trace elements. J. Sea Res., 82: 93–102.

Cardoso, J.F.M.F., J.I. Witte & H.W. van der Veer. 2009a. Differential reproductive strategies of two bivalves in the Dutch Wadden Sea. Estuar. Coast. Shelf Sci., 84(1): 37–44.

Cardoso, J.F.M.F., J.I. Witte & H.W. van der Veer. 2007. Growth and reproduction of the bivalve *Spisula subtruncata* (da Costa) in Dutch coastal waters. J. Sea Res., 57(4): 316–324.

Cardoso, J.F.M.F., J.I. Witte & H.W. van der Veer. 2009b. Reproductive investment of the American razor clam *Ensis americanus* in the Dutch Wadden Sea. J. Sea Res., 62(4): 295–298.

Carlier, A., L. Chauvaud, M. van der Geest, F. Le Loc'h, M. Le Duff, M. Vernet, J. Raffray, D. Diakhaté, P. Labrosse, A. Wagué, C. Le Goff, F. Gohin, B. Chapron & J. Clavier. 2015. Trophic connectivity between offshore upwelling and the inshore food web of Banc d'Arguin (Mauritania): New insights from isotopic analysis. Estuar. Coast. Shelf Sci., 165: 149–158.

Carlier, A., P. Riera, J. Amouroux, J. Bodiou, M. Desmalades & A. Grémare. 2008. Food web structure of two Mediterranean lagoons under varying degree of eutrophication. J. Sea Res., 60(4): 287–298.

Carlier, A., P. Riera, J.J.-M. Amouroux, J.-Y. Bodiou & A. Grémare. 2007. Benthic trophic network in the Bay of Banyuls-sur-Mer (northwest Mediterranean, France): An assessment based on stable carbon and nitrogen isotopes analysis. Estuar. Coast. Shelf Sci., 72(1-2): 1–15.

Carmichael, R.H., A.C. Shriver & I. Valiela. 2004. Changes in shell and soft tissue growth, tissue composition, and survival of quahogs, *Mercenaria mercenaria*, and softshell clams, *Mya arenaria*, in response to eutrophic-driven changes in food supply and habitat. J. Exp. Mar. Bio. Ecol., 313(1): 75–104.

Carreira, R.S., A.L.R. Wagener, J.W. Readman, T.W. Fileman & S.A. Macko. 2002. Changes in the sedimentary organic carbon pool of a fertilized tropical estuary, Guanabara Bay, Brazil: an elemental, isotopic and molecular marker approach. Mar. Chem., 79: 207–227.

Carriquiry, J.D., P. Jorgensen, J.A. Villaescusa & S.E. Ibarra-Obando. 2016. Isotopic and Elemental Composition of Marine Macrophytes as Biotracers of Nutrient Recycling Within a Coastal Lagoon in Baja California, Mexico. Estuaries and Coasts, 39(2): 451–461.

Carroll, M.L., B.J. Johnson, G.A. Henkes, K.W. McMahon, A. Voronkov, W.G. Ambrose & S.G. Denisenko. 2009. Bivalves as indicators of environmental variation and potential anthropogenic impacts in the southern Barents Sea. Mar. Pollut. Bull., 59(4-7): 193–206.

Castagna, M. & J. Kraeuter. 1977. *Mercenaria* culture using stone aggregate for predator protection. Proc Natl Shellfish Ass. Proc. Natl. Shellfish. Assoc., 67: 1–6.

Charles, F., J. Amouroux & A. Grémare. 1999. Comparative study of the utilization of bacteria and microalgae by the suspension-feeding bivalve: *Callista chione*. J. Mar. Biol. Assoc. UK, 79: 577–584.

Chauvaud, L., A. Lorrain, R.B. Dunbar, Y.-M. Paulet, G. Thouzeau, F. Jean, J.-M. Guarini & D. Mucciarone. 2005. Shell of the Great Scallop *Pecten maximus* as a high-frequency archive of paleoenvironmental changes. Geochemistry, Geophys. Geosystems, 6(8): Q08001.

Chauvaud, L., Y. Patry, A. Jolivet, E. Cam, C. Le Goff, Ø. Strand, G. Charrier, J. Thébault, P. Lazure, K. Gotthard & J. Clavier. 2012. Variation in size and growth of the great scallop *Pecten maximus* along a latitudinal gradient. PLoS One, 7(5): e37717.

Chauvaud, L., G. Thouzeau & Y.-M. Paulet. 1998. Effects of environmental factors on the daily growth rate of *Pecten maximus* juveniles in the Bay of Brest (France). J. Exp. Mar. Bio. Ecol., 227: 83–111.

Cherel, Y. & K.A. Hobson. 2007. Geographical variation in carbon stable isotope signatures of marine predators: a tool to investigate their foraging areas in the Southern Ocean. Mar. Ecol. Prog. Ser., 329: 281–287.

Chu, E.E. & J. Greaves. 1991. Metabolism of palmitic, linoleic, and linolenic acids in adult oysters, *Crassostrea virginica*. Mar. Biol., 236: 229–236.

Cifuentes, L.A., J.H. Sharp & M.L. Fogel. 1988. Stable carbon and nitrogen isotope biogeochemistry Delaware estuary. Limnol. Oceanogr., 33(5): 1102–1115.

Clarke, A. 1987. Temperature, latitude and reproductive effort. Mar. Ecol. Prog. Ser, 38: 89–99.

Cloern, J., E. Canuel & D. Harris. 2002. Stable carbon and nitrogen isotope composition of aquatic and terrestrial plants of the San Francisco Bay estuarine system. Limnol. Oceanogr., 47: 713–729.

CMEMS. Copernicus marine environment monitoring service. Available at: http://marine.copernicus.eu/ [Accessed January 1, 2016].

Coe, W.P. & H.J. Turner. 1938. Development of the gonads and gametes in the soft shell clam (*Mya arenaria*). J. Morphol., 62: 91–111.

Connelly, T.L., T.N. Businski, D. Deibel, C.C. Parrish & P. Trela. 2016. Annual cycle and spatial trends in fatty acid composition of suspended particulate organic matter across the Beaufort Sea shelf. Estuar. Coast. Shelf Sci., 181: 170–181.

Cortés-Sánchez, M., A. Morales-Muñiz, M.D. Simón-Vallejo, M.C. Lozano-Francisco, J.L. Vera-Peláez, C. Finlayson, J. Rodríguez-Vidal, A. Delgado-Huertas, F.J. Jiménez-Espejo, F. Martínez-Ruiz, M.A. Martínez-Aguirre, A.J. Pascual-Granged, M.M. Bergadà-Zapata, J.F. Gibaja-Bao, J.A. Riquelme-Cantal, J.A. López-Sáez, M. Rodrigo-Gámiz, S. Sakai, S. Sugisaki, G. Finlayson, D.A. Fa & N.F. Bicho. 2011. Earliest Known Use of Marine Resources by Neanderthals. PLoS One, 6(9): e24026.

Cresson, P., S. Ruitton, M.F. Fontaine & M. Harmelin-Vivien. 2012. Spatio-temporal variation of

suspended and sedimentary organic matter quality in the Bay of Marseilles (NW Mediterranean) assessed by biochemical and isotopic analyses. Mar. Pollut. Bull., 64(6): 1112–1121.

Crippa, G. 2013. The shell ultrastructure of the genus Glycymeris da Costa, 1778: A comparison between fossil and recent specimens. Riv. Ital. di Paleontol. e Stratigr., 119(3): 387–399.

Crippa, G., L. Angiolini, C. Bottini, E. Erba, F. Felletti, C. Frigerio, J.A.I. Hennissen, M.J. Leng, M.R. Petrizzo, I. Raffi, G. Raineri & M.H. Stephenson. 2016. Seasonality fluctuations recorded in fossil bivalves during the early Pleistocene: Implications for climate change. Palaeogeogr. Palaeoclimatol. Palaeoecol., 446: 234–251.

Crnčević, M., M. Peharda, D. Ezgeta-Balić & M. Pećarević. 2013. Reproductive cycle of *Glycymeris nummaria* (Mollusca: Bivalvia) from Mali Ston Bay, Adriatic Sea, Croatia. Sci. Mar., 77(2): 293–300.

Cruz, P., C. Rodriguez-Jaramillo & A.M. Ibarra. 2000. Environment and population origin effects on first sexual maturity of catarina scallop, *Argopecten ventricosus* (Sowerby II, 1842). J. Shellfish Res., 9(1): 89–94.

Cuif, J.-P., A. Bendounan, Y. Dauphin, J. Nouet & F. Sirotti. 2013. Synchrotron-based photoelectron spectroscopy provides evidence for a molecular bond between calcium and mineralizing organic phases in invertebrate calcareous skeletons. Anal. Bioanal. Chem., 405(27): 8739–8748.

Currin, C.A., S.Y. Newell & H.W. Paerl. 1995. The Role of Standing Dead Spartina-Alterniflora and Benthic Microalgae in Salt-Marsh Food Webs - Considerations Based on Multiple Stable-Isotope Analysis. Mar. Ecol. Ser., 121(1-3): 99–116.

Dalsgaard, J.J., M. St John, G. Kattner, D. Müller-Navarra, W. Hagen, M.S. John, M. St. John, G. Kattner, D. Müller-Navarra, W. Hagen, M. St John, G. Kattner, D. Müller-Navarra & W. Hagen. 2003. Fatty Acid Trophic Markers in the Pelagic Marine Environment. Adv. Mar. Biol., 46: 225–340.

Dame, R.F. 1996. *Ecology of Marine Bivalves. An Ecosystem Approach* Second. M. J. Kennish & P. L. Lutz, eds., Boca Raton, Florida: CRC Marine Science Series, CRC Press.

Danovaro, R., A. Dell'Anno, M. Fabiano, A. Pusceddu & A. Tselepides. 2001. Deep-sea ecosystem response to climate changes: The eastern Mediterranean case study. Trends Ecol. Evol., 16(9): 505–510.

Davenport, J., R.J. Smith & M. Packer. 2000. Mussels *Mytilus edulis*: significant consumers and destroyers of mesozooplankton. Mar. Ecol. Prog. Ser., 198: 131–137.

Delgado, M. & A. Pérez-Camacho. 2007. Estudio comparativo del desarrollo gonadal de *Ruditapes philippinarum* (Adams and Reeve) y *Ruditapes decussatus* (L.) (Mollusca: Bivalvia) Influencia de la temperatura. Sci. Mar., 71(3): 471–484.

DeMaster, D. 1991. Measuring biogenic silica in marine sediments and suspended matter. Mar. Part. Anal. Charact.: 363–367.

DeNiro, M.J. & S. Epstein. 1978. Influence of diet on the distribution of carbon isotopes in animals. , 42: 495–506.

Deudero, S., M. Cabanellas, A. Blanco & S. Tejada. 2009. Stable isotope fractionation in the digestive gland, muscle and gills tissues of the marine mussel *Mytilus galloprovincialis*. J. Exp. Mar. Bio. Ecol., 368(2): 181–188.

Dias, E., P. Morais, A. Cotter, C. Antunes & J. Hoffman. 2016. Estuarine consumers utilize marine, estuarine and terrestrial organic matter and provide connectivity among these food webs. Mar. Ecol. Prog. Ser., 554: 21–34.

Doi, H., M. Matsumasa, T. Toya, N. Satoh, C. Mizota, Y. Maki & E. Kikuchi. 2005. Spatial shifts in food sources for macrozoobenthos in an estuarine ecosystem: Carbon and nitrogen stable isotope analyses. Estuar. Coast. Shelf Sci., 64(2-3): 316–322.

Dolenec, M., P. Žvab, G. Mihelčić, Ž. Lambaša Belak, S. Lojen, G. Kniewald, T. Dolenec & N. Rogan Šmuc. 2011. Use of stable nitrogen isotope signatures of anthropogenic organic matter in the coastal environment: The case study of the Kosirina Bay (Murter Island, Croatia). Geol. Croat., 64: 143–152.

Dolenec, T., S. Lojen, G. Kniewald, M. Dolenec & N. Rogan. 2007. Nitrogen stable isotope composition as a tracer of fish farming in invertebrates *Aplysina aerophoba*, *Balanus perforatus* and *Anemonia sulcata* in central Adriatic. Aquaculture, 262(2-4): 237–249.

Drent, J. 2004. *The relative importance of temperature for growth and reproduction in an intertidal marine bivalve,* Macoma balthica*, along a latitudinal gradient. In: Drent J (ed) Life history variation of a marine bivalve (Macoma balthica) in a changing world.* State University Groningen.

Drummond, L., M. Mulcahy & S. Culloty. 2006. The reproductive biology of the Manila clam, *Ruditapes philippinarum*, from the North-West of Ireland. Aquaculture, 254(1-4): 326–340.

Dubois, S., H. Blanchet, A. Garcia, M. Massé, R. Galois, A. Grémare, K. Charlier, G. Guillou, P. Richard &

N. Savoye. 2014. Trophic resource use by macrozoobenthic primary consumers within a semi-enclosed coastal ecosystem: Stable isotope and fatty acid assessment. J. Sea Res., 88: 87–99.

Dubois, S., N. Savoye, A. Grémare, M. Plus, K. Charlier, A. Beltoise & H. Blanchet. 2012. Origin and composition of sediment organic matter in a coastal semi-enclosed ecosystem: An elemental and isotopic study at the ecosystem space scale. J. Mar. Syst., 94: 64–73.

Dupčić Radić, I., M. Carić, M. Najdek, N. Jasprica, J. Bolotin, M. Peharda & A. Bratoš Cetinić. 2014. Biochemical and fatty acid composition of *Arca noae* (Bivalvia: Arcidae) from the Mali Ston Bay, Adriatic Sea. Mediterr. Mar. Sci., 15(3): 520–531.

El-Karim, M.S.A., A.M.A. Mahmoud & M.H.H. Ali. 2016. Fatty Acids Composition and Sources of Organic Matter in Surface Sediments of Four River Nile Sub-Branches, Egypt. J. Fish. Aquat. Sci., 11(3): 216–224.

Elliot, M., K. Welsh, C. Chilcott, M. McCulloch, J. Chappell & B. Ayling. 2009. Profiles of trace elements and stable isotopes derived from giant long-lived *Tridacna gigas* bivalves: Potential applications in paleoclimate studies. Palaeogeogr. Palaeoclimatol. Palaeoecol., 280(1-2): 132–142.

Ezgeta-Balić, D., S. Lojen, T. Dolenec, P. Žvab Rožič, M. Dolenec, M. Najdek & M. Peharda. 2014. Seasonal differences of stable isotope composition and lipid content in four bivalve species from the Adriatic Sea. Mar. Biol. Res., 10(6): 625–634.

Ezgeta-Balić, D., M. Najdek, M. Peharda & M. Blažina. 2012. Seasonal fatty acid profile analysis to trace origin of food sources of four commercially important bivalves. Aquaculture, 334-337: 89–100.

Ezgeta-Balić, D., M. Peharda, C.A. Richardson, M. Kuzmanić, N. Vrgoč & I. Isajlović. 2011. Age, growth, and population structure of the smooth clam *Callista chione* in the eastern Adriatic Sea. Helgol. Mar. Res., 65: 457–465.

Faganeli, J., N. Ogrinc, N. Kovac, K. Kukovec, I. Falnoga, P. Mozetic & O. Bajt. 2009. Carbon and nitrogen isotope composition of particulate organic matter in relation to mucilage formation in the northern Adriatic Sea. Mar. Chem., 114(3-4): 102–109.

Faganeli, J., J. Pezdic, B. Ogorelec, M. Mišič & M. Najdek. 1994. The origin of sedimentary organic matter in the Adriatic. Cont. Shelf Res., 14(4): 365–384.

Fahl, K. & G. Kattner. 1993. Lipid Content and fatty acid composition of algal communities in sea-ice and water from the Weddell Sea (Antarctica). Polar Biol., 13(6): 405–409.

Falk-Petersen, S., J. Sargent & K. Tande. 1987. Lipid composition of zooplankton in relation to the sub-Arctic food web. Polar Biol., 8: 115–120.

Fischer, A.M., J.P. Ryan, C. Levesque & N. Welschmeyer. 2014. Characterizing estuarine plume discharge into the coastal ocean using fatty acid biomarkers and pigment analysis. Mar. Environ. Res., 99: 106–116.

Focken, U. & K. Becker. 1998. Metabolic fractionation of stable carbon isotopes: implications of different proximate compositions for studies of the aquatic food webs using $\delta^{13}C$ data. Oecologia, 115(3): 337–343.

Forster, G.R. 1981. The age and growth of *Callista chione*. J. Mar. Biol. Assoc. United Kingdom, 61: 881–883.

France, R.L. 1995. Carbon-13 enrichment in benthic compared to planktonic algae: foodweb implications. Mar. Ecol. Prog. Ser., 124(1-3): 307–312.

Frangoulis, C., N. Skliris, G. Lepoint, K. Elkalay, A. Goffart, J.K. Pinnegar & J.H. Hecq. 2011. Importance of copepod carcasses versus faecal pellets in the upper water column of an oligotrophic area. Estuar. Coast. Shelf Sci., 92(3): 456–463.

Freitas, L., M. Fernandez-Reiriz & U. Labarta. 2002. Fatty acid profiles of *Mytilus galloprovincialis* (Lmk) mussel of subtidal and rocky shore origin. Comp. Biochem. Physiol. Part B, 132: 453–461.

Fry, B. 2006. *Stable isotope ecology*, New York: Springer.

Fry, B. & Y.C. Allen. 2003. Stable isotopes in Zebra mussels as bioindicators of river-watershed linkages. River Res. Appl., 19(7): 683–696.

Fry, B. & E. Sherr. 1984. $\delta^{13}C$ measurements as indicators of carbon flow in marine and freshwater ecosystems. Contrib. Mar. Sci., 27: 13–47.

Gabbott, P.A. 1975. Storage cycles in marine molluscs: a hypothesis concerning the relationship between glycogen metabolism and gametogenesis. In Barnes, ed. *Proc 9th European Marine Biology Symposium*. Aberdeen: Aberdeen University Press, pp. 191–211.

Galap, C., P. Netchitaïlo, F. Leboulenger & J.-P. Grillot. 1999. Variations of fatty acid contents in selected tissues of the female dog cockle (*Glycymeris glycymeris* L., Mollusca, Bivalvia) during the annual cycle. Comp. Biochem. Physiol. Part A, 122: 241–254.

Galimany, E., M. Baeta, M. Durfort, J. Lleonart & M. Ramón. 2015. Reproduction and size at first maturity in a Mediterranean exploited *Callista chione* bivalve bed. Sci. Mar., 79(2): 233–242.

Galois, R., P. Richard & B. Fricourt. 1996. Seasonal Variations in Suspended Particulate Matter in the Marennes-Oléron Bay, France, using Lipids as Biomarkers. Estuar. Coast. Shelf Sci., 43(3): 335–357.

Gam, M., X. de Montaudouin & H. Bazairi. 2010. Population dynamics and secondary production of the cockle *Cerastoderma edule*: A comparison between Merja Zerga (Moroccan Atlantic Coast) and Arcachon Bay (French Atlantic Coast). J. Sea Res., 63(3-4): 191–201.

Gaspar, M.B. & C.C. Monteiro. 1998. Reproductive Cycles of the Razor Clam *Ensis siliqua* and the Clam *Venus striatula* off Vilamoura, Southern Portugal. J. Mar. Biol. Assoc. UK: 1247–1258.

Gaspar, M.E. 2004. Age and growth of *Chamelea gallina* from the Algarve coast (Southern Portugal): Influence of seawater temperature and gametogenic cycle on growth rate. J. Molluscan Stud., 70(4): 371–377.

Gillikin, D.P. 2005. *Geochemistry of Marine Bivalve Shells: the potential for paleoenvironmental reconstruction. Chapter 10: Barium uptake into the shells of the common mussel (Mytilus edulis) and the potential for estuarine paleo-chemistry reconstruction. PhD thesis.* University of Brussels.

Gillikin, D.P., K.A. Hutchinson & Y. Kumai. 2009. Ontogenic increase of metabolic carbon in freshwater mussel shells (*Pyganodon cataracta*). J. Geophys. Res., 114(G1): G01007.

Gillikin, D.P., A. Lorrain, S. Bouillon, P. Willenz & F. Dehairs. 2006. Stable carbon isotopic composition of *Mytilus edulis* shells: relation to metabolism, salinity, δ13CDIC and phytoplankton. Org. Geochem., 37(10): 1371–1382.

Gillikin, D.P., A. Lorrain, L. Meng & F. Dehairs. 2007. A large metabolic carbon contribution to the $\delta^{13}C$ record in marine aragonitic bivalve shells. Geochim. Cosmochim. Acta, 71(12): 2936–2946.

Gillikin, D.P., F. De Ridder, H. Ulens, M. Elskens, E. Keppens, W. Baeyens & F. Dehairs. 2005. Assessing the reproducibility and reliability of estuarine bivalve shells (*Saxidomus giganteus*) for sea surface temperature reconstruction: Implications for paleoclimate studies. Palaeogeogr. Palaeoclimatol. Palaeoecol., 228(1-2): 70–85.

Giraldo, C., A. Stasko, E.S. Choy, B. Rosenberg, A. Majewski, M. Power, H. Swanson, L. Loseto & J.D. Reist. 2016. Trophic variability of Arctic fishes in the Canadian Beaufort Sea: a fatty acids and stable isotopes approach. Polar Biol., 39(7): 1267–1282.

Goman, M., B. Ingram & A. Strom. 2008. Composition of stable isotopes in geoduck (*Panopea abrupta*) shells: A preliminary assessment of annual and seasonal paleoceanographic changes in the northeast Pacific. Quat. Int., 188: 117–125.

Gonçalves, A.M.M., U.M. Azeiteiro, M.A. Pardal & M. De Troch. 2012. Fatty acid profiling reveals seasonal and spatial shifts in zooplankton diet in a temperate estuary. Estuar. Coast. Shelf Sci., 109: 70–80.

Goodwin, D., B. Schöne & D. Dettman. 2003. Resolution and fidelity of oxygen isotopes as paleotemperature proxies in bivalve mollusk shells: models and observations. Palaios: 110–125.

Goodwin, D.H., K.W. Flessa & B.R. Schöne. 2001. Isotope Variation, and Temperature in the Gulf of California Bivalve Mollusk *Chione cortezi*: Implications for Paleoenvironmental Analysis. Palaios, 16: 387–398.

Goodwin, D.H., K.W. Flessa, B.R. Schöne & D.L. Dettman. 2001. Cross-Calibration of Daily Growth Increments, Stable Isotope Variation, and Temperature in the Gulf of California Bivalve Mollusk *Chione cortezi*: Implications for Paleoenvironmental Analysis. Palaios, 16: 387–398.

Goodwin, D.H., K.W. Flessa, M.A. Téllez-Duarte, D.L. Dettman, B.R. Schöne & G.A. Avila-Serrano. 2004. Detecting time-averaging and spatial mixing using oxygen isotope variation: a case study. Palaeogeogr. Palaeoclimatol. Palaeoecol., 205(1-2): 1–21.

Gosling, E. 2003. *Bivalve Molluscs. Biology, Ecology and Culture* Intergovernmental Panel on Climate Change, ed., Cambridge: Cambridge University Press.

Gosling, E. 2015. *Marine Bivalve Molluscs* Second Edi. J. Wiley & Sons, ed., West Sussex, England.

Goud, J. & G. Gulden. 2009. Description of a new species of *Glycymeris* (Bivalvia: Arcoidea) from Madeira, Selvagens and Canary Islands. Zool. Meded., 83(1997): 1059–1066.

Grall, J., F. Le Loc'h, B. Guyonnet & P. Riera. 2006. Community structure and food web based on stable isotopes ($\delta^{15}N$ and $\delta^{13}C$) analysis of a North Eastern Atlantic maerl bed. J. Exp. Mar. Bio. Ecol., 338(1): 1–15.

Gray, A., R. Seed & C. Richardson. 1997. Reproduction and growth of *Mytilus edulis chilensis* from the Falkland Islands. Sci. Mar., 61(2): 39–48.

Gribben, P.E., J. Helson & A.G. Jeffs. 2004. Reproductive cycle of the New Zealand Geoduck, *Panopea*

zelandica, in two North Island populations. Veliger, 47: 53–65.

Grossman, E.L. & T.-L. Ku. 1986. Oxygen and carbon isotope fractionation in biogenic aragonite: Temperature effects. Chem. Geol. Isot. Geosci. Sect., 59(February 2016): 59–74.

Guest, M.A., R.M. Connolly & N.R. Loneragan. 2004. Carbon movement and assimilation by invertebrates in estuarine habitats at a scale of metres. Mar. Ecol. Prog. Ser., 278(Odum 1979): 27–34.

Gutierrez-Mas, J.M. 2011. Glycymeris shell accumulations as indicators of recent sea-level changes and high-energy events in Cadiz Bay (SW Spain). Estuar. Coast. Shelf Sci., 92(4): 546–554.

Gutt, J. 2006. Coexistence of macro-zoobenthic species on the Antarctic shelf: an attempt to link ecological theory and results. Deep Sea Res. II, 53: 1009–1028.

Hall, C.A., W.A. Dollase & C.E. Corbató. 1974. Shell growth in *Tivela stultorum* (Mawe, 1823) and Callista chione (Linnaeus, 1758) (Bivalvia): annual periodicity, latitudinal differences, and diminution with age. Palaeogeogr. Palaeoclimatol. Palaeoecol., 15: 33–61.

Hallmann, N., B.R. Schöne, A. Strom & J. Fiebig. 2008. An intractable climate archive — Sclerochronological and shell oxygen isotope analyses of the Pacific geoduck, *Panopea abrupta* (bivalve mollusk) from Protection Island (Washington State, USA). Palaeogeogr. Palaeoclimatol. Palaeoecol., 269(1-2): 115–126.

Hamer, B., D. Medaković, D. Pavičić-Hamer, Ž. Jakšić, M. Štifanić, V. Nerlović, A. Travizi, R. Precali & K. Tjaša. 2010. Estimation of freshwater influx along the eastern Adriatic coast as a possible source of stress for marine organisms. Acta Adriat., 51(2): 191–194.

Hammer, Ø., D. Harper & P. Ryan. 2001. Past: Palaeontological Statistics Software Package for Education and Data Analysis. Palaeontol. Electron., 4(1): 9pp.

Harmelin-Vivien, M., V. Loizeau, C. Mellon, B. Beker, D. Arlhac, X. Bodiguel, F. Ferraton, R. Hermand, X. Philippon & C. Salen-Picard. 2008. Comparison of C and N stable isotope ratios between surface particulate organic matter and microphytoplankton in the Gulf of Lions (NW Mediterranean). Cont. Shelf Res., 28(August): 1911–1919.

Hedges, J.I., R.G. Keil & R. Benner. 1997. What happens to terrestrial organic matter in the ocean? Org. Geochem., 27(5): 195–212.

Honkoop, P. & J. van der Meer. 1998. Experimentally induced effects of water temperature and immersion time on reproductive output of bivalves in the Wadden Sea. J. Exp. Mar. Bio. Ecol., 220(2): 227–246.

Honkoop, P.J.C. & J.J. Beukema. 1997. Loss of body mass in winter of three interdital bivalve species: an experimental and observational study of the interacting effects between water temperature, feeding time and feeding behaviour. J. Exp. Mar. Biol. Ecol., 212: 277–297.

Hori, M., Y. Sano, A. Ishida, N. Takahata, K. Shirai & T. Watanabe. 2015. Middle Holocene daily light cycle reconstructed from the strontium/calcium ratios of a fossil giant clam shell. Sci. Rep., 5: 8734.

Huber, M. 2010. *Compendium of Bivalves*, Germany: ConchBooks.

Iglesias, J.I.P. & E. Navarro. 1991. Energetics of growth and reproduction in cockles (*Cerastoderma edule*): seasonal and age-dependent variations. Mar. Biol.: 359–368.

IPCC. 2014. *Climate Change: 2014: Synthesis Report. Contribution of Working Groups I, II and III to the Fifth Assessment Report of the Intergovernmental Panel on Climate Change*, Geneva, Switzerland.

Ivany, L.C., B.H. Wilkinson & D.S. Jones. 2003. Using Stable Isotopic Data to Resolve Rate and Duration of Growth throughout Ontogeny: An Example from the Surf Clam, *Spisula solidissima*. Palaios, 18(2): 126–137.

Jablonski, D. 1996. Body size and macroevolution. In D. et al. Jablonski, ed. *Evolutionary Paleobiology*. Chicago: University of Chicago Press, pp. 256–289.

Jackson, A.L., R. Inger, A.C. Parnell & S. Bearhop. 2011. Comparing isotopic niche widths among and within communities: SIBER - Stable Isotope Bayesian Ellipses in R. J. Anim. Ecol., 80: 595–602.

Jacob, D.E., A.L. Soldati, R. Wirth, J. Huth, U. Wehrmeister & W. Hofmeister. 2008. Nanostructure, composition and mechanisms of bivalve shell growth. Geochim. Cosmochim. Acta, 72(22): 5401–5415.

Jokela, J. & P. Mutikainen. 1995. Phenotypic plasticity and priority rules for energy allocation in a freshwater clam: a field experiment. Oecologia, 104(1): 122–132.

Jones, C.G., J.H. Lawton & M. Shachak. 1994. Organisms as ecosystem engineers. Oikos, 69: 373–386.

Jones, D.S. 1980. Annual cycle of shell growth increment formation in two continental shelf bivalves and its paleoecologic significance. Paleobiology, 6(03): 331–340.

Jones, D.S., D.F. Williams & M.A. Arthur. 1983. Growth history and ecology of the Atlantic surf clam, *Spisula solidissima* (Dillwyn), as revealed by stable isotopes and annual shell increments. J. Exp. Mar. Bio. Ecol., 73(3): 225–242.

Jones, D.S.D. & I.R. Quitmyer. 1996. Marking Time with Bivalve Shells: Oxygen Isotopes and Season of Annual Increment Formation. Palaios, 11(4): 340.

Jones, S.J., F.P. Lima & D.S. Wethey. 2010. Rising environmental temperatures and biogeography: poleward range contraction of the blue mussel, *Mytilus edulis* L., in the western Atlantic. J. Biogeogr., 37: 2243–2259.

Jurić, I., I. Bušelić, D. Ezgeta-Balić, N. Vrgoč & M. Peharda. 2012. Age, Growth and Condition Index of *Venerupis decussata* (Linnaeus, 1758) in the Eastern Adriatic Sea. Turkish J. Fish. Aquat. Sci., 12(3).

Kaiser, M.J., K. Ramsay, C.A. Richardson, F.E. Spence & A.R. Brand. 2000. Chronic fishing disturbance has changed shelf sea benthic community structure. J. Anim. Ecol., 69(3): 494–503.

Kalish, J. 1991. ^{13}C and ^{18}O isotopic disequilibria in fish otoliths: metabolic and kinetic effects. Mar. Ecol. Prog. Ser., 75: 191–203.

Kang, C., J. Kim, K. Lee, P. Lee & J. Hong. 2003. Trophic importance of benthic microalgae to macrozoobenthos in coastal bay systems in Korea: dual stable C and N isotope analyses. Mar. Ecol. Prog. Ser., 259: 79–92.

Kang, C.K., P. Sauriau, P. Richard & G.F. Blanchard. 1999. Food sources of the infaunal suspension-feeding bivalve *Cerastoderma edule* in a muddy sandflat of Marennes-Oléron Bay, as determined by analyses of carbon and nitrogen stable isotopes. Mar. Ecol. Prog. Ser., 187: 147–158.

Kasai, A., H. Horie & W. Sakamoto. 2004. Selection of food sources by *Ruditapes philippinarum* and *Mactra veneriformis* (Bivalva: Mollusca) determined from stable isotope analysis. Fish. Sci., 70(1): 11–20.

Kaustuv, R., D. Jablonski & J.W. Valentine. 2001. Climate change, species range limits and body size in marine bivalves. Ecol. Lett., 4: 366–370.

Kayama, M., S. Araki & S. Sato. 1989. Lipids of marine plants. In R. Ackman, ed. *Marine Biogenic Lipids, Fats, and Oils, vol. II.* Boca Raton: CRC Press, pp. 4–47.

Keller, N., D. Del Piero & A. Longinelli. 2002. Isotopic composition, growth rates and biological behaviour

of *Chamelea gallina* and *Callista chione* from the Gulf of Trieste (Italy). Mar. Biol., 140: 9–15.

Kelly, J.R. & R.E. Scheibling. 2012. Fatty acids as dietary tracers in benthic food webs. Mar. Ecol. Prog. Ser., 446: 1–22.

Kerhervé, P., M. Minagawa, S. Heussner & A. Monaco. 2001. Stable isotopes ($^{13}C/^{12}C$ and $^{15}N/^{14}N$) in settling organic matter of the northwestern Mediterranean Sea: biogeochemical implications. Oceanol. Acta, 24S: 77–85.

Kharlamenko, V., N. Zhukova, S. Khotimchenko, V. Svetashev & G. Kamenev. 1995. Fatty acids as markers of food sources in a shallow-water hydrothermal ecosystem (Kraternaya Bight, Yankich Island, Kurile Islands). Mar. Ecol. Prog. Ser., 120: 231–241.

Kharlamenko, V.I., S.I. Kiyashko, A.B. Imbs & D.I. Vyshkvartzev. 2001. Identification of food sources of invertebrates from the seagrass *Zostera marina* community using carbon and sulfur stable isotope ratio and fatty acid analyses. Mar. Ecol. Prog. Ser., 220: 103–117.

Kharlamenko, V.I., S.I. Kiyashko, S.A. Rodkina & A.B. Imbs. 2008. Determination of food sources of marine invertebrates from a subtidal sand community using analyses of fatty acids and stable isotopes. Russ. J. Mar. Biol., 34(2): 101–109.

Kharlamenko, V.I., S.I. Kiyashko, S.A. Rodkina & V.I. Svetashev. 2011. The composition of fatty acids and stable isotopes in the detritophage Acila insignis (Gould, 1861) (Bivalvia: Nuculidae): Searching for markers of a microbial food web. Russ. J. Mar. Biol., 37(3): 201–208.

Koike, H. 1980. Seasonal dating by growth line counting of the bivalve, *Meretrix lusoria*. Univ. Tokio Bull., 18: 1–20.

Krom, M.D., B. Herut & R.F.C. Mantoura. 2004. Nutrient budget for the Eastern Mediterranean: Implications for phosphorus limitation. Limnol. Oceanogr., 49(5): 1582–1592.

Kubota, K., K. Shirai, N. Murakami-Sugihara, K. Seike, M. Hori & K. Tanabe. 2017. Annual shell growth pattern of the Stimpson's hard clam *Mercenaria stimpsoni* as revealed by sclerochronological and oxygen stable isotope measurements. Palaeogeogr. Palaeoclimatol. Palaeoecol., 465: 307–315.

Langdon, C. & R. Newell. 1990. Utilization of detritus and bacteria as food sources by two bivalve suspension-feeders, the oyster *Crassostrea virginica* and the mussel *Geukensia demissa*. Mar. Ecol. Prog. Ser., 58: 299–310.

Lartaud, F., L. Emmanuel, M. de Rafelis, S. Pouvreau & M. Renard. 2010. Influence of food supply on the $\delta^{13}C$ signature of mollusc shells: implications for palaeoenvironmental reconstitutions. Geo-Marine Lett., 30(1): 23–34.

Layman, C. a., M.S. Araujo, R. Boucek, C.M. Hammerschlag-Peyer, E. Harrison, Z.R. Jud, P. Matich, A.E. Rosenblatt, J.J. Vaudo, L. a. Yeager, D.M. Post & S. Bearhop. 2012. Applying stable isotopes to examine food-web structure: An overview of analytical tools. Biol. Rev., 87: 545–562.

Leblanc, K., B. Quéguiner, N. Garcia, P. Rimmelin & P. Raimbault. 2003. Silicon cycle in the NW Mediterranean Sea: Seasonal study of a coastal oligotrophic site. Oceanol. Acta, 26: 339–355.

Lécuyer, C., V. Daux, P. Moissette, J.-J. Cornée, F. Quillévéré, E. Koskeridou, F. Fourel, F. Martineau & B. Reynard. 2012. Stable carbon and oxygen isotope compositions of invertebrate carbonate shells and the reconstruction of paleotemperatures and paleosalinities—A case study of the early Pleistocene of Rhodes, Greece. Palaeogeogr. Palaeoclimatol. Palaeoecol., 350-352: 39–48.

Lee Van Dover, C., J. Grassle, B. Fry, R. Garritt & V. Starczak. 1992. Stable isotope evidence for entry of sewage-derived organic material into a deep-sea food web. Nature, 356: 133–135.

Legac, M. & I. Fabijanić. 1994. Contribution to knowledge on the bivalve *Glycymeris bimaculata* (Poli, 1795) in Pag Bay. Period. Biol., 96(4): 450–451.

Legac, M. & M. Hrs-Brenko. 1999. A review of Bivalve species in the eastern Adriatic Sea. Nat. Croat., 8(1): 9–25.

Leontarakis, P.K. & C.A. Richardson. 2005. Growth of the smooth clam, Callista chione (Linnaeus, 1758) (Bivalvia: Veneridae) from the Thracian Sea, northeastern Mediterranean. J. Molluscan Stud., 71: 189–192.

Léveillé, J., C. Amblard & G. Bourdier. 1997. Fatty acids as specific algal markers in a natural lacustrian phytoplankton. J. Plankton Res., 19(4): 469–490.

Levitan, D.R. 1993. The importance of sperm limitation to the evolution of egg size in marine invertebrates. Am. Nat., 141: 517–536.

Lewis, D.E. & R.M. Cerrato. 1997. Growth uncoupling and the relationship between shell growth and metabolism in the soft shell clam *Mya arenaria*. Mar. Ecol. Prog. Ser., 158: 177–189.

Li, X., X. Fan, L. Han & Q. Lou. 2002. Fatty acids of some algae from the Bohai Sea. Phytochemistry, 59(2):

157–161.

Liénart, C., N. Susperregui, V. Rouaud, J. Cavalheiro, V. David, Y. Del Amo, R. Duran, B. Lauga, M. Monperrus, T. Pigot, S. Bichon, K. Charlier & N. Savoye. 2016. Dynamics of particulate organic matter in a coastal system characterized by the occurrence of marine mucilage – A stable isotope study. J. Sea Res., 116: 12–22.

Lopez, N., J. Navarro, C. Barria, M. Albo-Puigserver, M. Coll & I. Palomera. 2016. Feeding ecology of two demersal opportunistic predators coexisting in the northwestern Mediterranean Sea. Estuar. Coast. Shelf Sci., 175: 15–23.

Lord, J. & R. Whitlatch. 2014. Latitudinal patterns of shell thickness and metabolism in the eastern oyster *Crassostrea virginica* along the east coast of North America. Mar. Biol., 161(7): 1487–1497.

Lorenzen, C. & S. Jeffrey. 1978. Determination of chlorophyll in seawater. Unesco Tech. Pap. Mar. Sci.: 20pp.

Lorrain, A., Y. Paulet, L. Chauvaud, N. Savoye, A. Donval & C. Saout. 2002. Differential $\delta^{13}C$ and $\delta^{15}N$ signatures among scallop tissues: implications for ecology and physiology. J. Exp. Mar. Bio. Ecol., 275: 47–61.

Lorrain, A., Y.-M. Paulet, L. Chauvaud, R. Dunbar, D. Mucciarone & M. Fontugne. 2004. $\delta^{13}C$ variation in scallop shells: Increasing metabolic carbon contribution with body size? Geochim. Cosmochim. Acta, 68(17): 3509–3519.

Lorrain, A., N. Savoye, L. Chauvaud, Y. Paulet & N. Naulet. 2003. A decarbonation and preservation method for the analysis of organic C and N contents and stable isotope ratios of low-carbonated suspended particulate material. Anal. Chim. Acta, 491(February): 125–133.

Lucas, A. 1965. *Recherche sur la sexualité des mollusques bivalves. PhD thesis.* Université de Rennes.

MacDonald, B. & R. Thompson. 1986. Influence of temperature and food availability on the ecological energetics of the giant scallop *Placopecten magellanicus*. I. Growth rates of shell and somatic tissue. Mar. Ecol. Prog. Ser., 25: 279–94.

MacKenzie, K.M., M.R. Palmer, A. Moore, A.T. Ibbotson, W.R.C. Beaumont, D.J.S. Poulter & C.N. Trueman. 2011. Locations of marine animals revealed by carbon isotopes. Sci. Rep., 1(1): 21.

Magalhães, L., R. Freitas & X. de Montaudouin. 2016. Cockle population dynamics: recruitment predicts

adult biomass, not the inverse. Mar. Biol., 163(1): 16.

Mannino, M.A., K.D. Thomas, M.J. Leng & H.J. Sloane. 2008. Shell growth and oxygen isotopes in the topshell *Osilinus turbinatus*: Resolving past inshore sea surface temperatures. Geo-Marine Lett., 28: 309–325.

Marchitto, T.M., G.A. Jones, G.A. Goodfriend & C.R. Weidman. 2000. Precise Temporal Correlation of Holocene Mollusk Shells Using Sclerochronology. Quat. Res., 53(2): 236–246.

Marsden, I. & R. Pilkington. 1995. Spatial and temporal variations in the condition of *Austrovenus stutchburyi* Finlay, 1927 (Bivalvia: Veneridae) from the Avon–Heathcote estuary, Christchurch. N.Z. Nat. Sci., 22: 57–67.

Martínez del Rio, C., N. Wolf, S.A. Carleton & L.Z. Gannes. 2009. Isotopic ecology ten years after a call for more laboratory experiments. Biol. Rev., 84(1): 91–111.

Martínez-Pita, I., C. Sánchez-Lazo, E. Prieto & O. Moreno. 2011. The effect of diet on gonadal development of the smooth Venus clam *Callista chione* (Mollusca: Bivalvia). J. Shellfish Res., 30(2): 295–301.

Matijević, S., G. Kušpilić, M. Morović, B. Grbec, D. Bogner, S. Skejić & J. Veža. 2009. Physical and chemical properties of the water column and sediments at sea bass/sea bream farm in the middle Adriatic (Maslinova Bay). Acta Adriat., 50(1): 59–76.

Mayzaud, P., J. Chanut & R. Ackman. 1989. Seasonal changes of the biochemical composition of marine particulate matter with special reference to fatty acids and sterols. Mar. Ecol. Prog. Ser., 56: 189–204.

McConnaughey, T. a, J. Burdett, J.F. Whelan & C.K. Paull. 1997. Carbon isotopes in biological carbonates: respiration and photosynthesis. Geochim. Cosmochim. Acta, 61(3): 611–622.

McConnaughey, T.A. & D.P. Gillikin. 2008. Carbon isotopes in mollusk shell carbonates. Geo-Marine Lett., 28: 287–299.

McCutchan, J.H., W.M. Lewis, C. Kendall & C.C. McGrath. 2003. Variation in trophic shift for stable isotope ratios of carbon, nitrogen, and sulfur. Oikos, 102: 378–390.

Metaxatos, A. 2004. Population dynamics of the venerid bivalve *Callista chione* (L.) in a coastal area of the eastern Mediterranean. J. Sea Res., 52(4): 293–305.

Milano, S., B.R. Schöne & R. Witbaard. 2017. Changes of shell microstructural characteristics of *Cerastoderma edule* (Bivalvia) — A novel proxy for water temperature. Palaeogeogr. Palaeoclimatol. Palaeoecol., 465: 395–406.

Miller, D.C., R.J. Geider & H.L. MacIntyre. 1996. Microphytobenthos: The Ecological Role of the "Secret Garden" of Unvegetated, Shallow-Water Marine Habitats. II. Role in Sediment Stability and Shallow-Water Food Webs. Estuaries, 19(2): 202.

Miller, R.J. & H.M. Page. 2012. Kelp as a trophic resource for marine suspension feeders: a review of isotope-based evidence. Mar. Biol., 159(7): 1391–1402.

Minagawa, M. & E. Wada. 1986. Nitrogen isotope ratios of red tide organisms in the East China Sea: a characterization of biological nitrogen fixation. Mar. Chem., 19: 245–249.

Minagawa, M. & E. Wada. 1984. Stepwise enrichment of ^{15}N along food chains: Further evidence and the relation between $\delta^{15}N$ and animal age. Geochim. Cosmochim. Acta, 48(5): 1135–1140.

Mladineo, I., M. Peharda, S. Orhanović, J. Bolotin, M. Pavela-Vrančić & B. Treursić. 2007. The reproductive cycle, condition index and biochemical composition of the horse-bearded mussel *Modiolus barbatus*. Helgol. Mar. Res., 61(3): 183–192.

Möbius, J. 2013. Isotope fractionation during nitrogen remineralization (ammonification): Implications for nitrogen isotope biogeochemistry. Geochim. Cosmochim. Acta, 105: 422–432.

Moerdijk, P.W., A.D. Freddy, L. Dall, G. Newton & G. Newton. 2000. Glycymerididae (Mollusca, Bivalvia) from the North Sea Basin Family. Contr Tert Quatern Geol, 37: 3–21.

De Montaudouin, X. 1996. Factors involved in growth plasticity of cockles *Cerastoderma edule* (L.), identified by field survey and transplant experiments. J. Sea Res., 36(3-4): 251–265.

Montoya, J.P., E.J. Carpenter & D.G. Capone. 2002. Nitrogen fixation and nitrogen isotope abundances in zooplankton of the oligotrophic North Atlantic. Limnol. Oceanogr., 47(6): 1617–1628.

Morgan, E., R.M. O' Riordan & S.C. Culloty. 2013. Climate change impacts on potential recruitment in an ecosystem engineer. Ecol. Evol., 3(3): 581–594.

Morris, D. 1978. *The respiratory physiology of the subtidal bivalves* Glycymeris glycymeris *(L.),* Anomia ephippium *L. and* Modiolus modiolus *L.* Liverpool University.

Mortlock, R.A. & P.N. Froelich. 1989. A simple method for the rapid determination of biogenic opal in

pelagic marine sediments. Deep Sea Res. Part A. Oceanogr. Res. Pap., 36(9): 1415–1426.

Moura, P., M.B. Gaspar & C.C. Monteiro. 2009. Age determination and growth rate of a *Callista chione* population from the southwestern coast of Portugal. Aquat. Biol., 5: 97–106.

Moura, P., M.B. Gaspar & C.C. Monteiro. 2008. Gametogenic cycle of the smooth clam *Callista chione* on the south-western coast of Portugal. J. Mar. Biol. Assoc. UK, 88(1): 161–167.

Mutvei, H., E. Dunca, H. Timm & T. Slepukhina. 1996. Structure and growth rates of bivalve shells as indicators of environmental changes and pollution. Bull. du Musée océanographique Monaco, 14: 65–72.

Nadon, M.-O. & J.H. Himmelman. 2006. Stable isotopes in subtidal food webs: Have enriched carbon ratios in benthic consumers been misinterpreted? Limnol. Oceanogr., 51(6): 2828–2836.

Najdek, M. 1993. Factors influencing fatty acid and hydrocarbon composition of sedimenting particles in the northeastern Adriatic Sea. Mar. Chem., 41: 299–310.

Najdek, M., M. Blažina, D. Ezgeta-Balić & M. Peharda. 2013. Diets of fan shells (*Pinna nobilis*) of different sizes: fatty acid profiling of digestive gland and adductor muscle. Mar. Biol., 160(4): 921–930.

Najdek, M., D. Debobbis, D. Mioković & I. Ivančić. 2002. Fatty acid and phytoplankton compositions of different types of mucilaginous aggregates in the northern Adriatic. J. Plankton Res., 24: 429–441.

Najdek, M., D. Ezgeta-Balić, M. Blažina, M. Crnčević & M. Peharda. 2016. Potential food sources of *Glycymeris nummaria* (Mollusca: Bivalvia) during the annual cycle indicated by fatty acid analysis. Sci. Mar., 80(1): 123–129.

Napolitano, G.E., R.J. Pollero, A.M. Gayoso, B.A. MacDonald & R.J. Thompson. 1997. Fatty acids as trophic markers of phytoplankton blooms in the Bahia Blanca estuary (Buenos Aires, Argentina) and in Trinity Bay (Newfoundland, Canada). Biochem. Syst. Ecol., 25(8): 739–755.

Navarro, E., S. Méndez, M.B. Urrutia, U. Arambalza & I. Ibarrola. 2016. Digestive selection underlies differential utilization of phytoplankton and sedimentary organics by infaunal bivalves: Experiments with cockles (*Cerastoderma edule*) using cross-labelled mixed diets. Mar. Environ. Res., 120: 111–121.

Nerot, C., A. Lorrain, J. Grall, D.P. Gillikin, J.-M. Munaron, H. Le Bris & Y.-M. Paulet. 2012. Stable isotope variations in benthic filter feeders across a large depth gradient on the continental shelf. Estuar.

Coast. Shelf Sci., 96: 228–235.

Newton, P.P., R.S. Lampitt, T.D. Jickells, P. King & C. Boutle. 1994. Temporal and Spatial Variability of Biogenic Particle Fluxes during the JGOFS Northeast Atlantic Process Studies at 47°N, 20°W. Deep. Res. Part I-Oceanographic Res. Pap., 41(11-12): 1617–1642.

Nicol, D. 1964. An essay on size of marine pelecypods. J. Paleontol., 38(5): 968–974.

Ninčević Gladan, Ž., I. Marasović, B. Grbec, S. Skejić, M. Bužančić, G. Kušpilić, S. Matijević & F. Matić. 2009. Inter-decadal Variability in Phytoplankton Community in the Middle Adriatic (Kaštela Bay) in Relation to the North Atlantic Oscillation. Estuaries and Coasts, 33(2): 376–383.

Ninčević-Gladan, Ž., M. Bužančić, G. Kušpilić, B. Grbec, S. Matijević, S. Skejić, I. Marasović & M. Morović. 2015. The response of phytoplankton community to anthropogenic pressure gradient in the coastal waters of the eastern Adriatic Sea. Ecol. Indic., 56: 106–115.

Nishida, K., T. Ishimura, A. Suzuki & T. Sasaki. 2012. Seasonal changes in the shell microstructure of the bloody clam, *Scapharca broughtonii* (Mollusca: Bivalvia: Arcidae). Palaeogeogr. Palaeoclimatol. Palaeoecol., 363-364: 99–108.

Nolf, F. & F. Swinnen. 2013. The Glycymerididae of the NE Atlantic and the Mediterranean Sea. Neptunea, 12(2): 1–35.

Ogrinc, N., G. Fontolan, J. Faganeli & S. Covelli. 2005. Carbon and nitrogen isotope compositions of organic matter in coastal marine sediments (the Gulf of Trieste, N Adriatic Sea): indicators of sources and preservation. Mar. Chem., 95(3-4): 163–181.

Okaniwa, N., T. Miyaji, T. Sasaki & K. Tanabe. 2010. Shell growth and reproductive cycle of the Mediterranean mussel *Mytilus galloprovincialis* in Tokyo Bay, Japan: relationship with environmental conditions. Plankt. Benthos Res., 5: 214–220.

Orvain, F., S. Lefebvre, J. Montepini, M. Sébire, A. Gangnery & B. Sylvand. 2012. Spatial and temporal interaction between sediment and microphytobenthos in a temperate estuarine macro-intertidal bay. Mar. Ecol. Prog. Ser., 458: 53–68.

Oschmann, W. 2009. Sclerochronology: editorial. Int. J. Earth Sci., 98: 1–2.

Page, H.M. & M. Lastra. 2003. Diet of intertidal bivalves in the Ria de Arosa (NW Spain): Evidence from stable C and N isotope analysis. Mar. Biol., 143: 519–532.

Palacios, R., I. Racotta, E. Kraffe, Y. Marty, J. Moal & J. Samain. 2005. Lipid composition of the giant lion's paw scallop (*Nodipecten subnodosus*) in relation to gametogenesis I. Fatty acids. Aquaculture, 250: 270–282.

Pantoja, S., D.J. Repeta, J.P. Sachs & D.M. Sigman. 2002. Stable isotope constraints on the nitrogen cycle of the Mediterranean Sea water column. Deep. Res. I, 49: 1609–1621.

Parnell, A.C., R. Inger, S. Bearhop & A.L. Jackson. 2010. Source partitioning using stable isotopes: Coping with too much variation. PLoS One, 5(3): 1–5.

Parrish, C., T. Abrajano, S. Budge, R. Helleur, E. Hudson, K. Pulchan & C. Ramos. 2000. Lipid and phenolic biomarkers in marine ecosystems: analysis and applications. In P. Wangersky, ed. *The Handbook of Environmental Chemistry*. Berlin: Springer, pp. 193–223.

Parrish, C., C. McKenzie, B. MacDonald & E. Hatfield. 1996. Seasonal studies of seston lipids in relation to microplankton species composition and scallop growth in South Broad Cove, Newfoundland. Mar. Ecol. Prog. Ser., 129: 151–164.

Paulet, Y.M., A. Lorrain, J. Richard & S. Pouvreau. 2006. Experimental shift in diet $\delta^{13}C$: A potential tool for ecophysiological studies in marine bivalves. Org. Geochem., 37(10): 1359–1370.

Paulet, Y.-M., A. Lucas & A. Gerard. 1988. Reproduction and larval development in two *Pecten maximus* (L.) populations from Brittany. J. Exp. Mar. Bio. Ecol., 119: 145–156.

Peharda, M., B.A. Black, A. Purroy & H. Mihanović. 2016. The bivalve *Glycymeris pilosa* as a multidecadal environmental archive for the Adriatic and Mediterranean Seas. Mar. Environ. Res., 119: 79–87.

Peharda, M., M. Crnčević, I. Bušelić, C.A. Richardson & D. Ezgeta-Balić. 2012. Growth And Longevity of *Glycymeris nummaria* (Linnaeus, 1758) from the Eastern Adriatic, Croatia. J. Shellfish Res., 31(4): 947–950.

Peharda, M., D. Ezgeta-Balić, J. Davenport, N. Bojanić, O. Vidjak & Ž. Ninčević-Gladan. 2012. Differential ingestion of zooplankton by four species of bivalves (Mollusca) in the Mali Ston Bay, Croatia. Mar. Biol., 159(4): 881–895.

Peharda, M., D. Ezgeta-Balić, M. Radman, N. Sinjković, N. Vrgoč & I. Isajlović. 2012. Age, growth and population structure of *Acanthocardia tuberculata* (Bivalvia: Cardiidae) in the eastern Adriatic Sea. Sci. Mar., 76(March): 59–66.

Peharda, M., D. Ezgeta-Balić, N. Vrgoč & I. Isajlović. 2010. Description of bivalve community structure in the Croatian part of the Adriatic Sea-hydraulic dredge survey. Acta Adriat., 51(2): 141–158.

Peharda, M., D. Ezgeta-Balić, N. Vrgoč, I. Isajlović & D. Bogner. 2010. Description of bivalve community structure in the Croatian part of the Adriatic Sea - hydraulic dredge survey. Acta Adriat., 51(2): 141–158.

Peharda, M., I. Mladineo, L. Kekez, J. Bolotin, L. Kekez & B. Skaramuca. 2006. The reproductive cycle and potential protandric development of the Noah's Ark shell, *Arca noae* L.: Implications for aquaculture. Aquaculture, 252(2-4): 317–327.

Peharda, M., Z. Popović, D. Ezgeta-Balić, N. Vrgoć, S. Puljas & A. Frankić. 2013. Age and growth of *Venus verrucosa* (Bivalvia: Veneridae) in the eastern Adriatic Sea. Cah. Biol. Mar., 1: 281–286.

Peharda, M., S. Puljas, L. Chauvaud, B.R. Schöne, D. Ezgeta-Balić & J. Thébault. 2015. Growth and longevity of *Lithophaga lithophaga*: what can we learn from shell structure and stable isotope composition? Mar. Biol., 162: 1531–1540.

Peharda, M., C. Richardson, V. Onofri, A. Bratos & M. Crnčević. 2002. Age and growth of the bivalve *Arca noae* in the Croatian Adriatic Sea. J. Molluscan Stud., 68: 307–310.

Peharda, M., C.A. Richardson, I. Mladineo, S. Šestanović, Z. Popović, J. Bolotin & N. Vrgoč. 2007. Age, growth and population structure of *Modiolus barbatus* from the Adriatic. Mar. Biol., 151(2): 629–638.

Peharda, M., A. Soldo, A. Pallaoro, S. Matić & P. Cetinić. 2003. Age and growth of the Mediterranean scallop *Pecten jacobaeus* (Linnaeus 1758) in the Northern Adriatic Sea. J. Shellfish Res., 22(3): 639–642.

Peharda, M., N. Stagličić & D. Ezgeta. 2009. Distribution and population structure of *Arca noae* in the Pašman channel. Ribarstvo, 124(1): 3–10.

Peharda, M., I. Župan, L. Bavčević, A. Frankić & T. Klanjšček. 2007. Growth and condition index of mussel *Mytilus galloprovincialis* in experimental integrated aquaculture. Aquac. Res., 38: 1714–1720.

Pérez, V., F. Olivier, R. Tremblay, U. Neumeier, J. Thébault, L. Chauvaud & T. Meziane. 2013. Trophic resources of the bivalve, *Venus verrucosa*, in the Chausey archipelago (Normandy, France) determined by stable isotopes and fatty acids. Aquat. Living Resour., 26(3): 229–239.

Pernet, F., N. Malet, A. Pastoureaud, A. Vaquer, C. Quéré & L. Dubroca. 2012. Marine diatoms sustain growth of bivalves in a Mediterranean lagoon. J. Sea Res., 68: 20–32.

Peters, E., P. Yevich, J. Harshbarger & G. Zaroogian. 1994. Comparative histopathology of gonadal neoplasms in marine bivalve molluscs. Dis. Aquat. Organ., 20: 59–76.

Peterson, B.J. 1999. Stable isotopes as tracers of organic matter input and transfer in benthic food webs: A review. Acta Oecologica, 20(4): 479–487.

Peterson, B.J. & B. Fry. 1987. Stable isotopes in ecosystem studies. Annu. Rev. Ecol. Syst., 18: 293–320.

Peterson, C., P. Duncan, H. Summerson & G. Safrit. 1983. A mark-recapture test of annual periodicity of internal growth band deposition in shells of hard clams, *Mercenaria mercenaria*, from a population along the southeastern United States. Fish. Bull., 81(4): 765–779.

Philippart, C.J.M., H.M. van Aken, J.J. Beukema, O.G. Bos, G.C. Cadée & R. Dekker. 2003. Climate-related changes in recruitment of the bivalve *Macoma balthica*. Limnol. Oceanogr., 48(6): 2171–2185.

Philippart, C.J.M., R. Anadón, R. Danovaro, J.W. Dippner, K.F. Drinkwater, S.J. Hawkins, T. Oguz, G. O'Sullivan & P.C. Reid. 2011. Impacts of climate change on European marine ecosystems: Observations, expectations and indicators. J. Exp. Mar. Bio. Ecol., 400(1-2): 52–69.

Phillips, D.L., R. Inger, S. Bearhop, A.L. Jackson, J.W. Moore, A.C. Parnell, B.X. Semmens & E.J. Ward. 2014. Best practices for use of stable isotope mixing models in food-web studies. Can. J. Zool., 92(10): 823–835.

Pirini, M., M.P. Manuzzi, A. Pagliarani, F. Trombetti, A.R. Borgatti & V. Ventrella. 2007. Changes in fatty acid composition of *Mytilus galloprovincialis* (Lmk) fed on microalgal and wheat germ diets. Comp. Biochem. Physiol. Part B Biochem. Mol. Biol., 147(4): 616–626.

Popović, Z., I. Mladineo, D. Ezgeta-Balić, Ž. Trumbić, N. Vrgoč & M. Peharda. 2013. Reproductive cycle and gonad development of *Venus verrucosa* L. (Bivalvia: Veneridae) in Kaštela Bay, Adriatic Sea. Mar. Biol. Res., 9(January 2013): 229–239.

Poppe, Y. & G. Goto. 1993. *European seashells, Vol. 2 (Scaphopoda, Bivalvia, Cephalopoda)*, Wiesbaden: Verlag Christa Hemmen.

Pörtner, H.O. & A.P. Farrell. 2008. ECOLOGY: Physiology and Climate Change. Science, 322: 690–692.

Post, D.M. 2002. Using stable isotopes to estimate trophic position: models, methods, and assumptions.

Ecology, 83(3): 703–718.

Poutiers, J. 1996. Fiches FAO d'identification des espèces pour les besoins de la pêche. FAO/CEE, 1. Méditerranée Mer Noire, Zo. pêche 37, Révision 1 Bivalves.

Prins, T.C., A.C. Smaal & R.F. Dame. 1997. A review of the feedbacks between bivalve grazing and ecosystem processes. Aquat. Ecol., 31(4): 349–359.

Puccinelli, E., M. Noyon & C.D. McQuaid. 2016. Does proximity to urban centres affect the dietary regime of marine benthic filter feeders? Estuar. Coast. Shelf Sci., 169: 147–157.

Puljas, S., M. Peharda, I. Župan & F. Bukša. 2015. Maximum recorded life span of *Arca noae* Linnaeus, 1758 in the marine protected area Telaščica, Adriatic Sea. Cah. Biol. Mar., 56: 163–168.

Purroy, A., T. Šegvić-Bubić, A. Holmes, I. Bušelić, J. Thébault, A. Featherstone & M. Peharda. 2016. Combined Use of Morphological and Molecular Tools to Resolve Species Mis-Identifications in the Bivalvia The Case of Glycymeris glycymeris and G. pilosa. PLoS One, 11(9): e0162059.

R Core Team. 2015. R: A language and environment for statistical computing.

Radermacher, P., B.R. Schöne, E. Gischler, W. Oschmann, J. Thébault & J. Fiebig. 2009. Sclerochronology – a highly versatile tool for mariculture and reconstruction of life history traits of the queen conch, *Strombus gigas* (Gastropoda). Aquat. Living Resour., 22(3): 307–318.

Ragueneau, O., L. Chauvaud, A. Leynaert, G. Thouzeau, Y.-M. Paulet, S. Bonnet, A. Lorrain, J. Grall, R. Corvaisier & M. Le Hir. 2002. Direct evidence of a biologically active coastal silicate pump: Ecological implications. Limnol. Oceanogr., 47(6): 1849–1854.

Ramaswamy, V., B. Gaye, P.V. Shirodkar, P.S. Rao, A.R. Chivas, D. Wheeler & S. Thwin. 2008. Distribution and sources of organic carbon, nitrogen and their isotopic signatures in sediments from the Ayeyarwady (Irrawaddy) continental shelf, northern Andaman Sea. Mar. Chem., 111(3-4): 137–150.

Ramón, M. 2003. Population dynamics and secondary production of the cockle *Cerastoderma edule* (L.) in a backbarrier tidal flat of the Wadden Sea. Sci. Mar., 67(4): 429–443.

Ramón, M., J. Cano, J.B. Peña & M.J. Campos. 2005. Current status and perspectives of mollusc (bivalves and gastropods) culture in the Spanish Mediterranean. Boletín Inst. Español Oceanogr., 21: 361–373.

Ramón, M. & C.A. Richardson. 1990. Age determination and shell growth of *Chamelea gallina* (Bivalvia:

Veneridae) in the western Mediterranean.

Ramsay, K., M. Kaiser & C. Richardson. 2000. Can shell scars on dog cockles (*Glycymeris glycymeris* L.) be used as an indicator of fishing disturbance? J. Sea Res., 43: 167–176.

Ravera, O., G. Beone, P. Trincherini & N. Riccardi. 2007. Seasonal variations in metal content of two *Unio pictorum mancus* (Mollusca, Unionidae) populations from two lakes of different trophic state. J. Limnol., 66: 28–39.

Rees, A.P., C.S. Law & E.M.S. Woodward. 2006. High rates of nitrogen fixation during an in-situ phosphate release experiment in the Eastern Mediterranean Sea. Geophys. Res. Lett., 33(10): L10607.

Reynolds, D.J., P.G. Butler, S.M. Williams, J.D. Scourse, C.A. Richardson, A.D. Wanamaker, W.E.N. Austin, A.G. Cage & M.D.J. Sayer. 2013. A multiproxy reconstruction of Hebridean (NW Scotland) spring sea surface temperatures between AD 1805 and 2010. Palaeogeogr. Palaeoclimatol. Palaeoecol., 386: 275–285.

Reynolds, D.J., C.A. Richardson, J.D. Scourse, P.G. Butler, P. Hollyman, A. Román-González & I.R. Hall. 2017. Reconstructing North Atlantic marine climate variability using an absolutely-dated sclerochronological network. Palaeogeogr. Palaeoclimatol. Palaeoecol., 465: 333–346.

Ricardo, F., T. Pimentel, A.S.P. Moreira, F. Rey, M.A. Coimbra, M.R. Domingues, P. Domingues, M. Costa Leal & R. Calado. 2015. Potential use of fatty acid profiles of the adductor muscle of cockles (*Cerastoderma edule*) for traceability of collection site. Sci. Rep., 5(February): 11125.

Richardson, C., D. Crisp & N. Runham. 1979. Tidally deposited growth bands in the shell of the common cockle *Cerastoderma edule* (L.). Malacologia, 18: 277–290.

Richardson, C.A. 2001. Molluscs as archives of environmental change. Oceanogr. Mar. Biol. an Annu. Rev., 39: 103–164.

Richardson, C.A., M. Peharda, H. Kennedy, P. Kennedy & V. Onofri. 2004. Age, growth rate and season of recruitment of *Pinna nobilis* (L) in the Croatian Adriatic determined from Mg:Ca and Sr:Ca shell profiles. J. Exp. Mar. Bio. Ecol., 299(1): 1–16.

Riera, P. 2007. Trophic subsidies of *Crassostrea gigas*, *Mytilus edulis* and *Crepidula fornicata* in the Bay of Mont Saint Michel (France): A δ13C and δ15N investigation. Estuar. Coast. Shelf Sci., 72(1-2): 33–41.

Riera, P. & P. Richard. 1996. Isotopic Determination of Food Sources of *Crassostrea gigas* Along a Trophic Gradient in the Estuarine Bay of Marennes-Oléron. Estuar. Coast. Shelf Sci., 42(3): 347–360.

Rivetti, I., S. Fraschetti, P. Lionello, E. Zambianchi & F. Boero. 2014. Global Warming and Mass Mortalities of Benthic Invertebrates in the Mediterranean Sea. PLoS One, 9(12): e115655.

Romagnoli, F., J. Baena & L. Sarti. 2016. Neanderthal retouched shell tools and Quina economic and technical strategies: An integrated behaviour. Quat. Int., 407: 29–44.

Romanek, C.S., E.L. Grossman & J.W. Morse. 1992. Carbon isotopic fractionation in synthetic aragonite and calcite: Effects of temperature and precipitation rate. Geochim. Cosmochim. Acta, 56(1): 419–430.

Román-González, A., J.D. Scourse, P.G. Butler, D.J. Reynolds, C.A. Richardson, L.S. Peck, T. Brey & I.R. Hall. 2017. Analysis of ontogenetic growth trends in two marine Antarctic bivalves *Yoldia eightsi* and *Laternula elliptica*: Implications for sclerochronology. Palaeogeogr. Palaeoclimatol. Palaeoecol.

Root, T.L., J.T. Price, K.R. Hall, S.H. Schneider, C. Rosenzweigk & J.A. Pounds. 2003. Fingerprints of global warming on wild animals and plants. Nature, 421: 57–60.

Royer, C., J. Thébault, L. Chauvaud & F. Olivier. 2013. Structural analysis and paleoenvironmental potential of dog cockle shells (*Glycymeris glycymeris*) in Brittany, northwest France. Palaeogeogr. Palaeoclimatol. Palaeoecol., 373: 123–132.

Royer, J., C. Seguineau, K.-I. Park, S. Pouvreau, K.-S. Choi & K. Costil. 2008. Gametogenetic cycle and reproductive effort assessed by two methods in 3 age classes of Pacific oysters, *Crassostrea gigas*, reared in Normandy. Aquaculture, 277(3-4): 313–320.

Rueda, J.. & A.. Smaal. 2004. Variation of the physiological energetics of the bivalve *Spisula subtruncata* (da Costa, 1778) within an annual cycle. J. Exp. Mar. Bio. Ecol., 301(2): 141–157.

Sachs, J.P. & D.J. Repeta. 1999. Oligotrophy and Nitrogen Fixation During Eastern Mediterranean Sapropel Events. Science, 286(5449): 2485–2488.

Sampaio, L., A.M. Rodrigues & V. Quintino. 2010. Carbon and nitrogen stable isotopes in coastal benthic populations under multiple organic enrichment sources. Mar. Pollut. Bull., 60(10): 1790–802.

Sano, Y., S. Kobayashi, K. Shirai, N. Takahata, K. Matsumoto, T. Watanabe, K. Sowa & K. Iwai. 2012. Past

daily light cycle recorded in the strontium/calcium ratios of giant clam shells. Nat. Commun., 3: 761.

Šantić, D., S. Šestanović, M. Šolić, N. Krstulović, G. Kušpilić, M. Ordulj & Ž. Ninčević Gladan. 2013. Dynamics of the picoplankton community from coastal waters to the open sea in the Central Adriatic. Mediterr. Mar. Sci., 15(1): 179–188.

Santos, S., J.F.M.F. Cardoso, V. Borges, R. Witbaard, P.C. Luttikhuizen & H.W. van der Veer. 2012. Isotopic fractionation between seawater and the shell of *Scrobicularia plana* (Bivalvia) and its application for age validation. Mar. Biol., 159(3): 601–611.

Santos, S., J.F.M.F. Cardoso, C. Carvalho, P.C. Luttikhuizen & H.W. van der Veer. 2011. Seasonal variability in somatic and reproductive investment of the bivalve *Scrobicularia plana* (da Costa, 1778) along a latitudinal gradient. Estuar. Coast. Shelf Sci., 92(1): 19–26.

Sargent, J. & S. Falk-Petersen. 1988. The lipid chemistry of calanoid copepods. Hydrobiologia, 166/168: 101–114.

Sastry, A. & N.J. Blake. 1971. Regulation of gonad development in the Bay scallop, *Aequipecten irradians* Lamarck. Biol. Bull., 140: 274–283.

Sastry, A.N. 1979. Pelecypoda (excluding Ostreidae). In A. C. Giese & J. S. Pearse, eds. *Reproduction of marine invertebrates, Vol 5.* New York, NY: Academic Press.

Sastry, A.N. 1966. Temperature effects on reproduction of the bay scallop, *Aequipecten irradians* (Lamarck). Biol. Bull., 130: 118–134.

Sato, S. 1997. Shell microgrowth patterns of bivalves reflecting seasonal change of phytoplankon abundance. Paleontol. Res., 1(4): 260–266.

Sato, S. 1995. Spawning periodicity and shell microgrowth patterns of the venerid bivalve *Phacosoma japonicum* (Reeve, 1850). The Veliger, 38(1): 61–72.

Savoye, N., A. Aminot, P. Treguer, M. Fontugne, N. Naulet & R. Kerouel. 2003. Dynamics of particulate organic matter $\delta^{15}N$ and $\delta^{13}C$ during spring phytoplankton blooms in a macrotidal ecosystem (Bay of Seine, France). Mar. Ecol. Prog. Ser., 255: 27–41.

Savoye, N., V. David, F. Morisseau, H. Etcheber, G. Abril, I. Billy, K. Charlier, G. Oggian, H. Derriennic & B. Sautour. 2012. Origin and composition of particulate organic matter in a macrotidal turbid estuary:

The Gironde Estuary, France. Estuar. Coast. Shelf Sci., 108: 16–28.

Schöne, B.R. 2003. A “clam-ring”master-chronology constructed from a short-lived bivalve mollusc from the northern Gulf of California, USA. The Holocene, 1: 39–49.

Schöne, B.R. 2013. *Arctica islandica* (Bivalvia): A unique paleoenvironmental archive of the northern North Atlantic Ocean. Glob. Planet. Change, 111: 199–225.

Schöne, B.R. 2008. The curse of physiology - Challenges and opportunities in the interpretation of geochemical data from mollusk shells. Geo-Marine Lett., 28: 269–285.

Schöne, B.R., E. Dunca, J. Fiebig & M. Pfeiffer. 2005. Mutvei’s solution: An ideal agent for resolving microgrowth structures of biogenic carbonates. Palaeogeogr. Palaeoclimatol. Palaeoecol., 228(1-2): 149–166.

Schöne, B.R., J. Fiebig, M. Pfeiffer, R. Gleβ, J. Hickson, A.L. a. Johnson, W. Dreyer & W. Oschmann. 2005. Climate records from a bivalved Methuselah (*Arctica islandica*, Mollusca; Iceland). Palaeogeogr. Palaeoclimatol. Palaeoecol., 228(1-2): 130–148.

Schöne, B.R., A.D. Freyre Castro, J. Fiebig, S.D. Houk, W. Oschmann & I. Kröncke. 2004. Sea surface water temperatures over the period 1884–1983 reconstructed from oxygen isotope ratios of a bivalve mollusk shell (*Arctica islandica*, southern North Sea). Palaeogeogr. Palaeoclimatol. Palaeoecol., 212(3-4): 215–232.

Schöne, B.R. & D.P. Gillikin. 2013. Unraveling environmental histories from skeletal diaries — Advances in sclerochronology. Palaeogeogr. Palaeoclimatol. Palaeoecol., 373: 1–5.

Schöne, B.R., I. Kröncke & S.D. Houk. 2003. The cornucopia of chilly winters: ocean quahog (*Arctica islandica* L., Mollusca) master chronology reveals bottom water nutrient enrichment during colder winters (North. Senckenbergiana maritima, 32(1/2): 165–175.

Schöne, B.R., M. Pfeiffer, T. Pohlmann & F. Siegismund. 2005. A seasonally resolved bottom-water temperature record for the period AD 1866-2002 based on shells of *Arctica islandica* (Mollusca, North Sea). Int. J. Climatol., 25(7): 947–962.

Schöne, B.R., D.L. Rodland, A. Wehrmann, B. Heidel, W. Oschmann, Z. Zhang, J. Fiebig & L. Beck. 2007. Combined sclerochronologic and oxygen isotope analysis of gastropod shells (*Gibbula cineraria*, North Sea): life-history traits and utility as a high-resolution environmental archive for kelp forests. Mar. Biol., 150(6): 1237–1252.

Schöne, B.R. & D. Surge. 2012. Bivalve sclerochronology and geochemistry. In P. Seldon & J. Hardesty, eds. *Treatise online 46: Part N. Volume 1*. Lawrence: The University of Kansas, Paleontological Institute, pp. 1–24.

Schöne, B.R., K. Tanabe, D. Dettman & S. Sato. 2003. Environmental controls on shell growth rates and $\delta^{18}O$ of the shallow-marine bivalve mollusk *Phacosoma japonicum* in Japan. Mar. Biol., 142(3): 473–485.

Schubert, C. & S. Calvert. 2001. Nitrogen and carbon isotopic composition of marine and terrestrial organic matter in Arctic Ocean sediments: implications for nutrient utilization and organic matter. Deep Sea Res. Part I Oceanogr. Res. Pap., 48: 789–810.

Sebens, K.P. 1987. The Ecology of Indeterminate Growth in Animals. Annu. Rev. Ecol. Syst., 18(1): 371–407.

Seed, R. 1976. Ecology. In *Marine Mussels: Their Ecology and Physiology*. Cambridge: Cambridge University Press, pp. 13–65.

Sejr, M., K. Jensen & S. Rysgaard. 2002. Annual growth bands in the bivalve *Hiatella arctica* validated by a mark-recapture study in NE Greenland. Polar Biol., 25: 794–796.

Sejr, M.K., J.K. Petersen, K.T. Jensen & S. Rysgaard. 2004. Effects of food concentration on clearance rate and energy budget of the Arctic bivalve *Hiatella arctica* (L) at subzero temperature. J. Exp. Mar. Bio. Ecol., 311(1): 171–183.

Semmens, B.X., E.J. Ward, A.C. Parnell, D.L. Phillips, S. Bearhop, R. Inger, A. Jackson & J.W. Moore. 2013. Statistical basis and outputs of stable isotope mixing models: Comment on Fry (2013). Mar. Ecol. Prog. Ser., 490: 285–289.

Šestanović, S., M. Šolić & N. Krstulović. 2009. The influence of organic matter and phytoplankton pigments on the distribution of bacteria in sediments of Kaštela Bay (Adriatic Sea). Sci. Mar., 73(1): 83–94.

Shumway, S.E., R. Selvin & D.F. Schick. 1987. Food resources related to habitat in the scallop *Placopecten magellanicus* (Gmelin, 1791): A qualitative study. J. Shellfish Res., 6(2): 89–95.

Sivan, D., M. Potasman, A. Almogi-Labin, D.E. Bar-Yosef Mayer, E. Spanier & E. Boaretto. 2006. The *Glycymeris* query along the coast and shallow shelf of Israel, southeast Mediterranean. Palaeogeogr. Palaeoclimatol. Palaeoecol., 233(1-2): 134–148.

Smith, W. & F. Fitzpatrick. 1996. The eicosanoids: cyclooxygenase, lipoxygenase, and epoxygenase pathways. In D. Vance & J. Vance, eds. *Biochemistry of lipids, lipoproteins and membranes*. Amsterdam: Elsevier Science, pp. 283–308.

Sokolova, I.M., M. Frederick, R. Bagwe, G. Lannig & A.A. Sukhotin. 2012. Energy homeostasis as an integrative tool for assessing limits of environmental stress toleance in aquatic invertebrates. Mar. Environ. Res., 29: 1–15.

Sola, J.C. 1997. Reproduction, population dynamics, growth and production of *Scrobicularia plana* da costa (pelecypoda) in the Bidasoa estuary, Spain. Netherlands J. Aquat. Ecol., 30(4): 283–296.

Šolić, M., N. Krstulović, D. Šantić, S. Šestanović, M. Ordulj, N. Bojanić & G. Kušpilić. 2015. Structure of microbial communities in phosphorus-limited estuaries along the eastern Adriatic coast. J. Mar. Biol. Assoc. United Kingdom, 95(08): 1565–1578.

Soudant, P., K. van Ryckeghem, Y. Marty, J. Samain & P. Sorgeloos. 1999. Comparison of the lipid class and fatty acid composition between a reproductive cycle in nature and a standard hatchery conditioning of the Pacific oyster *Crassostrea gigas*. Comp. Biochem. Physiol. Part B, 123: 209–222.

Squires, R.L. 2010. Northeast Pacific Upper Cretaceous and Paleocene Glycymeridid Bivalves. J. Paleontol., 84(5): 895–917.

Steingrimsson, S.A. 1989. *A comparative ecological study of two Glycymeris glycymeris (L .) populations off the Isle of Man. PhD thesis.* University of Liverpool.

Stemmer, K. & G. Nehrke. 2014. The distribution of polyenes in the shell of *Arctica islandica* from North Atlantic localities: a confocal Raman microscopy study. J. Molluscan Stud., 80(4): 365–370.

Strickland, J. & T. Parsons. 1972. A practical handbook of sea-water analysis. J. Fish. Res. boar Canada, 167: 1–311.

Surić, M., R. Lončarić, N. Buzjak, S.T. Schultz, J. Šangulin, K. Maldini & D. Tomas. 2015. Influence of submarine groundwater discharge on seawater properties in Rovanjska-Modrič karst region (Croatia). Environ. Earth Sci., 74(7): 5625–5638.

Taipale, S.J. & E. Sonninen. 2009. The influence of preservation method and time on the $\delta^{13}C$ value of dissolved inorganic carbon in water samples. Rapid Commun. Mass Spectrom., 23(16): 2507–2510.

Taylor, R.& J.C. 1983. The Reproductive Cycle of the Bay Scallop, *Argopecten irradians irradians*

(Lamarck), in a Small Coastal Embayment on Cape Cod, Massachusetts. Estuaries, 6(4): 431.

Thomas, R. 1975. Functional morphology, ecology and evolutionary conservationism in the Glycymeridae (Bivalvia). Paleontology, 18: 217–254.

Thompson, D., R. Phillips, F. Stewart & S. Waldron. 2000. Low $\delta^{13}C$ signatures in pelagic seabirds: lipid ingestion as a potential source of ^{13}C-depleted carbon in the Procellariiformes. Mar. Ecol. Prog. Ser., 208: 265–271.

Thompson, I., D.S. Jones & D. Dreibelbis. 1980. Annual Internal Growth Banding and Life History of the Ocean Quahog *Arctica islandica* (Mollusca: Bivalvia). Mar. Biol., 57: 25–34.

Tieszen, L., T. Boutton, K. Tesdahl & N. Slade. 1983. Fractionation and turnover of stable carbon isotopes in animal tissues: implication for $\delta^{13}C$ analysis of diet. Oceanologia, 57: 32–37.

Tirado, C., C. Salas & J.I. López. 2002. Reproduction of *Callista chione* in the littoral of Málaga (Southern Spain). J. Shellfish Res., 21: 643–648.

Torres, T., J.E. Ortiz & I. Arribas. 2013. Variations in racemization/epimerization ratios and amino acid content of *Glycymeris* shells in raised marine deposits in the Mediterranean. Quat. Geochronol., 16: 35–49.

Turekian, K., J. Cochran, Y. Nozaki, I. Thompson & D. Jones. 1982. Determination of shell deposition rates of Arctica islandica from the New York Bight using natural 228Ra and 228Th and bomb-produced ^{14}C. Limnol. Oceanogr., 27: 737–741.

Uddin, M.J., H.-S. Yang, K.-J. Park, C.-K. Kang, H.-S. Kang & K.-S. Choi. 2012. Annual reproductive cycle and reproductive efforts of the Manila clam *Ruditapes philippinarum* in Incheon Bay off the west coast of Korea using a histology-ELISA combined assay. Aquaculture, 364-365: 25–32.

Underwood, A.., M.. Chapman & S.. Connell. 2000. Observations in ecology: you can't make progress on processes without understanding the patterns. J. Exp. Mar. Bio. Ecol., 250(1-2): 97–115.

Valli, G., E. Bidoli & C. Marussi. 1983. Osservazioni preliminari sulla riproduzione e sulla biometria di *Callista chione* (L.) (Mollusca, Bivalvia) del Golfo di Trieste. Nov. Thalass., 6: 97–103.

Valli, G., N. Marsich & M. Marsich. 1994. Riproduzione, biometria e contenuto di metalli in *Callista chione* (L.) (Mollusca, Bivalvia) del Golfo di Trieste nel corso di un ciclo annuale. Boll. della Soc. Adriat. di Sci. LXXV, Tomo II: 441–464.

Velasco, L.A. 2013. Esfuerzo reproductivo en moluscos: una revisión. Rev. Intropica, (18): 87–97.

Ventrella, V., M. Pirini, A. Pagliarani, F. Trombetti, M.P. Manuzzi & A.R. Borgatti. 2008. Effect of temporal and geographical factors on fatty acid composition of *M. galloprovincialis* from the Adriatic sea. Comp. Biochem. Physiol. Part B, 149(2): 241–250.

Verdelhos, T., P. Cardoso, M. Dolbeth & M. Pardal. 2011. Latitudinal gradients in *Scrobicularia plana* reproduction patterns, population dynamics, growth, and secondary production. Mar. Ecol. Prog. Ser., 442: 271–283.

Verdelhos, T., J.C. Marques & P. Anastácio. 2015. Behavioral and mortality responses of the bivalves *Scrobicularia plana* and *Cerastoderma edule* to temperature, as indicator of climate change's potential impacts. Ecol. Indic., 58: 95–103.

Vihtakari, M., P.E. Renaud, L.J. Clarke, M.J. Whitehouse, H. Hop, M.L. Carroll & W.G. Ambrose. 2016. Decoding the oxygen isotope signal for seasonal growth patterns in Arctic bivalves. Palaeogeogr. Palaeoclimatol. Palaeoecol., 446: 263–283.

Viladrich, N., L. Bramanti, G. Tsounis, B. Chocarro, A. Martínez-Quitana, S. Ambroso, T. Madurell & S. Rossi. 2016. Variation in lipid and free fatty acid content during spawning in two temperate octocorals with different reproductive strategies: surface versus internal brooder. Coral Reefs, 35(3): 1033–1045.

Vilibić, I., H. Mihanović, G. Kušpilić, A. Ivčević & V. Milun. 2015. Mapping of oceanographic properties along a middle Adriatic transect using Self-Organising Maps. Estuar. Coast. Shelf Sci., 163: 84–92.

Villalejo-Fuerte, M., F. Garcia-Dominguez & R.I. Ochoa-Baez. 1995. Reproductive cycle of *Glycymeris gigantea* (Reeve, 1843) (Bivalvia: Glycymerididae) in Bahia Concepcion, Baja California Sur, Mexico. Veliger, 38(2): 126–132.

Vizzini, S. & A. Mazzola. 2006. The effects of anthropogenic organic matter inputs on stable carbon and nitrogen isotopes in organisms from different trophic levels in a southern Mediterranean coastal area. Sci. Total Environ., 368(2-3): 723–731.

Volkman, J., A. Revill, P. Bonham & L. Clementson. 2007. Sources of organic matter in sediments from the Ord River in tropical northern Australia. Org. Geochem., 38: 1039–1060.

Wada, E., K. Ohki, S. Yoshikawa, P.. Parker, C. Van Baalen, G.I. Matsumoto, M. Noguchi Aita & T. Saino. 2012. Ecological aspects of carbon and nitrogen isotope ratios of cyanobacteria. Plankt. Benthos

Res., 7(3): 135–145.

Walliser, E.O., B.R. Schöne, T. Tütken, J. Zirkel, K.I. Grimm & J. Pross. 2015. The bivalve *Glycymeris planicostalis* as a high-resolution paleoclimate archive for the Rupelian (Early Oligocene) of central Europe. Clim. Past, 11(4): 653–668.

Walthert, L., U. Graf, A. Kammer, J. Luster, D. Pezzotta, S. Zimmermann & F. Hagedorn. 2010. Determination of organic and inorganic carbon, $\delta^{13}C$, and nitrogen in soils containing carbonates after acid fumigation with HCl. J. Plant Nutr. Soil Sci., 173(2): 207–216.

Wanamaker, A., A. Baker, P. Butler, C. Richardson, J. Scourse, I. Ridgway & D. Reynolds. 2009. A novel method for imaging internal growth patterns in marine mollusks: A fluorescence case study on the aragonitic shell of the marine bivalve *Arctica islandica* (Linnaeus). Limnol. Oceanogr. Methods, 7: 673–681.

Wanamaker, A.D., P.G. Butler, J.D. Scourse, J. Heinemeier, J. Eiríksson, K.L. Knudsen & C.A. Richardson. 2012. Surface changes in the North Atlantic meridional overturning circulation during the last millennium. Nat. Commun., 3: 899.

Ward, J. & S.E. Shumway. 2004. Separating the grain from the chaff: particle selection in suspension- and deposit-feeding bivalves. J. Exp. Mar. Bio. Ecol., 300(1-2): 83–130.

Watanabe, T. & T. Oba. 1999. Daily reconstruction of water temperature from oxygen isotopic ratios of a modern *Tridacna* shell using a freezing microtome sampling technique. J. Geophys. Res. Ocean., 104(C9): 20667–20674.

Weidman, C. & G. Jones. 1994. The long-lived mollusc *Arctica islandica*: A new paleoceanographic tool for the reconstruction of bottom temperatures for the continental shelves of the northern North. J. Geophys. Res., 99: 305–314.

Witbaard, R. 1996. A long-term growth record derived from *Arctica islandica* (Mollusca, Bivalvia) from the Fladen Ground (northern North Sea). ICES J. Mar. Sci. Mar. …, 53: 981–987.

Witbaard, R., G.C.A. Duineveld & M. Bergman. 2001. The effect of tidal resuspension on benthic food quality in the southern North Sea. Senckenbergiana maritima, 31(2): 225–234.

Yan, H., J. Chen & J. Xiao. 2014. A review on bivalve shell, a tool for reconstruction of paleo-climate and paleo-environment. Chinese J. Geochemistry, 33(3): 310–315.

Yan, L., B.R. Schöne, S. Li & Y. Yan. 2014. Shells of *Paphia undulata* (Bivalvia) from the South China Sea as potential proxy archives of the East Asian summer monsoon: a sclerochronological calibration study. J. Oceanogr., 70(1): 35–44.

Yokoyama, H., A. Tamaki & K. Harada. 2005. Variability of diet-tissue isotopic fractionation in estuarine macrobenthos. Mar. Ecol. Prog. Ser., 296: 115–128.

Yurkowski, D.J., S.H. Ferguson, C.A.D. Semeniuk, T.M. Brown, D.C.G. Muir & A.T. Fisk. 2016. Spatial and temporal variation of an ice-adapted predator's feeding ecology in a changing Arctic marine ecosystem. Oecologia, 180(3): 631–644.

Vander Zanden, M.J. & J.B. Rasmussen. 2001. Variation in $\delta^{15}N$ and $\delta^{13}C$ trophic fractionation: Implications for aquatic food web studies. Limnol. Oceanogr., 46(8): 2061–2066.

Zhao, L., B.R. Schöne & R. Mertz-Kraus. 2017. Controls on strontium and barium incorporation into freshwater bivalve shells (*Corbicula fluminea*). Palaeogeogr. Palaeoclimatol. Palaeoecol., 465: 386–394.

Zhukova, N. & V. Kharlamenko. 1999. Sources of essential fatty acids in the marine microbial loop. Aquat. Microb. Ecol., 17: 153–157.

Zucchetta, M., G. Cipolato, F. Pranovi, P. Antonetti, P. Torricelli, P. Franzoi & S. Malavasi. 2012. The relationships between temperature changes and reproductive investment in a Mediterranean goby: Insights for the assessment of climate change effects. Estuar. Coast. Shelf Sci., 101: 15–23.

Župan, I., M. Peharda, T. Dolenec, M. Dolenec, P.Ž. Rožič, S. Lojen, D. Ezgeta-Balić & J. Arapov. 2014. Aquaculture Assessment of Noah's Ark (*Arca noae Linnaeus*, 1758) in The Central Adriatic Sea (Croatia). J. Shellfish Res., 33(2): 433–441.

Žvab, P., T. Dolenec, S. Lojen, G. Kniewald, J. Vodopija, Z. Lambaša & M. Dolenec. 2010. Use of stable nitrogen ($\delta^{15}N$) isotopes in food web of the Adriatic Sea, Croatia. Mater. Geoenvironment, 57(1): 41–52.

Žvab Rožič, P., T. Dolenec, S. Lojen, G. Kniewald & M. Dolenec. 2015. Use of stable isotope composition variability of particulate organic matter to assess the anthropogenic organic matter in coastal environment (Istra Peninsula, Northern Adriatic). Environ. Earth Sci., 73(7): 3109–3118.

Zwarts, L. 1991. Seasonal variation in body weight of the bivalves *Macoma balthica*, *Scrobicularia plana*, *Mya arenaria* and *Cerastoderma edule* in the Dutch Wadden Sea. Netherlands J. Sea Res., 28: 231–245.

Table S1. Descriptive table of environmental and biochemical parameters in suspended particulate matter (SPM) and sediment (Sed) (mean ± SD). Abbreviations: Temperature (T; °C), salinity (ppm), Suspended particulate matter concentrations (SPM; mg/L), Chlorophyll *a* (Chl *a*; µg/L and µg/g), Chl *a* fraction within SPM (Chl *a*/SPM; %), biogenic silica (BSi; mg/L and %), BSi fraction within SPM (BSi/SPM; %), Particulate organic carbon and Chl *a* ratio (POC/Chl *a*), Inorganic carbon (IC; %) and Total carbon (TC; %).

				SPM								Sed			
Location	Year	Season	Month	T (°C)	Salinity (ppm)	SPM (mg/L)	Chl *a* (µg/L)	Chl *a*/SPM (%)	BSi (mg/L)	BSi/SPM (%)	POC/Chl *a*	Chl *a* (µg/g)	BSi (%)	IC (%)	TC (%)
PAG	2014	Summer	June	20.64	36.50	4.0±1.4	0.2±0.0	0.006	0.34±0.1	8.57	749.14	0.4±0.1	0.13	11.59	12.02
			July	23.64	37.21	1.5±0.0	0.2±0.0	0.007	0.10±0.0	6.79	961.73	0.8±0.1	0.18	11.02	11.40
			August	24.15	35.00	1.5±0.1	0.3±0.1	0.019	0.15±0.1	10.09	660.83	1.2±0.1	0.09	12.07	12.23
		Fall	September	20.66	36.60	0.9±0.1	0.5±0.0	0.057	0.11±0.0	11.93	326.14	0.5±0.0	0.10	11.73	11.85
			October	19.06	34.68	0.6±0.2	0.5±0.0	0.083	0.09±0.0	14.05	385.18	1.3±0.1	0.16	11.75	11.88
			November	15.84	36.87	0.8±0.1	0.3±0.0	0.035	0.03±0.0	3.64	1080.00	1.8±0.2	0.06	11.97	12.13
		Winter	December	13.27	36.89	0.6±0.1	0.3±0.1	0.055	0.11±0.0	18.33	519.57	1.8±0.2	0.13	12.14	12.27
	2015		January	10.42	36.21	0.7±0.1	0.6±0.1	0.086	0.06±0.0	8.65	280.02	NA	NA	NA	NA
			February	8.87	36.98	0.6±0.1	0.2±0.0	0.041	0.03±0.0	5.76	626.04	1.4±0.1	0.11	12.04	12.17
		Spring	March	9.81	36.22	1.1±0.4	0.6±0.0	0.096	0.05±0.0	4.68	235.29	0.4±0.3	0.12	11.01	11.67
			April	11.98	37.50	0.4±0.1	0.3±0.0	0.061	0.06±0.0	12.99	503.96	5.0±1.4	0.10	11.83	12.35
			May	16.31	37.20	0.6±0.4	0.3±0.0	0.057	0.03±0.0	5.64	417.48	0.6±0.0	0.11	11.48	12.21
		Summer	June	21.30	36.56	1.2±0.5	0.3±0.1	0.046	0.06±0.0	4.86	531.26	0.6±0.1	0.15	11.28	12.07
			July	24.59	37.97	0.9±0.1	0.4±0.1	0.037	0.04±0.0	4.59	663.64	0.6±0.1	0.11	10.65	11.42
			August	25.05	38.28	0.7±0.1	0.4±0.1	0.043	0.05±0.0	7.50	762.48	0.4±0.0	0.18	11.61	12.02
		Fall	September	21.35	37.64	0.5±0.0	0.4±0.0	0.096	0.08±0.0	16.50	513.06	3.1±0.1	0.20	11.99	12.27
			October	17.64	37.07	0.7±0.0	0.5±0.1	0.072	0.06±0.0	7.64	309.69	0.6±0.1	0.17	11.16	11.40
CETINA	2014	Summer	June	20.37	NA	0.8±0.1	0.2±0.0	0.027	NA	NA	820.72	1.6±0.2	NA	9.48	9.85
			July	23.92	36.12	1.1±0.2	0.3±0.0	0.024	0.11±0.0	9.69	865.76	2.3±0.2	0.14	10.24	10.64
			August	24.58	36.80	1.0±0.1	0.3±0.0	0.029	0.17±0.1	16.71	467.20	4.1±0.1	0.16	10.16	10.59

Table S1. (cont.)

Location	Year	Season	Month	SPM								Sed			
				T (°C)	Salinity (ppm)	SPM (mg/L)	Chl *a* (µg/L)	Chl *a*/SPM (%)	BSi (mg/L)	BSi/SPM (%)	POC/Chl *a*	Chl *a* (µg/g)	BSi (%)	IC (%)	TC (%)
CETINA		Fall	September	23.12	35.75	1.0±0.2	0.2±0.0	0.024	0.11±0.0	11.37	591.32	2.9±0.1	0.12	10.99	11.40
			October	21.29	35.70	0.9±0.1	0.6±0.2	0.071	0.11±0.0	12.34	565.34	2.4±0.1	0.17	10.86	11.28
			November	18.23	38.14	0.6±0.2	0.3±0.0	0.054	0.02±0.0	3.75	370.46	11.8±0.4	0.29	9.38	9.84
			December	16.41	37.39	1.0±0.2	0.4±0.1	0.038	0.12±0.0	11.38	527.97	5.0±0.7	0.23	11.08	11.56
	2015	Winter	January	13.90	37.20	0.7±0.2	0.4±0.1	0.051	0.05±0.0	6.75	544.48	6.5±0.1	0.16	10.43	10.89
			February	12.82	36.01	2.0±1.5	0.6±0.0	0.031	0.08±0.0	4.06	317.19	4.0±0.3	0.25	10.87	11.27
		Spring	March	12.67	32.20	0.9±0.4	0.5±0.0	0.050	0.07±0.0	7.66	296.08	6.8±0.3	0.22	7.59	7.95
			April	13.76	32.54	0.8±0.1	0.5±0.0	0.073	0.03±0.0	4.02	319.30	2.7±0.4	0.19	10.86	11.26
			May	17.27	36.60	0.9±0.5	0.6±0.1	0.067	0.05±0.0	5.51	300.24	2.3±0.3	0.13	11.49	11.91
		Summer	June	20.97	38.48	1.4±0.2	0.4±0.0	0.029	0.08±0.0	5.98	540.86	1.4±0.0	0.16	10.85	11.28
			July	23.44	36.30	0.6±0.1	0.2±0.1	0.040	0.06±0.0	9.89	719.22	1.1±0.0	0.15	11.07	11.48
			August	26.37	38.52	0.7±0.1	0.2±0.0	0.033	0.04±0.0	6.00	711.58	3.3±0.4	0.20	10.83	11.25
		Fall	September	23.46	37.52	0.5±0.0	0.3±0.0	0.062	0.08±0.0	14.68	532.45	3.1±0.3	0.21	11.04	11.46
			October	20.78	37.30	0.8±0.1	0.3±0.0	0.036	0.05±0.0	6.79	512.55	2.3±0.3	0.19	11.60	12.00

Table S2. Two-way ANOVA results of environmental parameters in suspended particulate matter (SPM) and sediment (Sed). Chlorophyll *a* (Chl *a*) in SPM (µg/L) and Sed (µg/g), Suspended particulate matter (SPM) in mg/L, Biogenic silica (BSi) in mg/L and Lipids in SPM (mg/g) and Sed (mg/g). Probabilities are expressed as: ** p < 0.001 and * p < 0.05.

Two-way ANOVA					
	df	**SS**	**MS**	***F***	**p**
Chl *a* (µg/L)					
site	1	0.00	0.00	0.00	0.997
month	1	0.05	0.05	2.43	0.122
site*month	1	0.00	0.00	0.15	0.698
Residuals	101	2.04	0.02		
Chl *a* (µg/g)					
site	1	156.25	156.25	38.06	< 0.001**
month	1	1.92	1.92	0.47	0.496
site*month	1	11.93	11.93	2.91	0.092
Residuals	97	398.21	4.11		
SPM (mg/L)					
site	1	0.88	0.88	1.55	0.215
month	1	9.77	9.77	17.31	< 0.001**
site*month	1	6.05	6.05	10.71	< 0.05*
Residuals	99	55.88	0.56		
BiSi (mg/L)					
site	1	0.002	0.002	1.29	0.259
month	1	0.04	0.04	34.44	< 0.001**
site*month	1	<0.001	<0.001	0.04	0.842
Residuals	90	0.108	0.001		
Lipids (mg/L)					
site	1	0.20	0.20	14.31	< 0.001**
month	1	0.19	0.19	13.57	< 0.001**
site*month	1	0.01	0.01	0.85	0.360
Residuals	68	0.97	0.01		
Lipids (mg/g)					
site	1	1.68	1.68	34.32	< 0.001**
month	1	0.00	0.00	0.06	0.810
site*month	1	2.64	2.64	53.99	< 0.001**
Residuals	65	3.18	0.05		

Table S3. Isotopic ($\delta^{13}C$, $\delta^{15}N$) (‰; mean ± SD) and elemental (C, N) (%; mean ± SD) composition and C:N molar ratio of food sources (suspended particulate matter [SPM] and sediment [Sed]) and consumers (*Glycymeris bimaculata* and *Callista chione*).

Sample	Year	Season	Month	PAG					CETINA				
				$\delta^{13}C$(‰)	$\delta^{15}N$(‰)	%C	%N	C:N	$\delta^{13}C$(‰)	$\delta^{15}N$(‰)	%C	%N	C:N
A. Food sources													
SPM	2014	Summer	June	-24.7±0.5	2.3±0.2	3.0±1.0	0.3±0.1	10.59	-24.2±0.1	5.3±0.5	5.0±0.4	0.8±0.1	7.41
			July	-24.4±0.3	5.3±0.5	5.8±0.7	0.8±0.1	8.32	-24.8±0.2	5.5±0.4	6.2±1.7	0.9±0.3	7.82
			August	-24.0±0.1	2.8±1.6	4.2±0.9	0.6±0.1	8.36	-24.4±0.1	2.5±1.9	3.6±0.3	0.5±0.0	7.84
		Fall	September	-23.4±0.1	4.7±0.2	4.2±0.8	0.7±0.1	7.27	-23.5±0.1	3.7±1.0	4.2±0.1	0.7±0.0	7.56
			October	-23.7±0.4	4.2±0.4	6.7±1.7	0.9±0.2	8.48	-24.4±0.3	4.4±1.3	8.9±3.5	1.0±0.3	10.11
			November	-23.6±0.2	6.1±0.3	6.9±3.8	1.0±0.6	8.04	-24.4±0.5	4.7±0.8	3.2±0.5	0.4±0.1	8.87
			December	-24.4±0.2	3.8±1.4	5.3±1.2	0.7±0.2	8.59	-26.2±1.3	4.5±1.7	5.1±3.0	0.5±0.3	11.15
	2015	Winter	January	-25.4±0.2	4.3±0.1	4.4±0.3	0.6±0.0	8.64	-25.3±0.1	4.0±0.4	3.9±0.8	0.5±0.1	8.98
			February	-25.5±0.1	4.5±0.3	4.3±0.3	0.6±0.0	8.76	-25.5±0.2	4.8±0.5	5.0±0.7	0.5±0.0	11.20
		Spring	March	-24.6±0.0	2.3±0.8	3.6±0.6	0.5±0.1	8.46	-25.7±0.4	3.4±1.4	4.3±0.7	0.6±0.1	8.62
			April	-25.6±0.6	5.5±1.9	5.8±0.9	0.8±0.0	8.65	-24.7±1.0	5.5±2.1	5.0±1.4	0.6±0.1	9.74
			May	-25.3±0.1	2.6±0.3	5.4±0.7	0.6±0.1	9.77	-25.4±0.6	3.0±0.5	4.9±1.9	0.7±0.2	8.61
		Summer	June	-24.6±0.2	1.6±1.2	5.2±0.8	0.7±0.2	8.13	-25.2±0.1	3.6±0.6	4.8±1.2	0.5±0.1	10.67
			July	-23.6±0.2	3.3±0.2	6.2±0.5	0.9±0.1	8.47	-25.6±0.1	3.5±0.3	3.9±1.8	0.5±0.2	9.28
			August	-23.8±0.3	3.9±0.4	6.7±0.7	0.8±0.1	9.51	-22.8±0.1	4.9±0.3	5.8±1.2	1.0±0.3	6.93
		Fall	September	-23.6±0.0	4.6±0.5	7.0±0.7	1.0±0.1	8.28	-23.8±0.1	5.6±0.5	5.9±1.0	0.8±0.1	8.29
			October	-24.1±0.1	4.2±0.8	4.0±0.1	0.6±0.0	8.38	-23.8±0.1	4.7±1.0	3.8±0.6	0.4±0.1	9.87
Sed	2014	Summer	June	n.a.	-2.1±0.4	0.4±0.3	0.0±0.0	14.59	n.a.	1.6±0.3	0.4±0.0	0.0±0.0	7.68
			July	-22.0±0.2	0.0±0.8	0.4±0.0	0.0±0.0	9.89	-26.5±0.0	1.0±0.3	0.4±0.0	0.0±0.0	8.05
			August	n.a.	-2.0±0.5	0.2±0.1	0.0±0.0	11.78	n.a.	2.3±0.5	0.4±0.0	0.0±0.0	7.67
		Fall	September	n.a.	-2.3±0.0	0.1±0.0	0.0±0.0	9.09	n.a.	1.9±0.1	0.4±0.0	0.0±0.0	6.95
			October	-22.5±0.1	-0.7±1.0	0.1±0.0	0.0±0.0	6.87	-26.5±0.3	2.3±0.0	0.4±0.0	0.0±0.0	6.73

Table S3. (cont.)

Sample	Year	Season	Month	PAG					CETINA				
				$\delta^{13}C$(‰)	$\delta^{15}N$(‰)	%C	%N	C:N	$\delta^{13}C$(‰)	$\delta^{15}N$(‰)	%C	%N	C:N
Sed			November	n.a.	-0.4±0.1	0.2±0.0	0.0±0.0	9.11	n.a.	3.2±0.1	0.5±0.0	0.0±0.0	8.68
		Winter	December	n.a.	3.9±0.2	0.1±0.0	0.0±0.0	5.17	n.a.	2.7±0.1	0.5±0.0	0.0±0.0	8.42
	2015		January	n.a.	n.a.	n.a.	n.a.	n.a.	n.a.	2.0±0.2	0.5±0.1	0.0±0.0	9.73
			February	-22.3±0.6	-0.1±0.1	0.1±0.0	0.0±0.0	6.52	-26.6±0.1	1.9±0.1	0.4±0.0	0.0±0.0	6.80
		Spring	March	n.a.	-1.1±1.4	0.7±0.0	0.0±0.0	31.12	n.a.	2.2±0.3	0.4±0.0	0.0±0.0	6.69
			April	n.a.	1.1±0.3	0.5±0.1	0.0±0.0	18.33	n.a.	1.1±0.1	0.4±0.0	0.0±0.0	8.22
			May	-22.7±0.1	1.5±0.1	0.7±0.1	0.0±0.0	13.76	-26.7±0.2	3.1±0.2	0.4±0.0	0.0±0.0	8.89
		Summer	June	n.a.	0.1±2.1	0.8±0.1	0.0±0.0	21.19	n.a.	3.3±0.2	0.4±0.0	0.0±0.0	8.46
			July	n.a.	-0.6±0.7	0.8±0.1	0.0±0.0	19.79	n.a.	2.7±0.4	0.4±0.0	0.0±0.0	7.25
			August	n.a.	1.7±1.0	0.4±0.0	0.0±0.0	11.01	n.a.	2.7±0.2	0.4±0.0	0.0±0.0	6.19
		Fall	September	n.a.	0.7±0.1	0.3±0.0	0.0±0.0	10.53	n.a.	3.0±0.4	0.4±0.0	0.0±0.0	7.25
			October	n.a.	0.8±0.4	0.2±0.1	0.0±0.0	11.32	n.a.	2.5±0.3	0.4±0.0	0.0±0.0	6.96
B. Consumers													
Glycymeris	2014	Summer	June	-22.9±0.3	1.3±0.2	40.2±1.8	7.2±0.1	6.55	-23.5±0.1	2.5±0.1	43.5±2.1	7.0±0.2	7.21
bimaculata			July	-22.8±0.3	1.3±0.0	37.0±3.7	6.8±0.3	6.36	-22.8±0.3	3.0±0.1	36.2±5.1	6.5±0.4	6.49
			August	-22.9±0.1	1.6±0.1	40.6±3.5	6.6±0.4	7.19	-23.1±0.1	3.2±0.1	41.9±0.5	6.6±0.3	7.41
		Fall	September	-22.1±0.1	1.7±0.0	39.4±1.8	7.2±0.4	6.43	-22.7±0.1	3.1±0.2	41.0±0.6	7.4±0.1	6.48
			October	-22.6±0.2	1.4±0.0	44.9±0.1	8.2±0.2	6.38	-23.0±0.6	3.0±0.2	44.1±1.7	7.9±0.7	6.59
			November	-23.0±0.4	1.8±0.1	45.3±4.4	7.5±0.2	6.99	-24.0±0.8	2.6±0.1	51.3±10.1	6.8±0.2	8.74
		Winter	December	-22.8±0.2	1.5±0.1	46.2±0.8	8.0±0.3	6.72	-22.4±0.4	2.9±0.1	42.6±2.6	8.2±0.4	6.09
	2015		January	-22.7±0.2	1.0±0.0	43.8±1.8	8.4±0.2	6.12	-23.5±0.1	2.3±0.1	47.5±1.3	7.7±0.2	6.86
			February	-23.5±0.2	0.4±0.0	47.8±0.5	8.2±0.1	6.77	-22.8±0.7	2.2±0.3	45.1±2.6	7.7±0.6	7.11
		Spring	March	-23.2±0.2	0.6±0.1	47.4±0.7	7.9±0.3	6.99	-23.7±0.1	2.0±0.1	46.7±1.4	7.9±0.2	6.94

Table S3. (cont.)

Sample	Year	Season	Month	PAG					CETINA				
				$\delta^{13}C$(‰)	$\delta^{15}N$(‰)	%C	%N	C:N	$\delta^{13}C$(‰)	$\delta^{15}N$(‰)	%C	%N	C:N
Glycymeris			April	-23.8±0.2	0.7±0.2	45.9±1.0	7.6±0.2	7.06	-23.7±0.2	2.0±0.2	47.5±1.1	7.5±0.3	7.41
bimaculata			May	-24.5±0.3	0.2±0.1	46.7±0.9	7.5±0.3	7.26	-23.9±0.1	1.8±0.0	45.2±1.8	7.4±0.1	7.14
		Summer	June	-24.5±0.3	0.6±0.3	46.5±1.4	7.2±0.3	7.58	-24.5±0.2	1.9±0.1	46.5±0.7	6.7±0.2	8.11
			July	-24.0±0.3	0.9±0.1	46.0±0.8	7.6±0.2	7.04	-24.2±0.1	2.2±0.1	46.1±0.6	7.1±0.1	7.53
			August	-23.9±0.2	1.1±0.0	48.8±1.2	7.2±0.2	7.91	-25.2±0.7	2.8±0.4	52.0±3.7	6.7±0.9	9.17
		Fall	September	-23.4±0.3	1.2±0.0	47.9±1.1	7.3±0.4	7.72	-23.3±0.3	2.8±0.1	46.5±0.8	7.7±0.4	7.07
			October	-23.0±0.2	1.2±0.0	47.4±0.7	7.7±0.2	7.15	-23.4±0.3	2.8±0.0	48.0±1.3	7.5±0.2	7.50
Callista	2014	Summer	June	-23.3±0.6	1.4±0.3	39.4±6.4	6.6±0.2	6.99	-25.0±0.2	2.5±0.0	47.0±3.8	5.6±0.2	9.81
chione			July	-24.1±0.7	1.8±0.0	44.9±8.6	6.0±0.4	8.65	-24.3±0.1	3.0±0.1	44.0±0.9	5.2±0.1	9.80
			August	-23.3±0.1	1.8±0.1	45.7±1.5	6.7±0.1	11.41	-24.6±0.3	3.2±0.3	52.3±2.8	5.4±0.3	11.41
		Fall	September	-23.0±0.2	1.4±0.2	43.0±2.4	6.8±0.0	7.39	-24.1±0.4	3.0±0.2	49.8±2.5	6.2±0.4	9.43
			October	-23.2±0.4	1.2±0.3	45.2±0.9	7.7±0.4	6.89	-24.1±0.1	2.5±0.2	49.2±0.4	6.5±0.2	8.78
			November	-24.0±0.1	1.4±0.2	51.3±3.1	7.0±0.4	8.53	-24.3±0.4	2.4±0.2	50.7±3.7	6.3±0.4	9.38
		Winter	December	-23.4±0.1	1.3±0.2	46.6±0.9	7.9±0.2	6.92	-23.7±0.6	2.7±0.0	48.3±2.2	7.5±0.4	7.55
	2015		January	-23.7±0.2	0.8±0.3	45.4±0.7	7.9±0.2	6.69	-23.1±0.5	2.5±0.3	44.7±2.4	7.2±0.7	7.96
			February	-24.5±0.1	0.4±0.2	47.8±0.7	7.3±0.8	7.73	-23.9±0.6	2.0±0.2	48.5±2.9	7.8±0.7	7.38
		Spring	March	-25.4±0.3	0.3±0.0	49.6±1.5	6.8±0.1	8.56	-24.5±0.6	1.9±0.3	50.5±2.4	7.2±1.0	8.33
			April	-25.5±0.3	0.8±0.1	57.1±13.2	8.2±2.1	8.14	-24.2±0.2	2.0±0.3	48.4±1.7	7.9±0.2	7.14
			May	-25.6±0.3	0.5±0.2	46.9±2.0	6.8±0.4	8.03	-25.3±0.3	1.6±0.1	46.0±1.8	6.8±0.4	7.94
		Summer	June	-25.5±0.3	0.8±0.4	47.6±2.3	6.9±0.4	8.06	-25.7±0.1	1.9±0.2	48.7±0.9	5.9±0.3	9.71
			July	-24.6±0.2	1.0±0.2	47.0±1.0	7.2±0.4	7.61	-25.6±0.3	2.4±0.2	49.3±2.3	6.3±0.6	9.20
			August	-24.7±0.5	1.1±0.3	51.7±2.2	6.6±0.7	9.16	-24.2±0.2	2.7±0.1	49.1±0.8	7.5±0.2	7.68
		Fall	September	-23.0±0.7	1.1±0.1	46.3±2.4	8.0±0.6	6.79	-25.4±0.8	2.7±0.1	54.1±3.3	6.4±1.0	10.10
			October	-23.0±0.3	1.0±0.1	47.6±0.8	8.0±0.3	6.94	-25.4±0.6	2.8±0.1	54.4±2.6	6.0±0.7	10.75

Table S4. Fatty acid contribution (mean % TFA ± SD) of food sources: (A) suspended particulate matter (SPM) in Pag, (B) SPM in Cetina and (C) sediment (Sed) in Pag, (D) Sed in Cetina. FA with annual mean proportions > 1% are shown. SFA: saturated FA; MUFA: monosaturated FA; PUFA: polyunsaturated FA; UND: unsaturation degree (Pirini et al. 2007) ; DETRITAL: detrital FA [15:0+15iso+15anteiso+17:0+17iso+17anteiso+18:1(n-7)] (Mayzaud et al. 1989, Najdek et al. 2002).

A. SPM - PAG												
FAME	May	June	July	August	September	October	November	December	January	February	March	April
C14:0	9.5±0.6	8.6±0.7	7.4±0.4	8.1±0.4	9.1±0.4	8.6±0.3	5.4±0.8	8.4±0.6	9.1±0.6	5.6±0.4	5.2±0.2	5.6±0.4
C15:0i	0.1±0.1	1.7±0.2	0±0	0±0	2.9±0.2	1±0.1	1.2±0.1	0±0	3.5±0.5	0.9±0	0.9±0	1.6±0.2
C15:0ai	0.2±0.1	1.8±0.1	0±0	0.6±0.2	1.5±0.1	1.5±0.1	1.1±0.2	0±0	0.5±0.1	1.2±0.1	1.7±0.3	0.7±0.2
C15:1	0±0	0±0	0±0	0±0	0±0	0±0	0±0	0±0	1.4±0.2	0±0	0±0	0±0
C15:0	0±0	1.4±0.1	2.5±0.1	2.9±0.2	1.9±0.2	2.9±0.2	1.2±0.3	1.9±0.2	3.6±0.4	1.5±0.1	1.6±0.1	2.1±0.2
C16:0i	0±0	1.2±0.1	0±0	0±0	0±0	0.9±0.1	0±0	0±0	0±0	0±0	0±0	0±0
C16:1	9.5±0.6	7±0.5	12.6±0.5	9±0.9	1.6±0.1	1.3±0.2	2.2±0.3	3.8±0.5	1.6±0.2	1.3±0.3	2.8±0.4	6.4±0.5
C16:0	33.8±1.3	31.1±1.2	35.7±1.1	30.2±0.5	35.2±0.4	31.4±0.8	40.8±0.8	34.9±1.2	33.4±1.1	46.2±1.4	37±1.5	37.6±1.5
17:0i	0.2±0	2.5±0.3	2.7±0.1	0.7±0.3	3.3±0.3	0.5±0.1	0.8±0.6	7.4±0.7	2.2±0.3	0.2±0	4.5±0.4	0.4±0
C17:0ai	0.2±0.1	0.9±0.6	1.2±0.1	0.6±0.5	2.2±0.4	0.8±0.1	1.3±0.9	2.1±0.4	1.7±0.4	0.1±0	0.6±0.1	1±0.1
C17:1	0±0	0±0	0±0	0±0	0±0	0.6±0.1	0±0	1.5±0.4	0±0	0±0	1.3±0.1	0±0
C17:0	1.3±0	1.8±0.1	1.5±0.1	5±0.1	1.3±0.2	1.6±0.1	1.6±0.6	1.8±0.2	3.7±0.4	1.2±0.1	1.5±0.1	2.1±0.1
C18:2 (n-6)	0±0	1.1±0.1	2.9±0.2	0±0	2±0	0.9±0.1	0±0	0.9±0.1	0.7±0.1	0±0	0±0	0±0
C18:1 (n-9)	1±0.1	6.4±0.6	3.2±0.2	5.6±0.5	6.6±0.5	5.5±0.5	1.2±0.2	5.9±0.2	5.2±0.5	1.5±0.1	1.4±0.3	0.7±0.1
C18:1 (n-7)	0±0	1.8±0.1	0±0	1.2±0.1	1.2±0.2	1±0.1	0±0	0.8±0.1	1.5±0.1	0±0	0±0	0±0
C18:0	30.5±0.6	10.5±0.6	13.9±0.9	13.9±0.2	16.3±0.3	26.7±1.1	31.9±2.9	12.2±0.7	13.1±0.9	26±0.5	23.7±0.5	21.8±0.6
19:0i	0.4±0.1	1.1±0.1	0±0	0.4±0	0±0	0±0	0±0	0±0	0±0	0±0	0±0	0±0
19:0ai	0.2±0	1.3±0.1	0±0	0±0	0±0	0±0	0±0	0±0	0±0	0±0	0±0	0±0
C20:4 (n-6)	0.4±0.2	1.9±0.3	1.9±0.3	1.4±0.1	0.3±0	0.1±0.1	0.1±0.1	0.5±0.1	0.3±0.1	0±0	0±0	0.5±0.2
C20:2	0±0	0±0	0±0	0±0	0±0	0±0	0±0	0.4±0.1	0±0	0±0	0±0	0.8±0.1
C20:1	1.5±0.1	0.8±0.3	0.1±0	1.7±0.2	2.7±0.1	4.3±0.1	1.8±0.4	2.9±0.2	4.1±0.6	0±0	0.4±0	3.7±0.2
C20:0	1±0.1	1.7±0.2	0.9±0.1	1.3±0.1	1.4±0.1	1.7±0	0.3±0.4	1.4±0.2	1.6±0.3	0.9±0	0.7±0	1.2±0.1
C22:5 (n-3)	0.4±0.1	0±0	0±0	0.5±0.1	0±0	0±0	0±0	0±0	0±0	0±0	0±0	0±0
C22:6 (n-3)	0.5±0.1	1.1±0.1	1±0.1	2.8±0.1	0.7±0	0.3±0.3	0.5±0.2	1.3±0.1	1.4±0.2	1.7±0.3	0.6±0	1.2±0.1
C22:3	0.1±0	0±0	0±0	0±0	0±0	0±0	0±0	0±0	0±0	0.7±0.1	0.5±0.1	1.8±0.1

Table S4. (cont.)

A. SPM - PAG												
FAME	May	June	July	August	September	October	November	December	January	February	March	April
C22:2 (n-6)	0.9±0.1	0±0	0±0	0±0	0±0	0±0	0±0	0±0	0±0	0±0	0.7±0	0±0
C22:1	3.2±0.1	1.9±0.3	2.6±0.1	2.4±0.3	1.1±0.1	1.4±0.1	3.6±0.3	2±0.1	3.5±0.2	4.3±0.6	8.3±0.4	4.7±0.7
C22:0	1±0.1	2.7±0.8	1.5±0.1	1.9±0.2	3.6±0.3	3.3±0.2	1.2±0.1	3.2±0.2	4.3±1.4	2±0.1	3.4±0.2	1.9±0.2
C24:1 (n-9)	1.2±0.3	0±0	0±0	0±0	0±0	0±0	0±0	0±0	0±0	0±0	0.3±0.1	0±0
C24:0	1.5±0.7	2.3±0.4	0.9±0	2.7±0.1	3.6±0.3	2.5±0.7	2.7±0.3	3.8±0.6	2.3±1	3.4±0.9	1.2±0	2.9±0.2
ΣSFA	79.7±0.6	69.9±1.4	67±1	68.8±1	80±0.3	82.7±0.8	88.3±1.7	75±0.2	77.3±1	89.1±0.7	81.3±1.2	77.9±0.8
ΣMUFA	16.3±0.4	17.8±1.2	18.5±0.7	19.9±1.3	13.3±0.5	14.3±0.3	8.8±0.3	16.8±0.5	17.3±0.8	7.1±0.9	14.6±0.8	15.5±0.8
ΣPUFA	3.4±0.4	11.1±0.4	12.8±0.4	10.6±0.3	4.1±0.1	2.3±0.6	1.1±0.2	5.9±0.1	3.8±0.2	3.5±0.2	3.3±0.3	5.2±0.3
ΣUND	0.4±0	1±0	1.1±0.1	1.1±0.1	0.3±0	0.3±0	0.2±0	0.6±0	0.5±0	0.3±0	0.3±0	0.4±0
ΣDETRITAL	2.6±0.3	15.6±0.8	7.9±0.2	12.4±0.9	14.2±0.5	10.2±0.6	7.3±2.3	14±1.2	16.7±0.2	5.2±0.2	10.7±0.6	7.9±0.3
C16:1/C16:0	0.3±0	0.2±0	0.4±0	0.3±0	0±0	0±0	0.1±0	0.1±0	0±0	0±0	0.1±0	0.2±0

B. SPM - CETINA												
FAME	May	June	July	August	September	October	November	December	January	February	March	April
C14:0	14.3±0.5	8.1±0.4	3.9±0.2	5.3±0.4	15.3±0.4	3.5±0.4	5.2±0.8	5.4±0.5	6.1±0.6	5±0.1	6.7±0.1	5.1±0.1
C15:0i	0±0	0±0	1±0.1	0±0	0±0	4.4±0.4	2.7±0.1	2.1±0.2	1.9±0.1	3.3±0	3.7±0.1	1.4±0.1
C15:0ai	0±0	0±0	1.4±0.1	0±0	0±0	4.1±0.1	1.6±0.1	1.8±0.2	1.7±0	0.3±0.1	1.5±0.2	0.9±0.1
C15:0	1.4±0.1	1.2±0.1	2.1±0.1	3.6±0.5	2±0.1	1.5±0.2	1.5±0.1	2.1±0.1	3.7±0.2	1.9±0.2	2.4±0.2	2.4±0
C16:0i	0±0	1.5±0.1	0±0	3.7±0.3	0±0	1.7±0.5	0±0	0±0	0±0	3±0.3	0±0	0±0
C16:1	3.5±0.4	12.4±0.1	11.8±0.3	7.5±0.3	4.8±0.2	5.5±0.4	5.9±0.3	10.8±1.1	10.2±0.2	9.8±0.8	8.8±0.3	9.4±0.2
C16:0	33.4±0.8	26.4±0.9	22.1±1	22.9±0.7	33.3±0.7	29±0.6	35.7±0.7	30.6±0.5	32.6±0.4	28.4±0.8	27.9±0.9	19.7±0.7
C17:0i	3±0.1	0±0	0±0	0±0	0±0	0±0	0±0	0±0	0±0	1.6±0	0±0	0±0
C17:0ai	4.6±0.4	0±0	0±0	0±0	0±0	0±0	0±0	0±0	0±0	3.7±0.2	0±0	0±0
C17:0	1.8±0.2	0.8±0.1	3.9±0.2	5.7±1	4.1±0.1	4.6±0.4	2.9±0.3	3.1±0.1	3.7±0.3	3.8±0.1	3.2±0.1	3.7±0.2
C18:2 (n-6)	0.2±0	0±0	6.6±0.1	5.2±0.2	0.3±0.1	2.3±0.1	0±0	1.2±0.1	1.7±0.2	0±0	0±0	4.3±0.2
C18:1 (n-9)	3.6±0.4	6.9±0.5	7.3±0.8	5.6±0.7	2.7±0.5	3.6±0.3	1.9±0.1	2.4±0.3	3±0.1	4±0.1	5±0.1	7.1±0.2
C18:1 (n-7)	1.1±0.1	0±0	0±0	0±0	0±0	0±0	0±0	0±0	0±0	0±0	0±0	0±0

Table S4. (cont.)

B. SPM - CETINA												
FAME	May	June	July	August	September	October	November	December	January	February	March	April
C18:0	16.5±0.6	17.1±0.7	14.1±1.1	15.7±0.4	20.8±1.1	7.6±0.3	21.7±1.7	17.9±0.7	13±0.1	12.3±0.2	14.3±0.4	14.6±0.4
19:0i	1.6±0.1	0±0	0±0	0±0	0±0	0±0	0±0	0±0	0±0	0±0	0±0	0±0
C19:0	0±0	0±0	0±0	0±0	0±0	7.4±0.4	0±0	0±0	0±0	0±0	0±0	0±0
C20:4 (n-6)	0.2±0	0.6±0	0.3±0	0.1±0	0±0	0±0	1.5±0.6	0.4±0.1	1.2±0.1	0.2±0	0.2±0.1	0.6±0.1
C20:5 (n-3)	0.3±0	2±0.2	3.1±0.1	1.2±0.1	1.5±0.1	0±0	2.3±0.2	0.7±0.2	2.9±0.1	1.2±0.1	0.9±0.1	1.4±0.2
C20:1	1.6±0.1	4.9±0.2	5.6±0.5	0±0	4.4±0.3	4.7±0.3	2.2±0.7	2.1±0.1	5.3±0.1	2.8±0.1	2.9±0.2	4.8±0.3
C20:0	1.2±0	2.5±0.1	2±0.1	1.6±0	1.8±0.1	1.6±0.2	1.5±0.1	1.8±0.1	2.7±0	3.3±0.2	3.8±0.2	4.8±0.2
C22:6 (n-3)	0.1±0	1.4±0.2	2.1±0.1	1.1±0.1	0.1±0	0±0	0±0	0±0	1.8±0.1	3.1±0.1	0.3±0	1.6±0.1
C22:3	0±0	0±0	0±0	0±0	0±0	0±0	0±0	0±0	0.2±0.3	0±0	0±0	0±0
C22:1	2.5±0.2	6.7±0.3	0±0	6.7±0.4	2.8±0.1	8.8±0.4	4.8±0.1	7.8±0.4	2.1±0.4	5.1±0.1	6.7±0.3	11.7±0.7
C22:0	3.3±0.2	7.1±0.1	7±0.1	8±0.2	3.5±0.2	6.7±0.4	4.2±0.1	5.5±0.2	2.7±0.1	3.2±0.1	3.8±0.1	2.5±0.1
C24:1 (n-9)	1.8±0.1	0±0	2.9±0.2	0±0	0±0	0±0	0±0	0±0	0±0	0±0	2.2±0.1	0±0
C24:0	3.5±0.1	0±0	2.6±0.2	5.6±0.4	2.1±0	2.5±0.6	3.4±0.1	4.1±0.1	3.2±0.5	3.8±0.5	5.3±0.3	3.9±0.1
ΣSFA	80±1.7	64.7±1.4	60±0.8	72±1	82.8±0.9	74.8±0	80.6±0.4	74.4±0.2	71.2±0.4	69.9±1	72.6±0.3	58.9±0.9
ΣMUFA	14.1±1	30.9±0.9	27.7±1	19.8±0.8	14.7±0.8	22.6±0.4	14.8±1	23.1±0.4	20.7±0.6	21.7±0.8	25.6±0.2	33±0.8
ΣPUFA	0.8±0	3.9±0.3	12.1±0.1	7.5±0.3	1.9±0.1	2.3±0.1	3.8±0.8	2.3±0.4	7.8±0.6	4.5±0.1	1.5±0	7.8±0.2
ΣUND	0.2±0	0.8±0.1	1.2±0	0.6±0	0.3±0	0.4±0	0.4±0	0.4±0	0.8±0	0.7±0	0.5±0	1±0
ΣDETRITAL	13.5±0.2	3.5±0.2	8.4±0.1	12.9±1.4	6.1±0.1	23.8±0.6	8.8±0.2	9.2±0.3	10.9±0.5	17.7±0.4	10.7±0.3	8.3±0.1
C16:1/C16:0	0.1±0	0.5±0	0.5±0	0.3±0	0.1±0	0.2±0	0.2±0	0.4±0	0.3±0	0.3±0	0.3±0	0.5±0

Sed - PAG												
FAME	May	June	July	August	September	October	November	December	January	February	March	April
C14:0	10.3±10.3	4.8±5	0±0	6.2±6.5	6.6±6.1	8.5±8.6	10.9±11.1	6.4±6.5	n.a.	3±3.1	0±0	0±0
C15:0i	0±0	0±0	0±0	3.6±3.5	2.5±2.5	2.5±2.6	0±0	0.8±0.8	n.a.	6.2±6.2	0±0	0±0
C15:0ai	0±0	0±0	0±0	3.4±3.6	0±0	2.1±2.1	0±0	0±0	n.a.	1.1±1.1	0±0	0±0
C15:1	0±0	0±0	0±0	0±0	0±0	0±0	0±0	0±0	n.a.	0±0	0±0	0±0
C15:0	2.6±2.6	2.4±2.5	0±0	3.6±3.5	4.4±4.3	6.6±6.5	3.4±3.5	1.5±1.5	n.a.	2.5±2.5	0±0	0±0

Table S4. (cont.)

	Sed - PAG											
FAME	May	June	July	August	September	October	November	December	January	February	March	April
C16:0i	0±0	0±0	0±0	0±0	0±0	0±0	0±0	1±1	n.a.	0±0	0±0	0±0
C16:1	8.3±8.2	4.2±4.4	7.1±6.5	8.2±8.5	5.2±5.1	3.8±3.8	3±3	6.6±6.5	n.a.	0±0	4±4.1	4.6±4.7
C16:0	41.5±41.7	34.7±34	30.7±30.5	33.2±32	38.2±38	36.2±36	41.7±41.5	32.7±32.8	n.a.	16.4±17	16.1±16	14.8±15
17:0i	0±0	5.2±5.2	5.7±4.6	1.1±1.3	1.8±1.8	0±0	0±0	5.5±4.9	n.a.	4.3±4.2	1.3±1.3	0±0
C17:0ai	0±0	3.4±3.3	0±0	0±0	0±0	0±0	0±0	1.4±1.4	n.a.	0±0	0±0	0±0
C17:1	0±0	0±0	0±0	0±0	0±0	0±0	0±0	0±0	n.a.	0±0	0±0	0±0
C17:0	3.2±3.1	2.7±2.8	4.9±4.6	3.3±3.5	2.5±2.4	0±0	1.9±1.9	1.6±1.5	n.a.	3.5±3.5	4.5±4.6	4.6±4.6
C18:3 (n-6)	0±0	0±0	0±0	0±0	0±0	0±0	0±0	0±0	n.a.	0±0	0±0	0±0
C18:0i	0±0	0±0	0±0	0±0	0±0	0±0	0±0	0±0	n.a.	0±0	0±0	0±0
C18:2 (n-6)	2.4±2.3	3.1±3.2	5.9±6.3	4.4±4.5	1.1±1	2.4±2.4	1.6±1.6	1.2±1.2	n.a.	2.5±2.5	3.1±3.1	4.7±4.8
C18:1 (n-9)	6.5±6.5	6.3±6.4	4.4±4.7	5.1±5	3±3.2	9±9	3.9±3.8	5.2±5.2	n.a.	8.7±8.7	15.5±16	17.5±18
C18:1 (n-7)	3.9±3.8	1.6±1.6	0±0	0±0	0±0	0±0	0±0	2.2±2.1	n.a.	0±0	0±0	0±0
C18:0	12.3±12.3	13±13	9.7±10.6	10.6±11	13.9±14.1	17.8±18	16.8±16.8	9.5±9.5	n.a.	7.8±7.9	6.3±6.2	3.5±3.4
19:0i	2.8±2.8	1.7±1.7	0±0	0±0	2.2±2.5	0±0	1.1±1.1	1.3±1.2	n.a.	1.7±1.7	0.7±0.7	5.9±5.9
19:0ai	0±0	0±0	0±0	0±0	0±0	0±0	0±0	0±0	n.a.	0±0	0±0	0±0
C19:0	0±0	0±0	0±0	0±0	0±0	0±0	0±0	0±0	n.a.	6.1±6.1	8.1±8.1	9.5±9.6
C20:4 (n-6)	0±0	0±0	0±0	0±0	0±0	0±0	0±0	0±0	n.a.	0±0	0±0	0±0
C20:5 (n-3)	0±0	0±0	0±0	0±0	0±0	0±0	0±0	0±0	n.a.	0±0	0±0	0±0
C20:2	0±0	0±0	0±0	0±0	0±0	0±0	0±0	0±0	n.a.	0±0	0±0	0±0
C20:1	0±0	9.7±9.7	5.3±5.6	1.8±1.6	5±5.4	0±0	1.7±1.7	5.8±6.7	n.a.	10.1±10	13.8±14	11.7±11
C20:0	1.1±1.1	1.1±1.1	4.6±4.7	3.5±3.4	1.5±1.7	4±4	1.3±1.3	1±0.9	n.a.	9.9±9.7	13.5±13	0.9±0.8
C22:5 (n-3)	0±0	0±0	0±0	0±0	0±0	0±0	0±0	0±0	n.a.	0±0	0±0	0±0
C22:6 (n-3)	0±0	0±0	0±0	0±0	0±0	0±0	0±0	0±0	n.a.	0±0	0±0	0±0
C22:3	0±0	0±0	0±0	0±0	0±0	0±0	0±0	0±0	n.a.	0±0	0±0	0±0
C22:2 (n-6)	0±0	0±0	0±0	0±0	0±0	0±0	0±0	0±0	n.a.	0±0	0±0	0±0
C22:1	0±0	2.3±2.3	7.7±7.9	3.6±3.6	3.9±3.8	0±0	0±0	4.8±5.4	n.a.	8.2±8.2	6.9±6.9	13.1±13
C22:0	1.2±1.3	3±2.9	9.2±9.3	3.5±3.3	3.8±3.8	4.6±4.5	5±5.1	2.4±2.3	n.a.	2.2±2.1	1.5±1.5	5.4±5.6

Table S4. (cont.)

Sed - PAG												
FAME	May	June	July	August	September	October	November	December	January	February	March	April
C24:1 (n-9)	0±0	0±0	0±0	0±0	0±0	0±0	0±0	3.4±2.6	n.a.	2±2	3.1±3.1	1.8±1.8
C24:0	3.8±3.9	0.5±0.5	4.1±3.8	4.4±4.5	4±4	2±2	7.1±7	3.6±3.8	n.a.	3.4±3.4	1.5±1.5	1.8±1.7
ΣSFA	78.9±79	69.1±69	68.8±68	76.5±76	82±81.8	84.3±84	89.3±89.4	67.4±66.8	n.a.	68.2±68	53.5±53	46.5±47
ΣMUFA	18.7±18.5	24.2±24	24.5±24.6	18.7±19	16.8±17.1	12.9±13	8.7±8.6	29.9±30.4	n.a.	28.9±29	43.4±44	48.8±49
ΣPUFA	2.4±2.3	3.1±3.2	5.9±6.3	4.4±4.5	0.7±0.6	2.4±2.4	1.6±1.6	1.2±1.2	n.a.	2.5±2.5	3.1±3.1	4.7±4.8
ΣUND	0.3±0.3	0.4±0.4	0.5±0.5	0.4±0.4	0.2±0.2	0.2±0.2	0.1±0.1	0.5±0.5	n.a.	0.5±0.5	0.9±0.9	1.3±1.3
ΣDETRITAL	12.5±12.4	17±17.1	10.6±9.2	15.1±15	13.7±13.9	11.2±11	6.4±6.5	15.3±14.5	n.a.	25.4±25	14.7±15	20.1±20
C16:1/C16:0	0.2±0.2	0.1±0.1	0.2±0.2	0.3±0.3	0.1±0.1	0.1±0.1	0.1±0.1	0.2±0.2	n.a.	0±0	0.3±0.3	0.3±0.3

D. Sed - CETINA												
FAME	May	June	July	August	September	October	November	December	January	February	March	April
C14:0	6.4±0.8	5.5±0.4	5±1	7.4±0.3	7.9±0.3	8.5±0.4	5.2±0.2	11.6±1.2	5.1±0.7	5.5±0.5	6.1±0.5	6.6±0.5
C15:0i	0.4±0.1	1.9±0.1	0.9±0.1	0.6±0.2	0.7±0.1	1±0.1	1.9±0.6	1.4±0.3	8.6±0.8	2±0.2	1.8±0.3	1.9±0.2
C15:0ai	0.7±0	1.2±0.1	0.3±0.2	0.8±0.1	0.6±0.1	0±0	0.4±0.1	1.8±0.1	0±0	2±0.3	1.8±0.1	0±0
C15:0	7.6±1.8	6.1±0.1	5±0.3	4.9±0.3	3.8±0.3	2.5±0.4	7.2±0.8	3.6±0.4	4.4±0.7	2.3±0.2	4.5±0.4	4±0.2
C16:0i	1±0.1	0.2±0.1	1.2±0.1	0.6±0.2	0±0	0±0	2.2±0.9	0±0	0±0	2.1±0.4	0.6±0.2	0±0
C16:1	6.6±0.5	8.1±0.5	11.4±1.1	10.7±0.6	4.7±0.4	8.5±0.7	12±1.4	2.7±0.3	4.7±0.4	4±0.2	5.9±1.1	4.8±1.1
C16:0	36.9±1.3	31.8±1.1	21.9±2.2	41.1±0.9	43.5±0.6	39.7±1.5	35.6±1.2	40.8±1.7	31.1±3.3	31.9±1.6	33.7±1.1	34.3±1.5
17:0i	1.8±0.1	4.3±0.3	5.8±0.4	1.6±0.5	0±0	1.3±0.1	4.6±0.5	0±0	1.4±0.3	3.4±0.6	2.5±0.4	3.4±0.4
C17:0ai	2.9±0.2	1.6±0.3	4.1±0.4	1.7±0.5	0.6±0.1	0.8±0.1	4.5±0.5	0±0	0.3±0.2	4.7±0.4	3.7±0.5	0±0
C17:1	1.8±0.2	3±0.1	0±0	1.7±0.3	0.7±0	0±0	0±0	0±0	0±0	0±0	3.1±0.1	0±0
C17:0	2.7±0.1	2.5±0.1	3.4±0.3	1.9±0.2	2.7±0.1	2.5±0.2	3±0.2	2.5±0.7	3.3±0.4	2.3±0.4	2.9±0.2	5.8±0.2
C18:2 (n-6)	0.6±0.1	1.8±0.2	3.4±0.4	0.5±0.1	0.5±0.1	0.6±0.1	0.9±0.2	0.7±0.1	0.6±0.1	0.7±0.1	0.9±0.1	1.5±0.3
C18:1 (n-9)	3±0.2	3.3±0.1	6.3±0.4	3.2±0.3	2.6±0.2	3.4±0.4	3.8±0.3	5.6±0.3	4.9±0.5	6.2±1.1	3.6±0.6	5.6±0.5
C18:1 (n-7)	1.2±0.2	1±0.1	1±0.3	1.3±0.1	1±0.1	1±0.1	1.5±0.2	0±0	0±0	0±0	1.5±0.4	0±0
C18:0	11.5±1.1	9.3±0.7	6.6±0.4	10.4±0.4	15.8±0.5	10.7±0.8	8±0.5	12.4±1.4	10.7±0.8	10.7±0.7	7.7±0.4	10.6±1.5
19:0i	0.7±0.1	1.3±0.1	1.8±0.3	0.4±0.1	0±0	1.1±0.1	0.9±0.2	0±0	3.4±0.5	2.5±0.5	1.4±0.6	0±0

Table S4. (cont.)

					D. Sed - CETINA							
FAME	May	June	July	August	September	October	November	December	January	February	March	April
19:0ai	0±0	0±0	0±0	1.2±0.2	0±0	0±0	0±0	0±0	0±0	0±0	0±0	0±0
C19:0	1.9±0.2	0.1±0	3.7±0.5	0.3±0.1	0±0	1.2±0.2	0±0	0±0	0±0	0±0	1.6±0.1	0±0
C20:1	1.4±0.1	3.1±0.4	3.1±0.4	1.8±0.8	0.3±0.1	2.9±0.1	1.6±0.1	0±0	0±0	4.8±0.6	1.5±0.1	0±0
C20:0	0.9±0.2	1.2±0.1	1.1±0.1	1±0	1.3±0.4	1.5±0.1	0.7±0.3	2.3±0.5	4.5±0.5	1.4±0.5	0.8±0.1	2.3±0.3
C22:1	1.7±0.1	4.6±0.3	2±0.1	2.4±0.1	1.3±0.1	2.7±0.2	1.4±0.1	1.2±0.1	3.6±0.4	3.3±0.2	1.8±0.3	6.3±0.5
C22:0	3.5±0.3	2.7±0.4	3.6±0.4	1.9±0.2	3.7±0.3	3.1±0.1	1.8±0.1	5.7±0.2	5.1±0.7	4.8±0.3	2.3±0.2	6.1±0.6
C24:1 (n-9)	0.8±0.2	0.4±0.1	3.6±0.4	0.3±0.1	1.3±0	1.3±0.3	0.5±0.4	1.9±0.2	2.7±0.6	0.7±0.2	4.5±0.4	2.9±0.1
C24:0	3.8±0.4	4.9±0.3	4.6±0.5	2.2±0.3	6.3±0.5	5±0.6	2±0.3	5.4±0.5	4.8±0.3	4.1±0.7	5.7±0.4	3.4±0.6
ΣSFA	79.7±0.6	73.7±1.1	66.1±3.7	76.1±1.1	86.4±0.1	77.9±1.1	73.6±2.1	87.6±0.2	82.5±0.9	75±1.1	73.3±1	75.2±3.3
ΣMUFA	16.5±1.3	23.2±0.8	26.8±2.5	21.3±0.6	11.9±0.2	19.9±0.8	20.8±2.3	11.4±0.2	15.9±1.1	19.1±1.5	21.9±0.6	23.3±4.4
ΣPUFA	0.6±0.1	1.5±0.5	2.7±1.2	1±0.4	0.5±0.1	0.6±0.1	0.9±0.2	0.7±0.1	0.6±0.1	0.7±0.1	0.9±0.1	1.1±0.8
ΣUND	0.2±0	0.4±0	0.5±0.1	0.3±0	0.1±0	0.3±0	0.3±0	0.1±0	0.2±0	0.3±0	0.3±0	0.3±0.1
ΣDETRITAL	20.8±1.9	20.2±0.4	27.3±1.2	15.1±1.6	9.5±0.2	11.3±0.6	26.2±1.5	9.3±1.3	21.5±1.4	21.3±0.4	22.2±0.9	15.1±0.3
C16:1/C16:0	0.2±0	0.3±0	0.5±0.1	0.3±0	0.1±0	0.2±0	0.3±0.1	0.1±0	0.2±0	0.1±0	0.2±0	0.1±0

Table S5. Fatty acid contribution (mean % TFA ± SD) of consumers: (PG) *Glycymeris bimaculata* from Pag, (PC) *Callista chione* from Pag, (CG) *Glycymeris bimaculata* from Cetina and (CC) *Callista chione* from Cetina. FA with annual mean proportions > 1% are shown. SFA: saturated FA; MUFA: monosaturated FA; PUFA: polyunsaturated FA; UND: unsaturation degree (Pirini et al. 2007) ; DETRITAL: detrital FA [15:0+15iso+15anteiso+17:0+17iso+17anteiso+18:1(n-7)] (Mayzaud et al. 1989, Najdek et al. 2002); DHA: C22:6(n-3); EPA: C20:5(n-3).

	PG. *Glycymeris bimaculata* - PAG											
FAME	May	June	July	August	September	October	November	December	January	February	March	April
C14:0	8.8±2.2	7.6±1.2	6.3±0.7	5.6±0.4	7.2±0.1	7.2±0	7.3±0.1	8.7±1.4	7.4±0.1	11±0.3	13.1±0.1	12.2±0.4
C15:0i	0±0	0.1±0.1	0.1±0	0.1±0	0.2±0	0.2±0	0.2±0	0.2±0	0.1±0.1	0.2±0	0.2±0	0.2±0
C15:0ai	0±0	0±0.1	0.1±0	0±0	0.1±0.1	0.2±0.1	0.1±0	0±0	0.1±0.1	0.1±0	0.1±0	0.1±0
C15:0	0.7±0.2	0.7±0	0.7±0.1	0.6±0.1	0.9±0	1.1±0	1±0.1	1±0	1.1±0.1	1.1±0	1.1±0	0.9±0
C16:1	12.5±0.2	10.5±0.2	14.8±0.9	13.5±0.3	9.2±0.3	10.1±1	6.3±0.5	6.3±0.6	6±2.4	7.3±1.2	8.6±2.8	10.6±0.8
C16:0	34.7±3.9	36.4±0.9	33.7±0.4	34.4±1.1	42.7±1.5	40±3.5	46.9±3	49.8±2.8	45.4±5.4	45.4±4.1	44.2±5.1	39.2±3
17:0i	0.9±0.4	1±0	0.9±0.1	0.9±0.2	1.6±0.7	2.3±0.3	1.6±0.4	1.1±0	0.9±0.3	1±0.2	1.1±0.1	0.8±0.2
C17:0ai	0±0	0.1±0.1	0.2±0	0.2±0.1	0.3±0	0.3±0.1	0.4±0.1	0.4±0.1	0.3±0.1	0.3±0	0.3±0	0.2±0
C17:1	0.1±0.1	0±0.1	0.2±0	0.2±0	0.2±0.1	0.2±0.1	0±0	0±0.1	0.1±0.1	0.1±0	0.1±0	0.1±0
C17:0	2.2±0.5	2.4±0.1	2.2±0.2	2.2±0.1	3.1±0.1	3±0.5	3.9±0.8	3.5±0.3	3.9±0.3	3.2±0.2	2.9±0.3	2.4±0.2
C18:3 (n-6)	1±0.3	0.8±0.1	0.7±0.1	0.5±0.2	0.3±0.1	0.3±0.1	0.3±0	0.3±0	0.4±0.2	0.5±0.2	0.4±0.1	0.9±0.3
C18:0i	0.3±0.1	0.3±0	0.3±0	0.3±0	0.4±0	0.4±0	0.5±0.1	0.4±0.1	0.4±0	0.4±0	0.4±0	0.3±0
C18:2 (n-6)	2.4±0.3	2.5±0.1	2.5±0.1	2.2±0.3	1.4±0.1	1.7±0.6	0.8±0.5	0.7±0.1	1.2±0.5	1.3±0.5	1.1±0.5	2±0.3
C18:1 (n-9)	9.9±0.5	10.9±1	11.3±0.5	9.7±0.1	8.6±0.3	9.6±1.4	6.2±2.2	5.8±0.2	8±2.3	6.6±1.2	5.6±1.5	8.5±0.4
C18:1 (n-7)	2.3±1	0.3±0.1	0.3±0	0.2±0	0.2±0.1	0.3±0.1	0.2±0.3	0.1±0.1	0.3±0.4	0.3±0.1	0.3±0.1	0.4±0
C18:0	12±1.1	12.1±0	10.3±0	11.6±0.6	14±1.1	14±0.7	17.3±1.9	16.5±0.5	16.5±2.8	13.5±0.4	12.8±2.2	10.7±1.1
19:0i	0.4±0.1	0.5±0	0.4±0	0.4±0.1	0.5±0	0.7±0.1	0.7±0.1	0.5±0	0.6±0	0.5±0	0.5±0	0.4±0
19:0ai	0±0	0±0.1	0±0.1	0±0.1	0.1±0.1	0.1±0.1	0.1±0.1	0.2±0.1	0.2±0.3	0.1±0	0.1±0.1	0.1±0
C19:0	0.4±0	0.4±0	0.3±0	0.3±0.1	0.4±0	0.5±0	0.5±0.1	0.5±0	0.5±0	0.4±0	0.4±0	0.3±0
C20:4 (n-6)	0.5±0.2	0.5±0.1	0.6±0	0.6±0.3	0.2±0	0.4±0.3	0±0	0.2±0.3	0.3±0.4	0.2±0.1	0.1±0.1	0.2±0.1
C20:5 (n-3)	2.3±1.2	2.5±0.4	3.3±0.3	2.6±0.5	0.4±0.2	0.8±0.6	0.1±0.1	0±0.1	0.2±0.3	0.6±0.6	0.8±0.8	0.9±0.4
C20:3	0.3±0	0.7±0	0.8±0.2	0.7±0.2	0.3±0.3	0.4±0.3	0.1±0.1	0±0	0±0	0.1±0.1	0.1±0.1	0.2±0.1
C20:2	0.3±0.5	0±0	0.1±0	0±0	0.2±0	0.2±0.1	0±0	0±0.1	0±0	0.1±0	0.1±0.1	0.2±0.1

Table S5. (cont.)

PG. *Glycymeris bimaculata* - PAG												
FAME	May	June	July	August	September	October	November	December	January	February	March	April
C20:1	3.5±0.9	4.6±0.1	3.9±0.7	6.6±1.4	3.9±0.2	3.3±0.9	3.2±0.7	2.5±0	3.4±1.3	3.2±0.9	2.8±0.7	4.3±1.4
C20:0	0.4±0	0.4±0.1	0.3±0.1	0.3±0	0.4±0	0.5±0	0.5±0	0.5±0.1	0.6±0.1	0.4±0	0.5±0	0.4±0
C22:5 (n-3)	0.2±0.1	0.2±0	0.2±0	0.1±0	0±0	0.1±0	0±0	0±0	0±0	0±0	0±0	0.1±0
C22:6 (n-3)	2±1.6	2.4±0.5	2.8±0.1	2.3±0.8	0.3±0.1	0.6±0.6	0±0	0±0	0.1±0	0.5±0.1	0.4±0.1	0.7±0.4
C22:3	0.3±0.1	0.4±0.2	0.3±0.2	0.1±0.1	0±0.1	0.1±0.2	0±0	0±0	0±0	0.1±0	0±0.1	0±0
C22:2	0.8±0.3	0.9±0.1	0.9±0.8	0.5±0.2	0.3±0.2	0.2±0.2	0±0	0±0	0±0	0.1±0.1	0.2±0	0.3±0.1
C22:1	0.2±0.3	0±0	0.6±0.2	2.4±1.3	1.7±1.3	0.3±0.2	0.5±0	0.3±0.1	1±0.4	0.4±0.3	0.9±0.2	1.2±0.5
C22:0	0.2±0	0.5±0	0.4±0	0.2±0	0.4±0.1	0.3±0.2	0.4±0.2	0.2±0.3	0.3±0.4	0.3±0.2	0.2±0	0.2±0.1
C24:0	0.3±0.1	0.5±0.1	0.4±0.1	0.3±0	0.5±0.2	0.6±0.1	0.7±0	0.2±0.3	0.8±0.1	0.4±0	0.5±0	0.4±0
ΣSFA	61.4±3.1	62.9±2.6	56.6±0.8	57.7±0.9	72.7±0.6	71.3±2.4	82.2±1.6	83.7±0	79±7.7	78.3±5.3	78.4±1.5	69±1.8
ΣMUFA	28.8±1.5	26.4±1.2	31.3±0.2	32.7±1.1	23.9±1.2	23.9±1.5	16.5±2.9	15±0.1	18.9±6.3	18.1±3.2	18.4±1.4	25.3±1.1
ΣPUFA	9.8±2.6	10.7±1.4	12.1±1	9.6±2.2	3.4±0.6	4.8±2.9	1.3±0.7	1.3±0.1	2.1±1.4	3.6±2.1	3.3±2.2	5.7±1.7
ΣUND	1.1±0.6	1.1±0.2	1.4±0.1	1.2±0.1	0.5±0	0.6±0.2	0.2±0.1	0.2±0	0.3±0.2	0.4±0.2	0.4±0.2	0.6±0.2
ΣDETRITAL	7.3±2	5.8±0.4	5.4±0.6	5.4±0.9	7.8±0.8	9±0.1	9.3±0.2	7.8±0.3	8.3±1.1	7.7±0.2	7.4±0.1	6.2±0.6
C16:1/C16:0	0.4±0.2	0.3±0	0.4±0	0.4±0	0.2±0	0.3±0	0.1±0.1	0.1±0	0.1±0.1	0.2±0	0.2±0.1	0.3±0
DHA/EPA	0.8±0.3	1±0	0.9±0	0.9±0.1	0.7±0	0.7±0.1	n.d.	n.d	n.d.	0.7±0.2	0.5±0	0.7±0.1

PC. *Callista chione* - PAG												
FAME	May	June	July	August	September	October	November	December	January	February	March	April
C14:0	9.7±0.4	7.9±1.1	6.2±0.4	6.4±0.3	6.9±0.1	9.2±1.2	9.3±0.1	10.5±0.2	12.8±1.8	10.8±0.3	11.5±1.5	11.9±0.2
C15:0i	0.2±0	0.2±0	0.2±0	0.3±0	0.3±0.1	0.3±0.1	0.3±0	0.3±0	0.4±0	0.3±0	0.3±0.1	0.3±0
C15:0ai	0.1±0	0.1±0	0.1±0	0.1±0	0.1±0.1	0.1±0	0.1±0	0.1±0	0.2±0	0.1±0	0.1±0.1	0.1±0
C15:0	1.1±0.1	0.9±0.1	0.9±0.1	1±0	1.4±0	1.6±0.1	1.5±0	1.9±0	2±0.3	1.8±0.1	1.4±0.1	1.4±0.1
C16:2	0±0	0.1±0	0±0	0±0	0±0	0±0	0±0	0.3±0.4	0±0	0±0	0.5±0.1	0.5±0
C16:1	13.2±0.6	12.9±1.4	16.5±0.2	19.1±1	14.6±0	12.9±1.2	14.7±0.7	10.4±1.1	10.1±1	14.1±0.3	14.8±1.7	14.9±0.2

Table S5. (cont.)

PC. *Callista chione* - PAG												
FAME	May	June	July	August	September	October	November	December	January	February	March	April
C16:0	28.8±0.1	29.6±0.9	27.5±0.2	34±1.2	40.4±1	38.8±3.2	33.8±0.5	37.8±0.2	42.1±4.3	36.1±1.2	33.1±2.2	31.3±2.2
17:0i	2.6±0.3	1.2±0.1	1.3±0.2	1.8±0.3	3.3±0.2	1.8±0.1	2.6±0	5.3±1.8	2.5±0.6	2.1±0.6	4.4±1.9	3.3±0.6
C17:0ai	0.8±0	0.6±0	0.6±0.1	0.7±0.1	1.2±0.2	0.9±0	1.1±0	1.3±0	1.2±0.1	0.9±0	0.8±0.2	0.7±0.2
C17:1	0.3±0.1	0.2±0	0.2±0.1	0.2±0.1	0.4±0.1	0.2±0	0.3±0	0.2±0.1	0.2±0	0.2±0	0.2±0.2	0.3±0.2
C17:0	1.5±0.1	1.2±0.1	1.2±0.1	1.4±0.1	2.2±0.1	1.8±0.2	1.8±0.1	2±0.1	2±0.2	1.7±0.2	1.7±0.1	1.4±0.1
C18:3 (n-6)	1.4±0	1.5±0.1	1.3±0.2	0.7±0	0.5±0.1	0.5±0.1	0.6±0	0.7±0	0.6±0.2	1.2±0.1	0.7±0	1.4±0.2
C18:0i	0.1±0	0.1±0	0±0.1	0.1±0	0.2±0	0.1±0	0.1±0	0.1±0	0.1±0	0.1±0	0.1±0.1	0.1±0
C18:2 (n-6)	2.7±0.1	2.9±0.1	2.6±0.1	1.9±0.1	1.3±0.1	1.4±0.4	2±0.1	1.3±0.3	1.2±0.5	1.9±0.2	1.4±0	2.3±0.2
C18:1 (n-9)	12.4±0.4	12.4±0.4	10.4±0.3	9.7±0.3	10.3±0.7	10.6±0.3	12.1±0.8	10.2±1.3	9.6±1.7	10.7±0.8	8.8±1.8	11.4±0.1
C18:1 (n-7)	0.3±0	0.4±0	0.2±0	0.2±0	0.2±0	0.2±0	0.3±0	0.1±0.2	0.3±0	0.4±0	0.4±0	0.3±0.1
C18:0	6.3±0.1	5.6±0.1	4.7±0.1	5.8±0.2	7.9±0.1	7.4±1.1	6.8±0.2	6.8±0.3	7.8±0.5	6.7±0.3	5.8±0.6	5±0.1
19:0i	0.3±0	0.1±0	0.1±0	0.1±0	0.2±0	0.1±0	0.2±0	0.4±0.2	0.3±0.2	0.1±0	0.4±0.3	0.2±0
19:0ai	0.2±0	0.1±0	0.1±0	0.1±0	0.1±0	0.1±0	0.2±0	0.3±0.1	0.1±0.2	0.1±0	0.3±0.2	0.2±0
C19:1	0.2±0	0.2±0	0.2±0	0.1±0	0.2±0.1	0.2±0	0.2±0.1	0.3±0.1	0.3±0.2	0.1±0	0.1±0.1	0.3±0
C19:0	0.3±0	0.2±0	0.2±0	0.2±0	0.4±0	0.3±0	0.3±0	0.4±0	0.5±0.2	0.3±0	0.3±0.1	0.2±0.1
C20:4 (n-6)	0.7±0.1	0.8±0.1	0.9±0	0.9±0	0.3±0	0.3±0.2	0.8±0.1	0.3±0.1	0.2±0.2	0.4±0.1	0.3±0	0.3±0
C20:5 (n-3)	3.3±0.2	5.4±0.1	8.9±0.2	5.6±0.3	1±0	0.7±0.5	1.7±0.1	0.6±0.1	0.3±0.2	1.5±0.2	1.9±0.2	1.1±1
C20:3	0.8±0.1	0.8±0	1±0.1	0.8±0.1	0.2±0	0.2±0.2	0.3±0	0.3±0	0.2±0.1	0.3±0.1	0.4±0.1	0.5±0
C20:2	1.7±0.1	1.7±0.2	1.7±0	1.4±0.2	1.1±0.1	1±0.2	1.5±0	0.8±0.3	0.7±0.5	1.3±0.1	1±0	1.4±0.1
C20:1	3±0.2	4.5±0.8	3.1±2	1.5±0.1	1.8±0.1	5.4±0.1	2.4±0.2	1.7±0.4	2.2±1.9	3±2.2	1.8±0	1.5±0.1
C20:0	0.3±0	0.2±0	0.2±0	0.3±0	0.3±0	0.3±0	0.3±0	0.3±0	0.3±0	0.2±0	0.2±0	0.2±0
C22:5 (n-3)	0±0	0±0	0±0	0.3±0	0.1±0	0.1±0	0.2±0	0.1±0	0±0	0.1±0	0.1±0	0.1±0
C22:6 (n-3)	3.4±0.1	5.1±0.2	6.9±0.5	3.2±0.4	0.5±0.1	0.4±0.3	1.3±0.1	0.3±0.2	0.2±0.2	1.1±0.2	0.6±0	1.5±0.2
C22:3	0.3±0	0.3±0	0.3±0	0.2±0	0.1±0	0.1±0	0.2±0	0.3±0.1	0.1±0	0.1±0	0.3±0.2	0.2±0
C22:2 (n-6)	1.7±0.8	0.6±0.5	1±0.1	0.9±0.1	0.9±0	0.7±0.2	1.2±0.1	1.3±0.9	0.5±0.1	0.8±0.3	2±2.1	1.9±0.2
C22:1	1.3±0.3	1.8±1.8	0.5±0	0.2±0.1	0.9±0.5	1.7±0.1	0.7±0.3	2.2±1.2	0.4±0.1	0.5±0.5	3.4±3.2	2±0.2

Table S5. (cont.)

PC. *Callista chione* - PAG												
FAME	May	June	July	August	September	October	November	December	January	February	March	April
C22:0	0.1±0.2	0.1±0	0.2±0	0.1±0	0.2±0	0.1±0	0.2±0	0.4±0.2	0.1±0	0.2±0.1	0.4±0.3	0.3±0
C24:0	0.2±0.1	0.1±0.1	0.1±0	0.1±0	0.1±0	0.1±0	0.1±0	0.3±0.1	0.2±0.1	0.2±0.1	0.2±0.1	0.2±0
ΣSFA	52.7±0.8	48.1±0.2	43.6±1.4	52.5±0.8	65.2±0.8	63.1±3.1	58.7±0.8	68.3±2.4	72.8±2	61.7±2.9	61±1.9	56.8±1.6
ΣMUFA	30.8±0.1	32.4±0.9	31.2±2	31.1±0.3	28.4±0.3	31.1±1.4	30.8±1.1	25.2±2	23.2±2	29.2±2.2	29.4±0.7	30.8±0.6
ΣPUFA	16.5±1	19.5±0.7	25.2±0.7	16.4±1.2	6.4±0.4	5.7±1.7	10.4±0.3	6.6±0.4	4±2	9.1±0.7	9.5±1.6	12.4±1
ΣUND	1.7±0	2.3±0	3.2±0.1	1.9±0.1	0.7±0	0.8±0.2	1.1±0	0.6±0.1	0.5±0.2	1±0.1	1±0.1	1.2±0
ΣDETRITAL	7.5±0.6	5±0	4.9±0.6	6±0.5	9.7±0.5	7.4±0.1	8.5±0.1	12.3±2.2	9.7±0.5	7.9±0.9	10.1±2	8.3±1
C16:1/C16:0	0.5±0	0.4±0.1	0.6±0	0.6±0	0.4±0	0.3±0.1	0.4±0	0.3±0	0.2±0	0.4±0	0.4±0	0.5±0
DHA/EPA	1±0	0.9±0.1	0.8±0	0.6±0	0.5±0.1	0.6±0	0.8±0	0.5±0.3	0.5±0.2	0.7±0.1	0.3±0	2.4±2.5

CG. *Glycymeris bimaculata* - CETINA												
FAME	May	June	July	August	September	October	November	December	January	February	March	April
C14:0	7.5±1.1	6.9±0.4	5.6±0	4.4±0.3	6.2±0.1	6.3±0.3	8.8±0.8	7.8±0.2	9±0.1	8.8±0.8	6.2±0.7	8.2±0.3
C15:0i	0.2±0	0.1±0	0.1±0	0.1±0.1	0.2±0	0.1±0.1	0.3±0	0.2±0	0.2±0	0.2±0	0.1±0.1	0.2±0.0
C15:0ai	0.1±0	0.1±0	0.1±0	0.1±0.1	0.1±0.1	0±0	0±0	0.1±0	0.1±0.1	0.1±0	0±0.1	0.1±0.0
C15:0	0.8±0	0.7±0	0.7±0	0.6±0	1.1±0.3	1±0	1.1±0.2	0.8±0	0.9±0	0.9±0.2	0.6±0.1	0.7±0.1
C16:0i	0.1±0	0.1±0	0.1±0	0.1±0	0.1±0	0±0	0.1±0	0.1±0	0.1±0	0.1±0	0.1±0.1	0.1±0.0
C16:1	7.4±2.2	9.3±0.4	12.9±0.3	9.3±1.1	6.1±0.1	5.4±0.1	9.4±0.8	9.8±0.7	10±0.8	10.6±0.1	8.2±2.9	11.6±0.2
C16:0	35.1±3.9	37.2±1.3	30.1±1.7	34.5±3.7	45.2±0	45.5±0.7	43.2±3.6	38.7±1.5	40.4±0.9	37.8±0.7	34.1±6.2	32.2±1.1
17:0i	0.8±0	0.8±0.1	0.9±0.1	0.9±0.3	1.4±0.8	0.9±0.2	1.2±0	0.8±0	0.8±0.1	0.8±0.2	0.5±0.1	0.7±0.1
C17:0ai	0.2±0	0.2±0	0.2±0	0.3±0	0.2±0	0.2±0	0.3±0	0.3±0	0.3±0	0.3±0	0.3±0.2	0.3±0.1
C17:1	0.1±0.1	0.2±0	0.2±0	0.2±0	0±0	0±0	0.1±0.2	0.2±0	0.2±0	0.2±0	0.1±0.1	0.2±0.1
C17:0	2.9±0.2	2.9±0.1	2.4±0.2	3±0.1	4.3±0.7	4±0.1	3.4±0.1	3.2±0.2	3.1±0.1	3±0.1	2.4±0.6	2.3±0.0
C18:3 (n-6)	0.6±0.5	0.4±0.1	0.7±0	0.5±0	0.4±0.1	0.2±0.1	0.3±0	0.5±0.1	0.4±0	0.6±0.1	1.3±0.9	1.1±0.1
C18:0i	0.4±0.1	0.3±0	0.4±0	0.5±0.1	0.6±0.2	0.4±0.2	0.5±0	0.5±0	0.4±0	0.4±0.2	0.3±0.1	0.3±0.0

Table S5. (cont.)

CG. *Glycymeris bimaculata* - CETINA												
FAME	May	June	July	August	September	October	November	December	January	February	March	April
C18:2 (n-6)	2.1±1.2	2.1±0.1	2.5±0.2	2.2±0.4	0.9±0.1	1.2±0.4	1.3±0.3	1.9±0.2	1.7±0.2	2±0.4	2.8±0.8	2.6±0.1
C18:1 (n-9)	9.1±1.1	10±0.1	9.2±0.2	9±0.7	6.5±0.1	6.9±1.2	6.7±1.3	8.7±0.4	7.7±0.1	8.3±1.2	10.1±1.5	9.8±0.1
C18:1 (n-7)	0.4±0.1	0.3±0	0.4±0	0.3±0	0.1±0.1	0±0	0.2±0	0.2±0	0.3±0	0.3±0	0.3±0.1	0.3±0.0
C18:0	13.5±2.9	13.1±0.7	11.1±0.6	15.5±0.9	21.1±2.3	18.9±1.7	14.3±0.1	13.4±1.3	13.2±0.1	12.3±1.7	12.8±4.2	10.1±0.2
19:0i	0.6±0.2	0.5±0	0.5±0	0.7±0.1	0.8±0.1	0.7±0.1	0.5±0	0.6±0.1	0.6±0.1	0.6±0	0.5±0.1	0.5±0.1
C19:0	0.7±0.3	0.5±0	0.4±0	0.5±0.1	0.7±0.1	0.7±0.1	0.5±0	0.5±0	0.5±0	0.4±0	0.4±0.1	0.4±0.1
C20:4 (n-6)	0.3±0.3	0.3±0	0.7±0.1	0.6±0.2	0±0	0±0	0.2±0.1	0.4±0.1	0.3±0.1	0.4±0.1	0.7±0.4	0.7±0.1
C20:5 (n-3)	1.2±1.6	0.8±0.2	3.7±0.6	1.8±0.7	0±0	0±0	0.4±0.2	0.9±0.3	0.7±0.1	1.5±0.6	2.6±2.2	4.2±0.1
C20:3	0.3±0.1	0.6±0	0.8±0.2	0.6±0.2	0.1±0.1	0±0	0.3±0.1	0.4±0	0.4±0.1	0.5±0.2	0.5±0.2	0.6±0.1
C20:2	0.1±0.1	0.2±0	0.2±0	0.2±0	0±0	0±0	0.1±0	0.2±0	0.1±0	0.2±0	0.2±0.2	0.4±0.1
C20:1	6.1±0.7	6.5±0.2	6.3±0.5	7.8±1.9	2.5±3.6	4.5±2	4.2±0.7	5.9±0.4	4.6±0.6	4.5±0.5	6.6±0	4.8±0.6
C20:0	0.5±0.1	0.5±0.1	0.4±0	0.6±0.1	0.7±0.1	0.8±0	0.5±0	0.5±0.1	0.5±0	0.4±0	0.4±0.1	0.4±0.1
C22:5 (n-3)	0.1±0.2	0.2±0	0.3±0	0.4±0.2	0±0	0±0	0.1±0.1	0.2±0.1	0.1±0	0.2±0	0.3±0	0.3±0.1
C22:6 (n-3)	1.5±1.9	0.9±0.3	3.6±0.9	2.1±0.7	0±0	0±0	0.3±0.2	1±0.5	0.6±0.1	1±0.9	2.7±2.6	2.8±0.1
C22:3	0±0.1	0±0	0.1±0	0.1±0.1	0±0	0±0	0±0	0±0	0±0	0±0	0.4±0.4	0.1±0.0
C22:2	0.8±0	0.8±0.1	0.8±0	1.1±0	0±0	0.1±0.2	0.4±0.1	0.2±0.3	0.3±0	0.5±0	0.8±0.1	0.5±0.0
C22:1	5.2±3.3	2.4±0.3	3.4±0.4	0.6±0	0.1±0.1	0.5±0.7	0.3±0.1	1.1±1.2	1.4±0.2	2.2±0.4	2.5±0.3	2.6±0.7
C22:0	0.5±0	0.5±0.1	0.5±0.1	0.6±0.1	0.3±0.5	0.8±0.2	0.6±0	0.5±0	0.4±0.3	0.5±0.1	0.4±0.2	0.4±0.1
C24:0	0.6±0.2	0.5±0.2	0.4±0	0.7±0	0.4±0.5	1.2±0.3	0.7±0.1	0.6±0.1	0.6±0	0.6±0	0.7±0.4	0.5±0.0
ΣSFA	64.5±1.6	64.9±1.1	54.1±2.6	63.2±0.9	83.4±1.7	81.3±1.8	75.8±1.3	68.4±1.3	71.1±1.1	67.2±1.3	59.9±0.6	57.4±1.1
ΣMUFA	28.3±0.8	28.8±1.2	32.6±0.8	27.2±3.6	15.2±0.8	17.2±1.8	20.8±1.1	25.9±2	24.1±0.5	26.1±0.9	27.8±0.5	29.4±0.5
ΣPUFA	7.2±5.8	6.3±0.9	13.3±1.8	9.6±2.2	1.3±0.1	1.5±0.1	3.4±1.2	5.7±1.3	4.8±0.6	6.7±0.5	12.3±1.2	13.2±0.7
ΣUND	0.9±0.5	0.8±0.1	1.6±0.3	1±0.3	0.2±0.1	0.3±0	0.4±0.1	0.7±0.1	0.6±0	0.7±0.4	1.3±0.9	1.5±0.1
ΣDETRITAL	7.1±0.8	6.5±0.2	6.4±0.2	7.1±0.8	9.5±2.1	7.9±0.5	8±0.2	7.2±0.5	7.3±0.2	7±0.2	5.6±1	5.9±0.6
C16:1/C16:0	0.2±0.1	0.3±0	0.4±0	0.3±0.1	0.1±0	0.1±0	0.2±0	0.3±0	0.2±0	0.3±0.1	0.3±0.1	0.4±0
DHA/EPA	1.4±0.3	1.1±0	1±0.1	1.1±0.1	n.d.	n.d.	0.8±0.2	1.1±0.1	0.8±0	0.6±0.1	0.9±0.2	0.7±0

Table S5. (cont.)

CC. *Callista chione* - CETINA												
FAME	May	June	July	August	September	October	November	December	January	February	March	April
C14:0	10.6±0.7	9.3±0.6	6.9±0.1	6.1±0.3	6.7±0.4	6.5±1.4	9.2±0.6	8±0.4	8.7±0	10±0.5	11.6±0	11.4±1
C15:0i	0.3±0	0.3±0	0.2±0	0.3±0	0.3±0	0.2±0	0.3±0	0.2±0	0.2±0	0.2±0	0.2±0	0.2±0
C15:0ai	0.1±0	0.1±0	0.1±0	0.1±0	0.1±0	0.1±0	0.1±0	0.1±0	0.2±0	0.1±0	0.1±0	0.1±0
C15:0	1.4±0	1.4±0.1	1.1±0	1.1±0.1	1.4±0.1	1.5±0.3	1.5±0.1	1.6±0.2	1.6±0	1.5±0.1	1.4±0.1	1.5±0
C16:0i	0.4±0.1	0.3±0.1	0.5±0	0.6±0	0.6±0	0.5±0.1	0.6±0	0.5±0	0.6±0	0.6±0	0.5±0	0.5±0
C16:1	13±0.7	16.1±1	16.3±0.5	15±0.9	13.7±2.1	11.1±1.2	13.1±1.4	11.9±0.5	10.6±0.2	13.1±0.8	13.8±0.3	13.1±0.3
C16:0	32.8±3.1	24.3±1.5	30.6±0.3	30.6±2.7	38.9±0.2	35.1±6.5	38.8±1	37.3±1.2	40.6±0.8	38.6±0.9	36.1±2.3	38.4±0.7
17:0i	1.4±0.1	1.5±0	1.3±0	1.6±0	2±0.2	2±0.1	2.1±0.1	2.1±0.2	1.8±0.4	1.7±0.1	1.4±0	1.4±0
C17:0ai	0.8±0	0.8±0	0.7±0	0.9±0	1±0.1	1±0.2	1.1±0.1	1.2±0	1.1±0	0.9±0	0.8±0	0.8±0.1
C17:1	0.2±0	0.3±0	0.2±0	0.3±0	0.2±0	0.2±0.1	0.3±0.1	0.3±0	0.2±0	0.2±0	0.2±0	0.1±0
C17:0	1.6±0	1.6±0.1	1.3±0.1	1.5±0.1	2.1±0.2	1.9±0.4	2.2±0.3	2.3±0.2	2.7±0.4	1.9±0	1.5±0.1	1.7±0
C18:3 (n-6)	0.5±0.4	0.1±0	1±0.1	0.4±0.4	0.4±0	0.5±0	0.5±0	0.5±0	0.5±0.1	0.6±0.1	1.1±0.2	0.5±0.1
C18:0i	0.6±0.7	1.2±0.2	0.1±0	0.4±0.5	0.1±0	0.1±0	0.2±0	0.2±0	0.2±0	0.2±0	0.1±0	0.1±0
C18:2 (n-6)	2.9±0.5	3.5±0.4	2.6±0.1	2.4±0.1	1.3±0.1	1.6±0.1	1.2±0.1	1.4±0.2	1.2±0.3	1.4±0.1	2.2±0.3	1.4±0.1
C18:1	12.2±0.8	13.5±0.1	10±0.1	10.8±0.2	10.9±0.4	10.5±1.2	9.5±0.4	10.5±0.4	9.4±0.7	9.8±0.3	11.5±0.4	10.8±0
C18:1 (n-7)	0.4±0.1	0.4±0	0.3±0	0.3±0	0.3±0	0.2±0	0.2±0	0.3±0	0.3±0	0.4±0	0.4±0	0.4±0
C18:0	6.5±0.1	5.9±0.3	5.1±0.1	5.7±0.5	8.3±0.9	7.3±1.5	8.4±0.6	9.1±0.8	10.2±0.2	8.4±0.2	6.4±0	8.1±0.5
19:0i	0.3±0.2	0.2±0	0.1±0	0.2±0	0.2±0	0.2±0	0.2±0	0.2±0.1	0.3±0	0.1±0	0.1±0	0.1±0
19:0ai	0.1±0	0.1±0	0.1±0	0.1±0	0.1±0	0.1±0	0.1±0	0.1±0	0.1±0	0±0.1	0.1±0	0±0.1
C19:1	0.3±0	0.3±0	0.1±0	0.2±0	0.2±0	0.2±0	0.2±0.1	0.1±0	0.2±0.1	0.1±0.1	0.3±0	0.2±0
C19:0	0.4±0	0.3±0	0.2±0	0.3±0	0.3±0	0.3±0.1	0.4±0.1	0.4±0	0.5±0.1	0.3±0	0.2±0	0.3±0
C20:4 (n-6)	0.3±0.1	0.5±0.2	0.8±0	0.7±0	0.2±0	0.2±0	0.2±0.1	0.4±0	0.2±0.1	0.3±0.1	0.3±0.1	0.2±0
C20:5 (n-3)	1.9±0.6	3.7±1.3	6.3±0.1	4.5±0.6	0.4±0	0.7±0.3	0.4±0.3	0.7±0.2	0.4±0.1	1±0.4	1.4±0.6	0.7±0.3
C20:3	0.5±0.1	0.7±0.1	0.9±0	0.8±0	0.3±0	0.2±0	0.3±0.2	0.3±0.1	0.3±0	0.2±0	0.3±0.2	0.1±0
C20:2	0.5±0.2	0.5±0	0.5±0	0.5±0.1	0.3±0	0.3±0	0.1±0.1	0.4±0.1	0.3±0.1	0.3±0.1	0.4±0.1	0.3±0

Table S5. (cont.)

CC. *Callista chione* - CETINA												
FAME	May	June	July	August	September	October	November	December	January	February	March	April
C20:1	5.5±1.1	6.8±0.6	6.1±0.1	6.8±0.5	5.4±0.8	6.4±2.6	5.4±0.3	4.8±0.5	4.1±0.4	4.2±0.5	3.7±0.3	4.2±0.3
C20:0	0.3±0	0.3±0	0.3±0	0.3±0	0.3±0	0.3±0	0.4±0	0.4±0	0.5±0	0.3±0	0.2±0	0.3±0
C22:5 (n-3)	0.2±0	0.3±0.1	0.4±0	0.3±0	0.1±0.1	0.1±0.1	0.1±0.1	0.1±0	0.1±0.1	0.1±0	0.1±0	0.1±0
C22:6 (n-3)	1.6±0.6	3.5±1.5	4.2±0.3	3.3±0.7	0.2±0	0.5±0.2	0.3±0.1	0.6±0.1	0.2±0	0.5±0.2	1±0.5	0.3±0.1
C22:3	0.1±0	0.2±0.1	0.2±0	0.2±0	0.1±0	0.1±0	0.1±0	0.2±0.1	0.1±0	0.1±0	0.1±0	0±0
C22:2	0.8±0	1±0.1	0.4±0.6	0.5±0.6	0.8±0.1	0.5±0.3	0.6±0	0.8±0.3	0.5±0	0.5±0.1	0.5±0.1	0.6±0.1
C22:1	1±0.5	0.8±0.3	0.7±0.4	2.6±2.4	1.6±1.6	8.5±11.1	1.2±0.1	0.9±0.6	0.7±0.1	0.6±0.3	0.5±0.1	0.6±0.1
C22:0	0.2±0.1	0.1±0	0.2±0	0.1±0	0.1±0.1	0.1±0	0.2±0.1	0.2±0	0.2±0.1	0.1±0.1	0.1±0	0.2±0
C24:1	0±0	0.1±0	0.1±0.1	0.4±0.5	0±0	0±0	0.2±0.2	0.6±0.5	0±0	0±0	0±0	0±0
C24:0	0.1±0	0.1±0	0.1±0	0.1±0	0.2±0	0.4±0.3	0.2±0.1	0.4±0	0.3±0.1	0.2±0	0.1±0	0.2±0.1
ΣSFA	58±1.8	47.7±2.4	48.9±0.1	49.9±1.4	62.7±1.1	57.6±1.6	66±0.8	64.1±0.8	69.7±0.9	65.3±1.5	60.8±0.6	65.3±0.9
ΣMUFA	32.7±1.3	38.3±1.2	33.9±1.2	36.3±0.9	32.3±0.2	37.1±1.2	30.1±0.2	29.5±0.5	25.7±0.5	28.5±0.2	30.4±0.3	29.4±0
ΣPUFA	9.3±1.5	14±3.6	17.3±1.3	13.7±0.5	5±0.9	5.3±0.6	3.9±0.6	6.4±0.2	4.7±0.4	6.2±1.3	8.8±0.3	5.3±0.9
ΣUND	1.1±0.2	2±0.4	2.2±0.1	1.9±0.3	0.7±0	1±0.4	0.6±0.1	0.8±0.1	0.6±0	0.7±0.1	1±0.2	0.7±0.1
ΣDETRITAL	7.9±0.4	8±0.1	6±0.1	7.3±0.2	8.5±0.4	8.2±1.3	9±0.4	9.1±0.3	9.6±0.2	8±0.3	6.6±0.2	7.2±0.2
C16:1/C16:0	0.4±0.1	0.7±0	0.5±0	0.5±0	0.4±0.1	0.3±0	0.3±0	0.3±0	0.3±0	0.3±0	0.4±0	0.3±0
DHA/EPA	0.8±0.1	0.9±0.1	0.7±0	0.7±0	0.5±0	0.8±0	0.7±0.1	0.9±0.3	0.5±0.1	0.5±0	0.7±0.1	0.5±0

Table S6. Similarity percentage analysis (SIMPER) identifying those FA profiles which contribute the most in differentiating SPM and Sed from Pag and Cetina.

SPM - Pag vs Cetina			Sed - Pag vs Cetina		
FA	Cont (%)	Cum (%)	FA	Cont (%)	Cum (%)
C16:1	14.94	14.94	C18:2 (n-6)	19.56	19.56
C18:2 (n-6)	13.52	28.46	PUFA	19.11	38.67
PUFA	12.44	40.90	C16:1	15.80	54.46
C20:5 (n-3) EPA	11.22	52.12	MUFA	12.52	66.99
C22:6 (n-3) DHA	9.69	61.81	DETRITAL	11.78	78.77
DETRITAL	9.31	71.11	C16:0	8.93	87.70
MUFA	8.24	79.35	UND	5.05	92.75
C20:4 (n-6) ARA	6.64	85.99	SFA	4.59	97.34
C16:0	4.52	90.50	C16:1/C16:0	2.66	100.00
UND	4.00	94.50			
C16:1/C16:0	3.11	97.60			
SFA	2.40	100.00			

Table S7. Similarity percentage analysis (SIMPER) identifying those FA profiles which contribute the most in differentiating the diet of *Callista chione* from Pag and Cetina (PC-CC), *Glycymeris bimaculata* from Pag and Cetina (PG-CG), between both species in Pag (PG-PC) and in Cetina (CG-CC).

PC-CC			PG-CG			PG-PC			CG-CC		
FA	Cont (%)	Cum (%)	FA	Cont (%)	Cum (%)	FA	Cont (%)	Cum (%)	FA	Cont (%)	Cum (%)
C20:5	18.21	18.21	PUFA	17.86	17.86	PUFA	18.08	18.08	PUFA	14.99	14.99
C22:6	17.46	35.67	C20:5	14.22	32.08	C20:5	14.38	32.46	C20:5	14.97	29.96
PUFA	15.75	51.42	C22:6	14.18	46.26	C22:6	13.67	46.13	C22:6	14.38	44.34
UND	8.40	59.82	UND	7.08	53.33	C16:1	8.49	54.62	C16:1	9.73	54.07
C18:2	6.63	66.45	C18:2	7.07	60.40	UND	8.07	62.69	UND	7.30	61.37
DETRITAL	5.79	72.24	C16:1	7.06	67.46	MUFA	6.24	68.92	MUFA	6.73	68.10
C20:4	4.94	77.18	MUFA	6.90	74.37	C18:2	5.62	74.55	C18:2	6.67	74.77
C16:1	4.44	81.63	DHA/EPA	6.77	81.13	DETRITAL	4.89	79.44	DHA/EPA	5.86	80.63
DHA/EPA	4.44	86.06	C20:4	4.84	85.97	DHA/EPA	4.56	84.00	C20:4	4.43	85.06
C16:0	4.09	90.16	DETRITAL	4.05	90.02	SFA	4.55	88.54	SFA	4.25	89.30
SFA	4.03	94.18	C16:0	3.97	93.98	C20:4	4.33	92.87	C16:0	3.91	93.22
MUFA	3.49	97.68	SFA	3.92	97.90	C16:0	4.21	97.08	DETRITAL	3.80	97.01
C16:1/C16:0	2.32	100.00	C16:1/C16:0	2.10	100.00	C16:1/C16:0	2.92	100.00	C16:1/C16:0	2.99	100.00

Fig S1. Chlorophyll *a* extracted from satellite data from the MODIS-Aqua sensor provided by the EU Copernicus Marine Service (CMEMS). Color bar represents concentration in mg/g

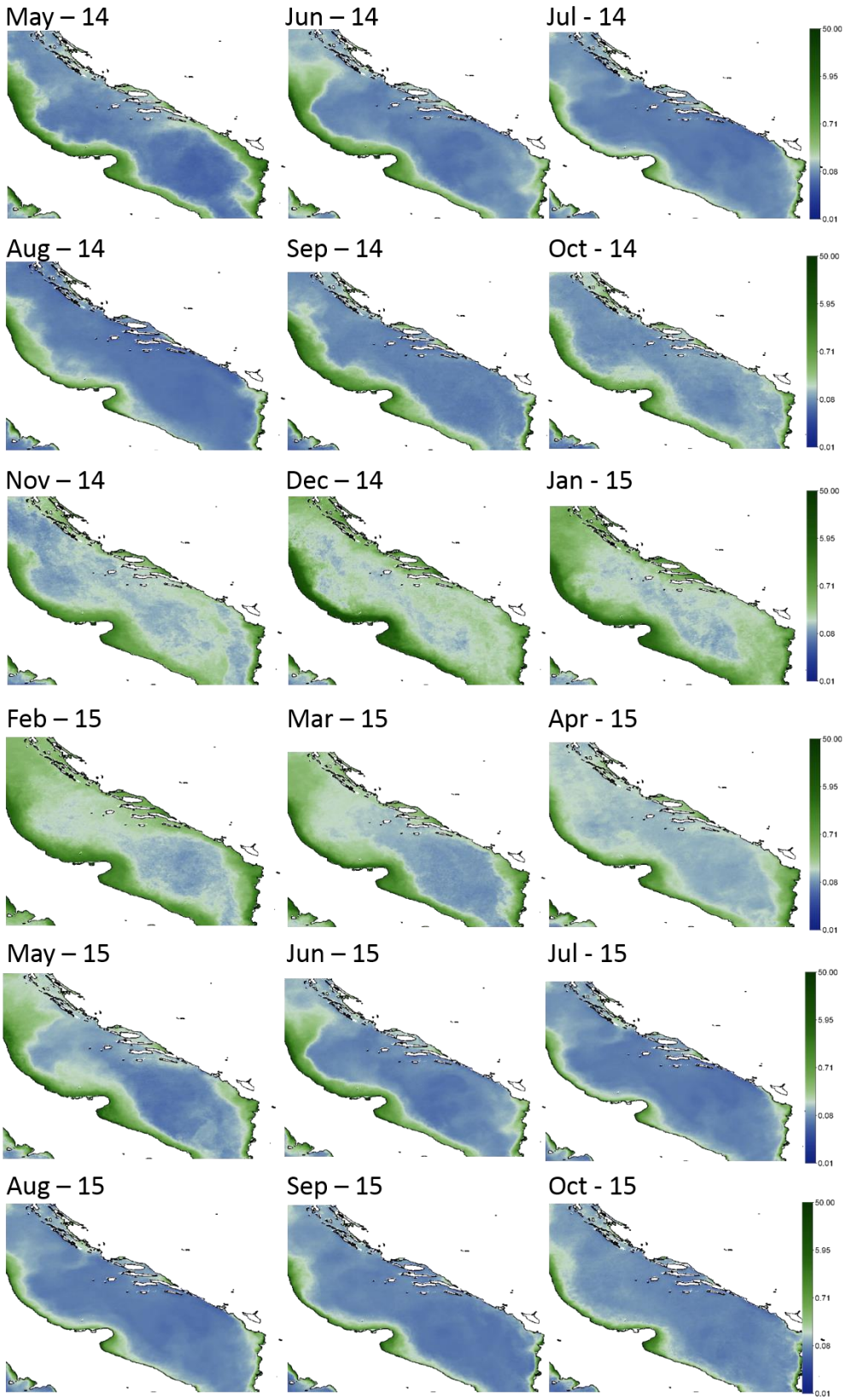

9. PROŠIRENI SAŽETAK

UVOD

Morski školjkaši nastanjuju litoralne obale i često žive u velikim agregacijama koje imaju važnu ulogu u ekosustavu sudjelujući u stvaranju, modificiranju i održavanju okolnog staništa (Jones i sur., 1994; Dame, 1996). S obzirom na njihovu široku geografsku i batimetrijsku raspodjelu, školjkaši mogu podnositi širok spektar okolišnih uvjeta koji reguliraju osobine životnog ciklusa (Gosling, 2015), što doprinosi zanimanju znanstvenika za njihovu primjenu u paleoklimatskim istraživanjima. Ljušture školjkaša ugrađuju informacije tijekom rasta što ih čini vrijednim arhivima ekoloških, bioloških i evolucijskih podataka (Richardson, 2001). Stoga, ljušture školjkaša mogu otkriti vrijedne podatke značajne za rekonstrukciju okolišnih varijacija i osobina životnog ciklusa od polarnih do tropskih staništa, te od slatkovodnih do morskih ekosustava (Goodwin i sur., 2001).

Posljednjih godina, brzo se razvijaju sklerokronološka istraživanja školjkaša, s ciljem da se istraže međugodišnje varijacije u rastu, kao i varijacije u geokemijskom sastavu ljuštura (Schöne i Gillikin, 2013). Ljušture mekušaca su prepoznate kao koristan arhiv podataka o okolišu u rasponu od nekoliko godina do tisućljeća (Schöne i sur., 2005; Butler i sur., 2010; Reynolds i sur., 2013). Školjkaši čuvaju zapise visoke rezolucije o okolišnim uvjetima i osobine životnog ciklusa u prstenovima prirasta svoje ljušture (Schöne i sur., 2005), a omjeri izotopa kisika ($\delta^{18}O$) u karbonatima ljušture mogu otkriti da li su razlike u godišnjoj stopi kalcifikacije kontrolirane egzogenim i endogenim čimbenicima (Gosling, 2015). Temperatura je ključni parametar pri proučavanju rasta ljuštura školjkaša, a detaljne studije su čak mogle odrediti i polu-dnevne obrasce rasta u nekim organizmima (prikaz u Schöne i Surge, 2012). Važnost svakog od čimbenika (primjerice temperature, saliniteta, gustoće fitoplanktona, cikličkih procesa, dobi i biološkog sata), u kontroli brzine i sezonalnosti rasta, varira među vrstama i prema latitudalnim gradijentima (Richardson, 2001). Upravo je kombinacija temperature, dostupnosti i kvalitete hrane, ona koja obično kontrolira unutar godišnji rast ljušture (Ansell, 1968; Witbaard, 1997; Ambrose i sur., 2012; Vihtakari i sur., 2016; Kubota i sur., 2017) iako je vjerojatno da će kombinacija različitih čimbenika rasta biti specifična za vrstu (Jones, 1980; Nishida i sur., 2012).

Isto tako, vrijeme i trajanje fizioloških procesa poput reproduktivnog ciklusa, mogu varirati i prostorno i vremenski, čak i unutar vrste (Cardoso i sur., 2007; Santos i sur., 2011; Verdelhos i sur., 2011; Magalhães i sur., 2016). To je rezultat složenih interakcija između egzogenih i endogenih čimbenika od kojih su okolišne varijable, npr. temperatura i opskrba hranom, glavni regulatori koji pokreću gametogenezu i mriještenje (Sastry 1979; MacDonald i Thompson 1986; Sebens 1987; De Montaudouin 1996; Honkoop i Beukema 1997; Philippart i sur., 2003; Drent 2004; Carmichael i sur. 2004; Sokolova i sur. 2012).

Da li je raspodjela energije uravnotežena ili usmjerena više na reprodukciju ili rast, može biti svojstveno vrsti i može ovisiti o latitudalnom gradijentu na kojem te vrste žive i izložene su varirajućim temperaturama ili dostupnosti hrane (npr. Cardoso i sur. 2007). Stoga je potrebno utvrditi prirodu okolišnih i fizioloških čimbenika koji potiču rast ljušture za većinu vrsta školjkaša. Studije o ekologiji i karakterizaciji osobina životnog ciklusa školjkaša čine osnovni korak za interpretaciju obrazaca rasta ljušture prije uporabe školjkaša kao ciljane skupine organizama za paleoklimatološke studije i studije starenja.

Početak sklerokronoloških istraživanja školjkaša u Sredozemlju zahtijeva identifikaciju ciljanih vrsta koje se mogu koristiti kao arhivi u paleoekologiji. Za ekološke interpretacije pri provođenju okolišnih rekonstrukcija na temelju obrazaca mikro-rasta ljušture, treba razumjeti osobine životnog ciklusa istraživane vrsta. Kombinacija detaljnih studija o okolišnim i biološkim čimbenicima, koji vode rastu ljušture, se rijetko primjenjuje, a to je izuzetno moćan alat za otkrivanje prisutnih promjena i testiranje ranijih evolucijskih hipoteza. Okolišni podatci visoke razlučivosti doprinose razumijevanju fizioloških procesa i drugih osobina životnog ciklusa, biogeografske rasprostranjenosti vrsta i učinkovitom upravljanju resursima ribarstva. Na temelju toga, ovaj rad analizira kombinirane učinke temperature mora, dostupnosti hrane, razmnožavanja i rasta, kod školjkaša iz Jadranskog mora.

Obrazloženje i ciljevi

Procjena promjena u morskom okolišu, uključujući promjene u bentosu, preduvijet je za implementaciju mjera zaštite okoliša od klimatskih promjena (IPCC 2001; IPCC 2007; IPCC 2014). Razumijevanje otiska okoliša na ljušturama školjkaša je od vitalnog značaja za bolje razumijevanje procesa koji su odgovorni za te promjene, kao i za predviđanje potencijalnih poremećaja na morskim organizmima i ekosustavima koje održavaju. U posljednjih nekoliko godina, sve veći broj sklerokronoloških istraživanja školjkaša pokušava rekonstruirati klimu u sjevernom Atlantiku kako bi se predvidjeli budući scenariji. Međutim, u drugim dijelovima svijeta, uključujući i Sredozemno more, poznavanje bioloških i ekološkim čimbenika koji utječu na rast ljuštura još je prilično ograničeno. Rekonstrukcija životnih ciklusa ciljanih vrsta na lokalnoj razini je iznimno utjecajna u smislu pokazivanja sposobnosti prilagodbe školjkaša na povoljne i nepovoljne uvjete, te će pružiti korisne informacije pri rekonstrukciji prijašnjih uvjeta. Interni obrasci rasta ljuštura će se vremenski kontekstualizirati kako bi se procijenilo što kontrolira unutar godišnje promjene u polaganju ljušturnog materijala. Cilj ovog rada je procijeniti ekološke i biološke čimbenike formiranja ljušture analizirajući: (1) varijable okoliša te, (2) razmnožavanje, (3) ekologiju ishrane i (4) rast ljuštura ciljanih vrsta školjkaša. Tri ciljane vrste su odabrane na temelju njihove brojnosti, relativno dugog životnog ciklusa i ekološke uloge u Jadranu, Sredozemnom moru i Atlantiku: *Callista chione*

(Linnaeus, 1758), gospodarski važna vrsta te dvije relativno dugoživuće vrste iz roda *Glycymeris*, *G. bimaculata* (Poli, 1795) i *G. pilosa* (Linnaeus, 1767). Uzorkovanje je provedeno na tri lokacije na istočnoj Jadranskoj obali, uključujući Paški zaljev, ušće rijeke Cetine i Pašmanski kanal s ciljem da se objasne biološke varijacije unutar i između i vrsta u različitim staništima. Ciljevi rada su:

- Analiza bentoske-pelagijske sprege u plitkim vodama srednjeg Jadrana kroz karakterizaciju lebdećih mikročestica (SPM) i sedimenta (Sed) na mjestima uzorkovanja
- Opis ciklusa razmnožavanja istraživanih vrsta primjenjujući dva metodološka pristupa: histološku analizu i analizu gonadosomatskog indeksa
- Opis indeksa tjelesne mase, reproduktivnog ulaganja, reproduktivnog rezultata i fekunditeta vrste *C. chione* uključujući usporedbu između dvije istraživane lokacije
- Procjena utjecaja okolišnih varijabli (tj. temperature) i opskrbe hranom na ciklus razmnožavanja
- Opis prostorno-vremenskih varijacija u ekologiji ishrane vrsta *Glycymeris sp*. i *C. chione* kroz kombiniranu primjenu analize stabilnih izotopa, masnih kiselina i drugih biomarkera (C:N omjer, Chl *a*, BSi)
- Procjena prehrambenih niša istraživanih vrsta školjkaša analizom izotopa i masnih kiselina primjenom modela miješanja dvaju izvora
- Opis mikro-obrazaca rasta ljušture primjenom sklerokemijskih metoda: mikro-mljevenje s vanjske površine ljušture vrste *C. chione* te mikro-mljevenje ljušturnog materijala iz poprečnih presjeka vrste *G. bimaculata*
- Međusobno povezivanje okolišnih i bioloških čimbenika i njihovih utjecaja na brzinu i sezonalnost rasta ljušture
- Utvrđivanje jesu li obrasci karakteristični za određenu vrstu ili određeno stanište

MATERIJAL I METODE

Područje istraživanja

Tri lokaliteta u istočnom dijelu srednjeg Jadrana, uključujući Paški zaljev, ušće rijeke Cetine i Pašmanski kanal, su izabrani na osnovu njihovih različitih okolišnih značajki i razlika u rastu školjkaša zabilježenih u ranijim istraživanjima (Ezgeta-Balić i sur. 2011). Sve lokacije su plitka obalna mjesta i uzorci su prikupljeni na dubinama u rasponu od 1 do 5 m.

Varijable okoliša

Temperatura mora je mjerena svaki sat putem *data logger*-a (*Tinytag, Gemini®*) razmještenih na svakoj lokaciji. Podaci o salinitetu zabilježeni su jednom mjesečno *in situ* sondom *YSB*. Mjesečni podaci o oborinama za meteorološke stanice Pag, Cetina (Split) i Pašman (Biograd) dobivene su iz Državnog hidrometeorološkog zavoda Republike Hrvatske.

Uzorci mora su prikupljeni ~ 0,5 m iznad morskog dna metodom autonomnog ronjenja i ronjenja na dah koristeći *Niskin* crpac (između 10 – 20 L). Prethodno izvagani nitrocelulozni filteri su korišteni za mjerenje lebdećih mikročestica (*SPM*) i biogenih sadržaja silicija (*BSi*), dok su prethodno paljeni (450°C, 6 h) i prethodno izvagani filteri od staklenih vlakana korišteni za mjerenje elementarnog sastava i omjera % C i % N, te njihovog izotopnog sastava ($\delta^{13}C$ i $\delta^{15}N$), masnih kiselina (FA) i koncentracija lipida. Koncentracija SPM je utvrđena na suhoj tvari ukupnih lebdećih čestica preostalih po jedinici volumena nakon sušenja (60°C, 24 h) (izraženo u mg/L). *SPM* filteri su također korišteni za analizu sadržaja *BSi* nakon sekvencijalne lužnate razgradnje (2 do 5 h) s $NaCO_3$ za razlikovanje silicija litogenog i biogenog porijekla (Mortlock i Froelich 1989; DeMaster 1991) Klorofil *a* je ekstrahiran u 90%-tnom acetonu (Strickland i Parsons 1972) i izmjeren u fluorometru *Turner Systems* (*Sunnyvale, CA*) / (*Trilogy)*. Sve kemijske analize su provedene na tri replike. Satelitski dobiveni podatci za klorofil *a* su izdvojeni iz senzora *MODIS-Aqua* od strane *EU Copernicus Marine Service (CMEMS)*.

Uzorci površine sedimenta (otprilike gornja 2 cm) (*Sed*) su prikupljeni mjesečno metodom autonomnog ronjenja pomoću plastičnog korera i pohranjeni na -20°C. Homogenizirani i samljeveni uzorci su korišteni za analize %C, %N i SI, uzorci klorofila *a* su ekstrahirani u 90%-tnom acetonu (4°C, 12 h) (Lorenzen i Jeffrey 1978), sadržaj *Bsi* mjeren je prema postupku za *SPM*, a ukupan ugljik (*TC*) je mjeren u analizatoru *LECO Truspec CN 2000*. Anorganski ugljik (*IC*) (izraženo u % suhe mase) je izračunat pomoću razlike između sadržaja *TC* i *OC*. Veličina zrna je određena u *HORIBA LA950V2* laserskom analizatoru raspodjele mikročestica nakon uklanjanja organske tvari u 20%-tnoj otopini vodikovog peroksida.

Ekologija ishrane

Elementarni i izotopni sadržaji partikularnog organskog ugljika i dušika mjereni su iz filtera sušenih na 50°C tijekom 24 sata, 50 mg za uzorak sedimenta (*Sed*) i 1 mg za uzorak digestivne žljezde (*DG*). Uzorci su liofilizirani i individualno homogenizirani koristeći ahatni mužar i tučak. Analize omjera stabilnih izotopa ugljika ($^{13}C/^{12}C$) i dušika ($^{15}N/^{14}N$), te elementarnih %C i %N, su provedene na analizatoru *Carlo Erba Elemental Analyzer EA1108* zajedno s masenim spektometrom *ThermoFinnigan MAT253* u Unidade de Técnicas Instrumentais de Investigación, Sveučilišta u A Coruña (Španjolska).

Model izotopnog miješanja dvaju izvora se izradio u paketu *MixSIAR*, grafičkom korisničkom sučelju (GUI) izrađenom na R softveru (Parnell i sur. 2010), koji koristi algoritam baziran na *Bayesian* statistici za određivanje raspodjele vjerojatnosti za proporcionalni doprinos izvora hrane kombiniranoj ishrani potrošača (Semmens i sur. 2013). Ovaj model objašnjava nesigurnost u vrijednostima izotopa pri procjeni doprinosa izvora u ishrani zbog razlike u ugradnji s obzirom na različita tkiva. Metoda *The Stable Isotope Bayesian Ellipses in R* (paket *SIBER*) se koristila za istraživanje niša izotopa proučavajući disperziju vrijednosti $\delta^{13}C$ i $\delta^{15}N$.

Za analize masnih kiselina (*FAs*), *SPM, Sed* i *DG* uzorci su prikupljeni u razdoblju od jedne godine i liofilizirani prije biokemijskih analiza. Za potpunu analizu lipida svi uzorci su vagani (*DG* uzorci su pomiješani), a kasnije je dodana smjesa (2:1) diklormetan-metanol (DCM: MeOH) izložena ultrazvučnom tretmanu u vodenoj kupelji na 30°C. Nakon odvajanja DCM faze su skupljene i osušene, te izvagane. Ukupni lipidi probavnih žlijezda su ponovno otopljeni u DCM-u, a neutralni lipidi su razdvojeni prema Pernet i suradnicima (2012). Svi ekstrakti (ukupni lipidi iz SPM i Sed i neutralni lipidi u DG) su saponificirani (1,2 M NaOH), zakiseljeni (6M HCl) i metilirani (14% BF3 u metanolu), a zatim ekstrahirani u DCM-u. Metil esteri masnih kiselina (*FAME*-ovi) su analizirani plinsko-tekućinskom kromatografijom *Agilent* (*GLC*), 6890 N GC sustavom opremljenim detektorom *5973 Network Mass Selective*, kapilarnom kolonom (25m x 0.3 mm x 0,25 µm, cross-linked 5% fenilmetilsiloksan) i helijem ultra visoke čistoće kao nosećim plinom. *FAs* su navedeni u postotcima ukupnih masnih kiselina (% TFA, srednja vrijednost ± SD) i grupirani kao *zasićene (SFA), mononezasićene (MUFA), PUFA i* detritične *masne kiseline* (*DETRITAL* 15:0 + 15iso + 15anteiso + 17:0 + 17iso + 17anteiso + 18.1(n-7); (Mayzaud i sur. 1989; Najdek i sur. 2002). Stupanj nezasićenosti (*UND*) izračunat je prema Pirini i suradnicima (2007).

Razmnožavanje: Histologija. U roku od tri sata od prikupljanja, školjkaši su otvoreni, komadić tkiva gonada seciran, fiksiran u 4% formaldehidu i pohranjen za kasniju laboratorijsku analizu. Obrada tkiva je provedena u laboratoriju dehidracijom u rastućim koncentracijama etanola (70%, 80%, 96% i 100%) i čišćenjem s *Bioclear*-om. Potom su uzorci tkiva uronjeni u parafin (*Histowax, Leica*), prerezani na mikrotomu (5 µm) i obojeni hematoksilinom i eozinom. Histološki preparati su ispitani pri 100x i 400x povećanju pomoću mikroskopa *Zeiss Axio Lab.A1*, određen je spol jedinki i faza razvoja gonada. Faze su opisane kao rana aktivna (3), kasnija faza razvoja (4), zrela faza (5), faza mriještenja (2) i neaktivna faza (1).

Srednji gonadni indeks (*MGI*) je izračunat zasebno za muške i ženske jedinke množenjem broja jedinki iz svake razvojne faze po numeričkom poretku dodijeljenom toj fazi i dijeleći ga s ukupnim brojem jedinki u pojedinom mjesecu uzorkovanja.

Histološka analiza vrste *Callista chione* je provedena na oko 20 jedinki mjesečno po lokalitetu prikupljenih u razdoblju od srpnja 2014. do srpnja 2015. godine. Uzorci vrste *Glycymeris bimaculata* su prikupljeni u razdoblju od srpnja 2014. do kolovoza 2015. Sakupljanje 20 jedinki mjesečno je provedeno i na Pagu i Cetini. Uzorci *vrste Glycymeris pilosa* su prikupljeni u razdoblju od rujna 2014. do kolovoza 2015. godine samo na lokaciji u Pašmanskom kanalu. Ova je vrsta bila vrlo rijetka na drugim lokacijama uzorkovanja, a Pašman je odabran kao mjesto s dovoljnim brojem dostupnih uzoraka za ovu analizu.

Razmnožavanje: Gonadosomatski indeks. Školjkaši (~ 20 mjesečno) su otvoreni i gonade su pažljivo odvojene od somatskog tkiva, te su oba dijela tkiva smještena u odvojene, prethodno izvagane porculanske posude. Uzorci su osušeni u pećnici na 60°C tijekom 48 sati i izvagani da se dobije indeks somatske mase *(SMI)* i indeks gonadne mase *(GMI)*. Ti indeksi su izračunati kao suha težina svakog dijela (somatski i gonadni) te podijeljena kubičnim dimezijama ljušture izražene u mg/cm^3. Da bi se odredilo relativno ulaganje u razmnožavanje, gonadosomatski indeks *(GSI)* je izračunat kao gonadna suha masa (*g*) podijeljena suhom masom cijelog tijela (*g*). Nadalje, indeks tjelesne mase (*BMI*), koji se određuje kao zbroj *SMI* i *GMI,* korišten je kao mjera indeksa tjelesnog stanja. Reproduktivni učinak je analiziran kao postotak gameta pušten u okoliš i plodnosti kao razlike u gonadnoj masi prije i poslije mriještenja, pokazujući moguće sposobnosti organizma da proizvodi reproduktivne jedinke.

Analiza *GSI* indeksa vrste *Callista chione* je provedena za uzorke prikupljene na Pagu i Cetini, dok je za vrstu *Glycymeris bimaculata* analiza GSI indeksa povedena samo za uzorke prikupljene na Pagu, zbog manje populacije ove vrste na području ušća rijeke Cetine.

Rast

Površinsko mikro-mljevenje ljuštura vrste *C. chione* te mikro-mljevenje ljušturnog materijala iz poprečnog presjeka ljuštura vrste *G. bimaculata* prikupljenih na području Paškog zaljeva i ušća rijeke Cetine primjenjeno je za prikupljanje uzoraka za analizu obrazaca mikro-rasta. Uzorci su prikupljeni prateći os maksimalnog rasta od ruba do mjesta rasta posljednje dvije godine. Koristila se bušilica *Dremell® Fortiflex* opremljena svrdlom od 0,3 mm (*C. chione*) i 1 mm (*G. bimaculata*) cilindričnog, dijamantom obloženog vrha zajedno sa stereomikroskopom opremljenim s dvostrukim reflektorskim glavnim osvjetljenjem (*Olympus Europa Highlight 3100*). Za prikupljanje dovoljno uzorka (od 50 do 120 µm), male plitke linije su mikro-mljevene usporedo s rubom ljušture.

Uzorci karbonata u prahu tretirani su 100%-tnom fosfornom kiselinom u borosilikatnim ampulicama ispranim helijem na 72°C. Spektrometar *GasBench II-coupled Thermo Finnigan MAT 253* u kontinuiranom modu je mjerio rezultirajući CO_2. Te analize su provedene na Institutu za geoznanosti Sveučilišta u Mainzu (Njemačka).

Uzorci morske vode za analizu stabilnih izotopa ($\delta^{18}O_{water}$) su prikupljeni na različitim mjestima unutar raspona gradijenta saliniteta od slatkovodnih (dobiveni iz estuarijskih i podmorskih izvora) do područja otvorenog mora. Odnos slanost-izotop kisika (linija miješanja) je obilježen svim mjerenjima omogućujući procjenu svojstava morske vode tijekom razdoblja uzorkovanja kako bi se dodijelila bolja procjena $\delta^{18}O_{water}$. Za rekonstrukciju temperature primjenila se paleotermometrijska jednadžba Grossman i Ku (1986.), s korekcijom od -0.27 ‰ (Dettman i sur., 1999.) koja se uobičajeno koristi kod aragonitnih ljuštura.

Nadalje, drugi tanki presjek ljušture svakog uzorka vrste *G. bimaculata* korišten za analizu starosti jedinke. Uzorci su uronjeni oko 20-40 minuta uz stalno miješanje u Mutvei-otopinu prema porotokolu Schöne i suradnika (2005). Nakon bojenja, presjeci su fotografirani digitalnim fotoaparatom *Canon EOS 550D* pričvršćenim na stereomikroskop *Wild Heerbrugg M8* opremljen dvostrukim reflektornim glavnim osvjetljenjem (*Schott VisiLED MC 1000*).

Za procjenu metaboličkog ugljika (C_M) uzorci vode su mjereni tijekom 4 mjeseca za dobivanje $\delta^{13}C_{DIC}$. Uzorci vode su prikupljeni u staklenim bočicama i 200 µl otopine $CuSO_4$ (osnovna otopina 25,6 g $CuSO_4$ * $5H_2O$ 100 mL^{-1}) je ubrizgano kako bi se spriječila biološka aktivnost prema Taipale i Sonninen (2009).

Statistička analiza

Statističke pretpostavke normalnosti (Shapiro test) i homogenost varianci (Levenov test) potvrđene su prije svih ANOVA analiza. Dvosmjerne ANOVA-e su primjenjene za testiranje utjecaja lokacije (2 razine) i mjeseca (17 razina) u izvorima hrane i potrošačima. Preklapanje izotopnih niša je testirano *SIBER* i *SIAR* paketima u *R* (Parnell i sur. 2010; Jackson i sur. 2011). *ANOSIM, SIMPER, PCA* i *nMDS* su korišteni za analiz masnih kiselina kako bi se predočile vremenske razlike u izvorima hrane i potrošačima.

Pearsonov koeficijent korelacije, hi-kvadrat test, dvosmjerne analize *ANOVA* i *ANCOVA* primjenjeni su za testiranje raznih parametara uključujući spol i duljinu ljušture između lokacija i kroz vrijeme.

Apsolutne stope rasta su određene kako bi se uklonili ontogenetski trendovi rasta za svaki uzorak (1) izračunavanjem metodom najmanjih kvadrata u ravnoj liniji prema svakom pojedinom skupu podataka i (2) dijeljenjem izmjerenih vrijednosti s predviđenim udaljenostima rasta ljušture od rezultirajuće funkcije, što je omogućilo usporedive stope rasta između različitih veličina jedinki. Pearsonove korelacije su izmjerene između vrijednosti $\delta^{13}C_{shell}$ i $\delta^{18}O_{shell.}$

Sve analize su povedene u *R v3.1.3* (Jackson i sur. 2011; R Core Team 2015) i *PAST 3.0* statističkim paketima (Hammer i sur. 2001).

REZULTATI

Okolišne varijable. Prosječne mjesečne vrijednosti temperature su pokazale jasan sezonski trend na svim lokacijama s rasponima od 8,9 do 25,1°C na Pagu, 12,7-26,4°C na ušću rijeke Cetine i 10,7-24,9°C na Pašmanu. Minimalne zabilježene temperature su bile 7,4, 10,9 i 6,1°C, a maksimalne one od 28,6, 28,6 i 28,3°C na Pagu, Cetini i Pašmanu, respektivno. Mjesečni rasponi saliniteta su oscilirali od 34,7 do 38,3 na Pagu, 32,2 do 38,5 u ušću rijeke Cetine i 36,8 do 38,3 na Pašmanu. Najviši mjesečni prosjek oborina zabilježen je na Pagu s 111,1 ± 86,0 mm/cm^3, a slijede Pašman 92,4 ± 78,3 mm/cm^3 i Cetina 85,4 ± 55,5 mm/cm^3.

Trofička ekologija dvije populacije vrsta *C. chione* i *G. bimaculata*

Izvori hrane. Koncentracije *SPM* su imale srednje vrijednosti od 1,02 ± 0,33 mg/L na Pagu i 0,92 ± 0,35 mg/L na Cetini i nisu se značajno razlikovale ($P > 0,05$) između lokacija. Vremenska varijacija Chl a_{SPM} je također bila slična na lokacijama ($P > 0,05$), i kretala se u rasponu od 0,2 do 0,6 µg/L na Pagu i 0,2-0,7 µg/L na Cetini. Uočene su značajne razlike u Chl a_{Sed} između lokacija ($P < 0,001$), s rasponima od 0,4 do 5,0 µg/g na Pagu i 1,1 do 11,8 µg/g na Cetini. Godišnji obrasci Chl a_{SPM} i Chl a_{Sed} su bili u značajnoj korelaciji u Cetini ($r = 0,49$, $P < 0,05$), ali ne i na Pagu ($r = 0,15$, $P > 0,05$), što ukazuje na učinkovitiju pelagijsko-bentosku vezu u Cetini. Koncentracija BSi_{SPM} je pokazala veliku vremensku varijabilnost u rasponu od 0,03 do 0,2 mg/L na Pagu i od 0,02 do 0,2 mg/L na Cetini, bez značajnih razlika između lokacija. Koncentracije BSi_{Sed} su bile u rasponu od 0,06 do 0,2% na Pagu i 0,1 do 0,3% na Cetini i pokazale su značajne razlike između lokacija (t-test, $P < 0,05$). BSi_{SPM} i BSi_{Sed} su bili povezani tijekom većeg dijela trajanja istraživanja.

Veličina zrna sedimenta je bila relativno konstantna s visokim sadržajem pijeska i šljunka, te niskog sadržaja mulja i gline (fini sediment), što je iznosilo <2%. Pijesak (2mm-63µm) je predstavljao veći dio u Cetini (87%) nego na Pagu (74%), dok je šljunka (> 2mm) bilo obilnije na Pagu (26% vs 11%).

Stabilni izotopi. U uzorcima stupca vode izotopna vremenska varijacija je bila u rasponu od -25,56 do -23,37 ‰ za $\delta^{13}C_{SPM}$ i 1,63-6,09 ‰ za $\delta^{15}N_{SPM}$ na Pagu i od -26,19 te -22,82 ‰ za $\delta^{13}C_{SPM}$ i 0,03-5,64 ‰ za $\delta^{15}N_{SPM}$ u Cetini. Obogaćenije izotopne vrijednosti zabilježene su tijekom ljeta i jeseni na obje lokacije. U sedimentu, izotopne vremenske varijacije su bile u rasponu od -22,74 do -22,0 ‰ za $\delta^{13}C_{Sed}$ i -2,26 do 3,92 ‰ za $\delta^{15}N_{Sed}$ na Pagu, a od -26,74 do 26,48 ‰ za $\delta^{13}C_{Sed}$ i 1,05-3,30 ‰ za $\delta^{15}N_{Sed}$ u Cetini. Nije bilo evidentnog godišnjeg trenda u molarnim omjerima C: N_{SPM} na bilo kojoj lokaciji, zabilježene vrijednosti su bile u rasponu od 7,3 do 10,6 na Pagu i od 6,9 do 11,2 na Cetini. Molarni omjeri C: N_{Sed} na Pagu su varirali od 5,2 do 21,19 dok su na Cetini bili od 6,2 do 9,7. Na Pagu su visoke vrijednosti zabilježene od proljeća do sredine ljeta.

Masne kiseline. Zabilježene su veće proporcije zasićenih masnih kiselina (*SFA*) s višim *TFA*% tijekom jeseni u uzorcima probavne žljezde školjkaša, vodenog stupca i sedimenta, te u probavnoj žljezdi također tijekom zime. Najniže vrijednosti *SFA* su zabilježene tijekom ljeta, kada je *PUFA* bila obilnija. Visoke vrijednosti *PUFA* i drugi pokazatelji svježeg materijala (*EFA*-ovi) u ljeto, a kasnije i proljeće, sugerirali su da su to razdoblja najviše kvalitete hrane u vodenom stupcu.

Koncentracija $lipids_{SPM}$ je bila u rasponu od 0,16 do 0,71 mg/L na Pagu i od 0,13 do 0,3 mg/L na Cetini prema sličnom vremenskom obrascu, s najnižom koncentracijom između kolovoza i listopada. U $lipids_{Sed}$ vrijednosti su se kretale od 0,36 do 1,20 mg / g na Pagu i 0,59 1,72 mg/g na Cetini i te su bile jedan red magnitude više od $lipids_{SPM}$.

Potrošači. *Stabilni izotopi*. Varijacija $\delta^{13}C_{DG}$ bila je ovisna o vrsti, s vrijednostima nešto više osiromašenim s ^{13}C u vrsti *C. chione*. Naprotiv, varijacija u $\delta^{15}N_{DG}$ je bila ovisna o lokalitetu, s vrijednostima više obogaćenim s ^{15}N u Cetini. Uočen je blagi vremenski pomak između $\delta^{13}C_{SPM}$ i $\delta^{13}C_{DG}$, gdje je varijacija u $\delta^{13}C_{DG}$ slijedila onaj $\delta^{13}C_{SPM}$ tjednima kasnije. Molarni omjer $C:N_{DG}$ je pokazao značajne razlike između lokacija, mjeseca i njihove interakcije za vrstu *C. chione* ($P < 0,001$), ali oni su bili manje vidljivi za vrstu *G. bimaculata* ($P > 0,001$).

Udio svakog izvora hrane u ishrani potrošača prema modelima *MixSIAR* je pokazao da su školjkaši koristili oba *SPM* i *Sed*, međutim, njegova relativna važnost se razlikovala među lokacijama. *Sed* kao izvor hrane je bio važniji za školjkaše s Paga, a tijekom ljeta mali udio činio je i *SPM*, dok je školjkašima s ušća Cetine SPM bio taj koji je najviše doprinosio njihovoj prehrani.

Masne kiseline. Na Pagu su vrijednosti *MUFA, PUFA, C18: 2, EPA, DHA, UND* i *C16:1* bile najviše u ljeto, osobito za vrstu *C. chione*. Detritusne masne kiseline su bile obilnije za vrijeme jeseni i zime, iako prisutne tijekom cijele godine. U Cetini je uočen sličan vremenski trend, a obje vrste školjkaša pokazale su više vrijednosti *MUFA, PUFA, C18:2, EPA, DHA* i *UND* tijekom ljeta i proljeća. Ljeto je sezona kada je gustoća detritusa bila najniža za razliku od jeseni i zime, dok je *C18:2 (n-6)* bila najobilnija tijekom proljeća i ljeta. Koncentracija lipida u digestivnoj žljezdi kretala se od 188,34 do 335,39 mg/g u uzorcima *C. chione* iz Paga, od 189,59 do 363,90 mg/g u uzorcima *C. chione* iz Cetine, od 130,53 do 255,36 mg/g u uzorcima *G. bimaculata* iz Paga i od 125,07 do 201,78 mg/g u uzorcima *G. bimaculata* iz Cetine.

Trofička ekologija dvije populacije vrste *G. pilosa*

Izvori hrane. Srednja koncentracija *SPM* je bila niža na Pašmanu (0,81 ± 0,31 mg/L) nego na Pagu (1,02 ± 0,33 mg/L). Vrijednosti $Chl\ a_{SPM}$ su bile u rasponu od 0,2 do 0,7 µg/L na Pašmanu i 0,2 do 0,6 µ/L na Pagu. Koncentracija BSi_{SPM} je također pokazala visoku vremensku varijabilnost na Pašmanu, u rasponu

od 0,04 do 0,44 mg/L. Koncentracija lipida u *SPM* je pokazala sveukupno više vrijednosti na Pagu, u prosjeku 0,23 ± 0,02 mg/L, nego na Pašmanu, u prosjeku 0,14 ± 0,02 mg/L.

Izotopni ciklus je bio prilično sinhroniziran između lokacija, a vrijednosti više obogaćene s ^{13}C zabilježene su tijekom ljeta i jeseni na obje lokacije. Iako su molarni omjeri $C{:}N_{SPM}$ pratili sličan obrazac za vrijeme jeseni i zime, oni su se značajno razlikovali među lokacijama ($P < 0,001$), s rasponom od 7,7 do 11,6 na Pašmanu i od 7,3 do 10,6 na Pagu.

Potrošač. Vrijednosti osiromašene s ^{13}C su zamijećene tijekom kraja zime i proljeća, dok je porast prema bogatijim vrijednostima varirao među populacijama. Na Pašmanu, vrijednosti su bile više obogaćene u jesen i ljeto, dok su na Pagu najveće vrijednosti prikazane u jesen i početkom zime. Molarni omjer $C{:}\ N_{DG}$ je pokazao značajne razlike između lokacije i mjeseca (sve na $P < 0,001$), ali ne u njihovoj interakciji ($P > 0,05$), što pokazuje da su se vremenske izotopne vrijednosti ponašale po sličnom obrascu među populacijama. Koncentracija lipida u probavnoj žljezdi je također analizirana sezonski na Pašmanu, te je uspoređena s istim mjesecima na Pagu. Prosječne vrijednosti na Pašmanu su bile 100,6 ± 7,1 mg/g, a one na Pagu su bile znatno više, 180,9 ± 5,3 mg/g.

Reproduktivni ciklus

Histološka analiza uzoraka vrste *Callista chione*. Ukupno 133 muških jedinki (54,3%), 105 ženskih (42,9%) i 7 hermafrodita (2,8%) su identificirani u populaciji s Paga, a 116 muških jedinki (52,7%), 97 ženskih (44,1%), 3 hermafrodita (1,4%) i 4 spolno neodređene jedinke (1,8%) su utvrđene u uzorcima iz Cetine. Omjer spolova se nije značajno razlikovao od 1:1 (chi-kvadrat = 3,294, P = 0,069 na Pagu i chi-kvadrat = 1,695, P = 0,193 u Cetini). Period mriještenja je počeo ranije na Cetini (u siječnju 2015), razdoblje s blažim temperaturama (na ~ 14°C) koje bi pogodovalo ranijem sazrijevanju gonada, s glavnim vrhuncem mriještenja u proljeće produljeno je do lipnja/srpnja. Na Pagu, period mriještenja je počeo kasnije, u travnju 2015 (pri ~ 12 ° C), a glavni vrhunac se dogodio tijekom ljeta, s kratkim vremenskom periodom otpuštanja gameta (uglavnom tijekom srpnja) ukazujući na značajnu gonadnu pohranu tijekom gametogeneze. Visoke vrijednosti srednjeg gonadnog indeksa (*MGI*) su bile u obrnutoj korelaciji s temperaturom.

Histološka analiza uzoraka vrsta *Glycymeris bimaculata i G. pilosa*

Ukupno 178 muških jedinki (55,6%), 141 ženskih (44,1%) i jedan hermafrodit (0,3%) su identificirani u populaciji *G. bimaculata* s Paga, te 149 muških (53,2%), 129 ženskih (46,1%), jedan hermafrodit (0,4%) i jedna spolno neodređena jedinka (0,4%) su utvrđene u uzorcima iz Cetine. Omjer spolova je bio 1,0: 1,3 na Pagu (chi-kvadrat = 4,292, P = 0,038), dok se na ušću rijeke Cetine nije značajno razlikovao od 1:1 (chi-kvadrat = 1,439, P = 0,230). Analizom uzoraka *Glycymeris pilosa* iz Pašmana identificirano je ukupno 129

muških (51,1%), 121 ženskih (48,5%) i jedan spolno neodređeni primjerak (0,4%). Omjer spolova nije se značajno razlikovao od 1:1 (chi-kvadrat = 0,256, P = 0,613).

Gametogeneza je počela oko listopada za vrstu *G. bimaculata* i u studenom za vrstu *G. pilosa*, nevezano s temperaturnim maksimumom. Period i vrijeme mriještenja populacija *G. bimaculata* u usporedbi s onima *C. chione* pokazali su neke sličnosti. Iako je razdoblje mriještenja bilo kraće za vrstu *G. bimaculata* nego za vrstu *C. chione*, glavni vrhunac mriještenja dogodio se također ranije na ušću Cetine (rujan 2014 i kolovoz 2015 godine) nego na Pagu (rujan/listopad 2014 i rujan/listopad 2015 godine), tijekom dva uzastopna razdoblja.

Gonadosomatski indeks

Najveće prosječne vrijednosti *BMI* za vrstu *C. chione* su bile 37,94 i 36,42 na Pagu (odnosi se na travanj i svibanj 2015 godine) i 33,56 i 30,95 na Cetini (odnosi se na srpanj 2014 i lipanj 2015 godine). Vrijednosti BMI su imale veće raspone varjabilnosti na Pagu nego na Cetini. Slično tome, vrijednosti *GSI* s Paga (0,050 ± 0,046) su bile znatno veće od onih s Cetine (0,037 ± 0,031) (Mann-Whitney $P < 0,001$). Kombinacija oba indeksa je pokazala pozitivnu korelaciju ($r = 0,77$, $P < 0,001$) na Pagu, što ukazuje na sinkronizaciju u vremenskom uzorku. Ovaj uzorak nije zabilježen na Cetini ($r = 0,13$, $P > 0,05$). Tijekom najzrelijih stadija, prije mriještenja, najveća gonadna proizvodnja opažena je na Pagu, srednje težine 348 ± 13 mg, dok je u Cetini bila 165 ± 6,70 mg. Na temelju srednjih populacijskih vrijednosti, uzorci s Paga otpustili su 82% gonada, dok su oni iz Cetine otpustili gotovo svu gonadnu masu (96%). U pogledu plodnosti, a uz pretpostavku jednake težine za muške i ženske jedinke, veći dio gonadne mase u razmnožavanje je uložen u Cetini, unatoč većim ulaganjima i produkciji iz populacije s Paga.

Za vrstu *G. bimaculata*, srednje vrijednosti *BMI* tijekom istraživanja su bile u prosjeku 22,4 ± 3,1. Najveća srednja mjesečna vrijednost *BMI* je bila 26,1 (kolovoz 2015 godine), a najniža prosječna je bila 18,4 (prosinac 2014 godine). Najviše prosječne mjesečne vrijednosti *GSI* su bile 0,192, 0,204 i 0,208 (u kolovozu 2014 godine, te kolovozu i rujnu 2015 godine), a one najniže su zabilježene u listopadu obje godine, i to 0,012 (2014 godine) i 0,018 (2015 godine). Ova dva indeksa su imala pozitivnu korelaciju ($r = 0,63$, $P < 0,001$), što ukazuje na sinkronizaciju u vremenskom uzorku. Tijekom najzrelijih faza, prije mriještenja, najviša srednja gonadna masa je bila 4,7 ± 1,3 g u kolovozu 2014 godine i od 5,3 ± 1,0 g, kako u kolovozu tako i rujnu, 2015. godine. Najveća zabilježena gonadna aktivnost u tom razdoblju je bila 6,8 g (kolovoz 2014. godine) i 7,4 g (rujan 2015. godine). Na temelju srednjih populacijskih vrijednosti, primjerci iz 2014. Godine otpustili su 93,8% gonada, a oni iz 2015. godine otpustili su 92,5%. U pogledu plodnosti, visok postotak gonadne mase uložen je u razmnožavanje.

Kombinacija histologije i gonadosmoatskog indeksa, je odredila ista glavna razdoblja mriještenja gdje su najviše vrijednosti gonadosomatskog indeksa korespondirale s mjesecima zrelosti i mriještenja. S druge strane, niske vrijednosti gonadosomatskog indeksa vezane su s neaktivnim i ranim razvojnih stadijima. Identificiran je prijelaz između zadnjeg događanja mriještenja i neaktivnog perioda.

Rast: Mikro-mljevenje ljuštura vrste *C. chione*. Međugodišnje amplitude izotopa kisika ljuštura s Paga su bile od -0,82 do 2,24 ‰ u uzorcima jedinke AC1, od -0,78 do 2,25 ‰ u uzorcima jedinke AC2 i od -0,77 do 2,46 ‰ u uzorcima jedinke AC3. Za ljušture iz Cetine ove amplitude su bile od -0,73 do 1,79 ‰ u uzorcima jedinke CC1, od -0,91 do 1,71 ‰ u uzorcima jedinke CC2 i od -0,84 do 1,51 ‰ u uzorcima jedinke CC3. Amplitude izotopa ugljika s Paga su bile u rasponu od -1,20 do 0,03 ‰ u uzorcima jedinke AC1, od -1,51 do -0,16 ‰ u u uzorcima jedinke AC2 i od -0,42 do -0,06 ‰ u uzorcima jedinke AC3. Za ljušture iz Cetine vrijednosti su bile u rasponu od -1,36 do 0,02 ‰ uzorcima jedinke u uCC1, od -1,02 do -0,07 ‰ u uzorcima jedinke CC2 i od -1,08 do -0,21 ‰ u uzorcima jedinke CC3. Značajne negativne korelacije postojale su između $\delta^{18}O_{shell}$ i $\delta^{13}C_{shell}$ osim za ljušturu CC3. Utvrđivanje vremena formiranja rasta ljušture usmjereno je na niz linija rasta koje su bili smještene između ljeta i rane jeseni. Otkrivene su temperaturne amplitude godišnje varijacije $\delta^{18}O_{shell}$, a sezona rasta utvrđena je za razdoblje od svibnja do prosinca. Svaka promjena od 4,34°C u temperaturi rezultira u pomaku od jednog promila u karbonatu ljušture, dakle, ljušture jedinki s Paga su pokrile raspon temperature od 13,2 - 14,0°C, dok su se vrijednosti rekonstruirane temperature iz uzoraka ljuštura jedinki s Cetine kretale od 10,2 - 11,4°C, što predstavlja nižu amplitudu od izmjerene temperature morske vode (16,2°C na Pagu, 13,7°C u Cetini). Rezultati istraživanja ukazuju da ljuštura prestaje rasti u razdoblju između siječnja i travnja, na obje lokacije.

Mjeseci s najvišim prosječnim stopama rasta ljušture na Pagu su bili srpanj (25,3%), kolovoz (19,7%) i svibanj (12,2%); a niže stope rasta su dobivene u rujnu (9,6%), listopadu (9,4%) i lipnju (7,1%). Na Cetini, najviše srednje vrijednosti rasta ljušture dobivene su u kolovozu (17,4%), listopadu (14,2%), lipnju (13,7%) i srpnju (23,0%); dok su niže srednje stope rasta dobivene u prosincu (6,5%) i svibnju (5,0%). Ljušture nisu rasle u razdoblju od siječnja do ožujka. Stope rasta ljušture su bile u korelaciji s temperaturom mora i povezane s gonadosomatskim indeksom i $\delta^{13}C_{SPM}$.

Rast: Mikro-mljevenje ljuštura vrste *G. bimaculata*. Međugodišnje amplitude izotopa kisika ljuštura s Paga su bile od -0,49 do 1,84‰ u uzorcima jedinke AB1 i od -0,47 do 1,67‰ u uzorcima jedinke AB3. Amplitude u analiziranim ljušturama iz Cetine su se kretale u rasponu od -0,83 do 2,24‰u uzorcima jedinke CB1, od -0,33 do 1,54‰ u uzorcima jedinke CB2 i od -0,57 do 2,44‰ u uzorcima jedinke CB3. Amplitude izotopa ugljika iz Paga su se kretale u rasponu od 0,03 do 1,25‰ u uzorcima jedinke AB1 i od

-0,52 do 0,38‰ u uzorcima jedinke AB3. U analiziranim uzorcima iz Cetine te vrijednosti su se kretale u rasponu od 0,35 do 1,77‰ (CB1), od 0,33 do 0,95‰ (CB2) i od 0,49 do 1,72‰ (CB3). Korelacije između $\delta^{18}O_{shell}$ i $\delta^{13}C_{shell}$ su varirale među uzorcima, pokazujući značajnu pozitivnu korelaciju u AB3 i negativne korelacije u drugim uzorkovanim ljušturama, iako su samo u CB1 i CB3 bile značajne. Rekonstruirane temperature na Pagu su bile u rasponu od 13,4 do 27,1°C (AB1) i 15,2 do 26,0°C (AB3), dok su u Cetini rasponi oscilirali između 14,0 do 28,9°C (CB1), 17,4 do 26,5°C (CB2) i 13.5 do 27.7°C (CB3). Ove vrijednosti su u okviru maksimalnih zabilježenih temperatura koje su bile 28,6°C na obje lokacije. Minimalne temperature su bile 7,4°C na Pagu i 10,9°C na Cetini što ukazuje na prestanak rasta ljuštura tijekom hladnijeg perioda u godini.

Razdoblja s najvećim rastom u ljušturi AB1 su bili lipanj s 13,6%, kolovoz s 22,7% i srpanj s 29,5%. U ljušturi AB3 su razdoblja s najvišom stopom rasta bili svibanj s 16,1%, srpanj s 22,6% i lipanj s 25,8%. Mjeseci s najmanjim rastom ljušture su bili studeni s 4,5 i 6,5% i prosinac s 4,5 i 0% za AB1 i AB2, respektivno. CB2 primjerak iz Cetine je pokazivao lipanj i srpanj kao mjesece s najvišim stopama rasta ljušture. U primjercima s Cetine, korišten je prosjek od 4 uzorka $\delta^{13}C_{DIC}$ kako bi se dobila gruba procjena metaboličkog ugljika, što je predstavljalo 8%.

RASPRAVA

Ova disertacija daje uvid u biološke i ekološke čimbenike koji utječu na rast ljuštura školjkaša. Rezultati su pokazali da dvije istraživane vrste, *C. chione* i *G. bimaculata*, iako s različitim okolišnim značajkama, ovisno o lokacijama, imaju zajedničko razdoblje prestanka rasta, sugerirajući opskrbljivanje hranom kao ograničavajući čimbenik. Smanjeni rast ljušture tijekom kasne jeseni i zime, kada su temperature mora i dostupnost hrane bili najniži, zajedno s početkom gametogeneze, ukazuju na smanjeni rast ljušture kao posljedicu nepovoljnih uvjeta okoliša i veću potrebu za reproduktivnim naporom. Glavni zaključci ove studije, koja obuhvaća okolišne karakteristike, hranjenje, razmnožavanje i rast, su sljedeći:

• Mješavina morskih i kopnenih izvora dominira vremenskom varijacijom mikročestica u obalnom dijelu srednjeg Jadrana.

• Niski *%C* i *%N* su karakteristični, potvrđujući slabu nutritivnu kvalitetu sedimenta u ovom oligotrofnom okolišu.

• Analize stabilnih izotopa i masnih kiselina upućuju da su proljeće i ljeto razdoblja s najboljom kvalitetom hrane u mikročesticama.

• $\delta^{13}C$ je bio specifičan za vrstu, s više obogaćenim vrijednostima u vrsti *G. bimaculata* nego vrsti *C.* chione, dok je δ15N bio specifičan za lokalitet, s više obogaćenim vrijednostima u Cetini.

• Nije uočeno preklapanje u ishrani između vrsta *G. bimaculata* i *C. chione* sugerirajući podjelu resursa. Populacije na Pagu su pokazale veći doprinos sedimenta u njihovoj ishrani, a prisutnost bentosne diazotrofne biomase je vjerojatno bila odgovorna za nisku $\delta_{15}N$ u njihovoj prehrani.

• Specifičnost lokaliteta je bila dominantna pri usporedbi izotopnog sastava dviju populacija vrste *G. pilosa*, s više obogaćenim vrijednostima na Pašmanu.

• Ovaj rad naglašava važnost uzimanja u obzir i prostornih i vremenskih promjena i prednosti kombiniranja skupa biokemijskih parametara u studijama ekologije prehrane.

• Histologija i gonadosomatski indeks su opisali glavne promjene u gametogenskom ciklusu dviju vrsta (*C chione* i *G. bimaculata*) s različitim reproduktivnim strategijama.

• Varijacije između lokacija, u vremenu i trajanju mriještenja *C. chione,* su najvjerojatnije rezultat razlika u temperaturi mora između istraživaih lolacija.

• Različite reproduktivne strategije između populacija *C. chione,* kao rezultat sposobnosti prilagodbe vrsta, predviđajući nepovoljne uvjete (Pag) resorpcijom gonada.

• Odgođen interval i vrijeme mriještenja u *Glycymeris* sp. je vjerojatno u vezi s potrebom za više vremena za pohranu energije uz postojeću opskrbu hranom.

• *BMI* ne može uvijek biti naveden kao pokazatelj stanja organizma u školjkaša.

• Sezonska varijacija u vrijednostima $\delta^{18}O_{shell}$ izmjerenim kod analizanih jedinki *C. chione* i *G. bimaculata*, ukazuje da se rast ljušture odvija u razdoblju između svibnja i prosinca.

• Linije godišnjeg rasta koje predstavljaju usporen rast ili zaustavljanje rasta ljušture su jasno vidljive na dijelovima ljušture položenim na kraju ljeta i početkom jeseni kod vrste *C. chione*. Kod mladih jedinki vrste *G. bimaculata* linije rasta nastaju u vrijeme temperaturnog maksimuma dok je kod odraslih jedinki ostalo nejasno kada dolazi do formiranja linije rasta.

• Temperatura je važna odrednica rasta ljušture, dok bi dostupnost hrane mogla postaviti granice sezone rasta ljušture.

• Sklerokronologija povezana s fiziološkim i ekološkim istraživanjima pridonosi boljem razumijevanju osobina životnih ciklusa vrsta.

10. BIOGRAPHY

Born on June 27th 1983 in Barcelona, I conducted my primary and secondary education in my hometown. I obtained a Bachelor degree in Biology from the Autonomous University of Barcelona (Bellaterra) in 2007. It was a 4-year degree plus one year abroad conducted at the University of California, Santa Cruz (USA) to get specialization in Marine Sciences. Pursuing my motivations, I took a 2-year Master in Science degree in Marine Biodiversity and Conservation as part of the EMBC European Program from which I graduated in 2010. The first year was taught at the University of the Algarve (Portugal) and the second year at the University of Oviedo (Spain). After that, I had the opportunity to work on my Master thesis at the Institut de Ciències del Mar, in Barcelona. I worked in the Benthic Ecology Lab and I remained there for a total of 3 years collaborating and participating in different projects. At the end of 2013 a Marie-Curie research fellowship (ITN) for Split to work on bivalve ecology came out, as part of the ARAMACC Project, and I was selected to start on April 1st next year. The Institute of Oceanography and Fisheries has hosted me during 3 years where I've written my PhD. During these years, several summer schools, workshops and conferences have been held and I've been able to participate on them travelling to the UK, Norway, Germany, the Nederland's, USA and Spain and learning about several aspects of sclerochronology.

Publications in journals indexed in Web of Science database:

Purroy A., T. Šegvić, A. Holmes, I. Bušelić, J. Thébault, A. Featherstone & M. Peharda. 2016. Combined use of morphological and molecular tools to resolve species mis-identifications in the Bivalvia – the case of *Glycymeris glycymeris* and *G. pilosa*. Plos One. 11(9): e0162059. doi: 10.1371/journal.pone.0162059

Grinyó J., A. Gori, S. Ambroso, **A. Purroy**, C. Calatayud, C. Dominguez-Carrió, M. Coppari, C. Lo Iacono, JP. López-González & JM. Gili. 2016. Diversity, distribution and population size structure of deep Mediterranean gorgonian assemblages (Menorca Channel Western Mediterranean Sea). Progr. Oceanogr., 145:42-56.

Peharda M., BA. Black, **A. Purroy** & H. Mihanović. 2016. The bivalve *Glycymeris pilosa* as a multidecadal environmental archive for the Adriatic and Mediterranean Seas. Mar. Environ. Res., 119: 79-87.

Purroy A., S. Requena Moreno, JM. Gili & R. Sardá. 2014. Spatial assessment of artisanal fisheries and potential impacts on the seabed: a study of the Cap de Creus region (northwestern Mediterranean Sea). Sci. Mar., 78(4): 449-459.

Ambroso S., C. Dominguez-Carrió, J. Grinyó, PJ. López-González, JM. Gili, **A. Purroy**, S. Requena & T. Madurell. 2013. In situ observations on withdrawal behavior of the sea pen *Virgularia mirabilis*. Mar. Biodiv., 43: 257-258.

Other publications:

Grinyó J., A. Gori, S. Ambroso, **A. Purroy**, C. Calatayud, C. Dominguez-Carrió, M. Coppari, C. Lo Iacono, P. López-González, JM. Gili. 2015. Spatial, bathymetrical and size distribution of Deep unexpected well preserved Mediterranean gorgonian assemblages (Menorca Channel, Western Mediterranean Sea). ICES 2015/D:19

Dominguez-Carrió C., S. Requena, JM. Gili, A. Gori, T. Madurell, E. Isla, A. Sabates, S. Ambroso, **A. Purroy**, J. Grinyó, A. Olariaga, C. Lo Iacono, A. Castellón, J. Prades, J. Sans, MJ. Uriz, R. Sardá, JP. Lozoya, L. Serrano. 2014. Sistema de Cañones Submarinos Occidentales del Golfo de León. Áreas de estudio del proyecto Proyecto LIFE + INDEMARES. Ed: Fundación Biodiversidad, Madrid, 100 pp.

Madurell T., C. Orejas, S. Requena, A. Gori, **A. Purroy**, C. Lo Iacono, A. Sabatés, C. Dominguez-Carrió & JM. Gili. 2012. The benthic communities of the Cap de Creus Canyon. In: Würtz M (ed.), Mediterranean Submarine Canyons: Ecology and Governance. Gland, Switzerland and Málaga, Spain: IUCN, pp. 123-132.

Gili JM., T. Madurell, S. Requena, C. Orejas, A. Gori, **A. Purroy**, C. Domínguez, C. Lo Iacono, E. Isla, JP. Lozoya, C. Carboneras & J. Grinyó. 2011. Caracterización física y ecológica del área marina del Cap de Creus. Informe final área LIFE+ INDEMARES (LIFE07/NAT/E/000732). Instituto de Ciencias del Mar/CSIC (Barcelona). Coordinación: Fundación Biodiversidad, Madrid, 272 pág.

Purroy A., S. Requena, R. Sardá, JM. Gili & E. Serrao. 2010. Spatial assessment and impact of artesanal fisheries' activity in Cap de Creus. Geographic Technologies applied to Marine Spatial Planning and Integrated Coastal Zone Management, 15-22.

ACKNOWLEDGEMENTS / AGRAÏMENTS

Gratitude unlocks the fullness of life…

A tots qui m'heu acompanyat durant tot aquest temps, i a aquells que us he anat trobant pel camí... volia agrair-vos l'haver-me inspirat d'una manera o altra! Per començar aquesta aventura Adriàtica, m'agradaria fer una passa enrera i començar per l'Institut de Ciències del Mar, on el meu interès per la recerca va anar creixent i va ser l'empenta per arribar fins aquí. Gràcies a tot el grup extens de bentos amb qui he compartit moments molt bons i han estat una gran part de l'arrel d'aquesta experiència. Gràcies **Jordi**, per incloure'm sempre i treballar amb tu de manera tan eficient i relaxada, recordo amb un gran somriure l'extàtic moment durant les filtracions a deshores al García del Cid… *let's pretend we don't exist…* les parades a port, i les estones a la sala de vídeos, ets collonut! A en **Carlos**, sobretot per la càlida acollida i els bons moments compartits, pel teu perfeccionisme inacabable… i aprofito per llençar un: si us plau, entrega ja! :) A la **Núria**, pel teu tarannà pacífic, suport i referent a l'inici d'aquesta aventura. Per les birretes cibernètiques, i les xerrades i viatges terapèutics. A la **Maria**, per la teva simpatia, les estones a gust, les connexions espaials, i per ser un bon estímul per a les remontades i recordar-me la importància de preguntar-se les coses. A la **Martina**, por todos los momentos de risas y risa desesperada, coffee breaks y repostería, por las divertidas salidas y por mostrarme las ventajas de la practicidad y de poner los pies en la tierra de vez en cuando. A l'**Stefano**, *bambolo*, *belle scarpe* & la **Rebeca**, pels bons moments *al cafè*, i l'especial estima que un guarda després de conviure més de dos mesos aïllats del món ;). Al **Jean Baptiste**, por nuestras charlas, tes y sensibilidades, por tu confianza y saber que puedo contar con tu apoyo, pour la fraternité! A l'**Elena**, la **Meli** & l'**Ana Mari**, por las gran compañeras y amigas de despacho que fuisteis, vuestro silencio, vuestras miradas y sobre todo vuestro cariño, ánimo, y conversas *más allá de* la ciencia. A l'**Ángela** & la **Miriam**, por vuestro carácter fuerte, luchador y pacificador, no es necesario tener largas charlas para compartir y aprender. A l'**Eli** (aupa volley!), l'**Alba**, l'**Andrea**, i tants més que ens hem creuat i viscut bon moments, i com no, en **Josep-Maria**. Gràcies per la oportunitat i per convidar-me a les campanyes, van ser genials! Gràcies a tots pel bon rotllo!

Quan una porta es tanca, una altra s'obre… i aquesta va ser la d'Split. *Dobrodošli*. This is how I was welcomed in the familiar environment, at the Institute of Oceanography and Fisheries where I've spent my last three years! I still remember hearing *tri godine* all the time, and then I knew I was the subject of the conversation, and that's pretty much all the Croatian I learnt. Melita, you were right… just kidding… ;) Gràcies al **Damián** per la transició, tot i que breu, va ser tranquilitzadora! I una cursa maratoniana va començar…

To my mentor **Melita**, I would honestly like to thank your warm welcome to Split and to the Institute, which gave me the comfort that I could count on you at any time. Thank you for your essential help in the field and the lab, facilitating all the set up, for being ready and willing to listen, talk or read at any moment and for your constructive comments.

Soon I realized that my experience wouldn't just be me based in Split but that I would become part of an extended community, and this was the ARAMACC! Paul as the table head, you are an energetic one… thank you for always setting a nice atmosphere around and for being encouraging at all times. It is been a great pleasure to meet all of you, **ARAMACCers**, **Juan**, **Maria**, **Fabian**, **Tamara** and **Amy**, and

Lars you too! brief and fun. And our *external* one, Ale-**Alejandro** (sorry about :) that) and to all supervisors… you are so many that consider yourself included! Our frequent meetings absorbed most of our time making it sometimes logistically c r a z y, but I enjoyed your company and fun times. Say *dinner time*! And I burst into laughter.

My secondment in Mainz wouldn't have meant the same without **Stef** and **Li** as awesome hosts and **Stella**'s friendly travel & lab company. *Oh* those basement journeys, although greyish, I remember them with smiles. **Irene**, esa complicidad no solo en compartir tópico sino en nuestra manera de ver y hacer, ha hecho que algunos momentos fueran mucho más fáciles. To all of you for our special connection and friendship which made our meetings and journeys, much warmer.
Thank you also to **Eric O.W.** and **Michael M.** for all your help in the geochemistry lab, tips, tricks, patience and selfless help.

Special thanks to **Julien Thébault** and **Bernd R. Schöne** for their meticulous and constructive comments in our joint collaborations. And to **Paul Butler** and **Rob Witbaard** to read through my thesis and give me your external viewpoint and constructive comments, I really appreciate it.

Thank you to my committee members **Nedo Vrgoč**, **Ivana Bočina** and **Ivan Župan** for their kind comments, professionality and flexibility.

This doctoral thesis would have not been possible without the help of a great team of colleagues and friends. I would like to thank all of you that help me at some stage of my sampling starting with **Ella**, **Nika**, **Marija**, **Marija E.**, **Hrvoje**, **Mišo**, Ivana, **Doris**, **Meri** and **Ranko**. Thank you to our visiting master students, **Claudia** and **Pedro** por vuestra alegría, ganas de participar en todo y vuestra compañía durante 4 meses! To **Inne** and **Gotje**, although it was a short stay, I can still hear the unstoppable and exciting tone of your talks and I keep hilarious times in my memory, força Barça! A ti **Lili**, por ese último muestreo tan especial, curioso-exploratorio y animador, qué mejor que tu compañía para esta tarea! Eres una gran inspiración para moverse por el mundo, con tu *espavilamiento*, tu salero, expresión y ganas de vida. Eres un ángel.
Special thanks to **Filip**, Ivan and **Mario** for their professionality and commitment every month, to collect my samples under any conditions. I can say we are one of the healthier samplers ever! We overcame Buras, Jugos and other storms, nature as it is. A special mention to the **Bukša family**, and a dedicated one to **Franći**, my Pag boat-mate, your firm, worker, familiar, friendly and giving character will be always in my memory, be in peace.
Thank you all! Without all your help, collecting and processing all the samples on time wouldn't have been possible. Needless to say… a tribute goes to all ***bivalves*** sacrificed in the pursuit of good science.

Hvala ti: **Ivona**, **Ivana B**, **Roman**, **Nikša**, **Danijela B**, **Krešo**, **Petra L**, **Anka**. For borrowing me keys, labs, chemicals, books, gloves, pens, company & smiles. In fact, I'm sure I've needed something from most of the personnel at IZOR, and you've kindly offered your help. So thank you to all **IZORians** for opening your doors at my questions and requests, and especially to those willing to share science and beyond science with me. *Hvala ti* Slaven and Tanja for that. **Slaven**, thank you so much for your flexibility, random talks in the hallways and stairs, for sharing your home and taking me to Istra! It's been relaxing and fun. *Oh*, and long life to *čuvarkuća*! **Tanja**, our fruitful collaboration and break talks made me realize what a resourceful woman you are, your mentality helped me to move through some bumps.

Thank you **Sanja Puljas** for your valuable help, patience and selfless teaching about all histological misteries. Your visits and company in the lab and while identifying all gonadal maturation stages, were a wanted, relaxed and productive time. Also I'd like to thank, you and Ivana B. for hosting me at your laboratory to sort out some sample problems. I'm also pleased to have met the devoted malacologist Prof. **Brian Morton**, I'm really amazed by your drawings and the microscopical detail you are able to incorporate in. I keep a nice memory of our couple trips, talks about life and scientific enthusiasm.

To my charming office-mate **Damir**, I guess I'm saying that cus you barely were there ;) your absence it's been great at some…mmm concentration points, but with you, storyteller, it's been always funnier. You may miss my silence, but I definately know you'll miss my *colours*. My next-door mates, **Igor** and later on **Petra** too. I may have not visited you enough, but if I needed smiles, I knew where to go. I love the way of *not not* knocking on office's door, and your expression after that. Coffee visits, printer visits, looking for visits, forgetting what visits. Always pleasant. **Sanja M** feel also included on the last ;) you always reminded me it was 9:ooh, time to focus on if I weren't, and I learned about croatian social interaction! **Hana**, you arrived quietly and became a nice company while writing the PhD, always calm and focused, you collaborated in creating the good environment, I wish you luck!
Someone came in late… **Daria**, I think saying *better late than never* summarizes our relationship. We've needed to speed up to catch up, and it has been fun. I would have rather having you around all this time, but *hej*, what a nice unexpected closing. Thanks for all the help offered and performed in such a short time! and for our gastronomic outings. Salut!

A PhD abroad appreciates the finding of a transitional family, and I met this reception with **Patricia**, **Tatiane** and even **Tin**, muchas gracias e muito obrigadinha! Habéis sido una gran medicina para distraerme y me sentí muy cómoda junto a vosotr@s. **Ivana**, with a little bit of time I got into your heart, thank you amiga, thank you also for introducing me to Mosor and discover many beautiful places around Croatia, for taking me with you in all adventures, for offering a hand in everything, and for our scenic lunch breaks. To **Ines**, for our connection, bike getaways and for the laughter. It's been inspiring and often a mirror to meet the multitasking croatian one :). To both of you for sharing the exciting pain and special feeling of silking around. Such a destroyer activity never felt so good. *Ljubavi*.

Special thanks to **Marjan** (Šuma!), to be there ALL the time as the best source of oxygen and relaxation everytime I needed it. Always so accessible.

All people that I met taking different paths and that influenced me through life, supported my career and encouraged me to follow my dreams… **Meri**, **Elena O**, **Mercè L**, **Laura B**, **Amélie**, the **Sneddon's**, **Bruno**, **EMBC crew**, **Catarina, Fletcher, Sunny**… you're always special to me.

En especial a la **Carla** i l'**Helena** per sentir-vos aprop meu. Des que vam trobar-nos, compartir aficions i maneres de fer han estat i són una gran inspiració per mi. Començant per la muntanya, viatges, trivias, manualitats, i les nostres idees i plans futurs, han fet que sigueu part de mi. Espero que les *distàncies* s'escurcin i tenir-vos sempre ben aprop meu.

A ti **Raquel**, por no importar donde nos encontremos y estar siempre en el corazón de la otra. Entendiéndonos entre nuestras dos ciencias, me ha enriquecido mucho y me ha ayudado a ver el otro lado de las cosas. Nuestra mútua admiración junto con tu positivismo y energia, son un gran apoyo… siempre. Así que, desde donde sea… por muchos años más!

Gràcies a l'extensa familia més propera que sempre té un ull per saber per on paro, què faig i com estic, gràcies **tiet**, **tieta**, **tata**, **Eric**, **Naiara**, **Eva** i **Ricky**, i parelles! En especial gràcies a la Naiara, al **Carlos** i a l'**Iker** per la vostra visita, una sorpresa molt agradable i un xut d'energia, tot i que també va ser una presa d'energia, amb *epípteros* nocturns ;).

A la **mama** i el **papa**, per donar-me sempre la llibertat de fer el que he cregut a cada moment i el vostre suport tot i no saber molt bé on anava o a fer què. Des que vaig desplegar les ales, he donat més voltes que una baldufa, he anat buscant i trobant, buscant i trobant, o simplement buscant, i sempre esteu al costat amb molts ànims. No sabeu l'incalculable valor que té aquest recolzament. Una estima eterna a l'**avi**, la **iaia** i la **Dana**, sou una part molt important de com sóc avui.

A tu te... **Àlex**, perquè sí, perquè sí, i perquè sí, perquè sempre has sigut i seràs el meu model. Davant d'una passa meva, n'hi ha una de teva, i és per això que connectem i compartim il.lusions i somnis, tot i lo diferents que som! Gràcies per les *extenses* xerrades, el missatge final i l'especial toc d'humor, que m'han donat forces per seguir endavant quan no he vist les coses clares. Per creure en mi i fer-me baixar del núvol quan cal. Tu sí que vals un món! Sempre amunt, *na na na*.

Y especialmente a ti **Enrique**, sin saber cómo agradecer todo tu apoyo?! Profesionalmente eres admirable, y he aprendido muchísimo de todos tus comentarios que, sin duda, han sido una parte muy importante de mi crecimiento. Aun en la distancia, has formado parte de todo este proceso y lo has vivido constante e intensamente junto a mí. Contar con tus consejos, tu paciencia, tu comprensión, tu ánimo, tu confianza y tu cariño ha sido muy muy muy reconfortante. Tus visitas han sido excelentes *vitaminas* para llevarlo mejor! Y juntos hemos explorado éste y otros terrenos llenos de aventuras, contigo siempre es más divertido i em sento molt afortunada ☺ *Viva la vida*!

Segurament m'he deixat a algú... Moltes gràcies!!!

Moltes gràcies!!!

Ariadna

"Només hi ha dos dies l'any en què no es pot fer res; un es diu ahir i un altre demà, per tant, avui és el dia ideal per estimar, creure, fer i principalment viure"

Dalai Lama

Doctorat en Ciències del Mar

CONTROLADORS BIOLÒGICS I ECOLÒGICS DEL CREIXEMENT DE LA CLOSCA EN ELS BIVALVES

Ariadna Purroy Albet

Tesi doctoral realitzada a l'Institut d'Oceanografia i Pesca, Split

Resum

Els mol·luscs bivalves incorporen en les seves closques aspectes de la història de vida durant el creixement, convertint-los en valuosos arxius d'informació ambiental, biològica i evolutiva. En aquesta tesi es proporciona informació detallada sobre els controladors biològics i ambientals del creixement de la closca a *Callista chione*, *Glycymeris bimaculata* i *G. pilosa*. L'estudi s'ha dut a terme a la costa mig-est del Mar Adriàtic (Abadia de Pag, desembocadura del riu Cetina i Canal de Pašman) des de maig del 2014 fins a l'octubre de 2015. Mitjançant l'anàlisi de diversos paràmetres bioquímics incloent-hi isòtops estables i la composició d'àcids grassos, s'ha caracteritzat l'ecologia alimentària d'aquestes espècies en el seu hàbitat. El comportament reproductiu s'ha estudiat aplicant dos enfocaments complementaris, la histologia i l'índex gonadosomàtic. Per últim, l'anàlisi d'isòtops estables de mostres carbonatades s'ha relacionat amb registres de temperatura d'alta resolució per descriure els patrons de microcreixement de la closca. Els períodes amb la millor qualitat alimentària a la matèria particulada van identificar-se a la primavera i a l'estiu. Es va observar una repartició dels recursos alimentaris entre *C. chione* i *G. bimaculata* a cada àrea d'estudi, i es va veure que la composició isotòpica del nitrogen al teixit dels bivalves estava influenciada per la presència de biomassa diazotròfica, i aquesta els diferenciava entre localitats. Les variacions en l'inici i durada de la fresa entre les àrees d'estudi estan probablement associades a la temperatura, mentre que a *Glycymeris* sp., la fresa no hi està directament conectada. Aquestes respostes biològiques a petita escala són essencials per fer front a les influències del canvi climàtic. La formació de la closca es va produir entre el maig i el desembre assenyalant (1) la temperatura com un determinant important del creixement de la closca (2) la disponibilitat de nutrients com a limitant de l'època de creixement i (3) l'inici de la gametogènesi prop de la formació de la línea de creixement, el que evidencia majors requeriments d'energia per a la reproducció. Aquests resultats contribueixen al coneixement sobre l'ecologia de bivalves al Mar Adriàtic i destaquen la importància d'unir estudis d'esclerocronologia i ecologia per entendre millor aspectes de la història de vida de les espècies.

Paraules clau: bivalves, ecologia alimentària, àcids grassos, isòtops estables, histologia, índex gonadosòmatic, creixement de la closca, escloroquímica, esclerocronologia, Mar Adriàtic.

"What is a scientist after all? It is a curious man looking through a keyhole, the keyhole of nature, trying to know what's going on"

Jacques Yves Cousteau